LIFERING, an E3 ligase, ubiquitinates the acyl-CoA dehydrogenase-like protein IBR3, and coordinates cell proliferation and death upon DNA damage

Brigitta M. Kállai[1], Edit Németh[2], Aladár Pettkó-Szandtner[3], Zaki Ahmad[2], Fruzsina Nagy[4,5], László Bögre[2], Zoltán Magyar[4], Tamás Mészáros[1#] & Beatrix M. Horváth[2#*]

1. Department of Molecular Biology Institute of Biochemistry and Molecular Biology, Semmelweis University, Budapest, Hungary,

2. Department of Biological Sciences, Royal Holloway, University of London, Egham, UK

3. Proteomics Research Group, Core Facility, Biological Research Centre, Szeged, Hungary

4. Institute of Plant Biology, HUN-REN Biological Research Centre, Szeged, Hungary

5. Doctoral School in Biology, Faculty of Science and Informatics, University of Szeged, H-6726, Szeged, Hungary

#: corresponding authors, contributed equally

* Current address: Education and Students Affairs, Wageningen University, Wageningen, The Netherlands

Short running title: DNA damage induced LIFERING ubiquitinates IBR3

ABSTRACT

Plants rapidly respond to environmental changes to ensure an optimal balance between growth and survival with intact genome. Here, we show that a DNA damage response gene, which we named *LIFERING*, is under the direct and independent regulation of ATM/ATR-SOG1 and RBR pathways. We demonstrate that LIFERING upon DNA damage plays an essential role in maintaining the balance between cell proliferation and cell death. Downstream of RBR, it is required to maintain proliferation, and in response to DNA damaging agents it initiates a cell death accompanied by rapid elongation and differentiation of the transit amplifying cells in the root meristem. LIFERING is a RING-between-RING E3 ligase; its ligase activity is dependent on the Cys392 residue located in the BRcat domain, responsible for the coordination of zinc ion binding. Using proximity labelling, we identified the acyl-CoA dehydrogenase-like protein IBR3, which is involved in the conversion of indole-3-butyric acid (IBA) to indole-3-acetic acid (IAA), as one of its targets. We provide evidence that IBR3 is ubiquitinated at several Lys residues in the presence of LIFERING. Our findings show that LIFERING rapidly responds to DNA damage and via ubiquitination of IBR3, is likely to be involved in the regulation of free-auxin level, indicating a link between DNA damage response and auxin regulation in the root.

Keywords:
DNA damage response (DDR), cell death, E3 ligase LIFERING, ubiquitination, acyl-CoA dehydrogenase-like protein (IBR3)

INTRODUCTION

During their entire lifecycle, plants are exposed both to exogenous and endogenous stresses and toxic compounds. Although sunlight is required for photosynthesis, the short-wave electromagnetic radiation causes cellular and DNA damage. Furthermore, other abiotic stresses, such as drought, salinity, and heavy metal contaminants also induce similar genotoxic effects (Yoshiyama *et al.*, 2013a; Pedroza-Garcia *et al.*, 2022). In addition, endogenous damage, spontaneously generated during DNA metabolism, replication and repair can also have an impact on the genome integrity. (Szurman-Zubrzycka *et al.*, 2023).

Protection of genome integrity is especially crucial in the stem cell niches. The plant RETINOBLASTOMA-RELATED (RBR) plays a central role in this process by two distinct mechanisms: (i) promoting the exit from cell proliferation to differentiation (Harashima & Sugimoto, 2016) (Cruz-Ramirez *et al.*, 2013), and (ii) directly regulating the expression of DNA damage response genes (Horvath *et al.*, 2017). RBR performs these functions in complex with the three canonical E2Fs (E2FA, E2FB, and E2FC) and other core components of the DREAM complex (dimerization partner (DP), retinoblastoma (RB)-like, E2F and MuvB), which are essential to establish transient and stable cellular quiescence and DNA damage response (Lang *et al.*, 2021; Gombos *et al.*, 2023). In addition to the transcriptional control of genes involved in S-phase progression, replication and cell-cycle checkpoint, RBR, primarily in conjunction with E2FA, directly regulates the expression of numerous damage response and repair genes, including *AtBRCA1* and *AtRAD51* (Biedermann *et al.*, 2017; Horvath *et al.*, 2017). This allows RBR to act rapidly to endogenous replication-induced DNA damage and initiates an ATM/ATR-SOG1 independent response pathway.

To mitigate the consequences of DNA damage, plants similarly to other organisms have evolved mechanisms to sense DNA lesions and initiate the DNA damage response (DDR)

pathways (LaRocque & McVey, 2023). The DDR signalling cascade is conserved in animals and plants (Clay & Fox, 2021; Herbst *et al.*, 2024); the double-strand breaks (DSB) activate the ATAXIA-TELANGIECTASIA MUTATED (ATM) kinase by the MRN complex (MRE11-RAD50-NBS1), while the ATAXIA-TELANGIECTASIA-AND-RAD3-RELATED (ATR) is mainly recruited to single stranded breaks (SSB) by the complex of Replication Protein (RPA) and ATR Interacting Protein (ATRIP). Though both ATM and ATR have distinct functions during signalling in response to genotoxic agents such as γ-irradiation, they show additive and complementary roles during DNA replication, cell cycle progression and repair (Nisa *et al.*, 2019; Herbst *et al.*, 2024) .

In plants, the activity of the ATM/ATR-driven signalling pathway merges with the phosphorylation of the plant-specific transcription factor, SUPPRESSOR OF GAMMA RESPONSE 1 (SOG1), which is considered to be the functional analogue of the mammalian p53 (Yoshiyama *et al.*, 2013a; Yoshiyama *et al.*, 2013b). Upon genotoxic stress, in parallel to RBR and E2Fs, the activated SOG1 regulates the expression of numerous DNA repair and cell cycle genes to coordinate repair with cell cycle progression (Bourbousse *et al.*, 2018; Ogita *et al.*, 2018).

Halted cell cycle resumes when the lesions are repaired via various pathways depending on the nature of the lesion (Raina *et al.*, 2021; Szurman-Zubrzycka *et al.*, 2023). However, in the case of severe damage, proliferating cells escape from further division and initiate processes of (i) cell death, especially in the stem and daughter cells (Furukawa *et al.*, 2010; Horvath *et al.*, 2017), (ii) endoreduplication (Adachi *et al.*, 2011; Lang & Schnittger, 2020), and/or (iii) differentiation. RBR plays a key role to establish the threshold at which cell death is initiated upon genotoxic stress (Horvath *et al.*, 2017).

Besides transcriptional regulation, posttranslational modifications, such as phosphorylation, ubiquitination and SUMOylation, also play an essential role in the regulation of the DNA damage response (Su *et al.*, 2020). Among the characterised plant-specific E3 ubiquitin ligases involved in DDR, the DNA damage response mutant 1 (DDRM1) and 2 (DDRM2) play a role in the early steps of damage recognition and recruitment of repair proteins to the damaged site**.** DDRM1 monoubiquitinates the phosphorylated SOG1, thereby promoting its stability (Wang *et al.*, 2022). Subsequently, SOG1 induces the expression of DDRM2, binding of which to AtRAD51 is required for its recruitment to the damaged DNA site labelled with γ-H2AX (Yu *et al.*, 2023). Upon DDR, the RBR-induced *KNOTEN1* (KNO1) also partially co-localises with γ-H2AX and is stabilised by the de-ubiquitinases, UBP12 and UBP13 (Chen *et al.*, 2023). After stabilisation, KNO1 mediates the K63-linked ubiquitination and autophagic degradation of RMI1 protein, a structural component of the Bloom syndrome complex, thereby increasing homologous recombination frequency (Chen *et al.*, 2023).

Studying the role of RBR in the protection of genome integrity, we found that the *At5g60250* transcript exhibited significantly higher expression levels than any other transcripts upon silencing of *RBR* (Horvath *et al.*, 2017). With genome-wide transcriptional analyses, *At5g60250* was also detected to be upregulated in response to a plethora of genotoxic conditions, including γ-radiation and oxidative stress (Culligan *et al.*, 2006; Yi *et al.*, 2014), radiomimetic drugs like hydroxyurea and bleomycin (Cools *et al.*, 2010; Yi *et al.*, 2014), metal toxicity (Sjogren *et al.*, 2015; Chen *et al.*, 2019), as well as due to mutations in genes, such as *fas-1* and *fas-2* (Schonrock *et al.*, 2006), and upon overexpression of AAR7 (Lee *et al.*, 2007). Despite extensive knowledge on the expression of *At5g60250* in various conditions, the role in DDR and its catalytic activity remains unknown.

Here we provide evidence that *At5g60250* hereafter named as LIFERING, is directly regulated by RBR in an independent pathway to ATM/ATR-SOG1. Our genetic analysis shows that upon genotoxic stress LIFERING is required to maintain meristematic activity by preventing the exit to differentiation as well as to regulate stem cell divisions downstream of RBR. We demonstrate that LIFERING is a functional ubiquitin E3 ligase; it is capable of autoubiquitination, and its activity depends on the Cys392 residue involved in the coordination of zinc ion binding. Using proximity-based labelling and protein interaction studies, we show that the most prominent interacting protein of LIFERING, the acyl-CoA dehydrogenase-like protein, IBR3 is involved in the conversion of indole-3-butyric acid (IBA) to indole-3-acetic acid (IAA). Both by *in vitro* and *in vivo* assays, we provide evidence that LIFERING ubiquitinates IBR3.

Based on these data, we suggest that the ubiquitination of IBR3 via LIFERING may connect the DDR and auxin responsive pathways upon DNA damage, to protect cells via auxin-driven cell death response.

MATERIALS AND METHODS

Plant material and growth conditions

Seeds were sterilised and grown as described earlier (Blilou *et al.*, 2005) except that seedlings used for qRT-PCR and microscopical analysis were germinated on 1.2 % plant agar. *Arabidopsis thaliana* ecotype Columbia 0 (Col-0) was used as wild type; the T-DNA insertion line, *lifering-1* (SM_3_34488) was obtained from the Nottingham *Arabidopsis* Stock Centre. The transgenic lines, *e2fa-1* (MPIZ_244, (Berckmans *et al.*, 2011) *sog1-1*, (Yoshiyama *et al.*, 2009) *Atbrca1-1* (Reidt et al., 2006)*, rRBr* (Blilou *et al.*, 2005), *amiRBR* (Cruz-Ramirez *et al.*, 2012) and *amiRBR*,*sog1-1* (Horvath *et al.*, 2017) were described earlier. SM_3_34488, is an JIC SM line, ordered via NASC. The T-DNA insertions, mutations were confirmed by PCR based genotyping or sequencing and gene silencing was demonstrated via gene expressional studies and phenotyping. To study the *lifering-1* (pgLIFERING-GFP) phenotype more than ten independent transformant were generated. The T-DNA insertion mutations were confirmed by PCR based genotyping or sequencing while gene silencing was demonstrated via gene expressional studies and phenotyping. *GFP* expression was followed by microscopical analysis. The list of primer pairs used in these experiments are listed in Supporting Information Table S1.

Chemical treatments and induction studies

To induce DNA damage response, 5-6 days-old seedlings (das) were transferred to tissue culture plates, containing fresh MS liquid medium without or with 10 µg ml^{-1} mitomycin C (MMC), and treated for a short period of 1-4 h or 16 h. Kinase inhibitory assays were carried out as described earlier (Horvath *et al.*, 2017). In each treatment, the relevant controls and mutants were studied simultaneously, the experiments were repeated at least three times

(n=biological repeat) with 15-20 (*N*=sample size) replicates. Although the level of MMC induction varied between the different biological experiments, the ratio of the relevant induction between the treated controls and samples in interest were comparable. Counting the number of propidium-iodide (PI)-stained cells in the columella stem cells (CSC) and lateral root cap initials (LRC) and their daughter cells was used to quantify cell death in the distal stem cell niche. In addition, cell death was also determined of the root-tip measuring the contiguously PI-stained cell area in the proximal meristematic vasculature directly adjacent to the QC.

Fluorescence microscopy and data processing

Leica SP2 or Olympus IX81-FV1000 inverted laser-scanning microscope equipped with different laser lines were used for phenotypic analysis of roots stained in 5 µg/ml propidium-iodide (PI), at 543nm for PI and at 488nm for GFP. For qualitative and quantitative comparison, images were taken in a single median section and recorded with identical microscope settings in all cases. Confocal images were converted to tiff files and processed with ImageJ software. Cell length was measured on the longitudinal axis in the middle of the cell, in the epidermis and/or cortex cell layers. The zone of the transit amplifying cells was defined by the boundary of cells with gradually increasing length. The distance from the QC to the first differentiating cell determined the start of differentiation.

Cloning

The coding sequence of *LIFERING* (accession number AT5G60250) was amplified from the RIKEN RAFL22-04-P06 clone, then inserted into pEU3-NII-HxHLICNot and pRT-HA-TurboID-LIC using LIC (Bardoczy *et al.*, 2008) and using *Nco*I and *Not*I restriction endonucleases into pRT-3xHA. R392 residue of the mutant LIFERING ORF (designated as

C392R) was restored to C392 (designated as wild-type, WT) by *in vitro* mutagenesis (Laible & Boonrod, 2009). The coding sequence of IBR3 (accession number AT3G06810) was amplified from pACT2CS cDNA library (Nemeth *et al.*, 1998) and inserted into pEU3-NII-GLICNot and pRT-9xMyc vectors as described above. Details on the vectors and primers used for cloning are provided in Supporting Information Table S2. Coding sequences of the constructs were verified by Sanger sequencing (Eurofins Genomics)

***In vitro* protein expression and ubiquitination**

The pEU3 vector constructs were used for *in vitro* transcription (Nagy *et al.*, 2020) and 2.5 µl of crude mRNA-containing reaction mixture was added to 10 µl of W7240 wheat germ extract (CellFree Sciences). The bilayer *in vitro* translation was prepared according to the manufacturer's recommendation, except that both layers were supplemented to contain 10 µM $ZnCl_2$ and incubation was done for 20 hours at 20°C.

The *in vitro* ubiquitination reactions were performed as described previously (Takahashi *et al.*, 2009) with minor modifications. The WT and C392R 12xHis-LIFERING-containing translation mixtures were diluted 1.25 times in the final volume of the ubiquitination reactions to contain 10 mM Tris-HCl pH 7.5, 5 mM $MgCl_2$ and 3 mM ATP. FLAG-ubiquitin was produced in *E. coli* cells as described in the Supporting Information and was added at 4 µM final concentration where indicated. The mixtures were incubated for 3–4 hours at 30°C either alone to test for the ubiquitination activity of LIFERING or were added to bead-bound GST-IBR3 to ubiquitinate it.

12xHis-LIFERING was purified using Dynabeads™ His-Tag Isolation and Pulldown Beads (Thermo Scientific). 230 µl ubiquitination reaction mixture was added to 15 µl beads equilibrated and resuspended in 230 µl 2X B/W buffer (100 mM sodium phosphate pH 8, 600

mM NaCl, 0.02% Tween-20), and incubated on a rotator for 1 h at room temperature. The beads were washed three times with 300 µl 1X B/W buffer for 5 minutes each, twice with 1.5 ml 1X B/W buffer and six times with 1.5 ml PBS.

GST-IBR3 was purified using Pierce Glutathione Beads (Thermo Scientific) prior to the ubiquitination reactions. 200 µl GST-IBR3-containing translation mixture was added to 30 µl beads equilibrated and resuspended in 1 ml Glut B/W buffer (125 mM Tris-HCl pH 8, 150 mM NaCl, 0.5% Triton-X), and incubated on a rotator for 1 hour at room temperature. Beads were washed five times with 300 µl Glut B/W buffer and then resuspended in 100 µl ubiquitination reaction mixtures containing 12xHis-LIFERING proteins. After incubation, the unbound fraction was retained and the bead-bound GST-IBR3 proteins were washed three times with 300 µl Glut B/W buffer for 5 minutes each, twice with 1.5 ml Glut B/W buffer and six times with 1.5 ml PBS. The reactions were analysed by Western blot and the bead-bound proteins were subjected to mass spectrometry as described in the Supporting Information.

Transient protoplast protein expression

C-terminally 3xHA-tagged wild-type and mutant C392R LIFERING and 9xMyc-tagged IBR3 were expressed driven by the *35S* promoter of pRT vectors through PEG-mediated transfection of $2x10^5$-$5x10^5$ protoplasts (Yoo *et al.*, 2007) isolated from Columbia (Col-0) *Arabidopsis thaliana* root cell suspension (Mathur & Koncz, 1998). Transfections and co-transfections were performed by using 5 µg of each vector. After 16 hours of incubation in the dark at room temperature, the cells were lysed by RIPA buffer and boiled in SDS-DTT sample buffer. The extracts were centrifuged at 13000 rpm for 10 minutes and the supernatants were analysed using Western blot. To study the stability of IBR3, 2 µg of each vector was used for the transfections, and after 16 hours incubation in the dark at room temperature, cycloheximide

(CHX) and MG132 were added to a final concentration of 50 μM and further incubated in the dark for the indicated times, followed by lysis as previously described.

The details of the proximity labelling experiment can be found in the Supporting Information.

SDS-PAGE and Western blot

For the SDS-PAGE analysis, the samples were mixed with SDS-DTT sample buffer and heated at 95°C for 5 minutes. Proteins were separated on SDS-PAGE or AnyKD (Bio-Rad) gels with Laemmli running buffer, then transferred to Immobilon®-FL low fluorescence PVDF membrane (Merck Millipore). The Dunn carbonate buffer system (Dunn, 1986) was used for protein transfer at 30 V for 16 hours at 4 °C. The Odyssey CLx Imager (LI-COR Biosciences) was used with automatic intensity settings for two-colours detection of FLAG-tagged and His-tagged proteins, Single detection of GST-, 3xHA-, and 9xMyc-tagged proteins and Revert 700 Total Protein Stain were carried out by following the manufacturer's detection protocols. The list of antibodies used are provided in Supporting Information Table S3.

RESULTS

The DNA damage response (DDR) gene, *LIFERING,* is regulated both by the RETINOBLASTOMA-RELATED and the ATM/ATR-SOG1 pathways

The elevated expression of *LIFERING* upon RBR silencing was shown by micro-array analysis (Horvath *et al.*, 2017). To corroborate these data, we followed its expression by qRT-PCR both in *rRBr* root-tips where *RBR* is silenced in the root meristem (Fig. 1a), and in *amiRBR* seedlings where the post-embryonic RBR levels are reduced constitutively using the *35S* promoter (Fig. 1b). The results obtained were in accordance with the microarray data, indicating that the transcriptional level of *LIFERING* was significantly higher in both *rRBr* and *amiRBR* lines. As *LIFERING* is co-expressed with *AtBRCA1* (Horvath *et al.*, 2017), a gene known to be an essential component of DDR and homologous recombination, we compared the expressional changes of *LIFERING* and *AtBRCA1* and found a significantly higher level of induction of LIFERING than of *AtBRCA1* (Fig. 1a and b).

To address whether RBR regulates *LIFERING* gene expression in conjunction with E2FA, we quantified its expression and found that it was elevated in both *e2fa-1* and *e2fa-2* mutants, but at a lower level than in *amiRBR* (Fig. 1b). The de-repression of *LIFERING* in the homozygous double mutant lines, *amiRBR;e2fa-1* and *amiRBR;e2fa-2* did not exceed the de-repression detected in *amiRBR* (Fig. 1b). These results suggest that RBR acts partly through E2FA in a co-repressor complex to regulate *LIFERING* expression.

The presence of the canonical E2F binding sites within a 1kb region from the translational start site (Fig. 1c, ATG) further suggested that RBR may regulate *LIFERING* expression through E2F proteins. To confirm whether RBR indeed directly regulates *LIFERING* expression, chromatin immunoprecipitation (ChIP)-PCR assays were carried out on root tissues using an RBR-antibody (Horvath *et al.*, 2006). Significant enrichment of RBR was detected in distinct

regions of the *LIFERING* promoter. The enrichment on fragment 1 (Fig. 1c) was comparable to that detected on the *PCNA1* promoter, (Fig. 1d). A slightly lower level of enrichment was also observed in the neighbouring region (fragment 2), likely to be due to the heterogeneous size of sonicated fragments in the range of 300 to 500 bp.

To investigate the regulation of *LIFERING* expression upon DNA damage, *Arabidopsis thaliana* Col-0 seedlings were treated with the DNA damage agent, mitomycin C (MMC) and the induction of *LIFERING* transcription was analysed using qRT-PCR. Upon MMC treatment, *LIFERING* expression was significantly higher than that of *AtBRCA1* (16h, 10μg ml^{-1}, Fig. 2a), consistent with the difference observed in mRNA levels of the same genes upon RBR silencing. To assess whether *LIFERING* induction depends on the activity of the ATM/ATR kinases, we inhibited the ATM/ATR driven pathways with specific chemicals developed to block the activity of these kinases (IATM, KU55933 and IATR, VE-821) and previously shown to be effective in plants (Horvath *et al.*, 2017). While *AtBRCA1* expression was equally reduced by both the ATM and ATR inhibitors, *LIFERING* expression was more sensitive to the inhibition of ATR. The simultaneous inhibition of the ATM and ATR kinases almost completely abolished the expression of both *LIFERING* and *AtBRCA1* (Fig. 2b).

As SOG1 regulates DDR gene expression upon DNA damage, we tested the expression of *LIFERING* in the *sog1-1* mutant after MMC treatment. Comparing the relative expression of *LIFERING* with and without genotoxic agent in the *sog1-1* mutant, we detected 1.5-2 times higher relative gene expression of *LIFERING* than *AtBRCA1* (16h, 10μg ml^{-1}, Fig. 2c). This indicates that the SOG1-independent induction is stronger in the case of *LIFERING* than *AtBRCA1*.

Lastly, we tested whether the regulation of *LIFERING* expression upon *RBR* silencing is independent of SOG1 function. To this end, we followed its transcript level in the double

amiRBR,sog1-1 and the single mutants as controls. In the *sog1-1* mutant, the level of *LIFERING* expression was only partially reduced in the *amiRBR* background, suggesting that the SOG1 and RBR control *LFR* expression independently (Fig. 2d).

Role of LIFERING in cell death vs cell differentiation upon DNA damage

To investigate the role of LIFERING in DDR, first, we studied the phenotypic changes of the *lifering-1* mutant (SM_3_34488) upon genotoxic stress. For this, we studied whether the mutation in the 2nd exon leads to full knock-out of the relevant transcript by RT-PCR. Indeed, no induction of the *LIFERING* transcript was detected in the mutant either in the presence or absence of MMC in the mutant compared to the control (MMC, 16h, 10µg ml^{-1}, Fig. S1a and b).

Under normal growth conditions, root development and growth of the *lifering-1* mutant was comparable to the wild-type (Fig. S1c and d). No difference was detected either in the structure of the root or in the organisation of the meristem (Fig. 3a and Fig. S1e). To be able to establish its role in the cellular processes upon DDR, first we followed the cell death response in the mutants, *lifering-1, Atbrca1-3* and Col-0 roots, in 5-6 days-old seedlings (das) upon MMC treatment (14-16h, 10µg ml^{-1}). As shown in Fig. 3, the cell death response was significantly weaker in the *lifering-1* mutant, compared to Col-0 and *Atbrca1-3*, both in the proximal and distal root meristems (Fig. 3a-c). It is important to note that high proportion of *lifering-1* seedlings did not display any cell death response. To verify this response, we counted the number of the roots with zero, one or more than one dead cell in the stem cell niche. Only 15% of the studied seedlings developed cell death in more than one cell in the *lifering-1* SCN compared to the 61% of Col-0 (Table S4). To provide evidence that this phenotype is

exclusively linked to the mutation in *LIFERING*, we complemented the mutant with the LIFERING-GFP construct, in which the genomic region of *LIFERING* was fused to GFP and expressed under its own promoter (pgLIFERING-GFP). In the three independent transformants, both the transcriptional and cell death responses were comparable to those of Col-0 upon MMC treatment (Fig. S2a-c). The fluorescence signal was detected only after inducing DNA damage, predominantly in the cytoplasm and was located along the entire meristem (Fig. S2d).

Enhanced endoreplication followed by terminal differentiation is a further response to genotoxic stress protects genome integrity. To determine whether LIFERING also involved in these processes, we measured the distance between the QC and the boundary of the transition between the zones of the transit amplifying cells and elongation in the *lifering-1* mutant and compared to Col-0. As Fig. 3a illustrates, upon MMC treatment in *lifering-1*, the root meristem size is reduced compared to Col-0 and the *Atbrca1-3* mutant (Fig. 3a), suggesting that LIFERING has a role in maintaining cell proliferation and preventing early exit to cell elongation upon genotoxic stress. Treatment with genotoxic agent also led to root hair differentiation closer to the root-tip in the *lifering-1* than in Col-0, further supporting this notion.

In conclusion, due to the lack of LIFERING function, the balance between multiple DNA damage responses is shifted. Reduced cell death response is compensated for, by faster exit from cell cycle and premature cell differentiation.

LIFERING acts downstream of RBR to maintain cell proliferation

Since LIFERING is directly repressed by RBR, we hypothesised that LIFERING is required for cell death induction and over-proliferation when *RBR* expression is silenced. To investigate

this, we focused on a well-characterised phenotype of cell death and over-proliferation in the distal stem and daughter cells of the root tip (Fig. 4).

To this end, we introgressed the *lifering-1* mutant into *amiRBR* and studied the double homozygous descendants of two independent crosses verified by genotyping, the presence of GFP fluorescence, a readout for *RBR* silencing (Fig 4a) and by the lack of *LIFERING* expression upon MMC treatment (Fig. S3).

To quantify cell death response, we counted the number of dead cells in the distal stem cell niche and daughter cells (CSC and LRC) at various stages of root growth. Both cell death and over-proliferation of stem cells progressively accumulated over time. Correspondingly, at 5 das, the number of dead cells was comparable between the *amiRBR* and *amiRBR;lifering-1* lines, however, at later time points, the number of cells with cell death response started to stagnate and became significantly fewer in the *amiRBR;lifering-1* lines compared to *amiRBR* (Fig. 4a and b). The observed suppression became even more apparent at 13 das, when the cell death was limited to only few cells in the distal stem cell niche (Fig. 4b).

Similar to the suppression of cell death, the excess number of columella cell layers and disorganization of the stem cell area that progressively evolved during the period of 5 to 13 das in the *amiRBR* were also repressed in the *amiRBR;lifering-1* lines (Fig. 4c).

Based on these data, we concluded that LIFERING functions downstream of RBR both for the initiation of cell death and for maintaining cell proliferation.

LIFERING is a plant-specific E3-ubiquitin ligase

To understand how LIFERING regulates cell proliferation and cell death, we investigated its biochemical activity. LIFERING is annotated as a putative E3 ubiquitin ligase. Our systematic

comparisons to known E3 ligases revealed that LIFERING shows protein sequence homology and structural similarity to the cluster of RING-between-RING (RBR) family of E3 ubiquitin ligases. It contains a conserved three-domain module comprising RING1, BRcat (benign-catalytic) and Rcat (required-for-catalysis), along with an N-terminal reverse transcriptase-like domain (Fig. 5a) (Marin, 2010; Spratt *et al.*, 2014). Accordingly, it has been suggested that LIFERING (At5g60250) belongs to the Plant II family of RING-between-RING class of E3 ubiquitin ligases (Marin, 2010).

Associated with the At5g60250 genomic region, two different protein variants, Q9LSS2 and Q681M6 has been deposited in the UniProt database, having the genomic sequence-based and the transcript-derived amino acid sequences, respectively. The two protein variants show six amino acids differences at the N-terminal region, and deviate also at position 392 where the transcript-derived amino acid sequence codes arginine instead of the default cysteine (Fig. S4). Using AlphaFold computational protein structure prediction combined with the AlphaFill algorithm (Fig. 5b), we assumed that the cysteine at position 392, along with cysteines at positions 387, 420, and 423, are part of one of the two zinc-binding sites of the BRcat domain and are liable to engage in zinc-binding (Fig. 5c) (Jumper *et al.*, 2021; Varadi *et al.*, 2022; Hekkelman *et al.*, 2023). To investigate the importance of this cysteine, we performed a multiple sequence alignment of this zinc-binding region in the BRcat domain of LIFERING with the two most widely studied human RING-between-RING (RBR) E3 ligases, Parkin and HHARI. We identified that Cys392 in LIFERING corresponds to the Cys281 of HHARI and Cys337 of Parkin (Fig. 5d) both of which are involved in coordination of zinc binding.

To study whether the LIFERING is a functional ubiquitin ligase, we cloned the *LIFERING* cDNA using the RIKEN clone (RAFL22-04-P06) into an *in vitro* translation vector fused with a 12xHis-tagged LIFERING. Subsequent sequencing of the coding sequence showed that the

original cDNA clone and the newly constructed *in vitro* translation vector coding the 12xHis-LIFERING contained arginine at position 392 of the protein instead of cysteine. To convert arginine to cysteine, we performed an *in vitro* mutagenesis (*C*GC to *T*GC) and termed this variant the wild-type LIFERING.

To investigate the predicted ubiquitin ligase activity of LIFERING, we produced both the wild-type and mutant C392R LIFERING variants using a wheat germ-based *in vitro* translation system supplemented with zinc. We assessed their ubiquitin ligase activity through *in vitro* protein ubiquitination assays. To this end, we supplemented the crude translation mixtures with FLAG-tagged ubiquitin (FLAG-Ub), while the control reaction was performed without ubiquitin. To detect the expression of the two LIFERING variants and the ubiquitination status, a polyhistidine-, and a FLAG-specific antibodies, respectively, were used in Western blot analysis (Fig. 5e). Although the wild-type and the C392R LIFERING proteins were detected in equal amounts in both the FLAG-Ub supplemented and control reactions, we observed a significantly higher level of ubiquitination in the protein extracts containing the wild-type protein compared to the mutant variant (Fig. 5e, lanes 3 and 4).
From these results we conclude that LIFERING exhibits ubiquitin ligase activity, which is critically dependent on the presence of Cys at position 392.

To investigate whether LIFERING undergoes autoubiquitination, we isolated both the wild-type and the mutant 12xHis-labelled LIFERING proteins from the ubiquitination reaction mixture (Fig. 5e, lanes 3 and 4) using immobilized metal affinity chromatography (IMAC) and performed an additional Western blot analysis using anti-FLAG antibodies. As Fig. 5e shows, we detected a ladder-like pattern of ubiquitination exclusively in the presence of the wild-type LIFERING. The proteins bound to the IMAC beads were further analysed using mass

spectrometry to reveal the position of the ubiquitinated amino acids. As a result of this analysis, isopeptide-linked ubiquitins were detected at Lys112 and Lys414 exclusively in the samples containing the wild-type LIFERING variant (Fig. S5), indicating that LIFERING can undergo autoubiquitination in the wheat germ-based *in vitro* translation system.

LIFERING ubiquitinates IBR3, the enzyme involved in the indole-3-acetic acid synthesis

To understand LIFERING's function, we set out to identify its target substrates for ubiquitination. We leveraged the TurboID-based biotin proximity labelling technique (Branon *et al.*, 2018). The wild-type and mutant LIFERING proteins were cloned in CaMV 35S promoter-driven vectors coding for TurboID at the N-terminal of the fusion proteins and *Arabidopsis* root cell suspension-derived protoplasts were transfected with these constructs. Using streptavidin-coated magnetic beads, the biotinylated proteins were isolated and subsequently identified by protein mass spectrometry. The spectral count data from numerous independently performed experiments with wild-type and mutant samples were analysed using SAINTexpress software (Teo *et al.*, 2014). Among the numerous potential targets, the acyl-CoA dehydrogenase IBR3 (At3g06810) was repeatedly identified as an interactor with both wild-type and mutant LIFERING proteins (FoldChange >100, Table S5) relative to the control runs with TurboID alone.

To validate the proximity labelling results, first we generated the GST-IBR3 fusion protein through *in vitro* translation, then we investigated in an *in vitro* ubiquitination assay the functional interaction between LIFERING and IBR3. The ubiquitination reactions were carried out with the crude translation mixtures containing wild-type or mutant 12xHis-LIFERING in the presence of GST-tagged IBR3 bound to the glutathione beads. The results of the pull-down

assay were analysed by Western blotting using different antibodies. Through application of polyHis-specific antibody, we found that both the wild-type and mutant LIFERING could interact with IBR3, and using FLAG- and GST-specific antibodies, we observed ubiquitination of the glutathione bound IBR3 exclusively by the wild-type LIFERING (Fig. 6a). The position of ubiquitination of IBR3 by LIFERING was also determined through mass spectrometry. Analysis of the bead-bound IBR3 treated either by the wild-type or mutant LIFERING corroborated the results obtained by Western blot. Four lysine residues of IBR3 (Lys170, 213, 311, and 536) were identified as ubiquitinated amino acids in the wild-type LIFERING containing sample. In contrast, no ubiquitination was detected in the reaction mixture containing the mutant C392R LIFERING (Fig. S6).

To determine whether LIFERING can also catalyse the ubiquitination of IBR3 *in vivo*, we co-transfected protoplasts derived from *Arabidopsis thaliana* root cell suspensions with different combinations of C-terminal Myc-tagged wild-type and mutant LIFERING variants and HA-tagged IBR3-encoding vectors. Immunoblot analysis of the protein extracts revealed that both the Myc- and HA-specific antibodies decorated the overexpressed proteins, confirming the production of the proteins of interest. A ladder-like pattern of IBR3 was also clearly visible when co-transfected with the wild-type LIFERING and using anti-HA antibody. Furthermore, the wild-type LIFERING also exhibited a ladder-like pattern not detected with the mutant variant by using the anti-Myc antibody (Fig. 6b). These *in vivo* observations were in line with the *in vitro* results, implying that only the wild-type Cys392-containing LIFERING is capable of autoubiquitination and the ubiquitination of IBR3.

Ubiquitination of proteins can lead to different outcomes, i.e. mono- and multi/mono-ubiquitination can often regulate protein activity and localisation, whereas polyubiquitination is conventionally regarded as a signal for proteasomal degradation. To study whether

ubiquitination of IBR3 by LIFERING results in its hydrolysis in the proteasome, we transfected the protoplasts with IBR3-encoding vector alone and with wild-type LIFERING-encoding vector together. After overnight incubation in the dark, the cells were treated with cycloheximide (CHX) and MG132 to block *de novo* protein synthesis and proteasomal activity, respectively. According to the Western blot analysis, IBR3 is a highly stable protein, with only a negligible difference in its protein levels detected even after 24 hours incubation in the presence of CHX. The combined addition of CHX and MG132 had no discernible effect on the protein amounts detected either (Fig. S6). The same phenomenon was observed with the co-transfected protoplast-derived samples. While the sign of ubiquitination, the ladder-like pattern of IBR3 was present, there was only an insignificant decrease in its level (Fig. S6). Our findings suggest that the ubiquitination of IBR3 by LIFERING may serve a distinct, yet to be identified function rather than proteasomal degradation.

DISCUSSION

The importance of RING domain proteins in plants is highlighted by their genomic over-representation compared to other eukaryotes (Kosarev *et al.*, 2002). Here, we show that LIFERING, a member of this protein family known to be rapidly upregulated upon many stress signals and is a catalytically active E3 ubiquitin ligase that ubiquitinates IBR3, the acyl-CoA dehydrogenase-like protein.

Structurally, LIFERING has a RING1-BRcat-Rcat signature and has been assigned to the Plant II subfamily of RING-between-RING-type E3 ubiquitin ligases (Marin, 2010). In addition to *in silico* analysis, we also performed biochemical experiments and demonstrated that LIFERING is an active ubiquitin ligase; its activity depends on the presence of zinc ions and Cys392 which corresponds to one of the zinc coordinating cysteines of Parkin, the human RBR type E3 ligase, one of the closest mammalian homologues of LIFERING. Previous research demonstrated that the biological activity of Parkin is altered by mutation of zinc-binding cysteines (Beasley *et al.*, 2007), which is in alignment with our observation.

LIFERING has an essential function to maintain genome stability *in planta*. It is a universal DNA damage and stress response gene; highly induced independently of whether the damage is caused by exogenous genotoxic agents or endogenous stresses due to mutations in genes involved in DNA replication and repair and their regulation, irrespective of the nature of the damage in the DNA structure. A genome-wide study to identify direct targets of SOG1 in response to γ-radiation also uncovered LIFERING as a target (Bourbousse *et al.*, 2018). Here we show that upstream to SOG1, LIFERING expression is regulated by ATM/ATR signalling. Independently and parallel to this, it is directly repressed by RBR, partly through E2FA.

As a response to DNA damage, besides induction of gene expression, cells mitigate the effects of dividing with damaged DNA by inhibition of cell cycle and induction of cell death.

LIFERING has a role in triggering both processes. It is essential to induce cell death response both upon exo- and endogenous DNA damage.

The so-far identified E3 ligases involved in DDR either play a role in the recognition of the damage site and/or its repair or in the regulation of cell cycle progression (Herbst *et al.*, 2024), and structurally do not belong to the RING1-BRcat-Rcat class of E3 ubiquitin ligases.
The limited data available on the members (22) of the largest Plant II subfamily of *Arabidopsis thaliana* RING-between-RING-type ligases suggest that they are mainly involved in phytohormone mediated regulation of stress responses (Wang *et al.*, 2020). RING FINGER OF SEED LONGEVITY1 (RSL1) (Bueso *et al.*, 2014a; Bueso *et al.*, 2014b), RING Finger ABA-Related1 (RFA1), and RFA4 (Fernandez *et al.*, 2020) target ABA receptors for degradation via proteasomal or vacuolar pathways. Similar to the members of PlantII subfamily, the ARIADNE12 (AtARI12) belongs to the Ariadne subfamily of plant RING-between-RING ubiquitin ligases (Mladek *et al.*, 2003) and is also stress responsive. Its expression is strongly up-regulated by UV-B irradiation and depends on the activity of the E3 ligase *CONSTITUTIVELY PHOTOMORPHOGENIC1 (COP1*), in both white and UV-B light (Xie *et al.*, 2015). As the increase of *AtARI12* mRNA levels did not correlate with the abundance of AtARI12 protein levels, moreover, using proteasome inhibitor MG132 had no effect on its stability, the authors proposed that AtARI12 protein levels are unlikely to be regulated by proteasome-mediated degradation (Xie *et al.*, 2015).

In searching for putative substrates of LIFERING, we found that it readily ubiquitinates the acyl-CoA dehydrogenase-like protein, IBR3, an enzyme involved in the conversion of IBA to indole-3-acetic acid IAA. IBR3 was ubiquitinated both *in vitro* and in the protoplast transient overexpression system, visualised by the characteristic ladder-like pattern of the protein with

different molecular weight. Furthermore, the ubiquitinated lysines of IBR3 protein were identified through mass spectrometry. The ubiquitin code can modify protein function in different ways. While K48-linked polyubiquitin chains mainly target proteins for proteasomal degradation, proteasome-independent processes are usually mediated by non-K48-linked ubiquitin chains affecting their stability, activity, interactions with other proteins and their subcellular localisation. In plants, the K63-linked chains are identified as the second most abundant modification and proposed to play proteasome-independent roles in hormonal responses and development, nutritional responses, biotic interactions and DNA repair and autophagy targeting (Romero-Barrios & Vert, 2018; Orosa-Puente & Spoel, 2022). Despite the application of proteosome and protein synthesis inhibitors (MG132 and CHX), no significant change in the IBR3 protein level could be detected, suggesting that ubiquitination of IBR3 by LIFERING likely has a different biological function than proteasomal degradation.

The conversion of IBA to IAA is a multistep enzymatic reaction during which the auxin precursor IBA undergoes peroxisomal oxidation to release free IAA (Damodaran & Strader, 2019). The conversion plays an essential role in the spatial determination of the auxin level, and thus controls a distinct set of plant developmental and growth effects (Strader *et al.*, 2011). It also provides a local auxin source in the root cap (Xuan *et al.*, 2015), while along the root axis, the IBA-derived auxin is responsible, on the one hand, for setting the local auxin level to position lateral root formation (Xuan *et al.*, 2015) and, on the other hand, in co-operation with cytokinin, for the formation of adventitious root (Damodaran & Strader, 2024).

In the root tip, IBR3 is localized to the lateral root cap; mostly to the lateral - and columella root cap cells, but also in the QC, dividing and young meristem cells, albeit at a lower level. In the differentiation zone, its expression was identified in the stele cells including the pericycle (Xuan et al., 2015; Ryu, KH et al., 2019). Importantly, the expression of IBR3 overlaps with that of LIFERING in the lateral - and columella root cap cells and the dividing meristematic

cells, albeit on a significantly lower level in non-genotoxic conditions (Ryu, KH et al., 2019). In the triple IBA response mutants, *ibr1,ibr3,ibr10,* the overall IAA level is unchanged (Strader *et al.*, 2010), while in the quadruple mutant, *ech2*,*ibr1,ibr3 ibr10*, the free auxin level is reduced with 20-25% in the root tip. As expected from the local auxin levels, the quadruple mutant develops a significantly shorter meristem (Strader *et al.*, 2011), and an overall reduced root system with fewer number of lateral roots (Xuan *et al.*, 2015). However, despite the morphological changes, no spontaneously developed cell death response was reported related to any of these mutants in normal growth conditions (Strader *et al.*, 2011).

How can we integrate our data in the existing knowledge on the connection between DNA damage response and hormonal regulation?

Root growth is dependent on the balance of the hormones, cytokinin and auxin (Salvi *et al.*, 2020). Upon DNA damage, however, the balance between cytokinin and auxin levels shifts. Through SOG1, DNA damage induces cytokinin synthesis and activates its signalling around the transition zone, thereby inhibiting downward auxin flow. With the reduction in auxin level, the position of auxin minima changes towards the stem cell niche, resulting in the G2 arrest of the dividing cells. Independent of G2 arrest, reduced auxin signalling also leads to stem cell death. In parallel, increased cytokinin signalling triggers early onset of endoreduplication. The combined effects of G2 arrest, early transition from division to endoreduplication and stem cell death, reduce meristematic activity and thus inhibit root growth to safeguard genome integrity (Davis *et al.*, 2016; Takahashi *et al.*, 2021). The fact that, in the absence of functional LIFERING, there was no or significantly reduced cell death in the root meristem, either upon treatment with genotoxic agent or in silencing of RBR, especially in the stem cell niche, we

suggest that LIFERING plays a role in setting the auxin level in the stem cell niche. Furthermore, closer endoreduplication in the meristem also indicates a shift in hormone balance.

Both the suppression of auxin signalling and auxin levels are prerequisites to the prompt local development of cell death response in the root meristem to protect genome integrity (Takahashi *et al.*, 2021). Upon DNA damage, the otherwise lowly expressed *IAA5* and *IAA29* genes, coding for the transcriptional repressors of auxin signalling, are directly induced by SOG1 in the vascular stem cells and daughters. This way, they can locally reduce the auxin response and ensure cell death upon damage in the stem cell niche and surrounding vascular cell layer. In contrast, in the double mutant *iaa5-1, iaa29-1*, due to lack of suppression of the local auxin level signalling, spatial reduction of the cell death response was detected in the apical meristem when challenged with DNA damage agent (Takahashi *et al.*, 2022). Similar to the *iaa5-1,iaa29-1*, the mutant line, *lifering-1* develops no or substantially weakened cell death response upon DNA damage and thus has significantly reduced number of dead cells in both the apical and distal meristems with no or only one dead cell either in the distal and/or in the vascular stem cell niche compared to the Col-0.

In line with the overlapping localisation of LIFERING and IBR3 and considering that LIFERING targets IBR3 for ubiquitination and consequently potentially inactivates it by an-as-yet-unknown mechanism, we propose that under normal growth conditions, in the absence of LIFERING in the root, the IBA to IAA conversion supplies auxin to support growth along the root meristem. In contrast, under stress, when *LIFERING* is rapidly induced, it attenuates the auxin supply, thereby leading to growth arrest and early differentiation. By setting the

balance between cell proliferation and differentiation, LIFERING through auxin signalling also regulates cell death response upon DNA damage.

In conclusion, we propose a working model according to which we suggest that by adjusting the level of free auxin available in the root meristem, LIFERING initiates a cell death response to prevent further division with damaged DNA and to fine-tune the auxin level in the QC and the surrounding area. Further experimentation should provide evidence to prove this model.

ACKNOWLEDGEMENT

We thank Hana Kourová and Pavla Binarová (Czech Academy of Sciences, Czech Republic) for their valuable advice during the experimentation. We thank Christian W.B. Bachem (Solynta, The Netherlands) for critically reading the manuscript.

AUTHORS CONTRIBUTIONS

B.M.H., L.B., B.M.K. and T.M. conceived and designed the original research plan. B.M.H., E.N., F.N., and Z.A. carried out the expressional, phenotypic and microscopical studies on the mutant and the complementation lines. B.M.K. and T.M. designed and carried out the *in vitro* translation, protoplast transient expression, pull-down and immuno-blotting assays, B.M.K. performed the ubiquitination assays, the Turbo-ID proximity labelling and generated the vector constructs essential for the above experiments. B.M.K. provided material for and A.P-Sz. carried out mass spectrometry analysis of proximity labelling derived samples. A.P-Sz. and B.M.K. evaluated the MS data. Z.M. and L.B. shared material and discussed the experiments and data. The manuscript was written by B.M.H., B.M.K, and T.M., it was read and commented by all the authors.

FUNDING SOURCES

B.M.H. was funded by a Marie-Curie IEF fellowship (FP7-PEOPLE-2012-IEF 330789), while B.M.K and T.M. by the TKP2021-EGA-24 grant of the Ministry of Innovation and Technology of Hungary from the National Research, Development and Innovation Fund. B.M.K. received funding from the National Scholarship for Young Talents NTP-NFTÖ-21-B-0075. Z.M., F.N. and E.N. were funded by the Hungarian National Research Funding (NKFI-139202) and with Campus Hungary, TÁMOP-4.2.4B/2-11/1-2012-0001 fellowship, respectively. L.B. was

supported by the BBSRC-NSF grant (BB/M025047/1) and A.P-Sz. by EU Horizon 2020 grant No. 739593; KIM NKFIA 2022-2.1.1-NL-2022-00005

CONFLICT OF INTEREST

The authors declare that they have no conflict of interest.

REFERENCES

Adachi S, Minamisawa K, Okushima Y, Inagaki S, Yoshiyama K, Kondou Y, Kaminuma E, Kawashima M, Toyoda T, Matsui M, et al. 2011. Programmed induction of endoreduplication by DNA double-strand breaks in Arabidopsis. *Proc Natl Acad Sci U S A* **108**(24): 10004-10009.

Bardoczy V, Geczi V, Sawasaki T, Endo Y, Meszaros T. 2008. A set of ligation-independent in vitro translation vectors for eukaryotic protein production. *BMC Biotechnol* **8**: 32.

Beasley SA, Hristova VA, Shaw GS. 2007. Structure of the Parkin in-between-ring domain provides insights for E3-ligase dysfunction in autosomal recessive Parkinson's disease. *Proc Natl Acad Sci U S A* **104**(9): 3095-3100.

Berckmans B, Vassileva V, Schmid SP, Maes S, Parizot B, Naramoto S, Magyar Z, Alvim Kamei CL, Koncz C, Bogre L, et al. 2011. Auxin-dependent cell cycle reactivation through transcriptional regulation of Arabidopsis E2Fa by lateral organ boundary proteins. *Plant Cell* **23**(10): 3671-3683.

Biedermann S, Harashima H, Chen P, Heese M, Bouyer D, Sofroni K, Schnittger A. 2017. The retinoblastoma homolog RBR1 mediates localization of the repair protein RAD51 to DNA lesions in Arabidopsis. *EMBO J* **36**(9): 1279-1297.

Blilou I, Xu J, Wildwater M, Willemsen V, Paponov I, Friml J, Heidstra R, Aida M, Palme K, Scheres B. 2005. The PIN auxin efflux facilitator network controls growth and patterning in Arabidopsis roots. *Nature* **433**(7021): 39-44.

Bourbousse C, Vegesna N, Law JA. 2018. SOG1 activator and MYB3R repressors regulate a complex DNA damage network in Arabidopsis. *Proc Natl Acad Sci U S A* **115**(52): E12453-E12462.

Branon TC, Bosch JA, Sanchez AD, Udeshi ND, Svinkina T, Carr SA, Feldman JL, Perrimon N, Ting AY. 2018. Efficient proximity labeling in living cells and organisms with TurboID. *Nat Biotechnol* **36**(9): 880-887.

Bueso E, Ibanez C, Sayas E, Munoz-Bertomeu J, Gonzalez-Guzman M, Rodriguez PL, Serrano R. 2014a. A forward genetic approach in Arabidopsis thaliana identifies a RING-type ubiquitin ligase as a novel determinant of seed longevity. *Plant Sci* **215-216**: 110-116.

Bueso E, Rodriguez L, Lorenzo-Orts L, Gonzalez-Guzman M, Sayas E, Munoz-Bertomeu J, Ibanez C, Serrano R, Rodriguez PL. 2014b. The single-subunit RING-type E3 ubiquitin ligase RSL1 targets PYL4 and PYR1 ABA receptors in plasma membrane to modulate abscisic acid signaling. *Plant J* **80**(6): 1057-1071.

Chen P, De Winne N, De Jaeger G, Ito M, Heese M, Schnittger A. 2023. KNO1-mediated autophagic degradation of the Bloom syndrome complex component RMI1 promotes homologous recombination. *EMBO J* **42**(10): e111980.

Chen P, Sjogren CA, Larsen PB, Schnittger A. 2019. A multi-level response to DNA damage induced by aluminium. *Plant J* **98**(3): 479-491.

Clay DE, Fox DT. 2021. DNA Damage Responses during the Cell Cycle: Insights from Model Organisms and Beyond. *Genes (Basel)* **12**(12).

Cools T, Iantcheva A, Maes S, Van den Daele H, De Veylder L. 2010. A replication stress-induced synchronization method for Arabidopsis thaliana root meristems. *Plant J* **64**(4): 705-714.

Cruz-Ramirez A, Diaz-Trivino S, Blilou I, Grieneisen VA, Sozzani R, Zamioudis C, Miskolczi P, Nieuwland J, Benjamins R, Dhonukshe P, et al. 2012. A bistable circuit involving SCARECROW-RETINOBLASTOMA integrates cues to inform asymmetric stem cell division. *Cell* **150**(5): 1002-1015.

Culligan KM, Robertson CE, Foreman J, Doerner P, Britt AB. 2006. ATR and ATM play both distinct and additive roles in response to ionizing radiation. *Plant J* **48**(6): 947-961.

Damodaran S, Strader LC. 2019. Indole 3-Butyric Acid Metabolism and Transport in Arabidopsis thaliana. *Front Plant Sci* **10**: 851.

Damodaran S, Strader LC. 2024. Factors governing cellular reprogramming competence in Arabidopsis adventitious root formation. *Dev Cell*.

Davis OM, Ogita N, Inagaki S, Takahashi N, Umeda M. 2016. DNA damage inhibits lateral root formation by up-regulating cytokinin biosynthesis genes in Arabidopsis thaliana. *Genes Cells* **21**(11): 1195-1208.

Dunn SD. 1986. Effects of the modification of transfer buffer composition and the renaturation of proteins in gels on the recognition of proteins on Western blots by monoclonal antibodies. *Anal Biochem* **157**(1): 144-153.

Fernandez MA, Belda-Palazon B, Julian J, Coego A, Lozano-Juste J, Inigo S, Rodriguez L, Bueso E, Goossens A, Rodriguez PL. 2020. RBR-Type E3 Ligases and the Ubiquitin-Conjugating Enzyme UBC26 Regulate Abscisic Acid Receptor Levels and Signaling. *Plant Physiol* **182**(4): 1723-1742.

Furukawa T, Curtis MJ, Tominey CM, Duong YH, Wilcox BW, Aggoune D, Hays JB, Britt AB. 2010. A shared DNA-damage-response pathway for induction of stem-cell death by UVB and by gamma irradiation. *DNA Repair (Amst)* **9**(9): 940-948.

Gombos M, Raynaud C, Nomoto Y, Molnar E, Brik-Chaouche R, Takatsuka H, Zaki A, Bernula D, Latrasse D, Mineta K, et al. 2023. The canonical E2Fs together with RETINOBLASTOMA-RELATED are required to establish quiescence during plant development. *Commun Biol* **6**(1): 903.

Harashima H, Sugimoto K. 2016. Integration of developmental and environmental signals into cell proliferation and differentiation through RETINOBLASTOMA-RELATED 1. *Curr Opin Plant Biol* **29**: 95-103.

Hekkelman ML, de Vries I, Joosten RP, Perrakis A. 2023. AlphaFill: enriching AlphaFold models with ligands and cofactors. *Nat Methods* **20**(2): 205-213.

Herbst J, Li QQ, De Veylder L. 2024. Mechanistic insights into DNA damage recognition and checkpoint control in plants. *Nat Plants* **10**(4): 539-550.

Horvath BM, Kourova H, Nagy S, Nemeth E, Magyar Z, Papdi C, Ahmad Z, Sanchez-Perez GF, Perilli S, Blilou I, et al. 2017. Arabidopsis RETINOBLASTOMA RELATED directly regulates DNA damage responses through functions beyond cell cycle control. *EMBO J* **36**(9): 1261-1278.

Jumper J, Evans R, Pritzel A, Green T, Figurnov M, Ronneberger O, Tunyasuvunakool K, Bates R, Zidek A, Potapenko A, et al. 2021. Highly accurate protein structure prediction with AlphaFold. *Nature* **596**(7873): 583-589.

Kosarev P, Mayer KF, Hardtke CS. 2002. Evaluation and classification of RING-finger domains encoded by the Arabidopsis genome. *Genome Biol* **3**(4): RESEARCH0016.

Laible M, Boonrod K. 2009. Homemade site directed mutagenesis of whole plasmids. *J Vis Exp*(27).

Lang L, Pettko-Szandtner A, Tuncay Elbasi H, Takatsuka H, Nomoto Y, Zaki A, Dorokhov S, De Jaeger G, Eeckhout D, Ito M, et al. 2021. The DREAM complex represses growth in response to DNA damage in Arabidopsis. *Life Sci Alliance* **4**(12).

Lang L, Schnittger A. 2020. Endoreplication - a means to an end in cell growth and stress response. *Curr Opin Plant Biol* **54**: 85-92.

LaRocque JR, McVey M. 2023. DNA Damage Response Mechanisms in Model Systems. *Genes (Basel)* **14**(7).

Lee DJ, Park JY, Ku SJ, Ha YM, Kim S, Kim MD, Oh MH, Kim J. 2007. Genome-wide expression profiling of ARABIDOPSIS RESPONSE REGULATOR 7(ARR7) overexpression in cytokinin response. *Mol Genet Genomics* **277**(2): 115-137.

Marin I. 2010. Diversification and Specialization of Plant RBR Ubiquitin Ligases. *PLoS One* **5**(7): e11579.

Mathur J, Koncz C. 1998. Establishment and maintenance of cell suspension cultures. *Methods Mol Biol* **82**: 27-30.

Mladek C, Guger K, Hauser MT. 2003. Identification and characterization of the ARIADNE gene family in Arabidopsis. A group of putative E3 ligases. *Plant Physiol* **131**(1): 27-40.

Nagy SK, Kallai BM, Andras J, Meszaros T. 2020. A novel family of expression vectors with multiple affinity tags for wheat germ cell-free protein expression. *BMC Biotechnol* **20**(1): 17.

Nemeth K, Salchert K, Putnoky P, Bhalerao R, Koncz-Kalman Z, Stankovic-Stangeland B, Bako L, Mathur J, Okresz L, Stabel S, et al. 1998. Pleiotropic control of glucose and hormone responses by PRL1, a nuclear WD protein, in Arabidopsis. *Genes Dev* **12**(19): 3059-3073.

Nisa MU, Huang Y, Benhamed M, Raynaud C. 2019. The Plant DNA Damage Response: Signaling Pathways Leading to Growth Inhibition and Putative Role in Response to Stress Conditions. *Front Plant Sci* **10**: 653.

Ogita N, Okushima Y, Tokizawa M, Yamamoto YY, Tanaka M, Seki M, Makita Y, Matsui M, Okamoto-Yoshiyama K, Sakamoto T, et al. 2018. Identifying the target genes of SUPPRESSOR OF GAMMA RESPONSE 1, a master transcription factor controlling DNA damage response in Arabidopsis. *Plant J* **94**(3): 439-453.

Orosa-Puente B, Spoel SH. 2022. Harnessing the ubiquitin code to respond to environmental cues. *Essays Biochem* **66**(2): 111-121.

Pedroza-Garcia JA, Xiang Y, De Veylder L. 2022. Cell cycle checkpoint control in response to DNA damage by environmental stresses. *Plant J* **109**(3): 490-507.

Raina A, Sahu PK, Laskar RA, Rajora N, Sao R, Khan S, Ganai RA. 2021. Mechanisms of Genome Maintenance in Plants: Playing It Safe With Breaks and Bumps. *Front Genet* **12**: 675686.

Reidt W, Wurz R, Wanieck K, Chu HH, Puchta H. 2006. A homologue of the breast cancer-associated gene BARD1 is involved in DNA repair in plants. *EMBO J* **25**(18): 4326-4337.

Romero-Barrios N, Vert G. 2018. Proteasome-independent functions of lysine-63 polyubiquitination in plants. *New Phytol* **217**(3): 995-1011.

Salvi E, Rutten JP, Di Mambro R, Polverari L, Licursi V, Negri R, Dello Ioio R, Sabatini S, Ten Tusscher K. 2020. A Self-Organized PLT/Auxin/ARR-B Network Controls the Dynamics of Root Zonation Development in Arabidopsis thaliana. *Dev Cell* **53**(4): 431-443 e423.

Schonrock N, Exner V, Probst A, Gruissem W, Hennig L. 2006. Functional genomic analysis of CAF-1 mutants in Arabidopsis thaliana. *J Biol Chem* **281**(14): 9560-9568.

Sjogren CA, Bolaris SC, Larsen PB. 2015. Aluminum-Dependent Terminal Differentiation of the Arabidopsis Root Tip Is Mediated through an ATR-, ALT2-, and SOG1-Regulated Transcriptional Response. *Plant Cell* **27**(9): 2501-2515.

Spratt DE, Walden H, Shaw GS. 2014. RBR E3 ubiquitin ligases: new structures, new insights, new questions. *Biochem J* **458**(3): 421-437.

Strader LC, Culler AH, Cohen JD, Bartel B. 2010. Conversion of endogenous indole-3-butyric acid to indole-3-acetic acid drives cell expansion in Arabidopsis seedlings. *Plant Physiol* **153**(4): 1577-1586.

Strader LC, Wheeler DL, Christensen SE, Berens JC, Cohen JD, Rampey RA, Bartel B. 2011. Multiple facets of Arabidopsis seedling development require indole-3-butyric acid-derived auxin. *Plant Cell* **23**(3): 984-999.

Su S, Zhang Y, Liu P. 2020. Roles of ubiquitination and SUMOylation in DNA damage response. *Current issues in molecular biology* **35**(1): 59-84.

Szurman-Zubrzycka M, Jedrzejek P, Szarejko I. 2023. How Do Plants Cope with DNA Damage? A Concise Review on the DDR Pathway in Plants. *Int J Mol Sci* **24**(3).

Takahashi H, Nozawa A, Seki M, Shinozaki K, Endo Y, Sawasaki T. 2009. A simple and high-sensitivity method for analysis of ubiquitination and polyubiquitination based on wheat cell-free protein synthesis. *BMC Plant Biol* **9**: 39.

Takahashi N, Inagaki S, Nishimura K, Sakakibara H, Antoniadi I, Karady M, Ljung K, Umeda M. 2021. Alterations in hormonal signals spatially coordinate distinct responses to DNA double-strand breaks in Arabidopsis roots. *Sci Adv* **7**(25).

Takahashi N, Ogita N, Koike T, Nishimura K, Inagaki S, Umeda M. 2022. Local induction of IAA5 and IAA29 promotes DNA damage-triggered stem cell death in Arabidopsis roots. *bioRxiv*: 2022.2009. 2002.506394.

Teo G, Liu G, Zhang J, Nesvizhskii AI, Gingras AC, Choi H. 2014. SAINTexpress: improvements and additional features in Significance Analysis of INTeractome software. *J Proteomics* **100**: 37-43.

Varadi M, Anyango S, Deshpande M, Nair S, Natassia C, Yordanova G, Yuan D, Stroe O, Wood G, Laydon A, et al. 2022. AlphaFold Protein Structure Database: massively expanding the structural coverage of protein-sequence space with high-accuracy models. *Nucleic Acids Res* **50**(D1): D439-D444.

M, Li X, Luo S, Fan B, Zhu C, Chen Z. 2020. Coordination and crosstalk between autophagosome and multivesicular body pathways in plant stress responses. *Cells* **9**(1): 119.

Xie L, Lang-Mladek C, Richter J, Nigam N, Hauser MT. 2015. UV-B induction of the E3 ligase ARIADNE12 depends on CONSTITUTIVELY PHOTOMORPHOGENIC 1. *Plant Physiol Biochem* **93**: 18-28.

Xuan W, Audenaert D, Parizot B, Moller BK, Njo MF, De Rybel B, De Rop G, Van Isterdael G, Mahonen AP, Vanneste S, Beeckman T. 2015. Root Cap-Derived Auxin Pre-patterns the Longitudinal Axis of the Arabidopsis Root. *Curr Biol* **25**(10): 1381-1388.

Yi D, Alvim Kamei CL, Cools T, Vanderauwera S, Takahashi N, Okushima Y, Eekhout T, Yoshiyama KO, Larkin J, Van den Daele H, et al. 2014. The Arabidopsis SIAMESE-RELATED cyclin-dependent kinase inhibitors SMR5 and SMR7 regulate the DNA damage checkpoint in response to reactive oxygen species. *Plant Cell* **26**(1): 296-309.

Yoo SD, Cho YH, Sheen J. 2007. Arabidopsis mesophyll protoplasts: a versatile cell system for transient gene expression analysis. *Nat Protoc* **2**(7): 1565-1572.

Yoshiyama K, Conklin PA, Huefner ND, Britt AB. 2009. Suppressor of gamma response 1 (SOG1) encodes a putative transcription factor governing multiple responses to DNA damage. *Proc Natl Acad Sci U S A* **106**(31): 12843-12848.

Yoshiyama KO, Kobayashi J, Ogita N, Ueda M, Kimura S, Maki H, Umeda M. 2013a. ATM-mediated phosphorylation of SOG1 is essential for the DNA damage response in Arabidopsis. *EMBO Rep* **14**(9): 817-822.

Yoshiyama KO, Sakaguchi K, Kimura S. 2013b. DNA damage response in plants: conserved and variable response compared to animals. *Biology (Basel)* **2**(4): 1338-1356.

Yu C, Hou L, Huang Y, Cui X, Xu S, Wang L, Yan S. 2023. The multi-BRCT domain protein DDRM2 promotes the recruitment of RAD51 to DNA damage sites to facilitate homologous recombination. *New Phytol* **238**(3): 1073-1084.

SUPPORTING INFORMATION

Supporting Information on Materials and Methods with References

Supporting Table S1: List of primers used for expressional studies *in planta.*

Supporting Table S2: Primers and vectors used for *in vitro* translation and transient protein expression experiments.

Supporting Table S3: List of antibodies used in this study.

Supporting Table S4: Ratio of the roots with different number of dead cells.

Supporting Table S5: Analysis of mass spectrometry spectral count data from TurboID proximity labelling experiments using SAINTexpress software (v3.6).

Supporting Figure S1: Expressional and phenotypic analysis of the *lifering-1* mutant.

Supporting Figure S2: Complementation of the *lifering-1* mutant

Supporting Figure S3: *LIFERING* expression in the double *amiRBR;lifering-1* mutant

Supporting Figure S4: Amino acid sequence alignment of UniProt Q9LSS2 and Q681M6

Supporting Figure S5: Mass spectrometry analysis of LIFERING (At5g60250) ubiqitination

Supporting Figure S6: Mass spectrometry analysis of IBR3's (At3g06810) ubiqitination

Supporting Figure S7: Effect of cycloheximide (CHX) and MG132 on the AtIBR3 protein level in *Arabidopsis* root cell suspension protoplasts

Supporting Information on Materials and Methods

Cloning

The N-terminal 3xHA-TurboID-tagging pRT-3xHA-Turbo-LIC vector was created by replacing AtMPK9 in the pRT-HA-AtMPK9 vector (Nagy *et al.*, 2015) with the 3xHA-TurboID coding sequence. Because the LIC cassette must contain unique *Ssp*I restriction site, the one found in the ampicillin resistance gene promoter of the original vector was removed through in

vitro mutagenesis (Liable & Boonrod, 2009). Subsequently, AtMPK9 insert was removed by digestion with *Nco*I and *Bam*HI. A template containing the coding sequence for 3xHA-TurboID was provided in a pMA-RQ vector. 3xHA-TurboID was amplified by PCR with primers coding for the *Ssp*I-harbouring ligation-independent cloning (LIC) cassette (Bardóczy *et al*, 2008) and inserted into the pRT-HA vector between the *Nco*I and *Bam*HI restriction sites.

To produce FLAG-tagged ubiquitin, the coding sequence of the ubiquitin monomer was optimized for wheat germ codons and checked for *E. coli* incompatible codons. The obtained sequence was chemically synthesized with LIC-compatible overhangs by Integrated DNA Technologies. Ubiquitin was amplified by PCR and inserted into the wheat-germ in vitro translation compatible pEU3-NII-FLAGLICNot vector (Nagy *et al*, 2020) using LIC. To produce larger amount of ubiquitin using the bacterial protein expression system, the FLAG-ubiquitin coding DNA was amplified by PCR from the pEU3-NII-FLAGLICNot_Ubiquitin vector described above and subcloned into the pET28a vector using *Nco*I and *Nde*I restriction endonucleases.

Bacterial FLAG-ubiquitin expression

FLAG-ubiquitin (FLAG-Ub) was expressed in BL21(DE3) competent *E. coli* cells (New England BioLabs) via autoinduction as previously described (Studier, 2005). A positive colony was inoculated into MDG non-inducing medium with 50 µg/ml kanamycin. After 5 hours of growth at 37°C, the starter culture was used to inoculate ZYM-5052 autoinducing medium with 50 µg/ml kanamycin at a 1:400 dilution and grown overnight at 37°C. The bacterial culture was centrifuged at 4000 rpm, 4°C for 20 minutes, and the resulting pellet was resuspended in 1/5–1/6 volume of extraction buffer (300 mM NaCl, 10 mM imidazole, 0.1% Triton-X) relative to the original culture volume. The resuspended cells were sonicated for 5 cycles of 30 seconds each (30s on, 30 s off. The cell lysate was then centrifuged at 13000 rpm and 4°C for 20 minutes.

The resulting supernatant was heated in 500 µl aliquots at 85°C for 5 minutes and chilled on ice. Following centrifugation at 13000 rpm for 10 minutes at 4°C, the soluble fraction of FLAG-Ub was purified using the flow-through from a 30K MWCO Amicon centrifugal filter (EMD Millipore) and concentrated with a 3K MWCO Amicon centrifugal filter (EMD Millipore). The concentration and purity of FLAG-Ub were determined by Tricine-SDS-PAGE (Haider *et al*, 2012) and densitometry analysis (data not shown). The concentration of the FLAG-Ub stock solution was adjusted to 200 µM, and aliquots were stored at -20°C.

Transient protein expression and proximity labelling

The Columbia (Col-0) *Arabidopsis thaliana* root-cell suspension culture was maintained according to Mathur and Koncz (Mathur & Koncz, 1998). Protoplast isolation and PEG-mediated protoplast transfection were conducted as previously described with slight modifications (Yoo *et al.*, 2007). To transfect $2x10^5$–$5x10^5$ protoplasts, 1 µg of HA-TurboID and HA-TurboID-LIFERING (wild-type and C392R) coding pRT plasmid DNAs were used. The transfected cells were cultured in 24-well plates for 16 hours in the dark at room temperature. Through empirical testing we identified the optimal biotin concentration and incubation time of biotin labelling as 50 µM and 3–4 hours, respectively (data not shown). Proximity labelling was then carried out by adding d-biotin at a final concentration of 50 µM, zeocin at a final concentration of 0.05 µg/µl, when indicated, and incubating for 4 hours in the dark at room temperature. For each sample, $2x10^6$ cells were harvested and lysed using a modified ice-cold RIPA buffer (50 mM Tris-HCl pH 7.8, 150 mM NaCl, 1% IGEPAL® CA-630, 0.5% sodium deoxycholate, 0.1% SDS, 1X protease inhibitor cocktail, 15 mM EGTA, 1 mM DTT, 1 mM NaF, 0.5 mM activated Na_3VO_4, 0.5 mM β-glycerophosphate, 1X PhosStop, 50 µM MG132) and incubation in an ultrasonic bath for 2 minutes. The extracts were centrifuged at 13000 rpm, 4°C for 15 minutes and the supernatants were desalted with 7K

MWCO Zeba™ Spin Desalting Column to remove free biotin and analysed by mass spectrometry.

Mass spectrometry sample preparation and analysis

In case of TurboID experiments, the biotinylated proteins were purified from the cleared extracts by using µMACS™ Streptavidin beads (Milteny Biotec). They were then digested in column with trypsin and analysed in a single run by mass spectrometry. The digestion mixtures were acidified and transferred to a single-use trapping mini-column (Evotip; 1/8 of the samples) and then analysed with a data-dependent LC-MS/MS method using an Evosep One (LC: 15 SPD; MS1: R:120,000) on-line coupled to a linear ion trap-Orbitrap (Orbitrap-Fusion Lumos, Thermo Fisher Scientific) mass spectrometer operating in positive ion mode. Data acquisition was carried out in data-dependent fashion, multiply charged ions were selected in cycle-time from each MS survey scan for ion-trap HCD fragmentation (MS spectra were acquired in the Orbitrap (R=60000) while MSMS in the ion-trap). The raw data was converted into peak lists using Proteome Discoverer (v1.4) and searched against the Uniprot Arabidopsis thaliana database (downloaded on 12 June 2019, containing 89,461 proteins) using our in-cloud Protein Prospector search engine (v5.15.1). Spectral counting was employed to estimate the relative abundance of individual proteins and were analysed by SAINTexpress (version 3.6; https://saint-apms.sourceforge.net/Main.html) using default parameters.

For the mass spectrometry analysis of in vitro ubiquitinated LIFERING and IBR3, 1/20 of the bead-bound protein samples were used for Gel-aided sample preparation (GASP) (Fischer & Kessler, 2015). The remaining LIFERING samples were concentrated using a 10kDa Amicon Ultra-0.5 Centrifugal Filter Unit and then mixed with 0.5 ml of Lysis Buffer (Miltenyi Biotec). They were then immunopurified using anti-FLAG antibody-coupled magnetic beads (MACS® Technology, Miltenyi Biotec, d=50 nm), digested in a column with trypsin, and analysed in a

single run by mass spectrometry (Kobayashi *et al*, 2015, Hubner *et al*, 2010, Jankovics *et al*, 2018). The digestion mixtures were acidified and transferred to a single-use trapping mini-column (Evotip; 1/8 of the samples). Subsequently, they were analysed using a data-dependent LC-MS/MS method. The LC-MS/MS method was performed using an Evosep One (LC: 15 SPD; MS1: R :120,000) on-line coupled to a linear ion trap-Orbitrap (Orbitrap-Fusion Lumos, Thermo Fisher Scientific) mass spectrometer operating in positive ion mode. Data acquisition was performed in a data-dependent manner. Multiply charged ions were selected in cycle-time from each MS survey scan for ion-trap HCD fragmentation. MS spectra were acquired in the Orbitrap (R=60000), while MSMS was acquired in the ion-trap. The raw data was converted into peak lists using the in-house Proteome Discoverer (v 1.4). The peak lists were then searched against the Uniprot WHEAT and Arabidopsis thaliana database, as well as 6 user-defined proteins (downloaded on 20th July 2022, containing 280426 proteins), using our in-cloud Protein Prospector search engine (v5.15.1). with the following parameters: enzyme: trypsin with maximum 2 missed cleavage; mass accuracies: 5 ppm for precursor ions and 0.6 Da for fragment ions (both monoisotopic); fixed modification: carbamidomethylation of Cys residues; variable modifications: acetylation of protein N-termini; Met oxidation; cyclization of N-terminal Gln residues, GlyGly (Uncleaved K), LeuArgGlyGly (Uncleaved K), Phospho (STY) allowing maximum 2 variable modifications per peptide. Acceptance criteria: minimum scores: 22 and 15; maximum E values: 0.01 and 0.05 for protein and peptide identifications, respectively.

Supporting Information References

Bardóczy, V., Géczi, V., Sawasaki, T., Endo, Y., & Mészáros, T. (2008). A set of ligation-independent in vitro translation vectors for eukaryotic protein production. *BMC biotechnology*, *8*(1), 1-7.

Branon, T. C., Bosch, J. A., Sanchez, A. D., Udeshi, N. D., Svinkina, T., Carr, S. A., ... & Ting, A. Y. (2018). Efficient proximity labeling in living cells and organisms with TurboID. *Nature biotechnology*, *36*(9), 880-887.

Fischer, R., & Kessler, B. M. (2015). Gel-aided sample preparation (GASP)—A simplified method for gel-assisted proteomic sample generation from protein extracts and intact cells. *Proteomics*, *15*(7), 1224-1229.

Haider, S. R., Reid, H. J., & Sharp, B. L. (2012). Tricine-sds-page. *Protein electrophoresis: methods and protocols*, 81-91.

Hubner, N. C., Bird, A. W., Cox, J., Splettstoesser, B., Bandilla, P., Poser, I., ... & Mann, M. (2010). Quantitative proteomics combined with BAC TransgeneOmics reveals in vivo protein interactions. *Journal of Cell Biology*, *189*(4), 739-754.

Jankovics, F., Bence, M., Sinka, R., Faragó, A., Bodai, L., Pettkó-Szandtner, A., ... & Erdélyi, M. (2018). Drosophila small ovary gene is required for transposon silencing and heterochromatin organization, and ensures germline stem cell maintenance and differentiation. *Development*, *145*(23), dev170639.

Kobayashi, K., Suzuki, T., Iwata, E., Nakamichi, N., Suzuki, T., Chen, P., ... & Ito, M. (2015). Transcriptional repression by MYB 3R proteins regulates plant organ growth. *The EMBO journal*, *34*(15), 1992-2007.

Laible, M., & Boonrod, K. (2009). Homemade site directed mutagenesis of whole plasmids. *JoVE (Journal of Visualized Experiments)*, (27), e1135.

Mathur, J., & Koncz, C. (1998). Establishment and maintenance of cell suspension cultures. *Arabidopsis Protocols*, 27-30.

Nagy, S. K., Darula, Z., Kállai, B. M., Bogre, L., Bánhegyi, G., Medzihradszky, F., ... & Mészáros, T. (2015). Activation of AtMPK9 through autophosphorylation that makes it independent of the canonical MAPK cascades.

Nagy, S. K., Kállai, B. M., András, J., & Mészáros, T. (2020). A novel family of expression vectors with multiple affinity tags for wheat germ cell-free protein expression. *BMC biotechnology*, *20*, 1-9.

Németh, K., Salchert, K., Putnoky, P., Bhalerao, R., Koncz-Kálmán, Z., Stankovic-Stangeland, B., ... & Koncz, C. (1998). Pleiotropic control of glucose and hormone responses by PRL1, a nuclear WD protein, in Arabidopsis. *Genes & development*, *12*(19), 3059-3073.

Studier, F. W. (2005). Protein production by auto-induction in high-density shaking cultures. *Protein expression and purification*, *41*(1), 207-234.

Yoo, Sang-Dong, Young-Hee Cho, and Jen Sheen. Arabidopsis mesophyll protoplasts: a versatile cell system for transient gene expression analysis. *Nature protocols* 2.7 (2007): 1565-1572.

Supporting Tables

Table S1: List of primers used for *in planta* expressional studies

Gene / primer name	Accession no. / sequence
A. qRT-PCR	
At3g18780	**ACTIN2**
qActinF	cgctgaccgtatgagcaaag
qActinR	ttcatgctgcttggtgcaa
At3g12280	**RETINOBLASTOMA-RELATED**
qRBRF2	ataataagcctgaaggtcaatgtc
qRBRR2	taaacattgtgcactgcagatact
At5g60250	**LIFERING**
qLIFERING F1	attgtacttgccggattca
qLIFERING R1	cagaagtgaggatagtcaggatgg
qLIFERING C-term	tttcacgaacccttttccatc
qLIFERING C-term	agcaaaagggtttggacctt
At2g21070	**BREAST CANCER ASSOCIATED-1**
qBRCA1F2	tcatgggagatttcgagctt
qBRCA1R2	atttagccaaggcttcagca
B. Chromatin immunoprecipitation	
At5g60250	**LIFERING**
LIFERING F1	aaacagcgtcgttttcagcta
LIFERING R1	tctgtttcggattttgtgtatga
LIFERING F2	atgacgttggtacccccttcc
LIFERING R2	cgcagagcttaaatcagcaa
LIFERING F3	gggtttggttagcgatgaga
LIFERING R3	gtcctcggatcaatgaatta
At1g07370	**PCNA1**
PCNA4F	aatgaccaaaaatatccatccaa
PCNA4R	cggctattttggaaagtgga
IR	**At3g03660-70**
IR1F	cattgaacacctattggtaggaa
IR1R	actgttttggtgccagattttcag
C. RT-PCR	
At2g37620	**ACTIN1**
ActinF	ggcgatgaagctcaatccaaa
ActinR	ggtcacgaccagcaagatcaag
At5g60250	**LIFERING**
LIFERING F1-RT	gattgtggctacgtgtggtg
LIFERING R1-RT	gtcctcggatcaatgcctta
D. Genotyping	
mutant/primer	
lifering-1	**At5g60250**
lifering-1 RP	ctaaagcaaaaggcaaaaccc
lifering-1 LP	aacataccctcagcaacgatg
SPM31	gcttgttgaaccgacacttttaacataag

SPM32 tacgaataagagcgtccattttagagtga

E. Cloning of LIFERING promoter and gene

pLIFERING F aaaacagcgtcgttttcagc
pLIFERING R *(cat)* acttgctctccgcagagctt
gLIFERING F atg gat ttc gat tcc gag tat gct
gLIFERING R *(tca)* gaa gtg agg ata gtc agg

Table S2: Primers and vectors used for *in vitro* translation and transient protein expression experiments

Primer name	Sequence (5'-3')
SspImut_forward	cctgataaatgcttcaataa**c**attgaaaaaggaag
SspImut_reverse	cttccttttcaat**g**ttattgaagcatttatcagg
NcoI-HA-Turbo_forward	ataccATGGCTAGTATGTACCCTTACGACG
Turbo_LIC_BamHI_reverse	tatggatcctgTTATCCACTTCCAATATTGGATTGGAAGTACGCCTTCTC AGCTGATCTAAGGC
XbaI-LIC-SmaI (SPY)_forward	gctctagagtacttccaatccaatattggaagtggataactcccggggcc
XbaI-LIC-SmaI (SPY)_reverse	ggccccgggagttatccacttccaatattggattggaagtactctagagc
LIFERINGmutC392_forward	CTGCCCTTACCCGAGG**TGC**TCGGCTTTGATGTCC
LIFERINGmutC392_reverse	GGACATCAAAGCCGA**GCA**CCTCGGGTAAGGGCAG
LIFERING_LIC_forward	tacttccaatccaatgcaATGGATTTCGATTCCGAGTATGCT
LIFERING_LIC_reverse	ttatccacttccaatgTCAGAAGTGAGGATAGTCAGGATG
LFR_LIC_reverse (noSTOP)	ttatccacttccaatgGAAGTGAGGATAGTCAGGATG
IBR3_LIC_forward	tacttccaatccaatgcaATGGGAAGCAGCACGGGCGATCT
IBR3_LIC_reverse	ttatccacttccaatgTCAGAGTTTTGAAGCTCTTTGCAGTTCTAAC
IBR3_LIC_reverse(noSTOP)	ttatccacttccaatgGAGTTTTGAAGCTCTTTGCAGTTCTAAC
LIC_forward (for FLAG-Ub)	tacttccaatccaatgca
LIC_reverse (for FLAG-Ub)	ttatccacttccaatgCTA
pET28a_NcoI_pEU3FLAG_forward	catgccATGGATTATAAGGACGACG
pET28a_NdeI_UbSTOP_reverse	ggaattccatatgTTAGCCGCCGCGGAG

Lowercase letters: non-coding sequences and LIC overhangs
Capital letters: gene-specific sequences
Bold and underlined: bases modified by in vitro mutagenesis
Underlined: restriction sites
Indented: START and STOP codons

Vector name	Description	Reference	Insert*	Expected MW
pEU3-NII-HxHLICNot	For in vitro translation of N-terminal 12xHis tagged proteins	Nagy *et al*, 2020	LIFERING (wt) LIFERING_C392R (mut)	77.9 kDa
pEU3-NII-GLICNot	For in vitro translation of N-terminal GST tagged proteins	Nagy *et al*, 2020	IBR3	117.7 kDa
pEU3-NII-FLAGLICNot	For in vitro translation of N-terminal 12xHis tagged proteins	Nagy *et al*, 2020	Ubiquitin	Not used in this work
pET28a_FLAG-Ub	For bacterial expression of N-terminal FLAG tagged ubiquitin	This work	Ubiquitin	10.7 kDa
pRT-3xHA-TurboID-LIC	For transient expression of N-terminal HA-TurboID tagged proteins under 35S promoter	This work	LIFERING (wt) LIFERING_C392R (mut)	112.7 kDa
pRT-3xHA	For transient expression of C-terminal 3xHA-tagged proteins under 35S promoter	Nagy *et al.*, 2015	IBR3	96.3 kDa
pRT-9xMyc	For transient expression of C-terminal 9xMyc-tagged proteins under 35S promoter	Nagy *et al.*, 2015	LIFERING (wt) LIFERING_C392R (mut)	88.6 kDa

*The insert-containing vectors were generated in this work.

Table S3: Antibodies used in this study

Antibody	Clone	Dilution	Source
Mouse anti-polyHistidine	HIS-1	1:2000	Sigma
Rabbit anti-GST	06-332	1:2000	Upstate, Merck KGaA
Rabbit anti-FLAG	F7425	1:1000	Sigma
Mouse anti-HA	HA-7	1:1000	Sigma
Mouse anti-c-Myc	9E10	1:1000	Roche
IRDye® 800CW goat anti-mouse	N/A	1:20000	LI-COR Biosciences
IRDye® 680RD goat anti-rabbit	N/A	1:20000	LI-COR Biosciences

Table S4: Summary of the roots with different number of dead cells

Table S4 summarises the number of roots with zero, one or more than one dead cells				
	total. number	roots with number of dead cells		
		n=0	n=1	n>1
Col-0	107	22	19	65
lifering-1	106	38	52	16
	ratio in (%)	n=0	n=1	n>1
		21%	18%	61%
		36%	49%	15%

Table S5: Analysis of mass spectrometry spectral count data from TurboID proximity labelling experiments using SAINTexpress software (v3.6)

Provided as separate file after the Supporting Figures.

Figure 1

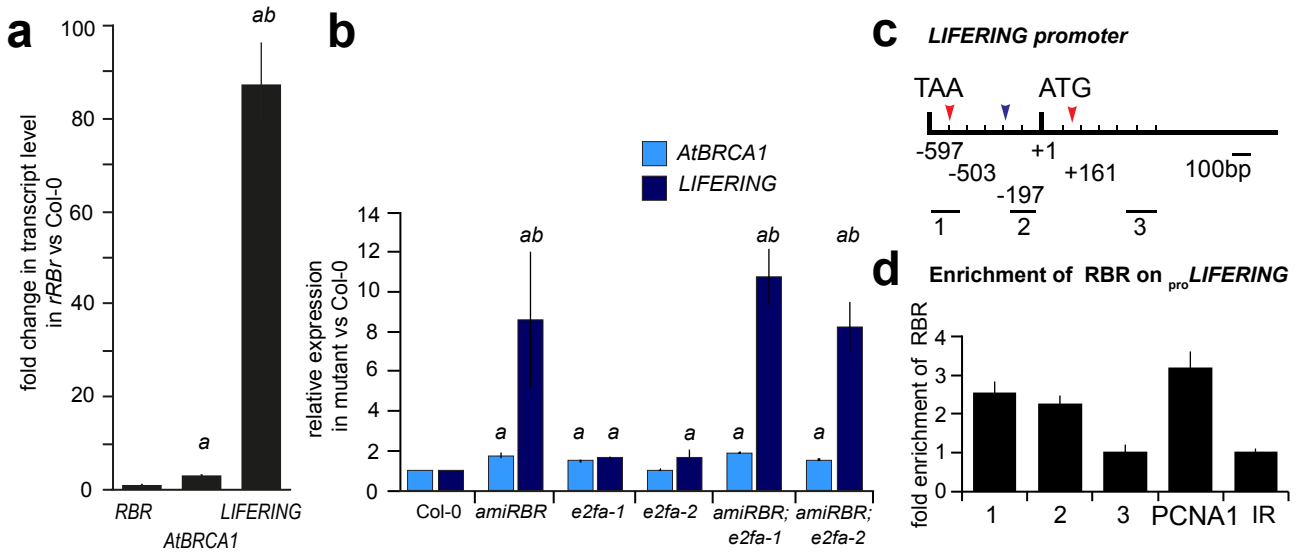

Figure 1. The expression of *LIFERING* is regulated by RBR through E2FA

(a) Bar chart shows the gene expression of *LIFERING* (At5g60250) compared to *RBR* and *AtBRCA1* expression determined by qRT-PCR. RNA was isolated from root-tips of 4-day old *rBRr* and Col-0 seedlings. Gene expression is given as the ratio between *rRBr* and Col-0. Fold change is given as *AtBRCA1* gene expression = 1.
(b) Relative transcript level of *LIFERING* and *AtBRCA1* as a control, upon *RBR* silencing in *amiRBR* and in the single: *e2fa-1, e2fa-2* and double mutants compared to Col-0, where the level of expression was set to 1 for both genes.
(c) Schematic representation of the *LIFERING* promoter. The positions of the following elements are indicated: start codon (ATG; +1), stop codon of the neighboring transcript (TAA; -597), putative E2F elements (red arrow-heads; -503:taggcccgcgaattt and +161:cggcgaaaa) and SOG1 binding site (black arrow; -197-169) as suggested by Bourbousse *et al* (2018). Black horizontal lines (1, 2, 3) indicate the position and length of the amplified regions in the qPCR analysis,
(d) Chromatin-Immuno Precipitation (ChIP) using RBR antibody; the chart shows fold enrichment calculated as a ratio of chromatin bound to the numbered sections of the promoter in (**c**) with or without antibody. The *PCNA1* promoter was used as a positive control, while IR (an intergenic region between At3g03360-70) as a negative control. Note that the enrichment of RBR on the *LIFERING* and *PCNA1* promoters are comparable.

Data information:
In (**a-c**): *a*: p<0.05 significance of the *AtBRCA1* expression in the mutant compared to Col-0 and *ab*: p<0.001 significance of the *LIFERING* expression in the mutant compared to Col-0 and to *AtBRCA1* calculated by the Student's *t*-test. Error bar: +/- StDev, *n*=3, *N*>100.

Figure 2

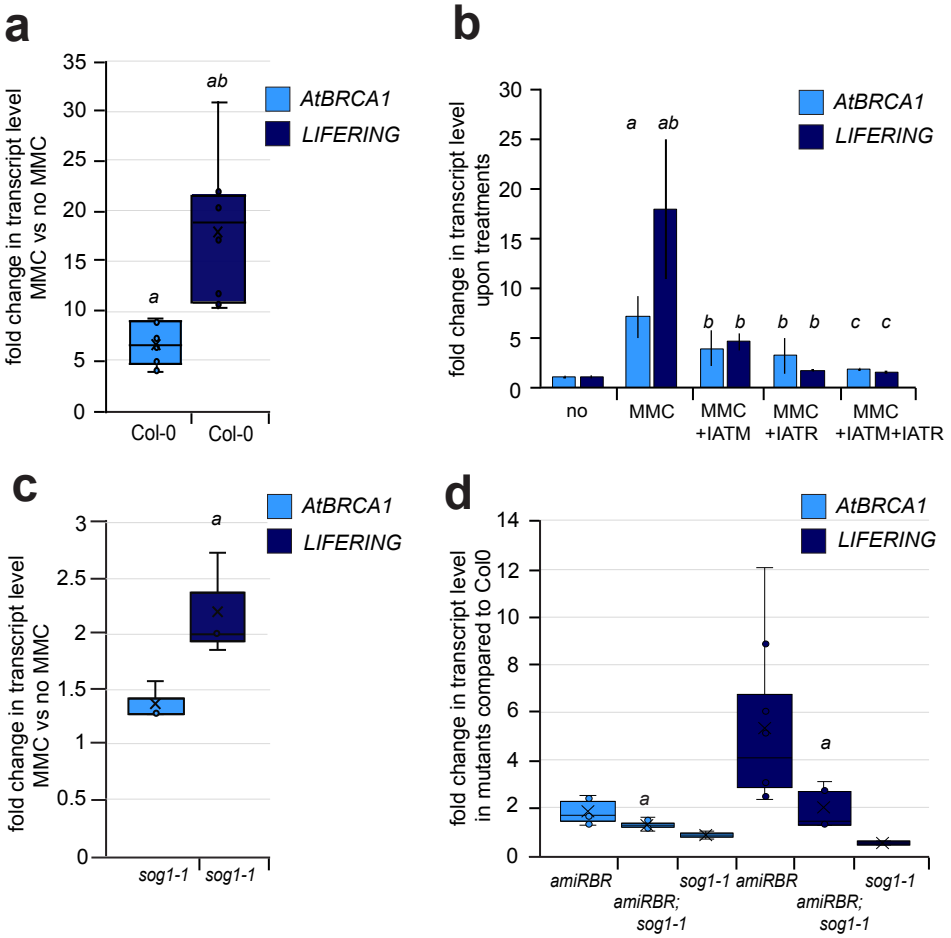

Figure 2. *LIFERING* expression is independently regulated by ATM/ATR-SOG1 and RBR pathways

(**a**) Chart of relative gene expression of *LIFERING* upon MMC (10μg ml^{-1}) treatment for 16h.The qRT-PCR was carried out on Col-0 seedlings. Relative expression of *AtBRCA1* is shown as a comparison. The values represent fold changes normalised to the values of the relevant genes in non-treated samples. *a*: p<0.01 significance compared to the non-treated control, *ab*:p<0.01 significance *LIFERING* to the non-treated control and of *AtBRCA1* transcript levels..
(**b**) Effect of the ATM and ATR inhibitors (IATM and IATR, respectively) on the induction of *LIFERING* expression upon DNA damage (16h, 10μg ml^{-1} MMC). Relative transcript levels of *LIFERING* and *AtBRCA1* as a control, were calculated comparing the expression levels to the non-treated sample which was set to 1. *a*: p<0.05 significance between MMC and no-MMC treated samples, *b*: p<0.05 significant difference upon applying inhibitors individually and *c*: p<0.05 upon applying both inhibitors.
(**c**) Chart of the relative expression of *LIFERING* in the *sog1-1* mutant upon MMC and non-MMC treatment (16h, 10μg ml^{-1}) in comparison to *AtBRCA1* expression. The values represent fold changes normalised to the values of the relevant gene in non-treated samples where the expression was set to 1. *a*: p<0.05 significant difference compared to the non-treated control.
(**d**) Effect of *sog1-1* mutation in the *amiRBR* background (*amiRBR;sog1-1*) both on *LIFERING* and *AtBRCA1* expression. Relative transcript levels were calculated comparing the expression levels to the relevant transcripts in Col-0 seedlings, in which the values were set to 1. *a*: p<0.05 significant difference in the double mutant compared to both single mutants.

Data information:
In (**a**-**d**), experiments were carried out on 5-6 das seedlings, *n*>3, *N*>100. Significance was calculated by the Student's *t*-test, error bars: +/- StDev.

Figure 3

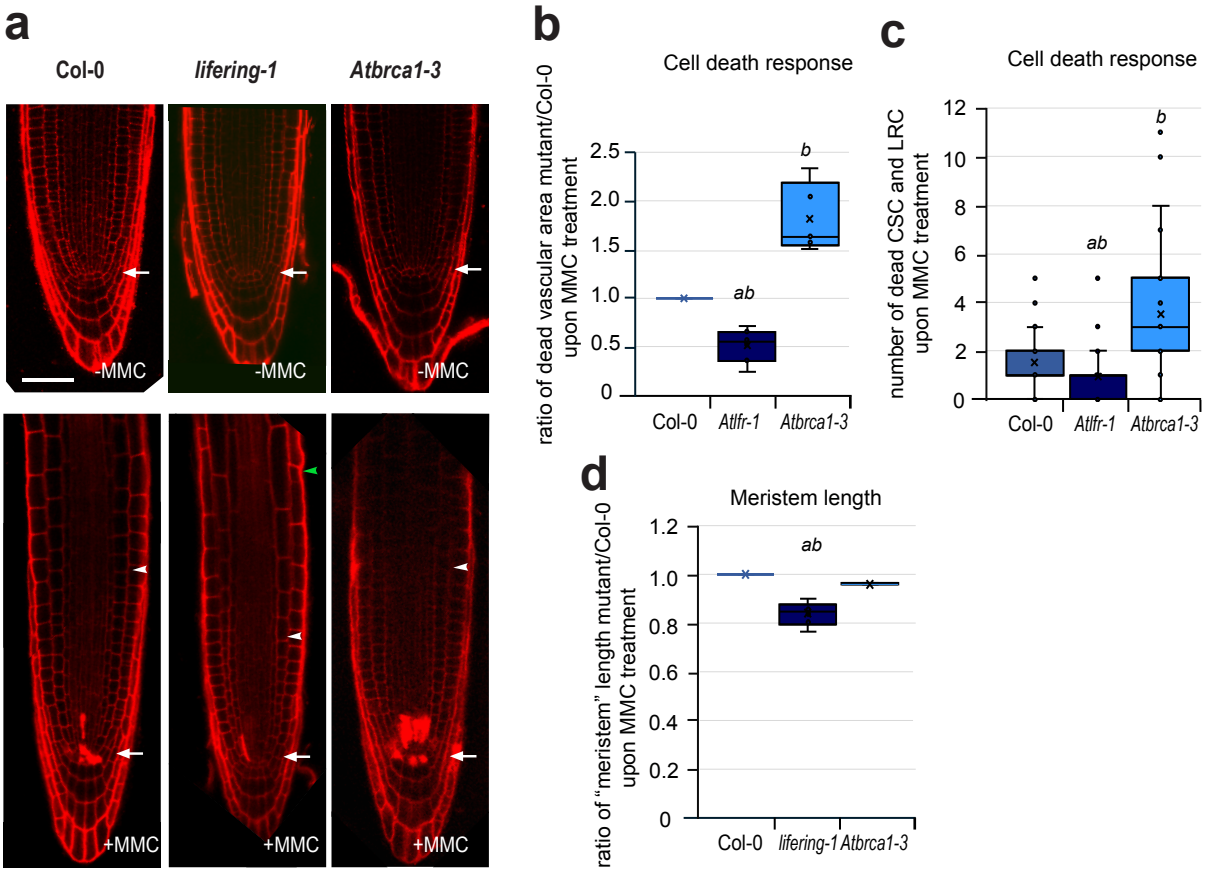

Figure 3. LIFERING is involved in DNA damage response upon genotoxic stress

(**a**) Representative confocal microscopy (CM) images of propidium-iodide (PI)-stained root-tips of Col-0, *lifering-1* and *Atbrca1-3* mutants; seedlings were grown without (-MMC, top line) and at 5-6 days, treated with MMC (+MMC, bottom line) for 16 h. Arrows indicate the position of the QC, white arrowheads in the cortical cell layer point towards the transition zone, while the green arrowhead shows the position of the first roothair forming epidermal cell in the MMC-treated *lifering-1* roots. Scale bar: 50µm. See Figure S1 for further comparison of Col0 and *lifering-1* root phenotype with and without MMC treatment.
(**b**) Cell death response was quantified in the proximal meristem by measuring the area of dead cells (PI-stained) in Col-0 and in the mutants, *lifering-1*, *Atbrca1-3*. The plot shows the ratio of PI-stained area in the relevant mutant and Col-0. The PI-stained area was measured in each experiment (n>4) from N>15 mutants and Col-0. Although, the mean of cell death area varied between the different biological repeats, the ratio between the mutant and Col-0 (setting the area of the wild-type to 1), allowing comparisons between independent experiments.
(**c**) Quantification of death response in the distal stem cell region by counting the dead columella stem and daughter cells (CSC) in addition to the lateral root initials and their descendants (LRC) in the median section as shown in (**a**). Data of n>5, N±90 seedlings. Further information about the distribution of the stem cell niche with 0, 1 and n>1 collapsed cells is given in Table S4.
(**d**) The ratio of the length of the meristematic region between the mutants and Col-0 calculated from n>4, N>10 in each experiments. Length of meristem is defined here as distance between the QC and the cortical cell boundary at the transition.

Data Information:
in (**b** and **c**), the box plot analysis shows both the median and mean. Significance was calculated using Student's *t*-test, *ab*: p<0.00001 indicates significant difference comparing *lifering-1* to Col-0 and *Atbrca1-3*, while *b*: p<0.00001 between *Atbrca1-3* and Col-0.
In (**d**) *ab*:p<0.00001 shows significance of *lifering-1* both to Col-0 and *Atbrca1-3*.

Figure 4

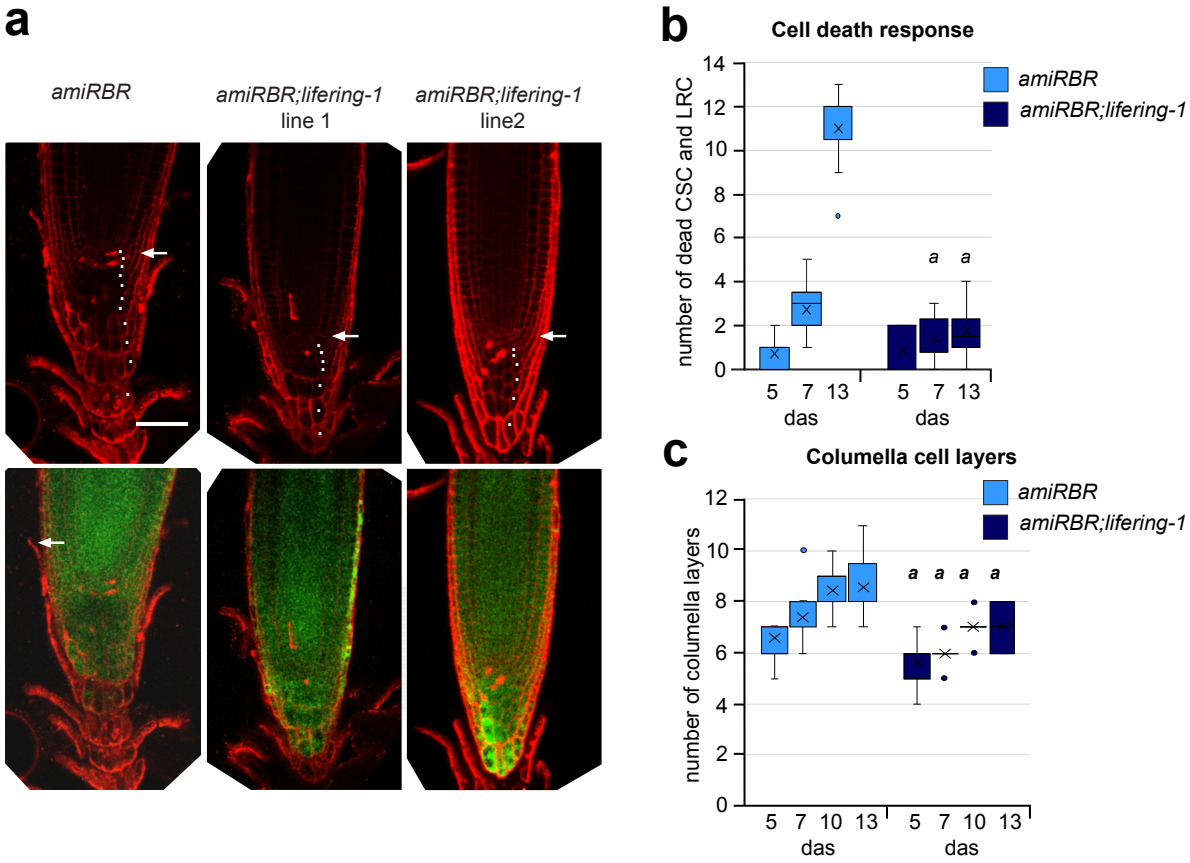

Figure 4. LIFERING affects cell proliferation downstream of RBR's function

(a) The representative CM images illustrate the cell death response (PI stained cells) and the number of columella and stem cell layers (white dots). PI-stained root-tips seedlings (12-13 das) from *amiRBR* and from the independent introgressed *amiRBR;lifering-1* lines 1 and 2 are shown. White arrows point to QC position in each image. The images with GFP signals show the presence and level of silencing in the mutant lines. Scale bar: 50µm,
(b) Cell death response of *amiRBR* and *amiRBR;lifering-1* seedlings at 5, 7 and 13 das. Total number of dead columella stem and daughter cells (CSC), lateral root cap initials and their descendants (LRC) were counted in the median sections as shown in (**a**). The boxplot shows the combined data of the introgressed lines, $n>3$ biological repeats, $N>15$, in each experiment.
a: $p<0.05$ significant difference between the introgessed lines and *amiRBR* at a given timepoint.
(c) Quantification of the number of columella stem and differentiated cell layers of 5, 7, 10 and 13 days-old roots from *amiRBR*, *amiRBR;lifering-1* lines 1 and 2. The boxplot shows the data of $n>3$, $N>15$ for each mutant in each experiment. *a*: $p<0.01$ significant difference between the introgessed lines and *amiRBR* at a given timepoint.

Figure 5

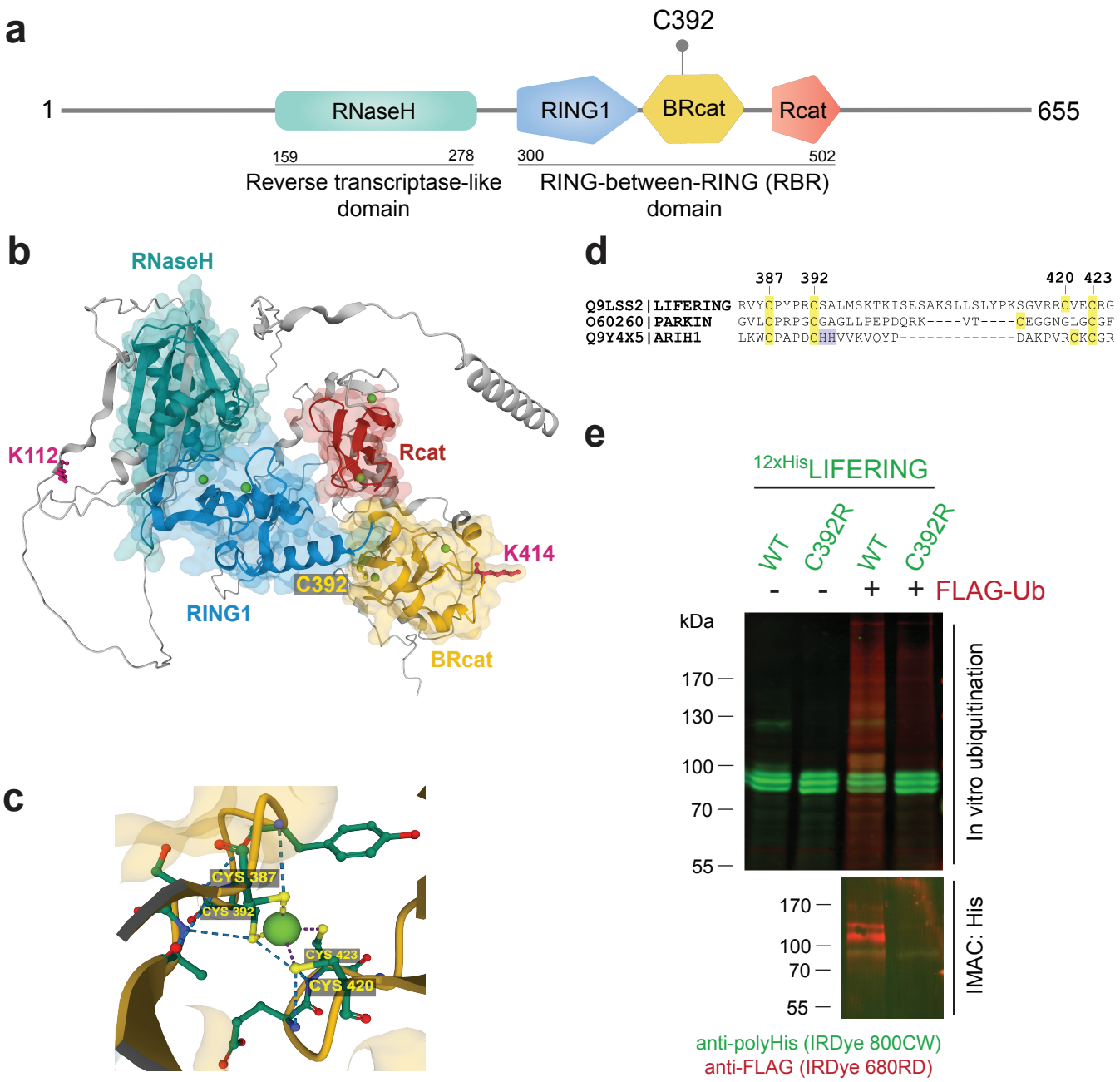

Figure 5. LIFERING is an E3 ubiquitin ligase

(a) Conserved domains of the LIFERING protein (UniProt: Q9LSS2) based on the InterPro database annotations. The Cys392 residue of the Q9LSS2 protein variant, which is Arg392 in the Q681M6 variant, is indicated.
(b) Prediction of the three-dimensional protein structure and ligand-binding of LIFERING using AlphaFold and AlphaFill, respectively. The domains identified in (**a**) are shown with the corresponding colours (green: RNaseH domain, blue: RING1, yellow: BRcat, red: Rcat), and the six zinc ions (green beads) predicted to be bound. The ubiquitinated lysine residues identified by mass spectrometry are shown in magenta, and the Cys392 residue in the BRcat domain is illustrated in yellow.
(c) Detailed representation of the first zinc-binding motif within the BRcat domain of LIFERING.
(d) Sequence alignment of the first zinc-binding motif in the BRcat domain of LIFERING, Parkin and HHARI (ARIH1). Zinc-binding cysteine residues are highlighted yellow. The numbers above indicate the position of the residues in LIFERING coding sequence.
(e) Western blot analysis of LIFERING *in vitro* ubiquitination reactions. The reactions were conducted using a combination of FLAG-tagged ubiquitin and total translation mixtures of the *in vitro* translated wild-type (WT) and C392R variants of 12xHis-LIFERING, as indicated. The E1 and E2 enzymes were sourced from endogenous wheat germ extract proteins used for *in vitro* translation. The ubiquitinated 12xHis-LIFERING proteins were isolated by pull-down (PD) using Dynabeads™ His-Tag Isolation and Pulldown beads and subsequently analysed by mass spectrometry. The proteins were separated by SDS-PAGE under reducing conditions. Multiplex detection was carried out using mouse anti-polyHis with IRDye 800CW goat anti-mouse conjugate (green) and rabbit anti-FLAG with IRDye 680RD goat anti-rabbit conjugate (red).

Figure 6

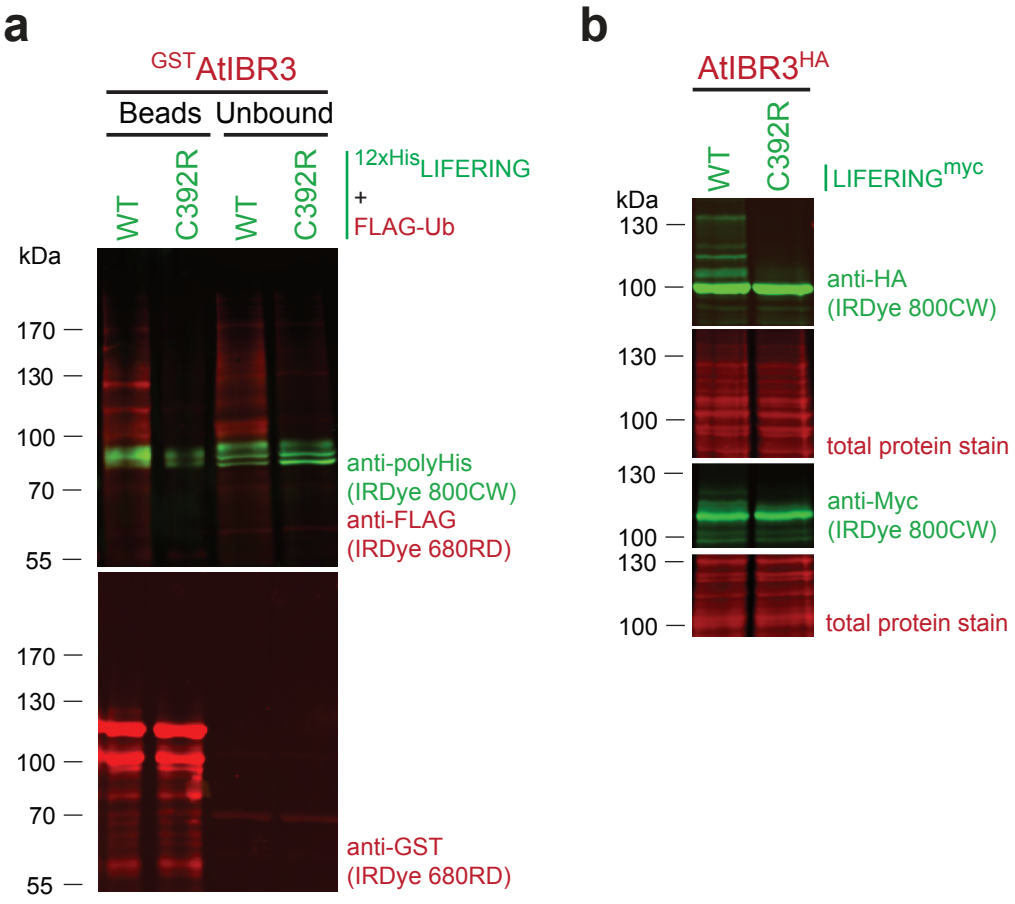

Figure 6. LIFERING ubiquitinates AtIBR3 *in vitro* and *in vivo*

(a) Western blot analysis of glutathione beads-bound AtIBR3 *in vitro* ubiquitination reactions in the presence of wild-type (WT) and C392R variants of LIFERING. FLAG-tagged ubiquitin and total translation mixtures of the *in vitro* translated wild-rype (WT) and C392R variants of 12xHis-LIFERING were added to the bead-bound AtIBR3, as indicated. Subsequently, the unbound fraction and washed beads were analysed following the *in vitro* ubiquitination reaction. The proteins were separated by SDS-PAGE under reducing conditions. Multiplex detection was carried out using mouse anti-polyHis antibody and rabbit anti-FLAG antibody. In the bottom part of (**a**), the singleplex detection of the bead-bound GST-IBR3 using rabbit anti-GST antibody is shown.
(b) Western blot analysis of *Arabidopsis* root cell suspension protoplasts co-transfected with wild-type or mutant Myc-tagged LIFERING and HA-tagged AtIBR3-encoding vectors. Singleplex detection was carried out using mouse anti-HA and mouse anti-Myc, and the membranes were stained with Revert 700 Total Protein Stain to check for loading consistency across the wells.

The secondary antibodies used in (**a** and **b**) were IRDye 680RD goat anti-rabbit conjugate (red) and IRDye 800CW goat anti-mouse conjugate (green).

Figure S1

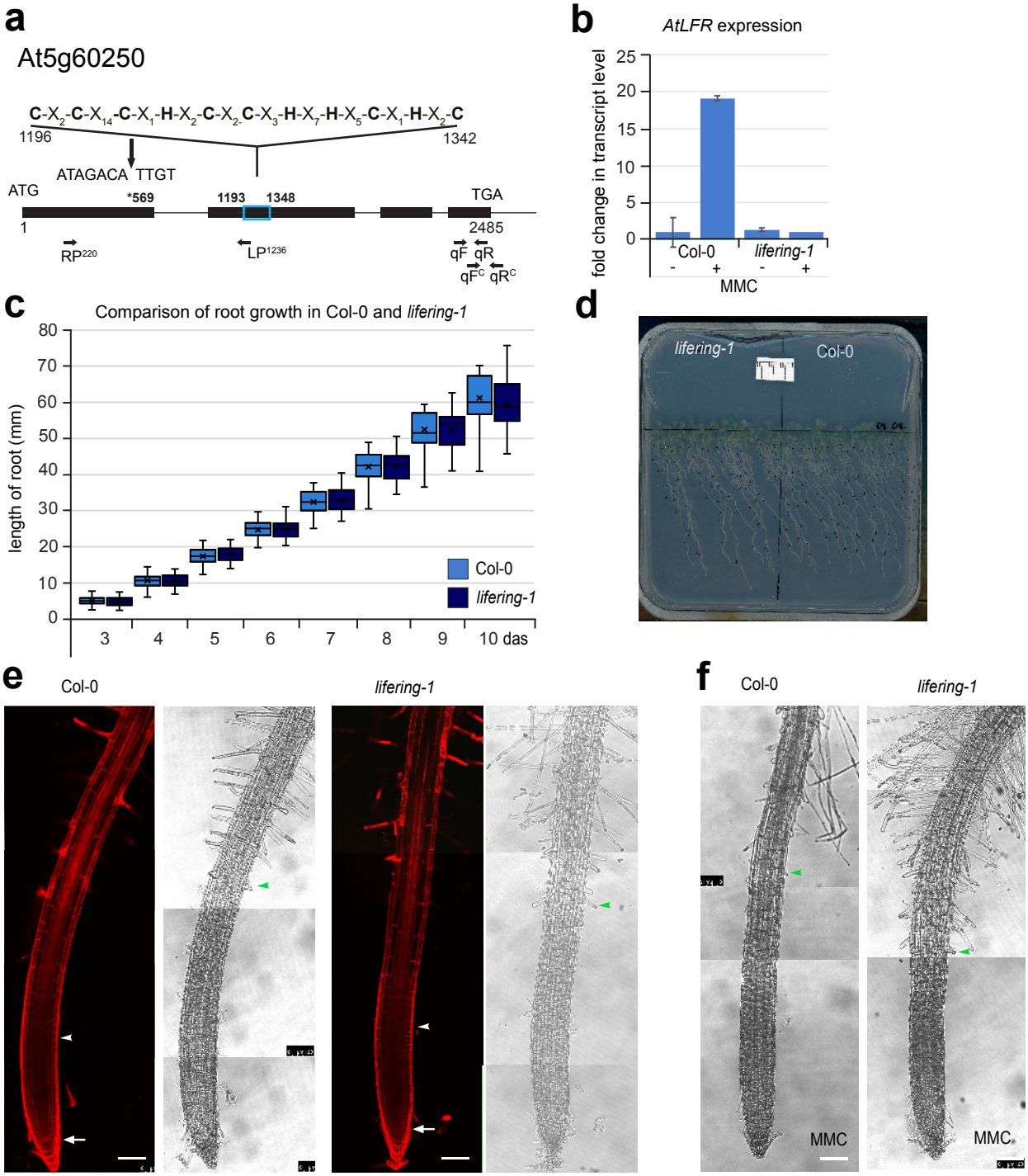

Figure S1 Expressional and phenotypic analysis of the *lifering-1* mutant

(**a**) The position of the insertion (*569) in the first exon of the coding region of the At5g60250 gene (*LIFERING*) in the insertion line, SM_3_34488 is shown. The RING-Ubox is labelled by the blue rectangle at position 1193-1348, the corresponding amino-acid sequence represents the C3HC4 RING-Between-RING finger domain at positions 1196-1342 of the genomic sequence. The primer pairs used for genotyping and expression analysis are located between positions: RP-LP**:** 220-1236 and qF-qR: 2304-2485, while for controlling the presence of the innate transcript in the lines for complementation, *lifering-1*(pgLIFERING): qF^C-qR^C 2446-2548. See Table S1 for primer sequences and Figure S2 for the complementation of the mutant.
(**b**) The level of *LIFERING* does not change upon induction with MMC treatment (- vs + MMC) in the mutant *lifering-1*, indicating that it is a full knock-out mutant. In contrast, in Col-0, upon MMC treatment, around 20 fold induction was detected. MMC treatment +/-16 h, 10µg ml^{-1}, *n*=2.
(c) Quantification of the root growth of Col-0 and *lifering-1* between 3 and 10 das. On a given day, no significant difference was detected between wild-type and mutant.
(d) The image corresponds to the root growth depicted in (**c**)**.**
(e) The corresponding PI-stained confocal and differential interference contrast (DIC) microscopy images illustrate the root zonation of Col-0 and *lifering-1* mutant. The white arrows point to the position of QC, while the white arrowheads mark the start of the transition zone towards the elongation zone.
(f) DIC images show the effect of MMC treatment (16-18h, 10µg ml^{-1}), on differentiation in Col-0 and *lifering-1*. In both (**e** and **f**), green arrowheads label the first differentiated epidermis cell. Scale bar: 100µm.

Figure S2

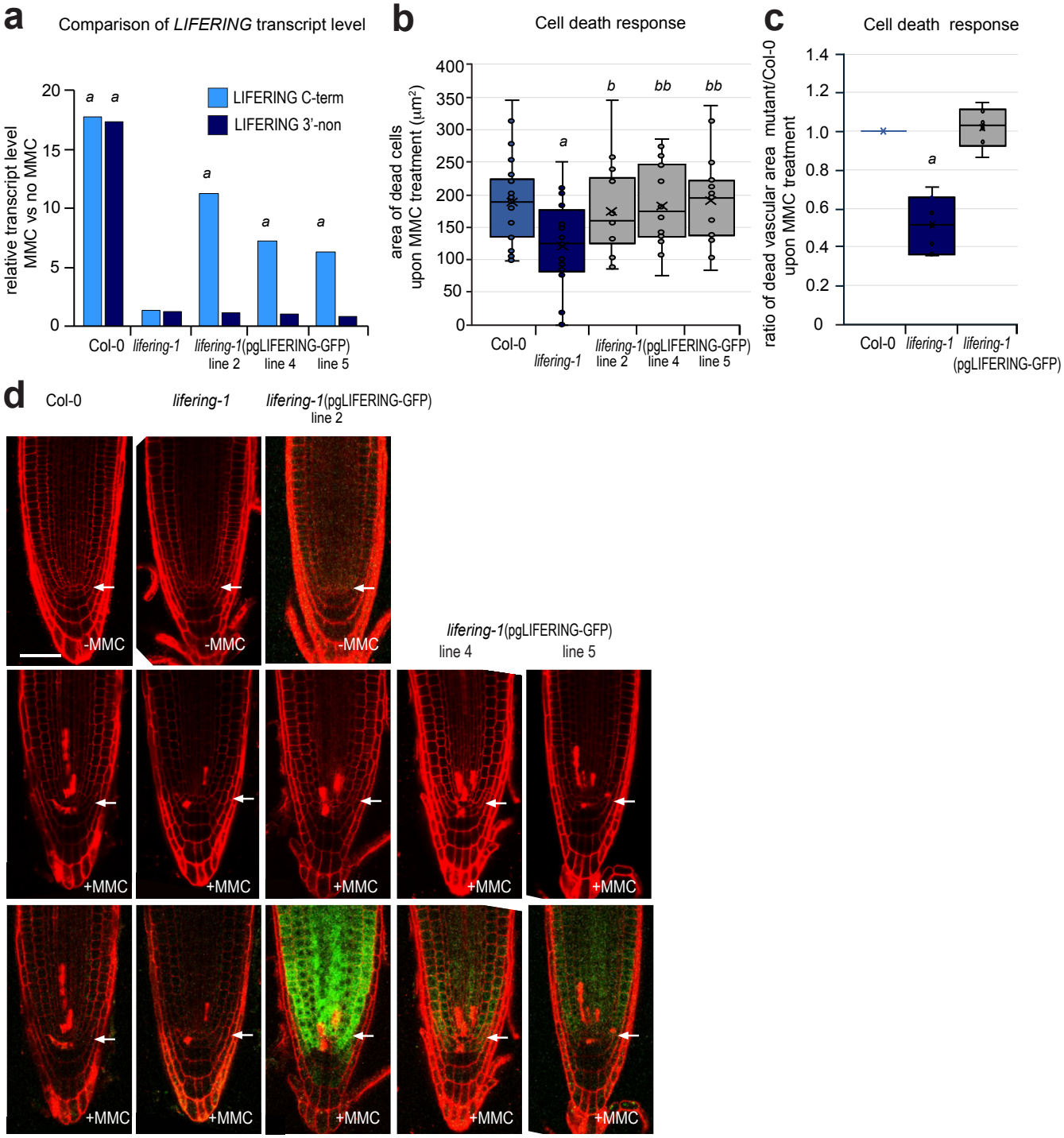

Figure S2. Introducing the *LIFERING* gene under its own promoter can complement the cell death response-phenotype of the *lifering-1* mutant

(**a**) The relative expression of *LIFERING* upon MMC treatment (10μg ml^{-1}) after 16 h. qRT-PCR was carried out on Col-0, *lifering-1* and *lifering-1*(pgLIFERING:GFP) lines (line 2, 4 and 5) on 5-6 das seedlings. Primer combinations, were located to the C-terminal (C-term) and to the 3' non-translated region (3'-non). Position of the primer pairs is indicated in Figure S1A. The values represent fold changes normalised to the values of the *LIFERING* gene in the non-treated samples where the expression was taken as 1.
(**b**, **c**) Comparison of the cell death response upon MMC treatment (10μg ml^{-1}, 16 h, 5-6das) in the *lifering-1* mutant and the complemented lines *lifering-1*(pgLIFERING:GFP).The cell death response was quantified by measuring the area of dead cells in the proximal meristem (μm^2, PI-stained area). (**b**) The graph shows the combined measurement of n=3, N>10 in each experiment. In the box-plot analysis the median was also included. *a*: p<0.002 significance comparing the cell death response between *lifering-1* and Col-0, *b*: p<0.05, *bb*:p<0.001 between the introgressed lines and the mutant using Student's *t*-test analysis. (**c**) illustrates ratio of cell death response of Col-0, *lifering-1* and *lifering-1*(pgLIFERING:GFP) where the measurements were combined for the three complemented lines.
(**d**) Confocal microscopy (CM) images of PI-stained root-tips of Col-0, *lifering-1* and *lifering-1*(pgLIFERING:GFP) lines 2, 4 and 5. Seedlings were grown without (-MMC) and treated with MMC (+MMC) for 16 h. To compare the level of *LIFERING* gene induction, see the two sets of images below, red channel shows the cell death response, while red and green channels combined, the location of the signal. For the microscopic analysis same settings were used through out the entire experiment. Scale bar: 50μm, white arrow: QC position in each image.

Figure S3

a

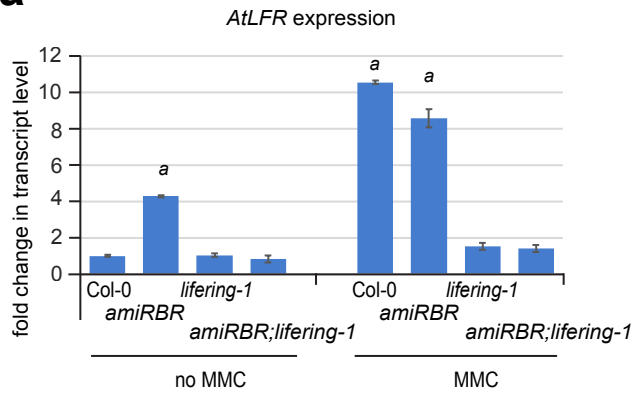

Figure S3 *LIFERING* expression in the double *amiRBR;lifering-1* compared to the single *amiRBR* and *lifering-1* mutants

(**a**) Comparison of the level of *LIFERING* expression in Col-0, in the single *amiRBR* and *lifering-1* mutants and in the double *amiRBR;lifering-1* mutant in the absence and presence of the genotoxic agent, MMC. No significant change was detected upon induction with MMC treatment in the *amiRBR;lifering-1*, indicating that the double mutant lacks the *LIFERING* transcript. MMC treatment +/-16 h, 10μg ml^{-1}, *n*=3, *a*: $p<0.01$ significant difference between the mutant lines compared to non-treated Col-0 expression, where the level of *LIFERING* was taken as 1.

Figure S4

```
                                 10        20        30        40        50
Q9LSS2/1-655       1 MDFDSEYAFRLQMEEALAASLSSQSRTPQRPPSPPIVATCGVLIVENNPNDSKTAKTSSG  60
Q681M6/1-649       1 ------DAFRLQMEEALAASLSSQSRTPQRPPSPPIVATCGVLIVENNPNDSKTAKTSSG  54

                                 70        80        90       100       110
Q9LSS2/1-655      61 YGFDFKRAVGGGNSKAKGKTHESVTGVRTDERNPNIGLGNSRSTSTGHGNTKPLPQETVR 120
Q681M6/1-649      55 YGFDFKRAVGGGNSKAKGKTHESVTGVRTDERNPNIGLGNSRSTSTGHGNTKPLPQETVR 114

                                130       140       150       160       170
Q9LSS2/1-655     121 PAQLVGEGSSRVNTAAGKINGNLLYRLYFKGLVSDENGKGKMTDVVSGFGVAICDQRDNL 180
Q681M6/1-649     115 PAQLVGEGSSRVNTAAGKINGNLLYRLYFKGLVSDENGKGKMTDVVSGFGVAICDQRDNL 174

                                190       200       210       220       230
Q9LSS2/1-655     181 LFEMKGPLIDNGMSRQGAELKALIRGLTEALKLGIKHIVFFCDSYPIFQYVTGKWMAKQK 240
Q681M6/1-649     175 LFEMKGPLIDNGMSRQGAELKALIRGLTEALKLGIKHIVFFCDSYPIFQYVTGKWMAKQK 234

                                250       260       270       280       290
Q9LSS2/1-655     241 KISLLLDDLQSIMQHFSSYQHVLVARNDVKFAYKLARESILSMVTPHEDPRQAKAVLKEE 300
Q681M6/1-649     235 KISLLLDDLQSIMQHFSSYQHVLVARNDVKFAYKLARESILSMVTPHEDPRQAKAVLKEE 294

                                310       320       330       340       350
Q9LSS2/1-655     301 CAICFNDIVAEGMFSVDKCRHRFCFQCVKQHVEVKLLHGMAPKCPHDGCKSELVIDACGK 360
Q681M6/1-649     295 CAICFNDIVAEGMFSVDKCRHRFCFQCVKQHVEVKLLHGMAPKCPHDGCKSELVIDACGK 354

                                370       380       390       400       410
Q9LSS2/1-655     361 LLTPKLSKLWQQRLQENAIPVTERVYCPYPRCSALMSKTKISESAKSLLSLYPKSGVRRC 420
Q681M6/1-649     355 LLTPKLSKLWQQRLQENAIPVTERVYCPYPRRSALMSKTKISESAKSLLSLYPKSGVRRC 414

                                430       440       450       460       470
Q9LSS2/1-655     421 VECRGLFCVDCKVPWHGNLSCTEYKKLHPEPPADDVKLKSLANNKMWRQCGKCQHMIELS 480
Q681M6/1-649     415 VECRGLFCVDCKVPWHGNLSCTEYKKLHPEPPADDVKLKSLANNKMWRQCGKCQHMIELS 474

                                490       500       510       520       530
Q9LSS2/1-655     481 QGCNHITCRCGHEFCYNCGGGWNKIMGTCLNRCPTWNEEYITRQDPARANVAANNYFDDE 540
Q681M6/1-649     475 QGCNHITCRCGHEFCYNCGGGWNKIMGTCLNRCPTWNEEYITRQDPARANVAANNYFDDE 534

                                550       560       570       580       590
Q9LSS2/1-655     541 DDDDVDGDYDYDDFFHPHFGHAMNDRNPEEPFDPFFDLPDGVLFTPQMLSSKSRQQLYLP 600
Q681M6/1-649     535 DDDDVDGDYDYDDFFHPHFGHAMNDRNPEEPFDPFFDLPDGVLFTPQMLSSKSRQQLYLP 594

                                610       620       630       640       650
Q9LSS2/1-655     601 DSDDSDDNATTQNAPAADENCPYFGKYGKYTIMYDSDGYELEDFTNPFHPDYPHF      655
Q681M6/1-649     595 DSDDSDDNATTQNAPAADENCPYFGKYGKYTIMYDSDGYELEDFTNPFHPDYPHF      649
```

Figure S4 Aminoacid sequence alignment of UniProt Q9LSS2 and Q681M6

Amino acid sequence alignment of UniProt Q9LSS2 genomic sequence-based and Q681M6 transcript-derived sequences, the putative protein products of the *AT5G60250* gene.

Figure S5

a

LIFERING (At5g60250)

Protein MW: 73467.9
Protein pI: 8.6
Protein Length: 655

Search Name	Num Unique	Peptide Count	% Cov	Best Disc Score	Best Expect Val
L_E_20230305_03_MT_KB_Ring_wt	85	333	72.2	7.05	1.9e-12
L_E_20230305_04_MT_KB_Ring_mut	104	441	85.6	7.50	2.8e-13

```
1    MDFDSEYAFR LQMEEALAAS LSSQSRTPQR PPSPPIVATC GVLIVENNPN DSKTAKTSSG YGFDFKRAVG GGNSKAKGKT
81   HESVTGVRTD ERNPNIGLGN SRSTSTGHGN TKPLPQETVR PAQLVGEGSS RVNTAAGKIN GNLLYRLYFK GLVSDENGKG
161  KMTDVVSGFG VAICDQRDNL LFEMKGPLID NGMSRQGAEL KALIRGLTEA LKLGIKHIVF FCDSYPIFQY VTGKWMAKQK
241  KISLLLDDLQ SIMQHFSSYQ HVLVARNDVK FAYKLARESI LSMVTPHEDP RQAKAVLKEE CAICFNDIVA EGMFSVDKCR
321  HRFCFQCVKQ HVEVKLLHGM APKCPHDGCK SELVIDACGK LLTPKLSKLW QQRLQENAIP VTERVYCPYP RCSALMSKTK
401  ISESAKSLLS LYPKSGVRRC VECRGLFCVD CKVPWHGNLS CTEYKKLHPE PPADDVKLKS LANNKMWRQC GKCQHMIELS
481  QGCNHITCRC GHEFCYNCGG GWNKIMGTCL NRCPTWNEEY ITRQDPARAN VAANNYFDDE DDDDVDGDYD YDDFFHPHFG
561  HAMNDRNPEE PFDPFFDLPD GVLFTPQMLS SKSRQQLYLP DSDDSDDNAT TQNAPAADEN CPYFGKYGKY TIMYDSDGYE
641  LEDFTNPFHP DYPHF
```

b

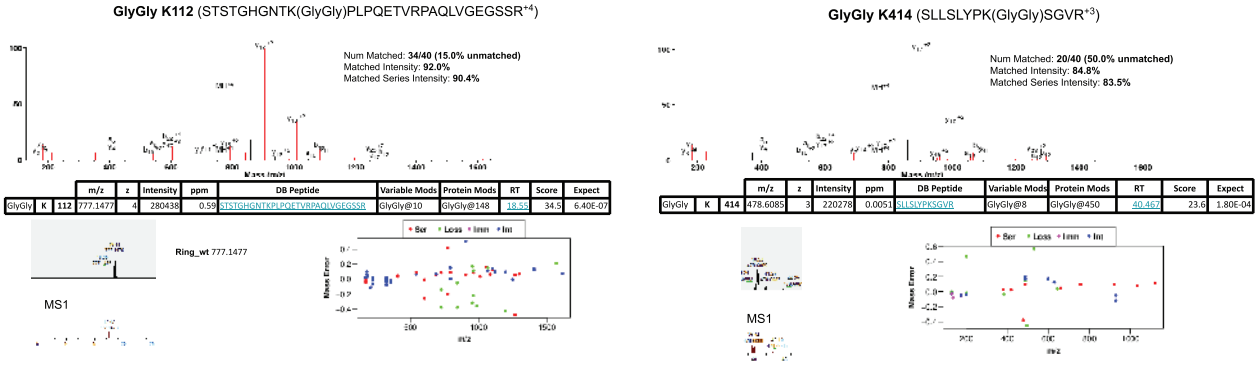

Figure S5. Mass spectrometry analysis of LIFERING (At5g60250) ubiqitination

The N-terminally 12xHis-tagged wild-type and mutant (C392R) LIFERING proteins were expressed using wheat germ extract-based *in vitro* translation. Following the *in vitro* ubiquitination reactions in the presence of FLAG-ubiquitin, the 12xHis-tagged proteins were isolated by immobilized metal-ion affinity chromatography (IMAC), and mass spectrometry was performed. Western blot analysis of the isolated proteins is shown in Fig. 5e.
(a) the detected peptide fragments of LIFERING (Uniprot: Q9LSS2) labelled in red.
(**b**) MS2 spectra of the annotated ubiquitinated peptides. LIFERING is intensively ubiquitinated on the K112 and K414 residues of the wild-type protein, but no MS1 signal, and therefore no ubiquitination, is detectable on the mutant protein.

Figure S6

a

IBR3 (At3g06810)

Protein MW: 91713.8
Protein pI: 8.6
Protein Length: 824

Num Unique	Peptide Count	% Cov	Best Disc Score	Best Expect Val
108	250	81.7	7.65	1.50E-13

```
  1 MGSSTGDLVT RIQSAHRFDH DALFRFAADN VSGFPTNPSQ FKVSQFGHGQ SNPTFLIEVG SGSSLKRYVL RKKPPGKLLQ
 81 SAHAVDREFQ VLRALGEHTQ VPVPKVFCLC TDPAVIGTAF YIMEFMEGRI FIDPKLPNVA PERRNAIYRA TAKALASLHS
161 ADVDAIGLEK YGRRGNYCKR QIDRWFKQYL ASTSEGKPER NPKMFELVDW LRKNIPAEDS TGATSGLVHG DFRIDNLVFH
241 PSEDRVIGII DWELSTLGNQ MCDVAYSCMH YIVNVQLDKE HVSEGFETTG LPEGMLSMPE FLLEYCSASG KPWPAANWKF
321 YVAFSLFRAA SIYTGVYSRW LMGNASAGER ARNTGVQANE LVESALGYIA RENVLPEHPP SVQRDVSPSY ESLVDGSGRF
401 IPNRKVLELR QKLIKFMETH IYPMENEFSK LAQSDMRWTV HPQEEKLKEM AKREGLWNLF VPVDSAARAR RELAATENKH
481 NLSGKSFDQL FGEGLTNLEY GYLCEIMGRS VWAPQVFNCG APDTGNMEVI LRYGNKEQIS EWLIPLLEGR IRSGFAMTEP
561 QVASSDATNI ECSIRRQGDS YVINGTKWWT SGAMDPRCRV LILMGKTDFN APKHKQQSMI LVDMRTPGIS VKRPLTVFGF
641 DDAPHGHAEI SFENVVVPAK NILLGEGRGF EIAQGRLGPG RLHHCMRLIG AAERGMELMA QRALSRKTFG KFIAQHGSFV
721 SDLAKLRVEL EGTRLLVLEA ADHLDKFGNK KARGILAMAK VAAPNMALKV LDTAIQVHGA AGVSSDTVLA HLWATARTLR
801 IADGPDEVHL GTIGKLELQR ASKL
```

b

			m/z	z	Intensity	ppm	DB Peptide	Variable Mods	Protein Mods	RT	Score	Expect
GlyGly	K	**170**	550.7895	4	290517	0.32	ALASLHSADVDAIGLEKYGR	GlyGly@17	GlyGly@170	37.8	33.3	1.0E-06
GlyGly	K	**213**	762.7086	3	82573	0.094	KNIPAEDSTGATSGLVHGDFR	GlyGly@1	GlyGly@213	20.17	46.8	1.3E-10
GlyGly	K	**311**	920.2291	5	39416	0.28	EHVSEGFETTGLPEGMLSMPEFLLEYCSASGKPWPAANWK	GlyGly@32	GlyGly@311	62.42	20.6	9.0E-05
GlyGly	K	**536**	753.731	3	41072	0.32	YGNKEQISEWLIPLLEGR	GlyGly@4	GlyGly@536	81.5	30.1	2.90E-07

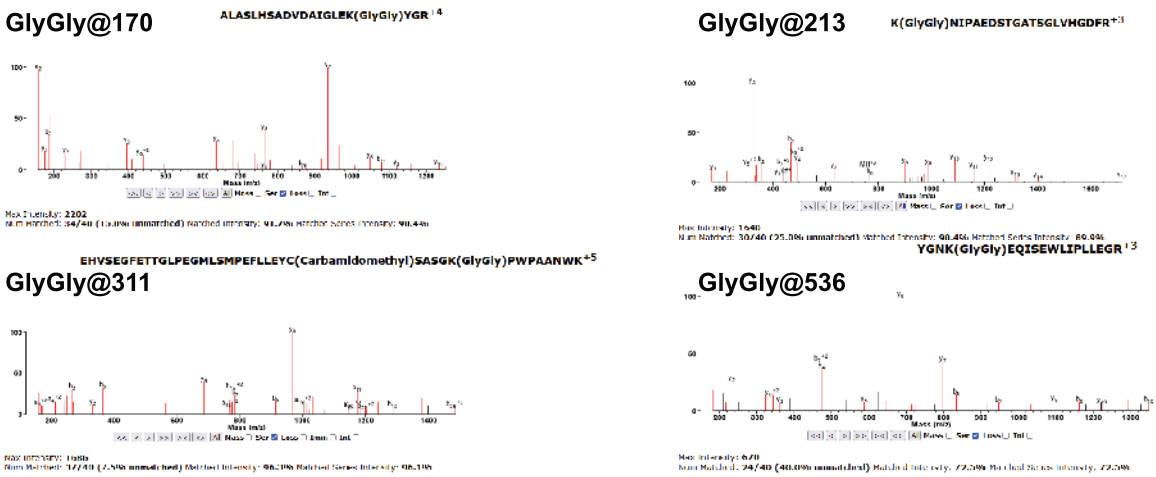

Figure S6. Mass spectrometry analysis of IBR3 (At3g06810) ubiquitination

The acyl-CoA dehydrogenase-like protein, IBR3, labelled with an N-terminal GST tag was expressed using wheat germ extract-based *in vitro* translation and purified with glutathione beads. The bead-bound IBR3 proteins were subjected to *in vitro* ubiquitination reactions in the presence of total translation mixtures containing wild-type or C392R mutant LIFERING proteins and FLAG-ubiquitin. The bead-bound proteins were analysed by mass spectrometry. Western blot analysis of the isolated proteins is shown in Fig. 6a.
(a) The detected peptide fragments of IBR3 (Uniprot: Q8RWZ3) labelled in red.
(b) MS2 spectra of the annotated ubiquitinated peptides. IBR3 is ubiquitinated on the K170, K213, K311, and K536 residues exclusively by the wild-type LIFERING.

Figure S7

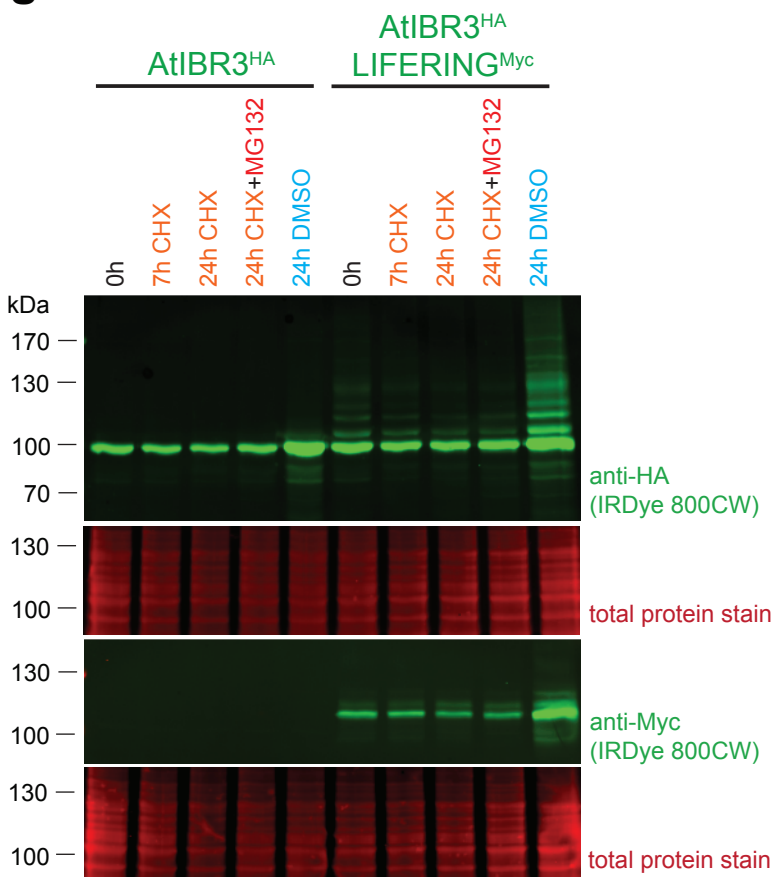

Figure S7. Effect of cycloheximide (CHX) and MG132 on the amount of AtIBR3 protein in *Arabidopsis* root cell suspension protoplasts

Western blot analysis of *Arabidopsis* root cell suspension protoplasts transfected with HA-tagged IBR3 or co-transfected with wild-type Myc-tagged AtLIFERING and HA-tagged AtIBR3-encoding vectors. Protoplasts were treated with 50 µM CHX and 50 µM MG132 for the indicated period is of time. Singleplex detection was performed using mouse anti-HA and mouse anti-Myc, and the membranes were stained with Revert 700 Total Protein Stain to check for loading consistency across the wells. The secondary antibody used was IRDye 800CW goat anti-mouse conjugate (green).

Supplementary Table S5.

Analysis of mass spectrometry spectral count data from TurboID proximity labelling experiments using SAINTexpress (v3.6). RINGwt is the wild-type LIFERING protein with Cys392, RINGmut is the mutant LIFERING with an arginine at position 392 of the protein coding sequence.

Identifier	Bait name	Zeocin treatment	Replicate
RINGmut	TurboID-RINGmut	no	1
RINGmut_z	TurboID-RINGmut	yes	1
RINGwt	TurboID-RINGwt	no	1
RINGwt_z	TurboID-RINGwt	yes	1
TbID_1	TurboID	no	1
TbID_2	TurboID	yes	2
TbID_3	TurboID	no	3

Bait: RINGwt	Prey	PreyGene	Spec	SpecSum	AvgSpec	NumReplicates	ctrlCounts	AvgP	MaxP	TopoAvgP	TopoMaxP	SaintScore	FoldChange	BFDR
RINGwt	Q0WV25	Tubulin alpha-4 chain	56	56	56,00	1	0|0|0	1,00	1,00	1,00	1,00	1,00	560,00	0,00
RINGwt	Q8RWZ3	Probable acyl-CoA dehydrogenase IBR3	34	34	34,00	1	0|0|0	1,00	1,00	1,00	1,00	1,00	340,00	0,00
RINGwt	P55737	Heat shock protein 90-2	15	15	15,00	1	0|0|0	1,00	1,00	1,00	1,00	1,00	150,00	0,00
RINGwt	P23321	Oxygen-evolving enhancer protein 1-1, chloroplastic	8	8	8,00	1	0|0|0	1,00	1,00	1,00	1,00	1,00	80,00	0,00
RINGwt	Q9S841	Oxygen-evolving enhancer protein 1-2, chloroplastic	7	7	7,00	1	0|0|0	1,00	1,00	1,00	1,00	1,00	70,00	0,00
RINGwt	Q9LZ45	Histone H2B.9	7	7	7,00	1	0|0|0	1,00	1,00	1,00	1,00	1,00	70,00	0,00
RINGwt	O22254	Putative 60S ribosomal protein L18-1	5	5	5,00	1	0|0|0	1,00	1,00	1,00	1,00	1,00	50,00	0,00
RINGwt	Q9STY6	40S ribosomal protein S20-2	5	5	5,00	1	0|0|0	1,00	1,00	1,00	1,00	1,00	50,00	0,00
RINGwt	Q9SU58	ATPase 4, plasma membrane-type	5	5	5,00	1	0|0|0	1,00	1,00	1,00	1,00	1,00	50,00	0,00
RINGwt	Q9SRH5	Mitochondrial outer membrane protein porin 1	5	5	5,00	1	0|0|0	1,00	1,00	1,00	1,00	1,00	50,00	0,00
RINGwt	Q9FM01	UDP-glucose 6-dehydrogenase 4	5	5	5,00	1	0|0|0	1,00	1,00	1,00	1,00	1,00	50,00	0,00
RINGwt	Q9FLV7	B3 domain-containing protein At5g24050	5	5	5,00	1	0|0|0	1,00	1,00	1,00	1,00	1,00	50,00	0,00
RINGwt	Q9ZP06	Malate dehydrogenase 1, mitochondrial	4	4	4,00	1	0|0|0	1,00	1,00	1,00	1,00	1,00	40,00	0,00
RINGwt	Q42589	Non-specific lipid-transfer protein 1	4	4	4,00	1	0|0|0	1,00	1,00	1,00	1,00	1,00	40,00	0,00
RINGwt	P48348	14-3-3-like protein GF14 kappa	4	4	4,00	1	0|0|0	1,00	1,00	1,00	1,00	1,00	40,00	0,00
RINGwt	Q07100	Serine/threonine-protein phosphatase PP2A-3 catalytic subunit	4	4	4,00	1	0|0|0	1,00	1,00	1,00	1,00	1,00	40,00	0,00
RINGwt	P57106	Malate dehydrogenase 2, cytoplasmic	4	4	4,00	1	0|0|0	1,00	1,00	1,00	1,00	1,00	40,00	0,00
RINGwt	Q8VZ19	60S ribosomal protein L30-2	4	4	4,00	1	0|0|0	1,00	1,00	1,00	1,00	1,00	40,00	0,00
RINGwt	P59230	60S ribosomal protein L10a-2	4	4	4,00	1	0|0|0	1,00	1,00	1,00	1,00	1,00	40,00	0,00
RINGwt	P21238	Chaperonin 60 subunit alpha 1, chloroplastic	3	3	3,00	1	0|0|0	1,00	1,00	1,00	1,00	1,00	30,00	0,00
RINGwt	O04316	Nitrile-specifier protein 4	3	3	3,00	1	0|0|0	1,00	1,00	1,00	1,00	1,00	30,00	0,00
RINGwt	P42699	Plastocyanin major isoform, chloroplastic	3	3	3,00	1	0|0|0	1,00	1,00	1,00	1,00	1,00	30,00	0,00

Bait: RINGwt	Prey	PreyGene	Spec	SpecSum	AvgSpec	NumReplicates	ctrlCounts	AvgP	MaxP	TopoAvgP	TopoMaxP	SaintScore	FoldChange	BFDR
RINGwt	Q8L3X8	Serine/arginine-rich SC35-like splicing factor SCL30	3	3	3,00	1	0|0|0	1,00	1,00	1,00	1,00	1,00	30,00	0,00
RINGwt	Q9FFR3	6-phosphogluconate dehydrogenase, decarboxylating 3, chloroplastic	3	3	3,00	1	0|0|0	1,00	1,00	1,00	1,00	1,00	30,00	0,00
RINGwt	O80929	60S ribosomal protein L36-1	3	3	3,00	1	0|0|0	1,00	1,00	1,00	1,00	1,00	30,00	0,00
RINGwt	Q9FGI6	NADH dehydrogenase [ubiquinone] iron-sulfur protein 1, mitochondrial	3	3	3,00	1	0|0|0	1,00	1,00	1,00	1,00	1,00	30,00	0,00
RINGwt	P10896	Ribulose bisphosphate carboxylase/oxygenase activase, chloroplastic	2	2	2,00	1	0|0|0	0,97	0,97	0,97	0,97	0,97	20,00	0,00
RINGwt	Q42556	ATPase 9, plasma membrane-type	2	2	2,00	1	0|0|0	0,97	0,97	0,97	0,97	0,97	20,00	0,00
RINGwt	Q8W4S4	V-type proton ATPase subunit a3	2	2	2,00	1	0|0|0	0,97	0,97	0,97	0,97	0,97	20,00	0,00
RINGwt	Q9ZU25	Probable mitochondrial-processing peptidase subunit alpha-1, mitochondrial	2	2	2,00	1	0|0|0	0,97	0,97	0,97	0,97	0,97	20,00	0,00
RINGwt	Q8VZB9	60S ribosomal protein L10a-1	2	2	2,00	1	0|0|0	0,97	0,97	0,97	0,97	0,97	20,00	0,00
RINGwt	Q8LF20	Putative clathrin assembly protein At2g25430	2	2	2,00	1	0|0|0	0,97	0,97	0,97	0,97	0,97	20,00	0,00
RINGwt	Q9FFC0	Histone H2B.10	10	10	10,00	1	1|2|0	1,00	1,00	1,00	1,00	1,00	10,00	0,00
RINGwt	P50318	Phosphoglycerate kinase 2, chloroplastic	1	1	1,00	1	0|0|0	0,00	0,00	0,00	0,00	0,00	10,00	0,51
RINGwt	Q8LCE1	Glutamine synthetase cytosolic isozyme 1-2	1	1	1,00	1	0|0|0	0,00	0,00	0,00	0,00	0,00	10,00	0,51
RINGwt	Q93Y35	26S proteasome non-ATPase regulatory subunit 6 homolog	1	1	1,00	1	0|0|0	0,00	0,00	0,00	0,00	0,00	10,00	0,51
RINGwt	Q9FXA2	Polyadenylate-binding protein 8	1	1	1,00	1	0|0|0	0,00	0,00	0,00	0,00	0,00	10,00	0,51
RINGwt	P48491	Triosephosphate isomerase, cytosolic	1	1	1,00	1	0|0|0	0,00	0,00	0,00	0,00	0,00	10,00	0,51
RINGwt	Q9FVE6	Histone deacetylase HDT1	1	1	1,00	1	0|0|0	0,00	0,00	0,00	0,00	0,00	10,00	0,51
RINGwt	Q941A6	Succinate dehydrogenase subunit 6, mitochondrial	1	1	1,00	1	0|0|0	0,00	0,00	0,00	0,00	0,00	10,00	0,51
RINGwt	Q9C6B3	Gamma carbonic anhydrase 2, mitochondrial	1	1	1,00	1	0|0|0	0,00	0,00	0,00	0,00	0,00	10,00	0,51
RINGwt	Q8VZU9	Derlin-1	1	1	1,00	1	0|0|0	0,00	0,00	0,00	0,00	0,00	10,00	0,51
RINGwt	Q8VYN2	Vesicle-associated protein 4-2	1	1	1,00	1	0|0|0	0,00	0,00	0,00	0,00	0,00	10,00	0,51

Bait: RINGwt	Prey	PreyGene	Spec	SpecSum	AvgSpec	NumReplicates	ctrlCounts	AvgP	MaxP	TopoAvgP	TopoMaxP	SaintScore	FoldChange	BFDR
RINGwt	Q9ZQ18	Cytoplasmic 60S subunit biogenesis factor REI1 homolog 2	1	1	1,00	1	0|0|0	0,00	0,00	0,00	0,00	0,00	10,00	0,51
RINGwt	Q9FXD6	Two-component response regulator ARR11	1	1	1,00	1	0|0|0	0,00	0,00	0,00	0,00	0,00	10,00	0,51
RINGwt	Q9FFU1	CRS2-associated factor 2, mitochondrial	1	1	1,00	1	0|0|0	0,00	0,00	0,00	0,00	0,00	10,00	0,51
RINGwt	Q9LV03	Glutamate synthase 1 [NADH], chloroplastic	1	1	1,00	1	0|0|0	0,00	0,00	0,00	0,00	0,00	10,00	0,51
RINGwt	P59233	Ubiquitin-40S ribosomal protein S27a-3	55	55	55,00	1	8|9|0	1,00	1,00	1,00	1,00	1,00	9,71	0,00
RINGwt	Q03251	Glycine-rich RNA-binding protein 8	6	6	6,00	1	0|0|2	0,96	0,96	0,96	0,96	0,96	9,00	0,01
RINGwt	Q03250	Glycine-rich RNA-binding protein 7	3	3	3,00	1	0|0|1	0,97	0,97	0,97	0,97	0,97	9,00	0,00
RINGwt	Q9LXJ2	Cytochrome b-c1 complex subunit 9, mitochondrial	3	3	3,00	1	0|0|1	0,97	0,97	0,97	0,97	0,97	9,00	0,00
RINGwt	P59232	Ubiquitin-40S ribosomal protein S27a-2	56	56	56,00	1	8|9|3	1,00	1,00	1,00	1,00	1,00	8,40	0,00
RINGwt	Q9FLQ4	2-oxoglutarate dehydrogenase E2 component (dihydrolipoamide succinyltransferase)	14	14	14,00	1	0|0|5	0,97	0,97	0,97	0,97	0,97	8,40	0,01
RINGwt	Q41188	Cold shock protein 2	8	8	8,00	1	1|1|1	1,00	1,00	1,00	1,00	1,00	8,00	0,00
RINGwt	Q8LD46	60S ribosomal protein L23a-1	24	24	24,00	1	4|3|3	1,00	1,00	1,00	1,00	1,00	7,20	0,00
RINGwt	P39207	Nucleoside diphosphate kinase 1	9	9	9,00	1	2|2|0	1,00	1,00	1,00	1,00	1,00	6,75	0,00
RINGwt	Q8H107	2-oxoglutarate dehydrogenase E2 component (dihydrolipoamide succinyltransferase)	13	13	13,00	1	0|0|6	0,94	0,94	0,94	0,94	0,94	6,50	0,01
RINGwt	Q9FE65	60S ribosomal protein L34-2	12	12	12,00	1	3|3|0	1,00	1,00	1,00	1,00	1,00	6,00	0,00
RINGwt	Q9SAJ4	Phosphoglycerate kinase 3, cytosolic	4	4	4,00	1	1|1|0	0,92	0,92	0,92	0,92	0,92	6,00	0,01
RINGwt	Q42560	Aconitate hydratase 1	4	4	4,00	1	0|2|0	0,86	0,86	0,86	0,86	0,86	6,00	0,02
RINGwt	Q9FE58	60S ribosomal protein L22-3	4	4	4,00	1	2|0|0	0,86	0,86	0,86	0,86	0,86	6,00	0,02
RINGwt	Q9LPI5	Polyadenylate-binding protein-interacting protein 11	2	2	2,00	1	0|1|0	0,79	0,79	0,79	0,79	0,79	6,00	0,02
RINGwt	P23686	S-adenosylmethionine synthase 1	26	26	26,00	1	7|7|0	0,99	0,99	0,99	0,99	0,99	5,57	0,00
RINGwt	Q9FJX3	Mitochondrial outer membrane protein porin 2	9	9	9,00	1	1|4|0	0,92	0,92	0,92	0,92	0,92	5,40	0,01

Bait: RINGwt	Prey	PreyGene	Spec	SpecSum	AvgSpec	NumReplicates	ctrlCounts	AvgP	MaxP	TopoAvgP	TopoMaxP	SaintScore	FoldChange	BFDR
RINGwt	P12411	Tubulin beta-1 chain	67	67	67,00	1	17|21|0	0,99	0,99	0,99	0,99	0,99	5,29	0,00
RINGwt	Q9SIM4	60S ribosomal protein L14-1	7	7	7,00	1	0|0|4	0,87	0,87	0,87	0,87	0,87	5,25	0,02
RINGwt	P17562	S-adenosylmethionine synthase 2	26	26	26,00	1	8|9|0	0,97	0,97	0,97	0,97	0,97	4,59	0,01
RINGwt	P92947	Monodehydroascorbate reductase, chloroplastic/mitochondrial	6	6	6,00	1	0|4|0	0,82	0,82	0,82	0,82	0,82	4,50	0,02
RINGwt	Q9SAJ6	Glyceraldehyde-3-phosphate dehydrogenase GAPCP1, chloroplastic	3	3	3,00	1	0|0|2	0,73	0,73	0,73	0,73	0,73	4,50	0,04
RINGwt	Q9LX65	V-type proton ATPase subunit H	3	3	3,00	1	0|2|0	0,73	0,73	0,73	0,73	0,73	4,50	0,04
RINGwt	Q9ZT91	Elongation factor Tu, mitochondrial	18	18	18,00	1	6|7|0	0,93	0,93	0,93	0,93	0,93	4,15	0,01
RINGwt	P27323	Heat shock protein 90-1	10	10	10,00	1	3|5|0	0,84	0,84	0,84	0,84	0,84	3,75	0,02
RINGwt	P29515	Tubulin beta-7 chain	88	88	88,00	1	26|36|10	0,79	0,79	0,79	0,79	0,79	3,67	0,03
RINGwt	P93819	Malate dehydrogenase 1, cytoplasmic	13	13	13,00	1	3|3|5	0,98	0,98	0,98	0,98	0,98	3,55	0,00
RINGwt	P29513	Tubulin beta-5 chain	55	55	55,00	1	17|22|8	0,97	0,97	0,97	0,97	0,97	3,51	0,01
RINGwt	P29516	Tubulin beta-8 chain	82	82	82,00	1	27|34|10	0,47	0,47	0,47	0,47	0,47	3,46	0,08
RINGwt	Q56YW9	Tubulin beta-2 chain	107	107	107,00	1	37|41|15	0,36	0,36	0,36	0,36	0,36	3,45	0,10
RINGwt	P29514	Tubulin beta-6 chain	54	54	54,00	1	16|21|10	1,00	1,00	1,00	1,00	1,00	3,45	0,00
RINGwt	P92549	ATP synthase subunit alpha, mitochondrial	20	20	20,00	1	8|10|0	0,65	0,65	0,65	0,65	0,65	3,33	0,04
RINGwt	Q9LUT2	S-adenosylmethionine synthase 4	27	27	27,00	1	12|13|0	0,45	0,45	0,45	0,45	0,45	3,24	0,08
RINGwt	O23255	Adenosylhomocysteinase 1	28	28	28,00	1	12|14|0	0,42	0,42	0,42	0,42	0,42	3,23	0,09
RINGwt	Q9SJL8	S-adenosylmethionine synthase 3	17	17	17,00	1	8|8|0	0,58	0,58	0,58	0,58	0,58	3,19	0,06
RINGwt	P29517	Tubulin beta-9 chain	70	70	70,00	1	26|33|8	0,02	0,02	0,02	0,02	0,02	3,13	0,25
RINGwt	P53494	Actin-4	29	29	29,00	1	13|15|0	0,26	0,26	0,26	0,26	0,26	3,11	0,12
RINGwt	P53497	Actin-12	29	29	29,00	1	13|15|0	0,26	0,26	0,26	0,26	0,26	3,11	0,12
RINGwt	O24456	Receptor for activated C kinase 1A	15	15	15,00	1	3|12|0	0,41	0,41	0,41	0,41	0,41	3,00	0,09
RINGwt	Q8RXU5	60S ribosomal protein L37a-2	11	11	11,00	1	0|0|11	0,53	0,53	0,53	0,53	0,53	3,00	0,06
RINGwt	P42645	14-3-3-like protein GF14 upsilon	6	6	6,00	1	2|4|0	0,57	0,57	0,57	0,57	0,57	3,00	0,06

Bait: RINGwt	Prey	PreyGene	Spec	SpecSum	AvgSpec	NumReplicates	ctrlCounts	AvgP	MaxP	TopoAvgP	TopoMaxP	SaintScore	FoldChange	BFDR
RINGwt	Q9SEU4	Serine/arginine-rich SC35-like splicing factor SCL33	5	5	5,00	1	0|0|5	0,60	0,60	0,60	0,60	0,60	3,00	0,05
RINGwt	Q9SIB9	Aconitate hydratase 3, mitochondrial	4	4	4,00	1	0|4|0	0,60	0,60	0,60	0,60	0,60	3,00	0,05
RINGwt	Q5E924	Glyceraldehyde-3-phosphate dehydrogenase GAPCP2, chloroplastic	3	3	3,00	1	0|0|3	0,58	0,58	0,58	0,58	0,58	3,00	0,05
RINGwt	Q9SF85	Adenosine kinase 1	3	3	3,00	1	2|1|0	0,52	0,52	0,52	0,52	0,52	3,00	0,07
RINGwt	P46077	14-3-3-like protein GF14 phi	3	3	3,00	1	1|2|0	0,52	0,52	0,52	0,52	0,52	3,00	0,07
RINGwt	Q01525	14-3-3-like protein GF14 omega	3	3	3,00	1	1|2|0	0,52	0,52	0,52	0,52	0,52	3,00	0,07
RINGwt	O04202	Eukaryotic translation initiation factor 3 subunit F	3	3	3,00	1	0|3|0	0,58	0,58	0,58	0,58	0,58	3,00	0,05
RINGwt	Q9LVI8	Glutamine synthetase cytosolic isozyme 1-3	1	1	1,00	1	0|1|0	0,00	0,00	0,00	0,00	0,00	3,00	0,51
RINGwt	Q9SHC8	Vesicle-associated protein 1-2, N-terminally processed	1	1	1,00	1	0|1|0	0,00	0,00	0,00	0,00	0,00	3,00	0,51
RINGwt	P24636	Tubulin beta-4 chain	71	71	71,00	1	29|35|8	0,00	0,00	0,00	0,00	0,00	2,96	0,32
RINGwt	Q9SQI8	Pyruvate dehydrogenase E2 component (dihydrolipoamide acetyltransferase)	23	23	23,00	1	0|0|25	0,10	0,10	0,10	0,10	0,10	2,76	0,19
RINGwt	Q8RYC2	Putative actin-5	11	11	11,00	1	4|4|4	0,63	0,63	0,63	0,63	0,63	2,75	0,05
RINGwt	P51818	Heat shock protein 90-3	15	15	15,00	1	5|12|0	0,15	0,15	0,15	0,15	0,15	2,65	0,16
RINGwt	O81127	Serine/arginine-rich splicing factor RSZ21	6	6	6,00	1	0|0|7	0,42	0,42	0,42	0,42	0,42	2,57	0,09
RINGwt	Q96300	14-3-3-like protein GF14 nu	5	5	5,00	1	2|4|0	0,33	0,33	0,33	0,33	0,33	2,50	0,11
RINGwt	Q42290	Probable mitochondrial-processing peptidase subunit beta, mitochondrial	5	5	5,00	1	2|4|0	0,33	0,33	0,33	0,33	0,33	2,50	0,11
RINGwt	Q9ASR1	Elongation factor 2	21	21	21,00	1	11|15|0	0,01	0,01	0,01	0,01	0,01	2,42	0,27
RINGwt	Q08682	40S ribosomal protein Sa-1	20	20	20,00	1	9|12|4	0,03	0,03	0,03	0,03	0,03	2,40	0,23
RINGwt	Q42351	60S ribosomal protein L34-1	12	12	12,00	1	3|3|9	0,09	0,09	0,09	0,09	0,09	2,40	0,19
RINGwt	Q8RWV0	Transketolase-1, chloroplastic	4	4	4,00	1	0|5|0	0,41	0,41	0,41	0,41	0,41	2,40	0,09
RINGwt	Q9SMX3	Mitochondrial outer membrane protein porin 3	25	25	25,00	1	15|16|2	0,00	0,00	0,00	0,00	0,00	2,27	0,33

Bait: RINGwt	Prey	PreyGene	Spec	SpecSum	AvgSpec	NumReplicates	ctrlCounts	AvgP	MaxP	TopoAvgP	TopoMaxP	SaintScore	FoldChange	BFDR
RINGwt	Q9C8P0	Pyruvate dehydrogenase E2 component (dihydrolipoamide acetyltransferase)	15	15	15,00	1	0|0|20	0,02	0,02	0,02	0,02	0,02	2,25	0,25
RINGwt	P42644	14-3-3-like protein GF14 psi	6	6	6,00	1	3|5|0	0,17	0,17	0,17	0,17	0,17	2,25	0,15
RINGwt	P49200	40S ribosomal protein S20-1	11	11	11,00	1	6|6|3	0,06	0,06	0,06	0,06	0,06	2,20	0,20
RINGwt	Q9C4Z6	Receptor for activated C kinase 1B	10	10	10,00	1	6|8|0	0,04	0,04	0,04	0,04	0,04	2,14	0,22
RINGwt	Q9SYG4	Oligouridylate-binding protein 1A	5	5	5,00	1	5|2|0	0,17	0,17	0,17	0,17	0,17	2,14	0,15
RINGwt	Q9LLC1	Biotin carboxyl carrier protein of acetyl-CoA carboxylase 2, chloroplastic	73	73	73,00	1	0|0|103	0,00	0,00	0,00	0,00	0,00	2,13	0,47
RINGwt	Q8L7B5	Chaperonin CPN60-like 1, mitochondrial	12	12	12,00	1	9|9|0	0,01	0,01	0,01	0,01	0,01	2,00	0,29
RINGwt	Q9LV28	Receptor for activated C kinase 1C	10	10	10,00	1	5|10|0	0,02	0,02	0,02	0,02	0,02	2,00	0,26
RINGwt	Q9LHP2	Serine/arginine-rich SC35-like splicing factor SCL30A	6	6	6,00	1	0|0|9	0,12	0,12	0,12	0,12	0,12	2,00	0,17
RINGwt	Q8LCL3	60S ribosomal protein L27-2	4	4	4,00	1	3|3|0	0,13	0,13	0,13	0,13	0,13	2,00	0,16
RINGwt	Q9LVM1	ABC transporter B family member 25, mitochondrial	2	2	2,00	1	0|0|3	0,33	0,33	0,33	0,33	0,33	2,00	0,11
RINGwt	Q9LHA4	V-type proton ATPase subunit d2	2	2	2,00	1	1|2|0	0,23	0,23	0,23	0,23	0,23	2,00	0,13
RINGwt	P83483	ATP synthase subunit beta-1, mitochondrial	17	17	17,00	1	9|12|5	0,00	0,00	0,00	0,00	0,00	1,96	0,34
RINGwt	P29197	Chaperonin CPN60, mitochondrial	21	21	21,00	1	16|15|2	0,00	0,00	0,00	0,00	0,00	1,91	0,38
RINGwt	Q42523	Methylcrotonoyl-CoA carboxylase subunit alpha, mitochondrial	156	156	156,00	1	7|13|227	0,00	0,00	0,00	0,00	0,00	1,89	0,50
RINGwt	Q9M9W1	60S ribosomal protein L22-2	5	5	5,00	1	4|3|1	0,06	0,06	0,06	0,06	0,06	1,88	0,21
RINGwt	Q42533	Biotin carboxyl carrier protein of acetyl-CoA carboxylase 1, chloroplastic	176	176	176,00	1	14|14|256	0,00	0,00	0,00	0,00	0,00	1,86	0,50
RINGwt	P0CJ46	Actin-1	26	26	26,00	1	14|17|11	0,00	0,00	0,00	0,00	0,00	1,86	0,40
RINGwt	P0CJ47	Actin-3	26	26	26,00	1	14|17|11	0,00	0,00	0,00	0,00	0,00	1,86	0,40
RINGwt	P29511	Tubulin alpha-6 chain	56	56	56,00	1	36|43|13	0,00	0,00	0,00	0,00	0,00	1,83	0,48
RINGwt	Q56WH4	Histone deacetylase HDT2	14	14	14,00	1	11|12|0	0,00	0,00	0,00	0,00	0,00	1,83	0,35

Bait: RINGwt	Prey	PreyGene	Spec	SpecSum	AvgSpec	NumReplicates	ctrlCounts	AvgP	MaxP	TopoAvgP	TopoMaxP	SaintScore	FoldChange	BFDR
RINGwt	Q9FVT2	Probable elongation factor 1-gamma 2	6	6	6,00	1	4|6|0	0,03	0,03	0,03	0,03	0,03	1,80	0,24
RINGwt	P42643	14-3-3-like protein GF14 chi	3	3	3,00	1	2|3|0	0,11	0,11	0,11	0,11	0,11	1,80	0,17
RINGwt	Q9LUW6	DEAD-box ATP-dependent RNA helicase 9, mitochondrial	3	3	3,00	1	3|2|0	0,11	0,11	0,11	0,11	0,11	1,80	0,17
RINGwt	P53496	Actin-11	29	29	29,00	1	17|18|14	0,00	0,00	0,00	0,00	0,00	1,78	0,43
RINGwt	P59259	Histone H4	13	13	13,00	1	0|2|20	0,00	0,00	0,00	0,00	0,00	1,77	0,34
RINGwt	Q9SEE9	Serine/arginine-rich splicing factor SR45	7	7	7,00	1	3|3|6	0,01	0,01	0,01	0,01	0,01	1,75	0,27
RINGwt	Q9SJT9	Coatomer subunit alpha-2	8	8	8,00	1	7|7|0	0,00	0,00	0,00	0,00	0,00	1,71	0,30
RINGwt	P0DH99	Elongation factor 1-alpha 1	102	102	102,00	1	69|82|30	0,00	0,00	0,00	0,00	0,00	1,69	0,50
RINGwt	Q94K05	T-complex protein 1 subunit theta	5	5	5,00	1	5|4|0	0,02	0,02	0,02	0,02	0,02	1,67	0,24
RINGwt	P53492	Actin-7	42	42	42,00	1	28|30|19	0,00	0,00	0,00	0,00	0,00	1,64	0,47
RINGwt	F4JWP9	109 kDa U5 small nuclear ribonucleoprotein component GFL	12	12	12,00	1	9|13|0	0,00	0,00	0,00	0,00	0,00	1,64	0,36
RINGwt	Q56WH1	Tubulin alpha-3 chain	34	34	34,00	1	24|31|8	0,00	0,00	0,00	0,00	0,00	1,62	0,46
RINGwt	B9DHQ0	Tubulin alpha-5 chain	34	34	34,00	1	24|31|8	0,00	0,00	0,00	0,00	0,00	1,62	0,46
RINGwt	P49227	60S ribosomal protein L5-2	19	19	19,00	1	17|20|0	0,00	0,00	0,00	0,00	0,00	1,54	0,43
RINGwt	Q9C522	ATP-citrate synthase beta chain protein 1	31	31	31,00	1	32|27|2	0,00	0,00	0,00	0,00	0,00	1,52	0,47
RINGwt	Q39043	Heat shock 70 kDa protein BIP2	35	35	35,00	1	27|27|16	0,00	0,00	0,00	0,00	0,00	1,50	0,48
RINGwt	Q9S9N1	Heat shock 70 kDa protein 5	30	30	30,00	1	15|21|24	0,00	0,00	0,00	0,00	0,00	1,50	0,47
RINGwt	Q93VP3	Eukaryotic translation initiation factor 5A-2	7	7	7,00	1	8|6|0	0,00	0,00	0,00	0,00	0,00	1,50	0,32
RINGwt	P42798	40S ribosomal protein S15a-1	5	5	5,00	1	2|5|3	0,01	0,01	0,01	0,01	0,01	1,50	0,29
RINGwt	Q9FVI6	Homeobox-leucine zipper protein HDG6	4	4	4,00	1	4|4|0	0,02	0,02	0,02	0,02	0,02	1,50	0,25
RINGwt	Q94AW8	Chaperone protein dnaJ 3	3	3	3,00	1	2|4|0	0,05	0,05	0,05	0,05	0,05	1,50	0,21
RINGwt	Q9SI61	Amidophosphoribosyltransferase 1, chloroplastic	1	1	1,00	1	1|1|0	0,00	0,00	0,00	0,00	0,00	1,50	0,51
RINGwt	Q8RXN4	3-hydroxyisobutyryl-CoA hydrolase-like protein 2, mitochondrial	1	1	1,00	1	0|2|0	0,00	0,00	0,00	0,00	0,00	1,50	0,51

Bait: RINGwt	Prey	PreyGene	Spec	SpecSum	AvgSpec	NumReplicates	ctrlCounts	AvgP	MaxP	TopoAvgP	TopoMaxP	SaintScore	FoldChange	BFDR
RINGwt	P29402	Calnexin homolog 1	1	1	1,00	1	0|2|0	0,00	0,00	0,00	0,00	0,00	1,50	0,51
RINGwt	Q94A52	Eukaryotic initiation factor 4A-III homolog	1	1	1,00	1	2|0|0	0,00	0,00	0,00	0,00	0,00	1,50	0,51
RINGwt	Q96292	Actin-2	22	22	22,00	1	18|18|9	0,00	0,00	0,00	0,00	0,00	1,47	0,45
RINGwt	Q9LKR3	Heat shock 70 kDa protein BIP1	34	34	34,00	1	26|28|16	0,00	0,00	0,00	0,00	0,00	1,46	0,48
RINGwt	Q9FGX1	ATP-citrate synthase beta chain protein 2	32	32	32,00	1	36|30|0	0,00	0,00	0,00	0,00	0,00	1,45	0,47
RINGwt	Q9FX54	Glyceraldehyde-3-phosphate dehydrogenase GAPC2, cytosolic	51	51	51,00	1	41|45|22	0,00	0,00	0,00	0,00	0,00	1,42	0,49
RINGwt	P11139	Tubulin alpha-1 chain	15	15	15,00	1	12|16|4	0,00	0,00	0,00	0,00	0,00	1,41	0,43
RINGwt	Q8LBI1	60S ribosomal protein L5-1	21	21	21,00	1	19|21|5	0,00	0,00	0,00	0,00	0,00	1,40	0,45
RINGwt	Q9ASS2	Protein FREE1	20	20	20,00	1	17|18|9	0,00	0,00	0,00	0,00	0,00	1,36	0,45
RINGwt	Q9LUW5	DEAD-box ATP-dependent RNA helicase 53, mitochondrial	10	10	10,00	1	10|9|3	0,00	0,00	0,00	0,00	0,00	1,36	0,39
RINGwt	Q9C9C5	60S ribosomal protein L6-3	9	9	9,00	1	0|0|20	0,00	0,00	0,00	0,00	0,00	1,35	0,37
RINGwt	P25858	Glyceraldehyde-3-phosphate dehydrogenase GAPC1, cytosolic	47	47	47,00	1	39|41|25	0,00	0,00	0,00	0,00	0,00	1,34	0,50
RINGwt	P51419	60S ribosomal protein L27-3	4	4	4,00	1	5|4|0	0,01	0,01	0,01	0,01	0,01	1,33	0,28
RINGwt	P42825	Chaperone protein dnaJ 2	4	4	4,00	1	4|5|0	0,01	0,01	0,01	0,01	0,01	1,33	0,28
RINGwt	O49485	D-3-phosphoglycerate dehydrogenase 1, chloroplastic	4	4	4,00	1	4|5|0	0,01	0,01	0,01	0,01	0,01	1,33	0,28
RINGwt	Q96293	Actin-8	22	22	22,00	1	20|20|10	0,00	0,00	0,00	0,00	0,00	1,32	0,46
RINGwt	P41377	Eukaryotic initiation factor 4A-2	25	25	25,00	1	22|27|9	0,00	0,00	0,00	0,00	0,00	1,29	0,48
RINGwt	P42794	60S ribosomal protein L11-2	12	12	12,00	1	11|14|3	0,00	0,00	0,00	0,00	0,00	1,29	0,43
RINGwt	Q9SCM3	40S ribosomal protein S2-4	6	6	6,00	1	7|7|0	0,00	0,00	0,00	0,00	0,00	1,29	0,35
RINGwt	Q94F49	Probable histone H2A.5	3	3	3,00	1	0|0|7	0,03	0,03	0,03	0,03	0,03	1,29	0,24
RINGwt	Q9S9K7	Probable histone H2AXb	3	3	3,00	1	0|0|7	0,03	0,03	0,03	0,03	0,03	1,29	0,24
RINGwt	O04848	Probable histone H2AXa	3	3	3,00	1	0|0|7	0,03	0,03	0,03	0,03	0,03	1,29	0,24
RINGwt	P41376	Eukaryotic initiation factor 4A-1	23	23	23,00	1	19|25|10	0,00	0,00	0,00	0,00	0,00	1,28	0,47
RINGwt	P31414	Pyrophosphate-energized vacuolar membrane proton pump 1	12	12	12,00	1	8|11|10	0,00	0,00	0,00	0,00	0,00	1,24	0,43

Bait: RINGwt	Prey	PreyGene	Spec	SpecSum	AvgSpec	NumReplicates	ctrlCounts	AvgP	MaxP	TopoAvgP	TopoMaxP	SaintScore	FoldChange	BFDR
RINGwt	Q56WD9	3-ketoacyl-CoA thiolase 2, peroxisomal	7	7	7,00	1	9|8|0	0,00	0,00	0,00	0,00	0,00	1,24	0,37
RINGwt	P40941	ADP,ATP carrier protein 2, mitochondrial	26	26	26,00	1	26|23|16	0,00	0,00	0,00	0,00	0,00	1,20	0,49
RINGwt	Q9SZY1	Nascent polypeptide-associated complex subunit alpha-like protein 4	10	10	10,00	1	9|9|7	0,00	0,00	0,00	0,00	0,00	1,20	0,42
RINGwt	Q9LFH5	60S ribosomal protein L12-2	6	6	6,00	1	8|7|0	0,00	0,00	0,00	0,00	0,00	1,20	0,36
RINGwt	Q9STW6	Heat shock 70 kDa protein 6, chloroplastic	6	6	6,00	1	3|4|8	0,00	0,00	0,00	0,00	0,00	1,20	0,37
RINGwt	P51427	40S ribosomal protein S5-2	6	6	6,00	1	7|8|0	0,00	0,00	0,00	0,00	0,00	1,20	0,36
RINGwt	Q9SRZ6	Cytosolic isocitrate dehydrogenase [NADP]	2	2	2,00	1	2|3|0	0,03	0,03	0,03	0,03	0,03	1,20	0,23
RINGwt	P31167	ADP,ATP carrier protein 1, mitochondrial	53	53	53,00	1	43|47|45	0,00	0,00	0,00	0,00	0,00	1,18	0,50
RINGwt	O81126	Serine/arginine-rich splicing factor RSZ22	9	9	9,00	1	1|0|22	0,00	0,00	0,00	0,00	0,00	1,17	0,41
RINGwt	Q9SJA6	Serine/arginine-rich splicing factor RSZ22A	7	7	7,00	1	0|0|18	0,00	0,00	0,00	0,00	0,00	1,17	0,37
RINGwt	Q1EBV4	Protein DNA-DAMAGE INDUCIBLE 1	16	16	16,00	1	19|12|11	0,00	0,00	0,00	0,00	0,00	1,14	0,46
RINGwt	Q9M352	60S ribosomal protein L36-2	8	8	8,00	1	1|1|19	0,00	0,00	0,00	0,00	0,00	1,14	0,40
RINGwt	Q9LNC5	110 kDa U5 small nuclear ribonucleoprotein component CLO	12	12	12,00	1	12|20|0	0,00	0,00	0,00	0,00	0,00	1,12	0,44
RINGwt	Q9ZW02	Pumilio homolog 3	3	3	3,00	1	4|4|0	0,00	0,00	0,00	0,00	0,00	1,12	0,30
RINGwt	Q42586	Orotidine 5'-phosphate decarboxylase	3	3	3,00	1	4|4|0	0,00	0,00	0,00	0,00	0,00	1,12	0,30
RINGwt	P34788	40S ribosomal protein S18	13	13	13,00	1	6|9|20	0,00	0,00	0,00	0,00	0,00	1,11	0,45
RINGwt	Q93ZM7	Chaperonin CPN60-like 2, mitochondrial	4	4	4,00	1	3|8|0	0,00	0,00	0,00	0,00	0,00	1,09	0,33
RINGwt	Q9LZ57	60S ribosomal protein L36-3	4	4	4,00	1	0|0|11	0,00	0,00	0,00	0,00	0,00	1,09	0,32
RINGwt	Q9M5K3	Dihydrolipoyl dehydrogenase 1, mitochondrial	4	4	4,00	1	4|7|0	0,00	0,00	0,00	0,00	0,00	1,09	0,34
RINGwt	Q9SSB5	26S proteasome regulatory subunit 7 homolog A	6	6	6,00	1	7|10|0	0,00	0,00	0,00	0,00	0,00	1,06	0,38
RINGwt	Q9SZ15	Protein HOMOLOG OF MAMMALIAN LYST-INTERACTING PROTEIN 5	21	21	21,00	1	25|22|13	0,00	0,00	0,00	0,00	0,00	1,05	0,49
RINGwt	Q9LIA8	UDP-glucose 6-dehydrogenase 2	7	7	7,00	1	10|10|0	0,00	0,00	0,00	0,00	0,00	1,05	0,41

Bait: RINGwt	Prey	PreyGene	Spec	SpecSum	AvgSpec	NumReplicates	ctrlCounts	AvgP	MaxP	TopoAvgP	TopoMaxP	SaintScore	FoldChange	BFDR
RINGwt	P51414	60S ribosomal protein L26-1	8	8	8,00	1	2|4|17	0,00	0,00	0,00	0,00	0,00	1,04	0,42
RINGwt	P41916	GTP-binding nuclear protein Ran-1	6	6	6,00	1	7|8|3	0,00	0,00	0,00	0,00	0,00	1,00	0,51
RINGwt	Q9FMG4	Serine/arginine-rich splicing factor SC35	5	5	5,00	1	0|0|15	0,00	0,00	0,00	0,00	0,00	1,00	0,51
RINGwt	Q9LDZ0	Heat shock 70 kDa protein 10, mitochondrial	5	5	5,00	1	9|6|0	0,00	0,00	0,00	0,00	0,00	1,00	0,51
RINGwt	Q9M5K2	Dihydrolipoyl dehydrogenase 2, mitochondrial	4	4	4,00	1	6|6|0	0,00	0,00	0,00	0,00	0,00	1,00	0,51
RINGwt	Q39172	NADPH-dependent oxidoreductase 2-alkenal reductase	3	3	3,00	1	3|6|0	0,00	0,00	0,00	0,00	0,00	1,00	0,51
RINGwt	Q9MAK9	26S proteasome regulatory subunit S10B homolog B	2	2	2,00	1	2|4|0	0,00	0,00	0,00	0,00	0,00	1,00	0,51
RINGwt	Q9SEI3	26S proteasome regulatory subunit 10B homolog A	2	2	2,00	1	2|4|0	0,00	0,00	0,00	0,00	0,00	1,00	0,51
RINGwt	P22953	Heat shock 70 kDa protein 1	103	103	103,00	1	124|137|58	0,00	0,00	0,00	0,00	0,00	0,97	0,51
RINGwt	Q9CAX6	40S ribosomal protein S14-2	7	7	7,00	1	11|11|0	0,00	0,00	0,00	0,00	0,00	0,95	0,51
RINGwt	Q9LJH8	Oligouridylate-binding protein 1C	7	7	7,00	1	11|7|4	0,00	0,00	0,00	0,00	0,00	0,95	0,51
RINGwt	Q9LTX9	Heat shock 70 kDa protein 7, chloroplastic	6	6	6,00	1	4|5|10	0,00	0,00	0,00	0,00	0,00	0,95	0,51
RINGwt	Q5XEP2	Hsp70-Hsp90 organizing protein 2	5	5	5,00	1	9|7|0	0,00	0,00	0,00	0,00	0,00	0,94	0,51
RINGwt	P57691	60S acidic ribosomal protein P0-3	5	5	5,00	1	5|11|0	0,00	0,00	0,00	0,00	0,00	0,94	0,51
RINGwt	Q8LC83	40S ribosomal protein S24-2	8	8	8,00	1	7|7|12	0,00	0,00	0,00	0,00	0,00	0,92	0,51
RINGwt	O65719	Heat shock 70 kDa protein 3	89	89	89,00	1	122|127|45	0,00	0,00	0,00	0,00	0,00	0,91	0,51
RINGwt	Q9LDD8	Methylcrotonoyl-CoA carboxylase beta chain, mitochondrial	66	66	66,00	1	3|6|209	0,00	0,00	0,00	0,00	0,00	0,91	0,51
RINGwt	P49209	60S ribosomal protein L9-1	20	20	20,00	1	26|28|12	0,00	0,00	0,00	0,00	0,00	0,91	0,51
RINGwt	Q0WNJ6	Clathrin heavy chain 1	17	17	17,00	1	25|31|0	0,00	0,00	0,00	0,00	0,00	0,91	0,51
RINGwt	P49692	60S ribosomal protein L7a-1	19	19	19,00	1	13|14|37	0,00	0,00	0,00	0,00	0,00	0,89	0,51
RINGwt	P25696	Bifunctional enolase 2/transcriptional activator	20	20	20,00	1	27|30|11	0,00	0,00	0,00	0,00	0,00	0,88	0,51
RINGwt	Q9T043	60S ribosomal protein L14-2	7	7	7,00	1	9|11|4	0,00	0,00	0,00	0,00	0,00	0,88	0,51
RINGwt	Q9LZH9	60S ribosomal protein L7a-2	16	16	16,00	1	10|11|34	0,00	0,00	0,00	0,00	0,00	0,87	0,51

Bait: RINGwt	Prey	PreyGene	Spec	SpecSum	AvgSpec	NumReplicates	ctrlCounts	AvgP	MaxP	TopoAvgP	TopoMaxP	SaintScore	FoldChange	BFDR
RINGwt	Q9LYJ9	DEAD-box ATP-dependent RNA helicase 46	8	8	8,00	1	13|15|0	0,00	0,00	0,00	0,00	0,00	0,86	0,51
RINGwt	Q9LHG8	Protein ELC	2	2	2,00	1	3|2|2	0,00	0,00	0,00	0,00	0,00	0,86	0,51
RINGwt	P46645	Aspartate aminotransferase, cytoplasmic isozyme 1	17	17	17,00	1	27|31|4	0,00	0,00	0,00	0,00	0,00	0,82	0,51
RINGwt	Q9ZU52	Fructose-bisphosphate aldolase 3, chloroplastic	3	3	3,00	1	2|2|7	0,00	0,00	0,00	0,00	0,00	0,82	0,51
RINGwt	O64728	Protein STICHEL	3	3	3,00	1	8|3|0	0,00	0,00	0,00	0,00	0,00	0,82	0,51
RINGwt	O64650	40S ribosomal protein S27-1	3	3	3,00	1	7|4|0	0,00	0,00	0,00	0,00	0,00	0,82	0,51
RINGwt	Q9LHA8	Heat shock 70 kDa protein 4	74	74	74,00	1	108|122|45	0,00	0,00	0,00	0,00	0,00	0,81	0,51
RINGwt	Q0WLB5	Clathrin heavy chain 2	16	16	16,00	1	28|31|0	0,00	0,00	0,00	0,00	0,00	0,81	0,51
RINGwt	P51413	60S ribosomal protein L17-2	8	8	8,00	1	5|7|18	0,00	0,00	0,00	0,00	0,00	0,80	0,51
RINGwt	Q8VZG7	Ribonuclease TUDOR 1	4	4	4,00	1	5|10|0	0,00	0,00	0,00	0,00	0,00	0,80	0,51
RINGwt	Q8S3C9	Dynamin-related protein 1D	4	4	4,00	1	4|3|8	0,00	0,00	0,00	0,00	0,00	0,80	0,51
RINGwt	P42697	Dynamin-related protein 1A	56	56	56,00	1	55|61|97	0,00	0,00	0,00	0,00	0,00	0,79	0,51
RINGwt	Q8H136	DEAD-box ATP-dependent RNA helicase 14	20	20	20,00	1	20|21|37	0,00	0,00	0,00	0,00	0,00	0,77	0,51
RINGwt	Q8L7U4	Co-chaperone protein p23-1	10	10	10,00	1	19|18|2	0,00	0,00	0,00	0,00	0,00	0,77	0,51
RINGwt	Q9SS17	40S ribosomal protein S24-1	8	8	8,00	1	8|9|14	0,00	0,00	0,00	0,00	0,00	0,77	0,51
RINGwt	Q9C7X7	Heat shock 70 kDa protein 18	61	61	61,00	1	95|100|45	0,00	0,00	0,00	0,00	0,00	0,76	0,51
RINGwt	Q9SRX2	60S ribosomal protein L19-1	16	16	16,00	1	7|8|48	0,00	0,00	0,00	0,00	0,00	0,76	0,51
RINGwt	P46286	60S ribosomal protein L8-1	16	16	16,00	1	13|16|34	0,00	0,00	0,00	0,00	0,00	0,76	0,51
RINGwt	Q940B0	60S ribosomal protein L18-3	14	14	14,00	1	13|11|32	0,00	0,00	0,00	0,00	0,00	0,75	0,51
RINGwt	P20649	ATPase 1, plasma membrane-type	8	8	8,00	1	14|18|0	0,00	0,00	0,00	0,00	0,00	0,75	0,51
RINGwt	Q9SIH0	40S ribosomal protein S14-1	7	7	7,00	1	11|11|6	0,00	0,00	0,00	0,00	0,00	0,75	0,51
RINGwt	Q9MAB3	Probable nucleolar protein 5-2	6	6	6,00	1	8|9|7	0,00	0,00	0,00	0,00	0,00	0,75	0,51
RINGwt	Q9SV20	Coatomer subunit beta-2	4	4	4,00	1	6|10|0	0,00	0,00	0,00	0,00	0,00	0,75	0,51
RINGwt	Q9STX5	Endoplasmin homolog	4	4	4,00	1	7|9|0	0,00	0,00	0,00	0,00	0,00	0,75	0,51
RINGwt	O04658	Probable nucleolar protein 5-1	2	2	2,00	1	3|5|0	0,00	0,00	0,00	0,00	0,00	0,75	0,51

Bait: RINGwt	Prey	PreyGene	Spec	SpecSum	AvgSpec	NumReplicates	ctrlCounts	AvgP	MaxP	TopoAvgP	TopoMaxP	SaintScore	FoldChange	BFDR
RINGwt	O64642	UTP:RNA uridylyltransferase 1	1	1	1,00	1	2|2|0	0,00	0,00	0,00	0,00	0,00	0,75	0,51
RINGwt	P22954	Heat shock 70 kDa protein 2	70	70	70,00	1	110|123|51	0,00	0,00	0,00	0,00	0,00	0,74	0,51
RINGwt	P41127	60S ribosomal protein L13-1	22	22	22,00	1	16|15|58	0,00	0,00	0,00	0,00	0,00	0,74	0,51
RINGwt	P49688	40S ribosomal protein S2-3	10	10	10,00	1	13|14|14	0,00	0,00	0,00	0,00	0,00	0,73	0,51
RINGwt	Q8LPJ7	40S ribosomal protein S26-2	6	6	6,00	1	0|0|25	0,00	0,00	0,00	0,00	0,00	0,72	0,51
RINGwt	Q8LF21	Dynamin-related protein 1C	35	35	35,00	1	41|46|60	0,00	0,00	0,00	0,00	0,00	0,71	0,51
RINGwt	Q42262	40S ribosomal protein S3a-2	13	13	13,00	1	19|19|17	0,00	0,00	0,00	0,00	0,00	0,71	0,51
RINGwt	Q42347	60S ribosomal protein L24-1	5	5	5,00	1	0|0|21	0,00	0,00	0,00	0,00	0,00	0,71	0,51
RINGwt	Q9FZ76	60S ribosomal protein L6-1	5	5	5,00	1	4|4|13	0,00	0,00	0,00	0,00	0,00	0,71	0,51
RINGwt	Q9LF33	UDP-glucose 6-dehydrogenase 3	5	5	5,00	1	8|13|0	0,00	0,00	0,00	0,00	0,00	0,71	0,51
RINGwt	Q9LNB6	Hsp70-Hsp90 organizing protein 1	30	30	30,00	1	44|45|39	0,00	0,00	0,00	0,00	0,00	0,70	0,51
RINGwt	Q9SJF1	GTPase LSG1-2	7	7	7,00	1	12|11|7	0,00	0,00	0,00	0,00	0,00	0,70	0,51
RINGwt	P49205	40S ribosomal protein S17-1	3	3	3,00	1	3|2|8	0,00	0,00	0,00	0,00	0,00	0,69	0,51
RINGwt	Q9FVQ1	Nucleolin 1	6	6	6,00	1	14|13|0	0,00	0,00	0,00	0,00	0,00	0,67	0,51
RINGwt	O23654	V-type proton ATPase catalytic subunit A	4	4	4,00	1	2|5|11	0,00	0,00	0,00	0,00	0,00	0,67	0,51
RINGwt	Q9LIK0	Plastidial pyruvate kinase 1, chloroplastic	2	2	2,00	1	4|5|0	0,00	0,00	0,00	0,00	0,00	0,67	0,51
RINGwt	Q9FLT0	Ribonuclease TUDOR 2	8	8	8,00	1	19|18|0	0,00	0,00	0,00	0,00	0,00	0,65	0,51
RINGwt	Q9M339	40S ribosomal protein S3-2	7	7	7,00	1	15|18|0	0,00	0,00	0,00	0,00	0,00	0,64	0,51
RINGwt	Q9ZUT9	40S ribosomal protein S5-1	6	6	6,00	1	5|7|16	0,00	0,00	0,00	0,00	0,00	0,64	0,51
RINGwt	Q9CAN8	Lysophospholipid acyltransferase 2	4	4	4,00	1	9|10|0	0,00	0,00	0,00	0,00	0,00	0,63	0,51
RINGwt	Q42064	60S ribosomal protein L8-3	13	13	13,00	1	14|16|33	0,00	0,00	0,00	0,00	0,00	0,62	0,51
RINGwt	Q9CAV0	40S ribosomal protein S3a-1	8	8	8,00	1	13|18|8	0,00	0,00	0,00	0,00	0,00	0,62	0,51
RINGwt	Q8L8Y0	40S ribosomal protein S2-1	6	6	6,00	1	10|11|8	0,00	0,00	0,00	0,00	0,00	0,62	0,51
RINGwt	Q93VB8	40S ribosomal protein S2-2	6	6	6,00	1	10|11|8	0,00	0,00	0,00	0,00	0,00	0,62	0,51
RINGwt	Q9SEI4	26S proteasome regulatory subunit 6B homolog	5	5	5,00	1	9|13|2	0,00	0,00	0,00	0,00	0,00	0,62	0,51

Bait: RINGwt	Prey	PreyGene	Spec	SpecSum	AvgSpec	NumReplicates	ctrlCounts	AvgP	MaxP	TopoAvgP	TopoMaxP	SaintScore	FoldChange	BFDR
RINGwt	Q8GUM2	Heat shock 70 kDa protein 9, mitochondrial	14	14	14,00	1	27|28|15	0,00	0,00	0,00	0,00	0,00	0,60	0,51
RINGwt	Q84VW9	Phosphoenolpyruvate carboxylase 3	8	8	8,00	1	24|16|0	0,00	0,00	0,00	0,00	0,00	0,60	0,51
RINGwt	Q9LUQ6	60S ribosomal protein L19-2	4	4	4,00	1	0|0|20	0,00	0,00	0,00	0,00	0,00	0,60	0,51
RINGwt	Q8LD03	40S ribosomal protein S7-3	3	3	3,00	1	7|8|0	0,00	0,00	0,00	0,00	0,00	0,60	0,51
RINGwt	Q9FFT4	Pyruvate decarboxylase 2	1	1	1,00	1	2|3|0	0,00	0,00	0,00	0,00	0,00	0,60	0,51
RINGwt	Q38929	Isopentenyl-diphosphate Delta-isomerase I, chloroplastic	1	1	1,00	1	2|3|0	0,00	0,00	0,00	0,00	0,00	0,60	0,51
RINGwt	Q93W34	Polyadenylate-binding protein RBP45C	1	1	1,00	1	2|3|0	0,00	0,00	0,00	0,00	0,00	0,60	0,51
RINGwt	F4ICD9	Protein transport protein SEC31 homolog A	1	1	1,00	1	0|0|5	0,00	0,00	0,00	0,00	0,00	0,60	0,51
RINGwt	Q9SIP7	40S ribosomal protein S3-1	8	8	8,00	1	17|18|6	0,00	0,00	0,00	0,00	0,00	0,59	0,51
RINGwt	O23515	60S ribosomal protein L15-1	14	14	14,00	1	13|11|48	0,00	0,00	0,00	0,00	0,00	0,58	0,51
RINGwt	Q9LJE5	YTH domain-containing protein ECT2	11	11	11,00	1	23|27|7	0,00	0,00	0,00	0,00	0,00	0,58	0,51
RINGwt	Q9FMU6	Mitochondrial phosphate carrier protein 3, mitochondrial	5	5	5,00	1	10|13|3	0,00	0,00	0,00	0,00	0,00	0,58	0,51
RINGwt	P49693	60S ribosomal protein L19-3	7	7	7,00	1	4|6|27	0,00	0,00	0,00	0,00	0,00	0,57	0,51
RINGwt	Q9ZPI1	Lysine--tRNA ligase, cytoplasmic	7	7	7,00	1	15|22|0	0,00	0,00	0,00	0,00	0,00	0,57	0,51
RINGwt	Q96266	Glutathione S-transferase F8, chloroplastic	4	4	4,00	1	8|13|0	0,00	0,00	0,00	0,00	0,00	0,57	0,51
RINGwt	Q8L5Y6	Cullin-associated NEDD8-dissociated protein 1	25	25	25,00	1	67|62|5	0,00	0,00	0,00	0,00	0,00	0,56	0,51
RINGwt	P0DH91	ADP-ribosylation factor 2-B	5	5	5,00	1	13|14|0	0,00	0,00	0,00	0,00	0,00	0,56	0,51
RINGwt	P29976	Phospho-2-dehydro-3-deoxyheptonate aldolase 1, chloroplastic	5	5	5,00	1	13|14|0	0,00	0,00	0,00	0,00	0,00	0,56	0,51
RINGwt	P19456	ATPase 2, plasma membrane-type	8	8	8,00	1	17|27|0	0,00	0,00	0,00	0,00	0,00	0,55	0,51
RINGwt	O50008	5-methyltetrahydropteroyltriglutamate --homocysteine methyltransferase 1	8	8	8,00	1	23|21|0	0,00	0,00	0,00	0,00	0,00	0,55	0,51
RINGwt	Q9LYK9	40S ribosomal protein S26-3	6	6	6,00	1	3|4|26	0,00	0,00	0,00	0,00	0,00	0,55	0,51
RINGwt	P46644	Aspartate aminotransferase 3, chloroplastic	4	4	4,00	1	11|11|0	0,00	0,00	0,00	0,00	0,00	0,55	0,51

Bait: RINGwt	Prey	PreyGene	Spec	SpecSum	AvgSpec	NumReplicates	ctrlCounts	AvgP	MaxP	TopoAvgP	TopoMaxP	SaintScore	FoldChange	BFDR
RINGwt	O04487	Probable elongation factor 1-gamma 1	2	2	2,00	1	5|6|0	0,00	0,00	0,00	0,00	0,00	0,55	0,51
RINGwt	Q9SEI2	26S proteasome regulatory subunit 6A homolog A	2	2	2,00	1	4|5|2	0,00	0,00	0,00	0,00	0,00	0,55	0,51
RINGwt	O04019	26S proteasome regulatory subunit 6A homolog B	2	2	2,00	1	4|5|2	0,00	0,00	0,00	0,00	0,00	0,55	0,51
RINGwt	Q9C658	Protein decapping 5	2	2	2,00	1	5|6|0	0,00	0,00	0,00	0,00	0,00	0,55	0,51
RINGwt	Q9LXG1	40S ribosomal protein S9-1	13	13	13,00	1	13|16|43	0,00	0,00	0,00	0,00	0,00	0,54	0,51
RINGwt	P49206	40S ribosomal protein S26-1	6	6	6,00	1	4|4|26	0,00	0,00	0,00	0,00	0,00	0,53	0,51
RINGwt	F4K1Z0	YTH domain-containing protein ECT3	4	4	4,00	1	8|7|8	0,00	0,00	0,00	0,00	0,00	0,52	0,51
RINGwt	P17094	60S ribosomal protein L3-1	23	23	23,00	1	36|42|58	0,00	0,00	0,00	0,00	0,00	0,51	0,51
RINGwt	P60039	60S ribosomal protein L7-3	9	9	9,00	1	14|17|22	0,00	0,00	0,00	0,00	0,00	0,51	0,51
RINGwt	Q9FEF8	rRNA 2'-O-methyltransferase fibrillarin 1	4	4	4,00	1	11|11|2	0,00	0,00	0,00	0,00	0,00	0,50	0,51
RINGwt	Q9SMW7	Basic transcription factor 3	3	3	3,00	1	8|8|2	0,00	0,00	0,00	0,00	0,00	0,50	0,51
RINGwt	Q945Q1	Cysteine proteinase inhibitor 1	2	2	2,00	1	4|4|4	0,00	0,00	0,00	0,00	0,00	0,50	0,51
RINGwt	Q9ZU46	Receptor protein kinase-like protein ZAR1	1	1	1,00	1	0|0|6	0,00	0,00	0,00	0,00	0,00	0,50	0,51
RINGwt	Q949R9	Mitochondrial pyruvate carrier 1	1	1	1,00	1	1|1|4	0,00	0,00	0,00	0,00	0,00	0,50	0,51
RINGwt	O82462	Glutamate--tRNA ligase, cytoplasmic	1	1	1,00	1	0|6|0	0,00	0,00	0,00	0,00	0,00	0,50	0,51
RINGwt	Q9MAH0	Phosphoenolpyruvate carboxylase 1	11	11	11,00	1	34|28|6	0,00	0,00	0,00	0,00	0,00	0,49	0,51
RINGwt	Q42340	40S ribosomal protein S16-3	9	9	9,00	1	12|11|32	0,00	0,00	0,00	0,00	0,00	0,49	0,51
RINGwt	P17745	Elongation factor Tu, chloroplastic	6	6	6,00	1	19|16|2	0,00	0,00	0,00	0,00	0,00	0,49	0,51
RINGwt	Q9SJQ9	Fructose-bisphosphate aldolase 6, cytosolic	31	31	31,00	1	82|66|48	0,00	0,00	0,00	0,00	0,00	0,47	0,51
RINGwt	Q9T029	40S ribosomal protein S25-4	3	3	3,00	1	5|6|8	0,00	0,00	0,00	0,00	0,00	0,47	0,51
RINGwt	P60040	60S ribosomal protein L7-2	10	10	10,00	1	16|23|26	0,00	0,00	0,00	0,00	0,00	0,46	0,51
RINGwt	O23212	Splicing factor U2af large subunit A	2	2	2,00	1	2|0|11	0,00	0,00	0,00	0,00	0,00	0,46	0,51
RINGwt	Q9LQ55	Dynamin-2B	35	35	35,00	1	54|60|118	0,00	0,00	0,00	0,00	0,00	0,45	0,51

Bait: RINGwt	Prey	PreyGene	Spec	SpecSum	AvgSpec	NumReplicates	ctrlCounts	AvgP	MaxP	TopoAvgP	TopoMaxP	SaintScore	FoldChange	BFDR
RINGwt	Q9C5U3	26S proteasome regulatory subunit 8 homolog A	3	3	3,00	1	10|11|0	0,00	0,00	0,00	0,00	0,00	0,43	0,51
RINGwt	P51430	40S ribosomal protein S6-2	8	8	8,00	1	17|20|20	0,00	0,00	0,00	0,00	0,00	0,42	0,51
RINGwt	Q9LF98	Fructose-bisphosphate aldolase 8, cytosolic	41	41	41,00	1	114|102|87	0,00	0,00	0,00	0,00	0,00	0,41	0,51
RINGwt	Q93VG5	40S ribosomal protein S8-1	10	10	10,00	1	28|32|14	0,00	0,00	0,00	0,00	0,00	0,41	0,51
RINGwt	Q9FLF0	40S ribosomal protein S9-2	4	4	4,00	1	0|0|29	0,00	0,00	0,00	0,00	0,00	0,41	0,51
RINGwt	Q05431	L-ascorbate peroxidase 1, cytosolic	3	3	3,00	1	11|11|0	0,00	0,00	0,00	0,00	0,00	0,41	0,51
RINGwt	Q94CE5	Gamma-aminobutyrate transaminase POP2, mitochondrial	2	2	2,00	1	7|8|0	0,00	0,00	0,00	0,00	0,00	0,40	0,51
RINGwt	Q9LFW1	UDP-arabinopyranose mutase 2	2	2	2,00	1	7|8|0	0,00	0,00	0,00	0,00	0,00	0,40	0,51
RINGwt	P49204	40S ribosomal protein S4-2	14	14	14,00	1	27|33|47	0,00	0,00	0,00	0,00	0,00	0,39	0,51
RINGwt	Q96327	ERBB-3 BINDING PROTEIN 1	8	8	8,00	1	31|23|7	0,00	0,00	0,00	0,00	0,00	0,39	0,51
RINGwt	P38666	60S ribosomal protein L24-2	5	5	5,00	1	5|6|27	0,00	0,00	0,00	0,00	0,00	0,39	0,51
RINGwt	Q9FNX5	Dynamin-related protein 1E	5	5	5,00	1	11|12|16	0,00	0,00	0,00	0,00	0,00	0,38	0,51
RINGwt	Q94BQ2	26S proteasome regulatory subunit 8 homolog B	3	3	3,00	1	10|12|2	0,00	0,00	0,00	0,00	0,00	0,38	0,51
RINGwt	P38420	DNA-directed RNA polymerase II subunit 2	1	1	1,00	1	3|5|0	0,00	0,00	0,00	0,00	0,00	0,38	0,51
RINGwt	O64843	Polyadenylate-binding protein-interacting protein 7	1	1	1,00	1	4|4|0	0,00	0,00	0,00	0,00	0,00	0,38	0,51
RINGwt	Q9XI93	Oleosin-B3-like protein	3	3	3,00	1	16|9|0	0,00	0,00	0,00	0,00	0,00	0,36	0,51
RINGwt	O48549	40S ribosomal protein S6-1	8	8	8,00	1	18|22|29	0,00	0,00	0,00	0,00	0,00	0,35	0,51
RINGwt	Q0WQ57	Auxilin-related protein 2	2	2	2,00	1	9|8|0	0,00	0,00	0,00	0,00	0,00	0,35	0,51
RINGwt	Q9SF40	60S ribosomal protein L4-1	23	23	23,00	1	23|26|154	0,00	0,00	0,00	0,00	0,00	0,34	0,51
RINGwt	P49691	60S ribosomal protein L4-2	22	22	22,00	1	24|27|144	0,00	0,00	0,00	0,00	0,00	0,34	0,51
RINGwt	Q9LTT8	Enhancer of mRNA-decapping protein 4	17	17	17,00	1	68|70|15	0,00	0,00	0,00	0,00	0,00	0,33	0,51
RINGwt	Q9SIV2	26S proteasome non-ATPase regulatory subunit 2 homolog A	3	3	3,00	1	10|17|0	0,00	0,00	0,00	0,00	0,00	0,33	0,51
RINGwt	Q08112	40S ribosomal protein S15-1	2	2	2,00	1	3|4|11	0,00	0,00	0,00	0,00	0,00	0,33	0,51

Bait: RINGwt	Prey	PreyGene	Spec	SpecSum	AvgSpec	NumReplicates	ctrlCounts	AvgP	MaxP	TopoAvgP	TopoMaxP	SaintScore	FoldChange	BFDR
RINGwt	Q9SL67	26S proteasome regulatory subunit 4 homolog B	2	2	2,00	1	9|9|0	0,00	0,00	0,00	0,00	0,00	0,33	0,51
RINGwt	Q9SE83	Dynamin-2A	24	24	24,00	1	55|65|102	0,00	0,00	0,00	0,00	0,00	0,32	0,51
RINGwt	Q9FJA6	40S ribosomal protein S3-3	4	4	4,00	1	15|17|6	0,00	0,00	0,00	0,00	0,00	0,32	0,51
RINGwt	Q5GM68	Phosphoenolpyruvate carboxylase 2	4	4	4,00	1	20|18|0	0,00	0,00	0,00	0,00	0,00	0,32	0,51
RINGwt	Q9FKA5	Uncharacterized protein At5g39570	9	9	9,00	1	39|36|16	0,00	0,00	0,00	0,00	0,00	0,30	0,51
RINGwt	Q9C514	40S ribosomal protein S7-1	1	1	1,00	1	3|4|3	0,00	0,00	0,00	0,00	0,00	0,30	0,51
RINGwt	Q9STH1	Hsp70-Hsp90 organizing protein 3	1	1	1,00	1	4|6|0	0,00	0,00	0,00	0,00	0,00	0,30	0,51
RINGwt	Q9LQ04	Bifunctional dTDP-4-dehydrorhamnose 3,5-epimerase/dTDP-4-dehydrorhamnose reductase	2	2	2,00	1	11|10|0	0,00	0,00	0,00	0,00	0,00	0,29	0,51
RINGwt	Q9LTT9	Varicose-related protein	8	8	8,00	1	49|34|5	0,00	0,00	0,00	0,00	0,00	0,27	0,51
RINGwt	Q9C5Z1	Eukaryotic translation initiation factor 3 subunit B	5	5	5,00	1	30|25|0	0,00	0,00	0,00	0,00	0,00	0,27	0,51
RINGwt	Q9SB63	Protein MODIFIER OF SNC1 1	3	3	3,00	1	17|16|0	0,00	0,00	0,00	0,00	0,00	0,27	0,51
RINGwt	Q38882	Phospholipase D alpha 1	33	33	33,00	1	176|159|68	0,00	0,00	0,00	0,00	0,00	0,25	0,51
RINGwt	Q9SIK2	40S ribosomal protein S25-2	1	1	1,00	1	2|4|6	0,00	0,00	0,00	0,00	0,00	0,25	0,51
RINGwt	Q39189	DEAD-box ATP-dependent RNA helicase 7	1	1	1,00	1	5|7|0	0,00	0,00	0,00	0,00	0,00	0,25	0,51
RINGwt	O82204	60S ribosomal protein L28-1	2	2	2,00	1	5|4|17	0,00	0,00	0,00	0,00	0,00	0,23	0,51
RINGwt	Q9LT08	26S proteasome non-ATPase regulatory subunit 14 homolog	1	1	1,00	1	3|10|0	0,00	0,00	0,00	0,00	0,00	0,23	0,51
RINGwt	P49690	60S ribosomal protein L23	2	2	2,00	1	3|3|22	0,00	0,00	0,00	0,00	0,00	0,21	0,51
RINGwt	O49160	Eukaryotic translation initiation factor 3 subunit C	2	2	2,00	1	13|17|0	0,00	0,00	0,00	0,00	0,00	0,20	0,51
RINGwt	P49637	60S ribosomal protein L27a-3	3	3	3,00	1	10|10|30	0,00	0,00	0,00	0,00	0,00	0,18	0,51
RINGwt	Q8S9J8	Probable clathrin assembly protein At4g32285	1	1	1,00	1	8|9|0	0,00	0,00	0,00	0,00	0,00	0,18	0,51
RINGwt	F4I1L3	Acetyl-CoA carboxylase 2	9	9	9,00	1	11|11|139	0,00	0,00	0,00	0,00	0,00	0,17	0,51
RINGwt	Q9LR33	60S ribosomal protein L27a-2	3	3	3,00	1	10|12|31	0,00	0,00	0,00	0,00	0,00	0,17	0,51
RINGwt	P11574	V-type proton ATPase subunit B1	4	4	4,00	1	31|29|24	0,00	0,00	0,00	0,00	0,00	0,14	0,51

Bait: RINGwt	Prey	PreyGene	Spec	SpecSum	AvgSpec	NumReplicates	ctrlCounts	AvgP	MaxP	TopoAvgP	TopoMaxP	SaintScore	FoldChange	BFDR
RINGwt	O04983	Biotin carboxylase, chloroplastic	7	7	7,00	1	5|9|150	0,00	0,00	0,00	0,00	0,00	0,13	0,51
RINGwt	P51418	60S ribosomal protein L18a-2	5	5	5,00	1	13|20|81	0,00	0,00	0,00	0,00	0,00	0,13	0,51
RINGwt	P59224	40S ribosomal protein S13-2	2	2	2,00	1	8|7|30	0,00	0,00	0,00	0,00	0,00	0,13	0,51
RINGwt	Q9LV09	Protein BOBBER 1	1	1	1,00	1	11|11|1	0,00	0,00	0,00	0,00	0,00	0,13	0,51
RINGwt	Q9T074	Phosphoenolpyruvate carboxykinase (ATP)	8	8	8,00	1	95|85|17	0,00	0,00	0,00	0,00	0,00	0,12	0,51
RINGwt	P49211	60S ribosomal protein L32-1	1	1	1,00	1	4|3|21	0,00	0,00	0,00	0,00	0,00	0,11	0,51
RINGwt	O82647	Pyruvate decarboxylase 1	1	1	1,00	1	14|13|0	0,00	0,00	0,00	0,00	0,00	0,11	0,51
RINGwt	O23254	Serine hydroxymethyltransferase 4	1	1	1,00	1	13|14|0	0,00	0,00	0,00	0,00	0,00	0,11	0,51
RINGwt	Q76E23	Eukaryotic translation initiation factor 4G	2	2	2,00	1	33|33|0	0,00	0,00	0,00	0,00	0,00	0,09	0,51
RINGwt	Q9FMM3	Protein ESSENTIAL FOR POTEXVIRUS ACCUMULATION 1	2	2	2,00	1	55|46|0	0,00	0,00	0,00	0,00	0,00	0,06	0,51
RINGwt	Q38970	Acetyl-CoA carboxylase 1	3	3	3,00	1	22|25|141	0,00	0,00	0,00	0,00	0,00	0,05	0,51

Bait: RINGwt_z	Prey	PreyGene	Spec	SpecSum	AvgSpec	NumReplicates	ctrlCounts	AvgP	MaxP	TopoAvgP	TopoMaxP	SaintScore	FoldChange	BFDR
RINGwt_z	Q8RWZ3	Probable acyl-CoA dehydrogenase IBR3	79	79	79,00	1	0|0|0	1,00	1,00	1,00	1,00	1,00	790,00	0,00
RINGwt_z	Q0WV25	Tubulin alpha-4 chain	68	68	68,00	1	0|0|0	1,00	1,00	1,00	1,00	1,00	680,00	0,00
RINGwt_z	P55737	Heat shock protein 90-2	34	34	34,00	1	0|0|0	1,00	1,00	1,00	1,00	1,00	340,00	0,00
RINGwt_z	P23321	Oxygen-evolving enhancer protein 1-1, chloroplastic	25	25	25,00	1	0|0|0	1,00	1,00	1,00	1,00	1,00	250,00	0,00
RINGwt_z	Q9S841	Oxygen-evolving enhancer protein 1-2, chloroplastic	22	22	22,00	1	0|0|0	1,00	1,00	1,00	1,00	1,00	220,00	0,00
RINGwt_z	Q94AR8	3-isopropylmalate dehydratase large subunit, chloroplastic	20	20	20,00	1	0|0|0	1,00	1,00	1,00	1,00	1,00	200,00	0,00
RINGwt_z	P57106	Malate dehydrogenase 2, cytoplasmic	14	14	14,00	1	0|0|0	1,00	1,00	1,00	1,00	1,00	140,00	0,00
RINGwt_z	Q9XFT3	Oxygen-evolving enhancer protein 3-1, chloroplastic	11	11	11,00	1	0|0|0	1,00	1,00	1,00	1,00	1,00	110,00	0,00
RINGwt_z	P50318	Phosphoglycerate kinase 2, chloroplastic	8	8	8,00	1	0|0|0	1,00	1,00	1,00	1,00	1,00	80,00	0,00
RINGwt_z	Q41932	Oxygen-evolving enhancer protein 3-2, chloroplastic	8	8	8,00	1	0|0|0	1,00	1,00	1,00	1,00	1,00	80,00	0,00
RINGwt_z	Q9LD57	Phosphoglycerate kinase 1, chloroplastic	8	8	8,00	1	0|0|0	1,00	1,00	1,00	1,00	1,00	80,00	0,00
RINGwt_z	Q9LZ45	Histone H2B.9	7	7	7,00	1	0|0|0	1,00	1,00	1,00	1,00	1,00	70,00	0,00
RINGwt_z	Q9SRH5	Mitochondrial outer membrane protein porin 1	7	7	7,00	1	0|0|0	1,00	1,00	1,00	1,00	1,00	70,00	0,00
RINGwt_z	Q9FM01	UDP-glucose 6-dehydrogenase 4	7	7	7,00	1	0|0|0	1,00	1,00	1,00	1,00	1,00	70,00	0,00
RINGwt_z	P21238	Chaperonin 60 subunit alpha 1, chloroplastic	7	7	7,00	1	0|0|0	1,00	1,00	1,00	1,00	1,00	70,00	0,00

Bait: RINGwt_z	Prey	PreyGene	Spec	SpecSum	AvgSpec	NumReplicates	ctrlCounts	AvgP	MaxP	TopoAvgP	TopoMaxP	SaintScore	FoldChange	BFDR
RINGwt_z	Q9STY6	40S ribosomal protein S20-2	6	6	6,00	1	0|0|0	1,00	1,00	1,00	1,00	1,00	60,00	0,00
RINGwt_z	Q9SU58	ATPase 4, plasma membrane-type	6	6	6,00	1	0|0|0	1,00	1,00	1,00	1,00	1,00	60,00	0,00
RINGwt_z	Q9ZP06	Malate dehydrogenase 1, mitochondrial	6	6	6,00	1	0|0|0	1,00	1,00	1,00	1,00	1,00	60,00	0,00
RINGwt_z	P48348	14-3-3-like protein GF14 kappa	6	6	6,00	1	0|0|0	1,00	1,00	1,00	1,00	1,00	60,00	0,00
RINGwt_z	P59230	60S ribosomal protein L10a-2	6	6	6,00	1	0|0|0	1,00	1,00	1,00	1,00	1,00	60,00	0,00
RINGwt_z	P10896	Ribulose bisphosphate carboxylase/oxygenase activase, chloroplastic	6	6	6,00	1	0|0|0	1,00	1,00	1,00	1,00	1,00	60,00	0,00
RINGwt_z	O49513	Ras-related protein RABA1e	6	6	6,00	1	0|0|0	1,00	1,00	1,00	1,00	1,00	60,00	0,00
RINGwt_z	Q9LVC9	60S acidic ribosomal protein P3-2	6	6	6,00	1	0|0|0	1,00	1,00	1,00	1,00	1,00	60,00	0,00
RINGwt_z	O22254	Putative 60S ribosomal protein L18-1	5	5	5,00	1	0|0|0	1,00	1,00	1,00	1,00	1,00	50,00	0,00
RINGwt_z	Q8VZ19	60S ribosomal protein L30-2	5	5	5,00	1	0|0|0	1,00	1,00	1,00	1,00	1,00	50,00	0,00
RINGwt_z	O04316	Nitrile-specifier protein 4	5	5	5,00	1	0|0|0	1,00	1,00	1,00	1,00	1,00	50,00	0,00
RINGwt_z	Q9FFR3	6-phosphogluconate dehydrogenase, decarboxylating 3, chloroplastic	5	5	5,00	1	0|0|0	1,00	1,00	1,00	1,00	1,00	50,00	0,00
RINGwt_z	Q9FGI6	NADH dehydrogenase [ubiquinone] iron-sulfur protein 1, mitochondrial	5	5	5,00	1	0|0|0	1,00	1,00	1,00	1,00	1,00	50,00	0,00
RINGwt_z	Q9ZU25	Probable mitochondrial-processing peptidase subunit alpha-1, mitochondrial	5	5	5,00	1	0|0|0	1,00	1,00	1,00	1,00	1,00	50,00	0,00
RINGwt_z	Q8LCE1	Glutamine synthetase cytosolic isozyme 1-2	5	5	5,00	1	0|0|0	1,00	1,00	1,00	1,00	1,00	50,00	0,00
RINGwt_z	Q9FXA2	Polyadenylate-binding protein 8	5	5	5,00	1	0|0|0	1,00	1,00	1,00	1,00	1,00	50,00	0,00
RINGwt_z	Q9ZQ18	Cytoplasmic 60S subunit biogenesis factor REI1 homolog 2	5	5	5,00	1	0|0|0	1,00	1,00	1,00	1,00	1,00	50,00	0,00
RINGwt_z	O03042	Ribulose bisphosphate carboxylase large chain	5	5	5,00	1	0|0|0	1,00	1,00	1,00	1,00	1,00	50,00	0,00
RINGwt_z	Q56WN1	Glutamine synthetase cytosolic isozyme 1-1	5	5	5,00	1	0|0|0	1,00	1,00	1,00	1,00	1,00	50,00	0,00
RINGwt_z	Q9FMD9	Glutamine synthetase cytosolic isozyme 1-4	5	5	5,00	1	0|0|0	1,00	1,00	1,00	1,00	1,00	50,00	0,00
RINGwt_z	P28769	T-complex protein 1 subunit alpha	5	5	5,00	1	0|0|0	1,00	1,00	1,00	1,00	1,00	50,00	0,00

Bait: RINGwt_z	Prey	PreyGene	Spec	SpecSum	AvgSpec	NumReplicates	ctrlCounts	AvgP	MaxP	TopoAvgP	TopoMaxP	SaintScore	FoldChange	BFDR
RINGwt_z	Q8L3X8	Serine/arginine-rich SC35-like splicing factor SCL30	4	4	4,00	1	0|0|0	1,00	1,00	1,00	1,00	1,00	40,00	0,00
RINGwt_z	Q42556	ATPase 9, plasma membrane-type	4	4	4,00	1	0|0|0	1,00	1,00	1,00	1,00	1,00	40,00	0,00
RINGwt_z	Q38900	Peptidyl-prolyl cis-trans isomerase CYP19-1	4	4	4,00	1	0|0|0	1,00	1,00	1,00	1,00	1,00	40,00	0,00
RINGwt_z	P93004	Aquaporin PIP2-7	4	4	4,00	1	0|0|0	1,00	1,00	1,00	1,00	1,00	40,00	0,00
RINGwt_z	P92939	Calcium-transporting ATPase 1, endoplasmic reticulum-type	4	4	4,00	1	0|0|0	1,00	1,00	1,00	1,00	1,00	40,00	0,00
RINGwt_z	P20115	Citrate synthase 4, mitochondrial	4	4	4,00	1	0|0|0	1,00	1,00	1,00	1,00	1,00	40,00	0,00
RINGwt_z	Q9M084	Aspartate--tRNA ligase 2, cytoplasmic	4	4	4,00	1	0|0|0	1,00	1,00	1,00	1,00	1,00	40,00	0,00
RINGwt_z	P56765	Acetyl-coenzyme A carboxylase carboxyl transferase subunit beta, chloroplastic	4	4	4,00	1	0|0|0	1,00	1,00	1,00	1,00	1,00	40,00	0,00
RINGwt_z	Q9SYP2	Pyrophosphate--fructose 6-phosphate 1-phosphotransferase subunit alpha 1	4	4	4,00	1	0|0|0	1,00	1,00	1,00	1,00	1,00	40,00	0,00
RINGwt_z	Q9ZPS7	Transmembrane 9 superfamily member 3	4	4	4,00	1	0|0|0	1,00	1,00	1,00	1,00	1,00	40,00	0,00
RINGwt_z	O80501	Ras-related protein RABH1b	4	4	4,00	1	0|0|0	1,00	1,00	1,00	1,00	1,00	40,00	0,00
RINGwt_z	P17597	Acetolactate synthase, chloroplastic	4	4	4,00	1	0|0|0	1,00	1,00	1,00	1,00	1,00	40,00	0,00
RINGwt_z	Q9LV21	T-complex protein 1 subunit delta	4	4	4,00	1	0|0|0	1,00	1,00	1,00	1,00	1,00	40,00	0,00
RINGwt_z	Q42589	Non-specific lipid-transfer protein 1	3	3	3,00	1	0|0|0	1,00	1,00	1,00	1,00	1,00	30,00	0,00
RINGwt_z	Q8W4S4	V-type proton ATPase subunit a3	3	3	3,00	1	0|0|0	1,00	1,00	1,00	1,00	1,00	30,00	0,00
RINGwt_z	Q8VZB9	60S ribosomal protein L10a-1	3	3	3,00	1	0|0|0	1,00	1,00	1,00	1,00	1,00	30,00	0,00
RINGwt_z	Q93Y35	26S proteasome non-ATPase regulatory subunit 6 homolog	3	3	3,00	1	0|0|0	1,00	1,00	1,00	1,00	1,00	30,00	0,00
RINGwt_z	Q9FVE6	Histone deacetylase HDT1	3	3	3,00	1	0|0|0	1,00	1,00	1,00	1,00	1,00	30,00	0,00
RINGwt_z	P0DH95	Calmodulin-1	3	3	3,00	1	0|0|0	1,00	1,00	1,00	1,00	1,00	30,00	0,00
RINGwt_z	P0DH96	Calmodulin-4	3	3	3,00	1	0|0|0	1,00	1,00	1,00	1,00	1,00	30,00	0,00
RINGwt_z	P25819	Catalase-2	3	3	3,00	1	0|0|0	1,00	1,00	1,00	1,00	1,00	30,00	0,00
RINGwt_z	Q8L7N0	T-complex protein 1 subunit zeta 2	3	3	3,00	1	0|0|0	1,00	1,00	1,00	1,00	1,00	30,00	0,00

Bait: RINGwt_z	Prey	PreyGene	Spec	SpecSum	AvgSpec	NumReplicates	ctrlCounts	AvgP	MaxP	TopoAvgP	TopoMaxP	SaintScore	FoldChange	BFDR
RINGwt_z	Q93VM8	Copper transporter 5	3	3	3,00	1	0|0|0	1,00	1,00	1,00	1,00	1,00	30,00	0,00
RINGwt_z	Q84WM9	Elongation factor 1-beta 1	3	3	3,00	1	0|0|0	1,00	1,00	1,00	1,00	1,00	30,00	0,00
RINGwt_z	Q9C9K3	Pyrophosphate--fructose 6-phosphate 1-phosphotransferase subunit alpha 2	3	3	3,00	1	0|0|0	1,00	1,00	1,00	1,00	1,00	30,00	0,00
RINGwt_z	Q680A5	Ribose-phosphate pyrophosphokinase 4	3	3	3,00	1	0|0|0	1,00	1,00	1,00	1,00	1,00	30,00	0,00
RINGwt_z	Q94A28	Aconitate hydratase 2, mitochondrial	3	3	3,00	1	0|0|0	1,00	1,00	1,00	1,00	1,00	30,00	0,00
RINGwt_z	Q9SIZ2	Eukaryotic translation initiation factor 2 subunit alpha homolog	3	3	3,00	1	0|0|0	1,00	1,00	1,00	1,00	1,00	30,00	0,00
RINGwt_z	Q4V3D3	Plant UBX domain-containing protein 9	3	3	3,00	1	0|0|0	1,00	1,00	1,00	1,00	1,00	30,00	0,00
RINGwt_z	Q03250	Glycine-rich RNA-binding protein 7	8	8	8,00	1	0|0|1	1,00	1,00	1,00	1,00	1,00	24,00	0,00
RINGwt_z	Q9SAJ4	Phosphoglycerate kinase 3, cytosolic	15	15	15,00	1	1|1|0	1,00	1,00	1,00	1,00	1,00	22,50	0,00
RINGwt_z	Q07100	Serine/threonine-protein phosphatase PP2A-3 catalytic subunit	2	2	2,00	1	0|0|0	0,97	0,97	0,97	0,97	0,97	20,00	0,00
RINGwt_z	P42699	Plastocyanin major isoform, chloroplastic	2	2	2,00	1	0|0|0	0,97	0,97	0,97	0,97	0,97	20,00	0,00
RINGwt_z	O80929	60S ribosomal protein L36-1	2	2	2,00	1	0|0|0	0,97	0,97	0,97	0,97	0,97	20,00	0,00
RINGwt_z	Q8LF20	Putative clathrin assembly protein At2g25430	2	2	2,00	1	0|0|0	0,97	0,97	0,97	0,97	0,97	20,00	0,00
RINGwt_z	Q8VZU9	Derlin-1	2	2	2,00	1	0|0|0	0,97	0,97	0,97	0,97	0,97	20,00	0,00
RINGwt_z	Q9ZVF3	MLP-like protein 328	2	2	2,00	1	0|0|0	0,97	0,97	0,97	0,97	0,97	20,00	0,00
RINGwt_z	P56780	Photosystem II reaction center protein H	2	2	2,00	1	0|0|0	0,97	0,97	0,97	0,97	0,97	20,00	0,00
RINGwt_z	Q39096	Protein EARLY RESPONSIVE TO DEHYDRATION 15	2	2	2,00	1	0|0|0	0,97	0,97	0,97	0,97	0,97	20,00	0,00
RINGwt_z	Q9MA79	Fructose-1,6-bisphosphatase, cytosolic	2	2	2,00	1	0|0|0	0,97	0,97	0,97	0,97	0,97	20,00	0,00
RINGwt_z	Q56XG6	DEAD-box ATP-dependent RNA helicase 15	2	2	2,00	1	0|0|0	0,97	0,97	0,97	0,97	0,97	20,00	0,00
RINGwt_z	Q9SB64	Protein NBR1 homolog	2	2	2,00	1	0|0|0	0,97	0,97	0,97	0,97	0,97	20,00	0,00
RINGwt_z	Q9M2Y6	Probable pectin methylesterase CGR2	2	2	2,00	1	0|0|0	0,97	0,97	0,97	0,97	0,97	20,00	0,00

Bait: RINGwt_z	Prey	PreyGene	Spec	SpecSum	AvgSpec	NumReplicates	ctrlCounts	AvgP	MaxP	TopoAvgP	TopoMaxP	SaintScore	FoldChange	BFDR
RINGwt_z	Q9SVY0	DNA-directed RNA polymerase I subunit 1	2	2	2,00	1	0|0|0	0,97	0,97	0,97	0,97	0,97	20,00	0,00
RINGwt_z	F4JRE0	Transmembrane 9 superfamily member 12	2	2	2,00	1	0|0|0	0,97	0,97	0,97	0,97	0,97	20,00	0,00
RINGwt_z	Q9ZPI6	Enoyl-CoA hydratase/3-2-trans-enoyl-CoA isomerase/3-hydroxybutyryl-CoA epimerase	2	2	2,00	1	0|0|0	0,97	0,97	0,97	0,97	0,97	20,00	0,00
RINGwt_z	Q9FHM7	Hypersensitive-induced response protein 4	2	2	2,00	1	0|0|0	0,97	0,97	0,97	0,97	0,97	20,00	0,00
RINGwt_z	Q8LAH8	Nucleoside diphosphate kinase IV, chloroplastic/mitochondrial	2	2	2,00	1	0|0|0	0,97	0,97	0,97	0,97	0,97	20,00	0,00
RINGwt_z	Q9LE54	Protein SPIRAL1-like 2	2	2	2,00	1	0|0|0	0,97	0,97	0,97	0,97	0,97	20,00	0,00
RINGwt_z	Q8RWF0	26S proteasome non-ATPase regulatory subunit 13 homolog A	2	2	2,00	1	0|0|0	0,97	0,97	0,97	0,97	0,97	20,00	0,00
RINGwt_z	O82663	Succinate dehydrogenase [ubiquinone] flavoprotein subunit 1, mitochondrial	2	2	2,00	1	0|0|0	0,97	0,97	0,97	0,97	0,97	20,00	0,00
RINGwt_z	Q9SX77	Succinate dehydrogenase subunit 5, mitochondrial	2	2	2,00	1	0|0|0	0,97	0,97	0,97	0,97	0,97	20,00	0,00
RINGwt_z	Q9LMA8	Protein TIFY 10A	2	2	2,00	1	0|0|0	0,97	0,97	0,97	0,97	0,97	20,00	0,00
RINGwt_z	Q9S7C0	Heat shock 70 kDa protein 14	2	2	2,00	1	0|0|0	0,97	0,97	0,97	0,97	0,97	20,00	0,00
RINGwt_z	Q9S7H8	Isochorismate synthase 1, chloroplastic	2	2	2,00	1	0|0|0	0,97	0,97	0,97	0,97	0,97	20,00	0,00
RINGwt_z	P93033	Fumarate hydratase 1, mitochondrial	2	2	2,00	1	0|0|0	0,97	0,97	0,97	0,97	0,97	20,00	0,00
RINGwt_z	Q93VR3	GDP-mannose 3,5-epimerase	2	2	2,00	1	0|0|0	0,97	0,97	0,97	0,97	0,97	20,00	0,00
RINGwt_z	Q9SEX2	Katanin p60 ATPase-containing subunit A1	2	2	2,00	1	0|0|0	0,97	0,97	0,97	0,97	0,97	20,00	0,00
RINGwt_z	B3LFA4	Cysteine--tRNA ligase 2, cytoplasmic	2	2	2,00	1	0|0|0	0,97	0,97	0,97	0,97	0,97	20,00	0,00
RINGwt_z	P42731	Polyadenylate-binding protein 2	2	2	2,00	1	0|0|0	0,97	0,97	0,97	0,97	0,97	20,00	0,00
RINGwt_z	Q94AH6	Cullin-1	2	2	2,00	1	0|0|0	0,97	0,97	0,97	0,97	0,97	20,00	0,00
RINGwt_z	Q9FLQ4	2-oxoglutarate dehydrogenase E2 component (dihydrolipoamide succinyltransferase)	32	32	32,00	1	0|0|5	1,00	1,00	1,00	1,00	1,00	19,20	0,00
RINGwt_z	Q8H107	2-oxoglutarate dehydrogenase E2 component (dihydrolipoamide succinyltransferase)	34	34	34,00	1	0|0|6	1,00	1,00	1,00	1,00	1,00	17,00	0,00

Bait: RINGwt_z	Prey	PreyGene	Spec	SpecSum	AvgSpec	NumReplicates	ctrlCounts	AvgP	MaxP	TopoAvgP	TopoMaxP	SaintScore	FoldChange	BFDR
RINGwt_z	Q9LVI8	Glutamine synthetase cytosolic isozyme 1-3	5	5	5,00	1	0|1|0	1,00	1,00	1,00	1,00	1,00	15,00	0,00
RINGwt_z	Q9SAJ6	Glyceraldehyde-3-phosphate dehydrogenase GAPCP1, chloroplastic	9	9	9,00	1	0|0|2	0,99	0,99	0,99	0,99	0,99	13,50	0,00
RINGwt_z	Q9LJE4	Chaperonin 60 subunit beta 2, chloroplastic	12	12	12,00	1	1|2|0	1,00	1,00	1,00	1,00	1,00	12,00	0,00
RINGwt_z	Q05758	Ketol-acid reductoisomerase, chloroplastic	12	12	12,00	1	1|2|0	1,00	1,00	1,00	1,00	1,00	12,00	0,00
RINGwt_z	Q42560	Aconitate hydratase 1	8	8	8,00	1	0|2|0	0,99	0,99	0,99	0,99	0,99	12,00	0,00
RINGwt_z	P59233	Ubiquitin-40S ribosomal protein S27a-3	63	63	63,00	1	8|9|0	1,00	1,00	1,00	1,00	1,00	11,12	0,00
RINGwt_z	P46077	14-3-3-like protein GF14 phi	11	11	11,00	1	1|2|0	1,00	1,00	1,00	1,00	1,00	11,00	0,00
RINGwt_z	P92947	Monodehydroascorbate reductase, chloroplastic/mitochondrial	14	14	14,00	1	0|4|0	0,98	0,98	0,98	0,98	0,98	10,50	0,00
RINGwt_z	Q9SIB9	Aconitate hydratase 3, mitochondrial	14	14	14,00	1	0|4|0	0,98	0,98	0,98	0,98	0,98	10,50	0,00
RINGwt_z	Q03251	Glycine-rich RNA-binding protein 8	7	7	7,00	1	0|0|2	0,98	0,98	0,98	0,98	0,98	10,50	0,00
RINGwt_z	P92994	Trans-cinnamate 4-monooxygenase	7	7	7,00	1	1|0|1	1,00	1,00	1,00	1,00	1,00	10,50	0,00
RINGwt_z	Q01525	14-3-3-like protein GF14 omega	10	10	10,00	1	1|2|0	1,00	1,00	1,00	1,00	1,00	10,00	0,00
RINGwt_z	P57752	Acyl-CoA-binding domain-containing protein 6	1	1	1,00	1	0|0|0	0,00	0,00	0,00	0,00	0,00	10,00	0,51
RINGwt_z	Q9SW21	Acyl carrier protein 4, chloroplastic	1	1	1,00	1	0|0|0	0,00	0,00	0,00	0,00	0,00	10,00	0,51
RINGwt_z	P36210	50S ribosomal protein L12-1, chloroplastic	1	1	1,00	1	0|0|0	0,00	0,00	0,00	0,00	0,00	10,00	0,51
RINGwt_z	Q96262	Plasma membrane-associated cation-binding protein 1	1	1	1,00	1	0|0|0	0,00	0,00	0,00	0,00	0,00	10,00	0,51
RINGwt_z	P10796	Ribulose bisphosphate carboxylase small chain 1B, chloroplastic	1	1	1,00	1	0|0|0	0,00	0,00	0,00	0,00	0,00	10,00	0,51
RINGwt_z	Q9SS94	Cell division control protein 48 homolog C	1	1	1,00	1	0|0|0	0,00	0,00	0,00	0,00	0,00	10,00	0,51
RINGwt_z	Q9ZSK4	Actin-depolymerizing factor 3	1	1	1,00	1	0|0|0	0,00	0,00	0,00	0,00	0,00	10,00	0,51
RINGwt_z	Q9ZW85	3-isopropylmalate dehydratase small subunit 1	1	1	1,00	1	0|0|0	0,00	0,00	0,00	0,00	0,00	10,00	0,51
RINGwt_z	Q6NLH0	DNA-directed RNA polymerases II, IV and V subunit 9A	1	1	1,00	1	0|0|0	0,00	0,00	0,00	0,00	0,00	10,00	0,51
RINGwt_z	O49453	Uncharacterized protein At4g28440	1	1	1,00	1	0|0|0	0,00	0,00	0,00	0,00	0,00	10,00	0,51

Bait: RINGwt_z	Prey	PreyGene	Spec	SpecSum	AvgSpec	NumReplicates	ctrlCounts	AvgP	MaxP	TopoAvgP	TopoMaxP	SaintScore	FoldChange	BFDR
RINGwt_z	Q42418	Profilin-2	1	1	1,00	1	0|0|0	0,00	0,00	0,00	0,00	0,00	10,00	0,51
RINGwt_z	Q9LZZ7	Spindle and kinetochore-associated protein 1 homolog	1	1	1,00	1	0|0|0	0,00	0,00	0,00	0,00	0,00	10,00	0,51
RINGwt_z	O81153	Proteasome subunit beta type-3-B	1	1	1,00	1	0|0|0	0,00	0,00	0,00	0,00	0,00	10,00	0,51
RINGwt_z	O81148	Proteasome subunit alpha type-4-A	1	1	1,00	1	0|0|0	0,00	0,00	0,00	0,00	0,00	10,00	0,51
RINGwt_z	Q84JT6	Peptide methionine sulfoxide reductase B9	1	1	1,00	1	0|0|0	0,00	0,00	0,00	0,00	0,00	10,00	0,51
RINGwt_z	Q3EBL9	Vacuolar protein-sorting-associated protein 37 homolog 2	1	1	1,00	1	0|0|0	0,00	0,00	0,00	0,00	0,00	10,00	0,51
RINGwt_z	O48962	Probable 3-beta-hydroxysteroid-Delta(8),Delta(7)-isomerase	1	1	1,00	1	0|0|0	0,00	0,00	0,00	0,00	0,00	10,00	0,51
RINGwt_z	Q9FNH6	NDR1/HIN1-like protein 3	1	1	1,00	1	0|0|0	0,00	0,00	0,00	0,00	0,00	10,00	0,51
RINGwt_z	Q94BV4	DEAD-box ATP-dependent RNA helicase 6	1	1	1,00	1	0|0|0	0,00	0,00	0,00	0,00	0,00	10,00	0,51
RINGwt_z	Q42404	U1 small nuclear ribonucleoprotein 70 kDa	1	1	1,00	1	0|0|0	0,00	0,00	0,00	0,00	0,00	10,00	0,51
RINGwt_z	Q96303	Inorganic phosphate transporter 1-4	1	1	1,00	1	0|0|0	0,00	0,00	0,00	0,00	0,00	10,00	0,51
RINGwt_z	Q9STX2	3-oxo-Delta(4,5)-steroid 5-beta-reductase	1	1	1,00	1	0|0|0	0,00	0,00	0,00	0,00	0,00	10,00	0,51
RINGwt_z	Q9C8J1	DEAD-box ATP-dependent RNA helicase 34	1	1	1,00	1	0|0|0	0,00	0,00	0,00	0,00	0,00	10,00	0,51
RINGwt_z	Q9SB50	AP-4 complex subunit mu	1	1	1,00	1	0|0|0	0,00	0,00	0,00	0,00	0,00	10,00	0,51
RINGwt_z	Q9SW96	Asparagine--tRNA ligase, cytoplasmic 1	1	1	1,00	1	0|0|0	0,00	0,00	0,00	0,00	0,00	10,00	0,51
RINGwt_z	Q9LXS7	Citrate synthase 1, peroxisomal	1	1	1,00	1	0|0|0	0,00	0,00	0,00	0,00	0,00	10,00	0,51
RINGwt_z	Q9FFA0	DUF724 domain-containing protein 10	1	1	1,00	1	0|0|0	0,00	0,00	0,00	0,00	0,00	10,00	0,51
RINGwt_z	Q8LPS1	Long chain acyl-CoA synthetase 6, peroxisomal	1	1	1,00	1	0|0|0	0,00	0,00	0,00	0,00	0,00	10,00	0,51
RINGwt_z	Q9ZU97	Protein VAC14 homolog	1	1	1,00	1	0|0|0	0,00	0,00	0,00	0,00	0,00	10,00	0,51
RINGwt_z	Q9M2N5	Zinc finger BED domain-containing protein DAYSLEEPER	1	1	1,00	1	0|0|0	0,00	0,00	0,00	0,00	0,00	10,00	0,51
RINGwt_z	P48641	Glutathione reductase, cytosolic	1	1	1,00	1	0|0|0	0,00	0,00	0,00	0,00	0,00	10,00	0,51
RINGwt_z	P54888	Delta-1-pyrroline-5-carboxylate synthase B	1	1	1,00	1	0|0|0	0,00	0,00	0,00	0,00	0,00	10,00	0,51

Bait: RINGwt_z	Prey	PreyGene	Spec	SpecSum	AvgSpec	NumReplicates	ctrlCounts	AvgP	MaxP	TopoAvgP	TopoMaxP	SaintScore	FoldChange	BFDR
RINGwt_z	Q9S7P3	Kinesin-like protein KIN-7N	1	1	1,00	1	0|0|0	0,00	0,00	0,00	0,00	0,00	10,00	0,51
RINGwt_z	Q8LPK4	AP-2 complex subunit alpha-2	1	1	1,00	1	0|0|0	0,00	0,00	0,00	0,00	0,00	10,00	0,51
RINGwt_z	Q9LYN7	Protein MEI2-like 4	1	1	1,00	1	0|0|0	0,00	0,00	0,00	0,00	0,00	10,00	0,51
RINGwt_z	F4I460	Myosin-8	1	1	1,00	1	0|0|0	0,00	0,00	0,00	0,00	0,00	10,00	0,51
RINGwt_z	P59232	Ubiquitin-40S ribosomal protein S27a-2	65	65	65,00	1	8|9|3	1,00	1,00	1,00	1,00	1,00	9,75	0,00
RINGwt_z	P39207	Nucleoside diphosphate kinase 1	13	13	13,00	1	2|2|0	1,00	1,00	1,00	1,00	1,00	9,75	0,00
RINGwt_z	Q8LD46	60S ribosomal protein L23a-1	30	30	30,00	1	4|3|3	1,00	1,00	1,00	1,00	1,00	9,00	0,00
RINGwt_z	P42645	14-3-3-like protein GF14 upsilon	18	18	18,00	1	2|4|0	1,00	1,00	1,00	1,00	1,00	9,00	0,00
RINGwt_z	Q9FJX3	Mitochondrial outer membrane protein porin 2	15	15	15,00	1	1|4|0	0,99	0,99	0,99	0,99	0,99	9,00	0,00
RINGwt_z	Q5E924	Glyceraldehyde-3-phosphate dehydrogenase GAPCP2, chloroplastic	9	9	9,00	1	0|0|3	0,97	0,97	0,97	0,97	0,97	9,00	0,01
RINGwt_z	Q9SHC8	Vesicle-associated protein 1-2, N-terminally processed	3	3	3,00	1	0|1|0	0,97	0,97	0,97	0,97	0,97	9,00	0,00
RINGwt_z	Q42406	Peptidyl-prolyl cis-trans isomerase CYP18-4	3	3	3,00	1	0|1|0	0,97	0,97	0,97	0,97	0,97	9,00	0,00
RINGwt_z	O80446	Pyridoxal 5'-phosphate synthase PDX1-like 4	3	3	3,00	1	0|1|0	0,97	0,97	0,97	0,97	0,97	9,00	0,00
RINGwt_z	P45434	Translocon-associated protein subunit alpha	3	3	3,00	1	1|0|0	0,97	0,97	0,97	0,97	0,97	9,00	0,00
RINGwt_z	P42643	14-3-3-like protein GF14 chi	14	14	14,00	1	2|3|0	1,00	1,00	1,00	1,00	1,00	8,40	0,00
RINGwt_z	Q9LUW6	DEAD-box ATP-dependent RNA helicase 9, mitochondrial	14	14	14,00	1	3|2|0	1,00	1,00	1,00	1,00	1,00	8,40	0,00
RINGwt_z	Q9FFC0	Histone H2B.10	8	8	8,00	1	1|2|0	1,00	1,00	1,00	1,00	1,00	8,00	0,00
RINGwt_z	P23686	S-adenosylmethionine synthase 1	36	36	36,00	1	7|7|0	1,00	1,00	1,00	1,00	1,00	7,71	0,00
RINGwt_z	Q96300	14-3-3-like protein GF14 nu	15	15	15,00	1	2|4|0	1,00	1,00	1,00	1,00	1,00	7,50	0,00
RINGwt_z	Q9SIM4	60S ribosomal protein L14-1	10	10	10,00	1	0|0|4	0,95	0,95	0,95	0,95	0,95	7,50	0,01
RINGwt_z	Q9LX65	V-type proton ATPase subunit H	5	5	5,00	1	0|2|0	0,93	0,93	0,93	0,93	0,93	7,50	0,01
RINGwt_z	Q9SI61	Amidophosphoribosyltransferase 1, chloroplastic	5	5	5,00	1	1|1|0	0,98	0,98	0,98	0,98	0,98	7,50	0,00

Bait: RINGwt_z	Prey	PreyGene	Spec	SpecSum	AvgSpec	NumReplicates	ctrlCounts	AvgP	MaxP	TopoAvgP	TopoMaxP	SaintScore	FoldChange	BFDR
RINGwt_z	Q94A52	Eukaryotic initiation factor 4A-III homolog	5	5	5,00	1	2|0|0	0,93	0,93	0,93	0,93	0,93	7,50	0,01
RINGwt_z	P12411	Tubulin beta-1 chain	94	94	94,00	1	17|21|0	1,00	1,00	1,00	1,00	1,00	7,42	0,00
RINGwt_z	P17562	S-adenosylmethionine synthase 2	42	42	42,00	1	8|9|0	1,00	1,00	1,00	1,00	1,00	7,41	0,00
RINGwt_z	P93819	Malate dehydrogenase 1, cytoplasmic	27	27	27,00	1	3|3|5	1,00	1,00	1,00	1,00	1,00	7,36	0,00
RINGwt_z	P92549	ATP synthase subunit alpha, mitochondrial	42	42	42,00	1	8|10|0	1,00	1,00	1,00	1,00	1,00	7,00	0,00
RINGwt_z	O24456	Receptor for activated C kinase 1A	35	35	35,00	1	3|12|0	0,98	0,98	0,98	0,98	0,98	7,00	0,00
RINGwt_z	Q9FE65	60S ribosomal protein L34-2	14	14	14,00	1	3|3|0	1,00	1,00	1,00	1,00	1,00	7,00	0,00
RINGwt_z	Q41188	Cold shock protein 2	7	7	7,00	1	1|1|1	0,99	0,99	0,99	0,99	0,99	7,00	0,00
RINGwt_z	Q9SF85	Adenosine kinase 1	7	7	7,00	1	2|1|0	0,99	0,99	0,99	0,99	0,99	7,00	0,00
RINGwt_z	O04202	Eukaryotic translation initiation factor 3 subunit F	7	7	7,00	1	0|3|0	0,92	0,92	0,92	0,92	0,92	7,00	0,01
RINGwt_z	Q8L7B5	Chaperonin CPN60-like 1, mitochondrial	40	40	40,00	1	9|9|0	1,00	1,00	1,00	1,00	1,00	6,67	0,00
RINGwt_z	Q8RWV0	Transketolase-1, chloroplastic	11	11	11,00	1	0|5|0	0,93	0,93	0,93	0,93	0,93	6,60	0,01
RINGwt_z	Q9ZT91	Elongation factor Tu, mitochondrial	28	28	28,00	1	6|7|0	1,00	1,00	1,00	1,00	1,00	6,46	0,00
RINGwt_z	P27323	Heat shock protein 90-1	17	17	17,00	1	3|5|0	0,99	0,99	0,99	0,99	0,99	6,38	0,00
RINGwt_z	P42644	14-3-3-like protein GF14 psi	17	17	17,00	1	3|5|0	0,99	0,99	0,99	0,99	0,99	6,38	0,00
RINGwt_z	Q9C4Z6	Receptor for activated C kinase 1B	29	29	29,00	1	6|8|0	0,99	0,99	0,99	0,99	0,99	6,21	0,00
RINGwt_z	P29515	Tubulin beta-7 chain	144	144	144,00	1	26|36|10	1,00	1,00	1,00	1,00	1,00	6,00	0,00
RINGwt_z	P42825	Chaperone protein dnaJ 2	18	18	18,00	1	4|5|0	0,99	0,99	0,99	0,99	0,99	6,00	0,00
RINGwt_z	Q9FE58	60S ribosomal protein L22-3	4	4	4,00	1	2|0|0	0,86	0,86	0,86	0,86	0,86	6,00	0,02
RINGwt_z	Q9SJJ5	Cyclin-dependent kinases regulatory subunit 2	4	4	4,00	1	1|1|0	0,92	0,92	0,92	0,92	0,92	6,00	0,01
RINGwt_z	Q9LXJ2	Cytochrome b-c1 complex subunit 9, mitochondrial	2	2	2,00	1	0|0|1	0,79	0,79	0,79	0,79	0,79	6,00	0,02
RINGwt_z	Q9LPI5	Polyadenylate-binding protein-interacting protein 11	2	2	2,00	1	0|1|0	0,79	0,79	0,79	0,79	0,79	6,00	0,02
RINGwt_z	Q2V4F9	SPX domain-containing membrane protein At1g63010	2	2	2,00	1	0|1|0	0,79	0,79	0,79	0,79	0,79	6,00	0,02

Bait: RINGwt_z	Prey	PreyGene	Spec	SpecSum	AvgSpec	NumReplicates	ctrlCounts	AvgP	MaxP	TopoAvgP	TopoMaxP	SaintScore	FoldChange	BFDR
RINGwt_z	Q9ZUA0	Dolichyl-diphosphooligosaccharide--protein glycosyltransferase subunit 1B	2	2	2,00	1	0|1|0	0,79	0,79	0,79	0,79	0,79	6,00	0,02
RINGwt_z	O64888	Ribose-phosphate pyrophosphokinase 5, chloroplastic	2	2	2,00	1	1|0|0	0,79	0,79	0,79	0,79	0,79	6,00	0,02
RINGwt_z	P29514	Tubulin beta-6 chain	89	89	89,00	1	16|21|10	1,00	1,00	1,00	1,00	1,00	5,68	0,00
RINGwt_z	P53494	Actin-4	53	53	53,00	1	13|15|0	0,99	0,99	0,99	0,99	0,99	5,68	0,00
RINGwt_z	P53497	Actin-12	53	53	53,00	1	13|15|0	0,99	0,99	0,99	0,99	0,99	5,68	0,00
RINGwt_z	P51818	Heat shock protein 90-3	32	32	32,00	1	5|12|0	0,98	0,98	0,98	0,98	0,98	5,65	0,00
RINGwt_z	P29516	Tubulin beta-8 chain	131	131	131,00	1	27|34|10	1,00	1,00	1,00	1,00	1,00	5,54	0,00
RINGwt_z	Q9LUT2	S-adenosylmethionine synthase 4	46	46	46,00	1	12|13|0	0,99	0,99	0,99	0,99	0,99	5,52	0,00
RINGwt_z	Q8LCL3	60S ribosomal protein L27-2	11	11	11,00	1	3|3|0	0,99	0,99	0,99	0,99	0,99	5,50	0,00
RINGwt_z	Q94AW8	Chaperone protein dnaJ 3	11	11	11,00	1	2|4|0	0,97	0,97	0,97	0,97	0,97	5,50	0,00
RINGwt_z	P29513	Tubulin beta-5 chain	86	86	86,00	1	17|22|8	1,00	1,00	1,00	1,00	1,00	5,49	0,00
RINGwt_z	P29197	Chaperonin CPN60, mitochondrial	60	60	60,00	1	16|15|2	1,00	1,00	1,00	1,00	1,00	5,45	0,00
RINGwt_z	Q93ZM7	Chaperonin CPN60-like 2, mitochondrial	20	20	20,00	1	3|8|0	0,96	0,96	0,96	0,96	0,96	5,45	0,01
RINGwt_z	Q9SQI8	Pyruvate dehydrogenase E2 component (dihydrolipoamide acetyltransferase)	45	45	45,00	1	0|0|25	0,95	0,95	0,95	0,95	0,95	5,40	0,01
RINGwt_z	Q9SRZ6	Cytosolic isocitrate dehydrogenase [NADP]	9	9	9,00	1	2|3|0	0,99	0,99	0,99	0,99	0,99	5,40	0,00
RINGwt_z	Q9LQI9	Oligouridylate-binding protein 1B	14	14	14,00	1	5|3|0	0,97	0,97	0,97	0,97	0,97	5,25	0,00
RINGwt_z	Q9LV28	Receptor for activated C kinase 1C	26	26	26,00	1	5|10|0	0,97	0,97	0,97	0,97	0,97	5,20	0,00
RINGwt_z	Q9LHG8	Protein ELC	12	12	12,00	1	3|2|2	1,00	1,00	1,00	1,00	1,00	5,14	0,00
RINGwt_z	Q9C8P0	Pyruvate dehydrogenase E2 component (dihydrolipoamide acetyltransferase)	34	34	34,00	1	0|0|20	0,94	0,94	0,94	0,94	0,94	5,10	0,01
RINGwt_z	Q9SIF2	Heat shock protein 90-5, chloroplastic	5	5	5,00	1	0|3|0	0,82	0,82	0,82	0,82	0,82	5,00	0,02
RINGwt_z	Q56YW9	Tubulin beta-2 chain	153	153	153,00	1	37|41|15	1,00	1,00	1,00	1,00	1,00	4,94	0,00
RINGwt_z	Q9SJT9	Coatomer subunit alpha-2	23	23	23,00	1	7|7|0	0,98	0,98	0,98	0,98	0,98	4,93	0,00

Bait: RINGwt_z	Prey	PreyGene	Spec	SpecSum	AvgSpec	NumReplicates	ctrlCounts	AvgP	MaxP	TopoAvgP	TopoMaxP	SaintScore	FoldChange	BFDR
RINGwt_z	O23255	Adenosylhomocysteinase 1	42	42	42,00	1	12|14|0	0,98	0,98	0,98	0,98	0,98	4,85	0,00
RINGwt_z	P42798	40S ribosomal protein S15a-1	16	16	16,00	1	2|5|3	1,00	1,00	1,00	1,00	1,00	4,80	0,00
RINGwt_z	Q9SEU4	Serine/arginine-rich SC35-like splicing factor SCL33	8	8	8,00	1	0|0|5	0,86	0,86	0,86	0,86	0,86	4,80	0,02
RINGwt_z	F4ICD9	Protein transport protein SEC31 homolog A	8	8	8,00	1	0|0|5	0,86	0,86	0,86	0,86	0,86	4,80	0,02
RINGwt_z	P29517	Tubulin beta-9 chain	107	107	107,00	1	26|33|8	1,00	1,00	1,00	1,00	1,00	4,79	0,00
RINGwt_z	F4JWP9	109 kDa U5 small nuclear ribonucleoprotein component GFL	35	35	35,00	1	9|13|0	0,97	0,97	0,97	0,97	0,97	4,77	0,00
RINGwt_z	Q9ASR1	Elongation factor 2	41	41	41,00	1	11|15|0	0,97	0,97	0,97	0,97	0,97	4,73	0,00
RINGwt_z	Q9SYG4	Oligouridylate-binding protein 1A	11	11	11,00	1	5|2|0	0,92	0,92	0,92	0,92	0,92	4,71	0,01
RINGwt_z	P24636	Tubulin beta-4 chain	112	112	112,00	1	29|35|8	1,00	1,00	1,00	1,00	1,00	4,67	0,00
RINGwt_z	Q42547	Catalase-3	6	6	6,00	1	2|2|0	0,97	0,97	0,97	0,97	0,97	4,50	0,00
RINGwt_z	Q8RXN4	3-hydroxyisobutyryl-CoA hydrolase-like protein 2, mitochondrial	3	3	3,00	1	0|2|0	0,73	0,73	0,73	0,73	0,73	4,50	0,04
RINGwt_z	Q67XG0	Two-on-two hemoglobin-3	3	3	3,00	1	2|0|0	0,73	0,73	0,73	0,73	0,73	4,50	0,04
RINGwt_z	O80605	Sucrose transport protein SUC3	3	3	3,00	1	0|2|0	0,73	0,73	0,73	0,73	0,73	4,50	0,04
RINGwt_z	P51419	60S ribosomal protein L27-3	13	13	13,00	1	5|4|0	0,95	0,95	0,95	0,95	0,95	4,33	0,01
RINGwt_z	Q9SJL8	S-adenosylmethionine synthase 3	23	23	23,00	1	8|8|0	0,95	0,95	0,95	0,95	0,95	4,31	0,01
RINGwt_z	Q8RYC2	Putative actin-5	17	17	17,00	1	4|4|4	1,00	1,00	1,00	1,00	1,00	4,25	0,00
RINGwt_z	Q8L828	Coatomer subunit beta'-3	7	7	7,00	1	3|2|0	0,92	0,92	0,92	0,92	0,92	4,20	0,01
RINGwt_z	Q42290	Probable mitochondrial-processing peptidase subunit beta, mitochondrial	8	8	8,00	1	2|4|0	0,86	0,86	0,86	0,86	0,86	4,00	0,02
RINGwt_z	Q9MAK9	26S proteasome regulatory subunit S10B homolog B	8	8	8,00	1	2|4|0	0,86	0,86	0,86	0,86	0,86	4,00	0,02
RINGwt_z	Q9SEI3	26S proteasome regulatory subunit 10B homolog A	8	8	8,00	1	2|4|0	0,86	0,86	0,86	0,86	0,86	4,00	0,02
RINGwt_z	Q38799	Pyruvate dehydrogenase E1 component subunit beta-1, mitochondrial	8	8	8,00	1	3|3|0	0,91	0,91	0,91	0,91	0,91	4,00	0,01
RINGwt_z	Q9LHA4	V-type proton ATPase subunit d2	4	4	4,00	1	1|2|0	0,78	0,78	0,78	0,78	0,78	4,00	0,03

Bait: RINGwt_z	Prey	PreyGene	Spec	SpecSum	AvgSpec	NumReplicates	ctrlCounts	AvgP	MaxP	TopoAvgP	TopoMaxP	SaintScore	FoldChange	BFDR
RINGwt_z	Q9FGK5	Ras-related protein RABA5a	4	4	4,00	1	2|1|0	0,78	0,78	0,78	0,78	0,78	4,00	0,03
RINGwt_z	O80845	Peroxisomal membrane protein 11D	4	4	4,00	1	0|0|3	0,74	0,74	0,74	0,74	0,74	4,00	0,03
RINGwt_z	B9DFS6	Sorting nexin 2B	4	4	4,00	1	0|3|0	0,74	0,74	0,74	0,74	0,74	4,00	0,03
RINGwt_z	Q9LUW5	DEAD-box ATP-dependent RNA helicase 53, mitochondrial	28	28	28,00	1	10|9|3	1,00	1,00	1,00	1,00	1,00	3,82	0,00
RINGwt_z	P83483	ATP synthase subunit beta-1, mitochondrial	33	33	33,00	1	9|12|5	1,00	1,00	1,00	1,00	1,00	3,81	0,00
RINGwt_z	O23016	Probable voltage-gated potassium channel subunit beta	5	5	5,00	1	2|2|0	0,88	0,88	0,88	0,88	0,88	3,75	0,01
RINGwt_z	Q95748	NADH dehydrogenase [ubiquinone] iron-sulfur protein 3	5	5	5,00	1	1|3|0	0,75	0,75	0,75	0,75	0,75	3,75	0,03
RINGwt_z	O49485	D-3-phosphoglycerate dehydrogenase 1, chloroplastic	11	11	11,00	1	4|5|0	0,84	0,84	0,84	0,84	0,84	3,67	0,02
RINGwt_z	Q9SMX3	Mitochondrial outer membrane protein porin 3	40	40	40,00	1	15|16|2	0,82	0,82	0,82	0,82	0,82	3,64	0,02
RINGwt_z	Q8VZG7	Ribonuclease TUDOR 1	18	18	18,00	1	5|10|0	0,77	0,77	0,77	0,77	0,77	3,60	0,03
RINGwt_z	P54609	Cell division control protein 48 homolog A	8	8	8,00	1	2|5|0	0,71	0,71	0,71	0,71	0,71	3,43	0,04
RINGwt_z	P0CJ46	Actin-1	47	47	47,00	1	14|17|11	1,00	1,00	1,00	1,00	1,00	3,36	0,00
RINGwt_z	P0CJ47	Actin-3	47	47	47,00	1	14|17|11	1,00	1,00	1,00	1,00	1,00	3,36	0,00
RINGwt_z	Q9FVT2	Probable elongation factor 1-gamma 2	11	11	11,00	1	4|6|0	0,70	0,70	0,70	0,70	0,70	3,30	0,04
RINGwt_z	Q9LVA0	BAG family molecular chaperone regulator 7	14	14	14,00	1	6|7|0	0,65	0,65	0,65	0,65	0,65	3,23	0,04
RINGwt_z	Q8LD03	40S ribosomal protein S7-3	16	16	16,00	1	7|8|0	0,60	0,60	0,60	0,60	0,60	3,20	0,05
RINGwt_z	P53496	Actin-11	52	52	52,00	1	17|18|14	1,00	1,00	1,00	1,00	1,00	3,18	0,00
RINGwt_z	Q56WD9	3-ketoacyl-CoA thiolase 2, peroxisomal	18	18	18,00	1	9|8|0	0,55	0,55	0,55	0,55	0,55	3,18	0,06
RINGwt_z	Q9LNC5	110 kDa U5 small nuclear ribonucleoprotein component CLO	33	33	33,00	1	12|20|0	0,17	0,17	0,17	0,17	0,17	3,09	0,15
RINGwt_z	Q9SCM3	40S ribosomal protein S2-4	14	14	14,00	1	7|7|0	0,47	0,47	0,47	0,47	0,47	3,00	0,08
RINGwt_z	P28186	Ras-related protein RABE1c	8	8	8,00	1	4|4|0	0,58	0,58	0,58	0,58	0,58	3,00	0,05
RINGwt_z	O81127	Serine/arginine-rich splicing factor RSZ21	7	7	7,00	1	0|0|7	0,59	0,59	0,59	0,59	0,59	3,00	0,05

Bait: RINGwt_z	Prey	PreyGene	Spec	SpecSum	AvgSpec	NumReplicates	ctrlCounts	AvgP	MaxP	TopoAvgP	TopoMaxP	SaintScore	FoldChange	BFDR
RINGwt_z	Q9SCX3	Elongation factor 1-beta 2	6	6	6,00	1	1|5|0	0,56	0,56	0,56	0,56	0,56	3,00	0,06
RINGwt_z	Q94JQ3	Serine hydroxymethyltransferase 3, chloroplastic	5	5	5,00	1	1|4|0	0,56	0,56	0,56	0,56	0,56	3,00	0,06
RINGwt_z	P42813	Ribonuclease 1	5	5	5,00	1	3|2|0	0,59	0,59	0,59	0,59	0,59	3,00	0,05
RINGwt_z	Q93Z16	Dolichyl-diphosphooligosaccharide--protein glycosyltransferase subunit 2	3	3	3,00	1	2|1|0	0,52	0,52	0,52	0,52	0,52	3,00	0,07
RINGwt_z	O23676	Protein mago nashi homolog	3	3	3,00	1	0|3|0	0,58	0,58	0,58	0,58	0,58	3,00	0,05
RINGwt_z	P49689	40S ribosomal protein S30	3	3	3,00	1	0|0|3	0,58	0,58	0,58	0,58	0,58	3,00	0,05
RINGwt_z	Q8W4R3	DEAD-box ATP-dependent RNA helicase 30	3	3	3,00	1	1|2|0	0,52	0,52	0,52	0,52	0,52	3,00	0,07
RINGwt_z	P92966	Serine/arginine-rich splicing factor RS41	3	3	3,00	1	0|0|3	0,58	0,58	0,58	0,58	0,58	3,00	0,05
RINGwt_z	F4J077	Protein PAT1 homolog 1	3	3	3,00	1	0|3|0	0,58	0,58	0,58	0,58	0,58	3,00	0,05
RINGwt_z	P29402	Calnexin homolog 1	2	2	2,00	1	0|2|0	0,53	0,53	0,53	0,53	0,53	3,00	0,07
RINGwt_z	F4JFN3	Heat shock protein 90-6, mitochondrial	2	2	2,00	1	0|2|0	0,53	0,53	0,53	0,53	0,53	3,00	0,07
RINGwt_z	Q8RXN3	Phosphoenolpyruvate/phosphate translocator 1, chloroplastic	2	2	2,00	1	1|1|0	0,47	0,47	0,47	0,47	0,47	3,00	0,08
RINGwt_z	Q8L953	40S ribosomal protein S27-3	2	2	2,00	1	2|0|0	0,53	0,53	0,53	0,53	0,53	3,00	0,07
RINGwt_z	Q04613	ATP synthase protein MI25	2	2	2,00	1	0|0|2	0,53	0,53	0,53	0,53	0,53	3,00	0,07
RINGwt_z	O81146	Proteasome subunit alpha type-6-A	2	2	2,00	1	0|2|0	0,53	0,53	0,53	0,53	0,53	3,00	0,07
RINGwt_z	Q9FZ48	Ubiquitin-conjugating enzyme E2 36	1	1	1,00	1	0|1|0	0,00	0,00	0,00	0,00	0,00	3,00	0,51
RINGwt_z	Q9FFD8	Protein METHYLENE BLUE SENSITIVITY 2	1	1	1,00	1	0|0|1	0,00	0,00	0,00	0,00	0,00	3,00	0,51
RINGwt_z	Q94JX9	Nascent polypeptide-associated complex subunit alpha-like protein 2	1	1	1,00	1	1|0|0	0,00	0,00	0,00	0,00	0,00	3,00	0,51
RINGwt_z	Q9SP35	Mitochondrial import inner membrane translocase subunit TIM17-2	1	1	1,00	1	1|0|0	0,00	0,00	0,00	0,00	0,00	3,00	0,51
RINGwt_z	Q9FFN9	Probable E3 ubiquitin-protein ligase ARI13	1	1	1,00	1	1|0|0	0,00	0,00	0,00	0,00	0,00	3,00	0,51
RINGwt_z	Q42351	60S ribosomal protein L34-1	14	14	14,00	1	3|3|9	0,37	0,37	0,37	0,37	0,37	2,80	0,10
RINGwt_z	P49200	40S ribosomal protein S20-1	14	14	14,00	1	6|6|3	0,75	0,75	0,75	0,75	0,75	2,80	0,03

Bait: RINGwt_z	Prey	PreyGene	Spec	SpecSum	AvgSpec	NumReplicates	ctrlCounts	AvgP	MaxP	TopoAvgP	TopoMaxP	SaintScore	FoldChange	BFDR
RINGwt_z	P53492	Actin-7	71	71	71,00	1	28|30|19	0,99	0,99	0,99	0,99	0,99	2,77	0,00
RINGwt_z	Q08682	40S ribosomal protein Sa-1	23	23	23,00	1	9|12|4	0,33	0,33	0,33	0,33	0,33	2,76	0,11
RINGwt_z	Q9LJH8	Oligouridylate-binding protein 1C	20	20	20,00	1	11|7|4	0,42	0,42	0,42	0,42	0,42	2,73	0,09
RINGwt_z	Q9M5K3	Dihydrolipoyl dehydrogenase 1, mitochondrial	10	10	10,00	1	4|7|0	0,33	0,33	0,33	0,33	0,33	2,73	0,10
RINGwt_z	Q9ZU52	Fructose-bisphosphate aldolase 3, chloroplastic	10	10	10,00	1	2|2|7	0,37	0,37	0,37	0,37	0,37	2,73	0,09
RINGwt_z	O64650	40S ribosomal protein S27-1	10	10	10,00	1	7|4|0	0,33	0,33	0,33	0,33	0,33	2,73	0,10
RINGwt_z	Q9SEI2	26S proteasome regulatory subunit 6A homolog A	10	10	10,00	1	4|5|2	0,59	0,59	0,59	0,59	0,59	2,73	0,05
RINGwt_z	Q9FZ76	60S ribosomal protein L6-1	19	19	19,00	1	4|4|13	0,13	0,13	0,13	0,13	0,13	2,71	0,16
RINGwt_z	O23654	V-type proton ATPase catalytic subunit A	16	16	16,00	1	2|5|11	0,15	0,15	0,15	0,15	0,15	2,67	0,16
RINGwt_z	P0DH99	Elongation factor 1-alpha 1	158	158	158,00	1	69|82|30	0,00	0,00	0,00	0,00	0,00	2,62	0,47
RINGwt_z	Q9FVI6	Homeobox-leucine zipper protein HDG6	7	7	7,00	1	4|4|0	0,36	0,36	0,36	0,36	0,36	2,62	0,10
RINGwt_z	P31414	Pyrophosphate-energized vacuolar membrane proton pump 1	25	25	25,00	1	8|11|10	0,50	0,50	0,50	0,50	0,50	2,59	0,08
RINGwt_z	Q9C522	ATP-citrate synthase beta chain protein 1	52	52	52,00	1	32|27|2	0,00	0,00	0,00	0,00	0,00	2,56	0,38
RINGwt_z	Q9FGX1	ATP-citrate synthase beta chain protein 2	55	55	55,00	1	36|30|0	0,00	0,00	0,00	0,00	0,00	2,50	0,40
RINGwt_z	P41916	GTP-binding nuclear protein Ran-1	15	15	15,00	1	7|8|3	0,35	0,35	0,35	0,35	0,35	2,50	0,10
RINGwt_z	Q9M5K2	Dihydrolipoyl dehydrogenase 2, mitochondrial	10	10	10,00	1	6|6|0	0,18	0,18	0,18	0,18	0,18	2,50	0,14
RINGwt_z	Q84W89	DEAD-box ATP-dependent RNA helicase 37	5	5	5,00	1	2|4|0	0,33	0,33	0,33	0,33	0,33	2,50	0,11
RINGwt_z	O64728	Protein STICHEL	9	9	9,00	1	8|3|0	0,19	0,19	0,19	0,19	0,19	2,45	0,14
RINGwt_z	O04487	Probable elongation factor 1-gamma 1	9	9	9,00	1	5|6|0	0,18	0,18	0,18	0,18	0,18	2,45	0,14
RINGwt_z	Q1EBV4	Protein DNA-DAMAGE INDUCIBLE 1	34	34	34,00	1	19|12|11	0,03	0,03	0,03	0,03	0,03	2,43	0,22
RINGwt_z	Q9LFH5	60S ribosomal protein L12-2	12	12	12,00	1	8|7|0	0,08	0,08	0,08	0,08	0,08	2,40	0,19
RINGwt_z	Q9ASS2	Protein FREE1	35	35	35,00	1	17|18|9	0,00	0,00	0,00	0,00	0,00	2,39	0,31
RINGwt_z	P41376	Eukaryotic initiation factor 4A-1	42	42	42,00	1	19|25|10	0,00	0,00	0,00	0,00	0,00	2,33	0,38

Bait: RINGwt_z	Prey	PreyGene	Spec	SpecSum	AvgSpec	NumReplicates	ctrlCounts	AvgP	MaxP	TopoAvgP	TopoMaxP	SaintScore	FoldChange	BFDR
RINGwt_z	Q9LHP2	Serine/arginine-rich SC35-like splicing factor SCL30A	7	7	7,00	1	0|0|9	0,25	0,25	0,25	0,25	0,25	2,33	0,13
RINGwt_z	Q94K05	T-complex protein 1 subunit theta	7	7	7,00	1	5|4|0	0,18	0,18	0,18	0,18	0,18	2,33	0,14
RINGwt_z	Q9FLF0	40S ribosomal protein S9-2	22	22	22,00	1	0|0|29	0,00	0,00	0,00	0,00	0,00	2,28	0,31
RINGwt_z	Q39043	Heat shock 70 kDa protein BIP2	53	53	53,00	1	27|27|16	0,00	0,00	0,00	0,00	0,00	2,27	0,39
RINGwt_z	Q9LKR3	Heat shock 70 kDa protein BIP1	53	53	53,00	1	26|28|16	0,00	0,00	0,00	0,00	0,00	2,27	0,40
RINGwt_z	Q96292	Actin-2	34	34	34,00	1	18|18|9	0,00	0,00	0,00	0,00	0,00	2,27	0,35
RINGwt_z	O04658	Probable nucleolar protein 5-1	6	6	6,00	1	3|5|0	0,17	0,17	0,17	0,17	0,17	2,25	0,15
RINGwt_z	Q9LHE5	Mitochondrial import receptor subunit TOM40-1, N-terminally processed	6	6	6,00	1	3|5|0	0,17	0,17	0,17	0,17	0,17	2,25	0,15
RINGwt_z	Q9FMV1	Gamma carbonic anhydrase-like 1, mitochondrial	3	3	3,00	1	2|2|0	0,26	0,26	0,26	0,26	0,26	2,25	0,13
RINGwt_z	Q96528	Catalase-1	3	3	3,00	1	2|2|0	0,26	0,26	0,26	0,26	0,26	2,25	0,13
RINGwt_z	Q9LXV4	Zinc finger CCCH domain-containing protein 56	3	3	3,00	1	2|2|0	0,26	0,26	0,26	0,26	0,26	2,25	0,13
RINGwt_z	Q94CE5	Gamma-aminobutyrate transaminase POP2, mitochondrial	11	11	11,00	1	7|8|0	0,04	0,04	0,04	0,04	0,04	2,20	0,22
RINGwt_z	Q8RXU5	60S ribosomal protein L37a-2	8	8	8,00	1	0|0|11	0,12	0,12	0,12	0,12	0,12	2,18	0,17
RINGwt_z	O04019	26S proteasome regulatory subunit 6A homolog B	8	8	8,00	1	4|5|2	0,10	0,10	0,10	0,10	0,10	2,18	0,18
RINGwt_z	P29511	Tubulin alpha-6 chain	66	66	66,00	1	36|43|13	0,00	0,00	0,00	0,00	0,00	2,15	0,46
RINGwt_z	P41377	Eukaryotic initiation factor 4A-2	41	41	41,00	1	22|27|9	0,00	0,00	0,00	0,00	0,00	2,12	0,42
RINGwt_z	Q9SEI4	26S proteasome regulatory subunit 6B homolog	17	17	17,00	1	9|13|2	0,00	0,00	0,00	0,00	0,00	2,12	0,31
RINGwt_z	Q9S9N1	Heat shock 70 kDa protein 5	42	42	42,00	1	15|21|24	0,00	0,00	0,00	0,00	0,00	2,10	0,38
RINGwt_z	Q9C9C5	60S ribosomal protein L6-3	14	14	14,00	1	0|0|20	0,01	0,01	0,01	0,01	0,01	2,10	0,27
RINGwt_z	Q0WNJ6	Clathrin heavy chain 1	39	39	39,00	1	25|31|0	0,00	0,00	0,00	0,00	0,00	2,09	0,43
RINGwt_z	Q9SV20	Coatomer subunit beta-2	11	11	11,00	1	6|10|0	0,02	0,02	0,02	0,02	0,02	2,06	0,26
RINGwt_z	Q56WH1	Tubulin alpha-3 chain	43	43	43,00	1	24|31|8	0,00	0,00	0,00	0,00	0,00	2,05	0,44
RINGwt_z	B9DHQ0	Tubulin alpha-5 chain	43	43	43,00	1	24|31|8	0,00	0,00	0,00	0,00	0,00	2,05	0,44

Bait: RINGwt_z	Prey	PreyGene	Spec	SpecSum	AvgSpec	NumReplicates	ctrlCounts	AvgP	MaxP	TopoAvgP	TopoMaxP	SaintScore	FoldChange	BFDR
RINGwt_z	Q9SZ15	Protein HOMOLOG OF MAMMALIAN LYST-INTERACTING PROTEIN 5	41	41	41,00	1	25|22|13	0,00	0,00	0,00	0,00	0,00	2,05	0,42
RINGwt_z	Q96293	Actin-8	34	34	34,00	1	20|20|10	0,00	0,00	0,00	0,00	0,00	2,04	0,41
RINGwt_z	Q9FX54	Glyceraldehyde-3-phosphate dehydrogenase GAPC2, cytosolic	73	73	73,00	1	41|45|22	0,00	0,00	0,00	0,00	0,00	2,03	0,47
RINGwt_z	Q9M339	40S ribosomal protein S3-2	22	22	22,00	1	15|18|0	0,00	0,00	0,00	0,00	0,00	2,00	0,37
RINGwt_z	Q9SJF1	GTPase LSG1-2	20	20	20,00	1	12|11|7	0,00	0,00	0,00	0,00	0,00	2,00	0,34
RINGwt_z	Q9FEF8	rRNA 2'-O-methyltransferase fibrillarin 1	16	16	16,00	1	11|11|2	0,00	0,00	0,00	0,00	0,00	2,00	0,33
RINGwt_z	Q9LF46	2-hydroxyacyl-CoA lyase	8	8	8,00	1	6|6|0	0,03	0,03	0,03	0,03	0,03	2,00	0,22
RINGwt_z	Q9FJH6	ABC transporter F family member 1	8	8	8,00	1	5|7|0	0,03	0,03	0,03	0,03	0,03	2,00	0,22
RINGwt_z	O82355	Desiccation-related protein At2g46140	4	4	4,00	1	3|3|0	0,13	0,13	0,13	0,13	0,13	2,00	0,16
RINGwt_z	Q9LVM1	ABC transporter B family member 25, mitochondrial	2	2	2,00	1	0|0|3	0,33	0,33	0,33	0,33	0,33	2,00	0,11
RINGwt_z	Q9SIT1	Receptor-like kinase TMK3	2	2	2,00	1	2|1|0	0,23	0,23	0,23	0,23	0,23	2,00	0,13
RINGwt_z	P31265	Translationally-controlled tumor protein 1	2	2	2,00	1	0|0|3	0,33	0,33	0,33	0,33	0,33	2,00	0,11
RINGwt_z	F4K0J3	Kinesin-like protein KIN-4C	2	2	2,00	1	0|3|0	0,33	0,33	0,33	0,33	0,33	2,00	0,11
RINGwt_z	Q8GUM2	Heat shock 70 kDa protein 9, mitochondrial	46	46	46,00	1	27|28|15	0,00	0,00	0,00	0,00	0,00	1,97	0,44
RINGwt_z	Q56WH4	Histone deacetylase HDT2	15	15	15,00	1	11|12|0	0,00	0,00	0,00	0,00	0,00	1,96	0,33
RINGwt_z	P49227	60S ribosomal protein L5-2	24	24	24,00	1	17|20|0	0,00	0,00	0,00	0,00	0,00	1,95	0,39
RINGwt_z	Q42523	Methylcrotonoyl-CoA carboxylase subunit alpha, mitochondrial	160	160	160,00	1	7|13|227	0,00	0,00	0,00	0,00	0,00	1,94	0,50
RINGwt_z	P25858	Glyceraldehyde-3-phosphate dehydrogenase GAPC1, cytosolic	68	68	68,00	1	39|41|25	0,00	0,00	0,00	0,00	0,00	1,94	0,47
RINGwt_z	P42794	60S ribosomal protein L11-2	18	18	18,00	1	11|14|3	0,00	0,00	0,00	0,00	0,00	1,93	0,36
RINGwt_z	Q9CAX6	40S ribosomal protein S14-2	14	14	14,00	1	11|11|0	0,00	0,00	0,00	0,00	0,00	1,91	0,33
RINGwt_z	Q9LZ57	60S ribosomal protein L36-3	7	7	7,00	1	0|0|11	0,05	0,05	0,05	0,05	0,05	1,91	0,21
RINGwt_z	P40941	ADP,ATP carrier protein 2, mitochondrial	41	41	41,00	1	26|23|16	0,00	0,00	0,00	0,00	0,00	1,89	0,44
RINGwt_z	P11139	Tubulin alpha-1 chain	20	20	20,00	1	12|16|4	0,00	0,00	0,00	0,00	0,00	1,88	0,38

Bait: RINGwt_z	Prey	PreyGene	Spec	SpecSum	AvgSpec	NumReplicates	ctrlCounts	AvgP	MaxP	TopoAvgP	TopoMaxP	SaintScore	FoldChange	BFDR
RINGwt_z	Q5XEP2	Hsp70-Hsp90 organizing protein 2	10	10	10,00	1	9|7|0	0,01	0,01	0,01	0,01	0,01	1,88	0,29
RINGwt_z	Q9M9W1	60S ribosomal protein L22-2	5	5	5,00	1	4|3|1	0,06	0,06	0,06	0,06	0,06	1,88	0,21
RINGwt_z	F4J8K6	rRNA biogenesis protein RRP5	5	5	5,00	1	6|2|0	0,08	0,08	0,08	0,08	0,08	1,88	0,19
RINGwt_z	Q9SIP7	40S ribosomal protein S3-1	25	25	25,00	1	17|18|6	0,00	0,00	0,00	0,00	0,00	1,83	0,42
RINGwt_z	Q9SIH0	40S ribosomal protein S14-1	17	17	17,00	1	11|11|6	0,00	0,00	0,00	0,00	0,00	1,82	0,36
RINGwt_z	P31167	ADP,ATP carrier protein 1, mitochondrial	81	81	81,00	1	43|47|45	0,00	0,00	0,00	0,00	0,00	1,80	0,49
RINGwt_z	Q8LBI1	60S ribosomal protein L5-1	27	27	27,00	1	19|21|5	0,00	0,00	0,00	0,00	0,00	1,80	0,43
RINGwt_z	Q38929	Isopentenyl-diphosphate Delta-isomerase I, chloroplastic	3	3	3,00	1	2|3|0	0,11	0,11	0,11	0,11	0,11	1,80	0,17
RINGwt_z	Q9LK22	Plant UBX domain-containing protein 1	3	3	3,00	1	3|1|1	0,10	0,10	0,10	0,10	0,10	1,80	0,18
RINGwt_z	P93733	Phospholipase D beta 1	3	3	3,00	1	3|2|0	0,11	0,11	0,11	0,11	0,11	1,80	0,17
RINGwt_z	Q0WLB5	Clathrin heavy chain 2	35	35	35,00	1	28|31|0	0,00	0,00	0,00	0,00	0,00	1,78	0,45
RINGwt_z	P46644	Aspartate aminotransferase 3, chloroplastic	13	13	13,00	1	11|11|0	0,00	0,00	0,00	0,00	0,00	1,77	0,35
RINGwt_z	Q9T043	60S ribosomal protein L14-2	14	14	14,00	1	9|11|4	0,00	0,00	0,00	0,00	0,00	1,75	0,36
RINGwt_z	Q9SEE9	Serine/arginine-rich splicing factor SR45	7	7	7,00	1	3|3|6	0,01	0,01	0,01	0,01	0,01	1,75	0,27
RINGwt_z	Q39189	DEAD-box ATP-dependent RNA helicase 7	7	7	7,00	1	5|7|0	0,01	0,01	0,01	0,01	0,01	1,75	0,27
RINGwt_z	Q9CAN8	Lysophospholipid acyltransferase 2	11	11	11,00	1	9|10|0	0,00	0,00	0,00	0,00	0,00	1,74	0,33
RINGwt_z	Q93VP3	Eukaryotic translation initiation factor 5A-2	8	8	8,00	1	8|6|0	0,00	0,00	0,00	0,00	0,00	1,71	0,30
RINGwt_z	P57691	60S acidic ribosomal protein P0-3	9	9	9,00	1	5|11|0	0,00	0,00	0,00	0,00	0,00	1,69	0,31
RINGwt_z	P0DH91	ADP-ribosylation factor 2-B	15	15	15,00	1	13|14|0	0,00	0,00	0,00	0,00	0,00	1,67	0,38
RINGwt_z	Q39172	NADPH-dependent oxidoreductase 2-alkenal reductase	5	5	5,00	1	3|6|0	0,03	0,03	0,03	0,03	0,03	1,67	0,24
RINGwt_z	Q9LLC1	Biotin carboxyl carrier protein of acetyl-CoA carboxylase 2, chloroplastic	57	57	57,00	1	0|0|103	0,00	0,00	0,00	0,00	0,00	1,66	0,49
RINGwt_z	Q9FJA6	40S ribosomal protein S3-3	21	21	21,00	1	15|17|6	0,00	0,00	0,00	0,00	0,00	1,66	0,43
RINGwt_z	Q8L8Y0	40S ribosomal protein S2-1	16	16	16,00	1	10|11|8	0,00	0,00	0,00	0,00	0,00	1,66	0,39

Bait: RINGwt_z	Prey	PreyGene	Spec	SpecSum	AvgSpec	NumReplicates	ctrlCounts	AvgP	MaxP	TopoAvgP	TopoMaxP	SaintScore	FoldChange	BFDR
RINGwt_z	Q93VB8	40S ribosomal protein S2-2	16	16	16,00	1	10|11|8	0,00	0,00	0,00	0,00	0,00	1,66	0,39
RINGwt_z	P46645	Aspartate aminotransferase, cytoplasmic isozyme 1	34	34	34,00	1	27|31|4	0,00	0,00	0,00	0,00	0,00	1,65	0,46
RINGwt_z	Q9LIA8	UDP-glucose 6-dehydrogenase 2	11	11	11,00	1	10|10|0	0,00	0,00	0,00	0,00	0,00	1,65	0,35
RINGwt_z	P59259	Histone H4	12	12	12,00	1	0|2|20	0,00	0,00	0,00	0,00	0,00	1,64	0,35
RINGwt_z	Q05431	L-ascorbate peroxidase 1, cytosolic	12	12	12,00	1	11|11|0	0,00	0,00	0,00	0,00	0,00	1,64	0,36
RINGwt_z	Q9C658	Protein decapping 5	6	6	6,00	1	5|6|0	0,01	0,01	0,01	0,01	0,01	1,64	0,27
RINGwt_z	Q9STW6	Heat shock 70 kDa protein 6, chloroplastic	8	8	8,00	1	3|4|8	0,00	0,00	0,00	0,00	0,00	1,60	0,32
RINGwt_z	P51427	40S ribosomal protein S5-2	8	8	8,00	1	7|8|0	0,00	0,00	0,00	0,00	0,00	1,60	0,32
RINGwt_z	Q9FMG4	Serine/arginine-rich splicing factor SC35	8	8	8,00	1	0|0|15	0,00	0,00	0,00	0,00	0,00	1,60	0,31
RINGwt_z	Q9LDZ0	Heat shock 70 kDa protein 10, mitochondrial	8	8	8,00	1	9|6|0	0,00	0,00	0,00	0,00	0,00	1,60	0,32
RINGwt_z	Q9SSB5	26S proteasome regulatory subunit 7 homolog A	9	9	9,00	1	7|10|0	0,00	0,00	0,00	0,00	0,00	1,59	0,34
RINGwt_z	Q9LTX9	Heat shock 70 kDa protein 7, chloroplastic	10	10	10,00	1	4|5|10	0,00	0,00	0,00	0,00	0,00	1,58	0,36
RINGwt_z	P51414	60S ribosomal protein L26-1	12	12	12,00	1	2|4|17	0,00	0,00	0,00	0,00	0,00	1,57	0,37
RINGwt_z	P22953	Heat shock 70 kDa protein 1	166	166	166,00	1	124|137|58	0,00	0,00	0,00	0,00	0,00	1,56	0,51
RINGwt_z	Q9FVQ1	Nucleolin 1	14	14	14,00	1	14|13|0	0,00	0,00	0,00	0,00	0,00	1,56	0,39
RINGwt_z	Q9SZY1	Nascent polypeptide-associated complex subunit alpha-like protein 4	13	13	13,00	1	9|9|7	0,00	0,00	0,00	0,00	0,00	1,56	0,38
RINGwt_z	Q42533	Biotin carboxyl carrier protein of acetyl-CoA carboxylase 1, chloroplastic	147	147	147,00	1	14|14|256	0,00	0,00	0,00	0,00	0,00	1,55	0,50
RINGwt_z	Q8L7U4	Co-chaperone protein p23-1	20	20	20,00	1	19|18|2	0,00	0,00	0,00	0,00	0,00	1,54	0,44
RINGwt_z	Q8H136	DEAD-box ATP-dependent RNA helicase 14	39	39	39,00	1	20|21|37	0,00	0,00	0,00	0,00	0,00	1,50	0,48
RINGwt_z	P25696	Bifunctional enolase 2/transcriptional activator	34	34	34,00	1	27|30|11	0,00	0,00	0,00	0,00	0,00	1,50	0,47
RINGwt_z	P49209	60S ribosomal protein L9-1	33	33	33,00	1	26|28|12	0,00	0,00	0,00	0,00	0,00	1,50	0,47
RINGwt_z	P20649	ATPase 1, plasma membrane-type	16	16	16,00	1	14|18|0	0,00	0,00	0,00	0,00	0,00	1,50	0,42

Bait: RINGwt_z	Prey	PreyGene	Spec	SpecSum	AvgSpec	NumReplicates	ctrlCounts	AvgP	MaxP	TopoAvgP	TopoMaxP	SaintScore	FoldChange	BFDR
RINGwt_z	Q9LYJ9	DEAD-box ATP-dependent RNA helicase 46	14	14	14,00	1	13|15|0	0,00	0,00	0,00	0,00	0,00	1,50	0,40
RINGwt_z	Q9LNU4	26S proteasome non-ATPase regulatory subunit 3 homolog A	7	7	7,00	1	7|7|0	0,00	0,00	0,00	0,00	0,00	1,50	0,32
RINGwt_z	Q8RWN9	Pyruvate dehydrogenase E2 component (dihydrolipoamide acetyltransferase)	5	5	5,00	1	0|0|10	0,02	0,02	0,02	0,02	0,02	1,50	0,26
RINGwt_z	Q9FLT9	Chloroplastic import inner membrane translocase subunit HP30-2	5	5	5,00	1	3|4|3	0,01	0,01	0,01	0,01	0,01	1,50	0,29
RINGwt_z	Q9ZW02	Pumilio homolog 3	4	4	4,00	1	4|4|0	0,02	0,02	0,02	0,02	0,02	1,50	0,25
RINGwt_z	P38420	DNA-directed RNA polymerase II subunit 2	4	4	4,00	1	3|5|0	0,02	0,02	0,02	0,02	0,02	1,50	0,25
RINGwt_z	Q8W117	Suppressor of mec-8 and unc-52 protein homolog 1	4	4	4,00	1	4|4|0	0,02	0,02	0,02	0,02	0,02	1,50	0,25
RINGwt_z	Q949U7	Peroxiredoxin-2E, chloroplastic	3	3	3,00	1	3|3|0	0,04	0,04	0,04	0,04	0,04	1,50	0,21
RINGwt_z	Q9FPJ8	Polyadenylate-binding protein RBP45A	3	3	3,00	1	3|3|0	0,04	0,04	0,04	0,04	0,04	1,50	0,21
RINGwt_z	Q9FMR9	RuvB-like protein 1	3	3	3,00	1	4|2|0	0,05	0,05	0,05	0,05	0,05	1,50	0,21
RINGwt_z	O64642	UTP:RNA uridylyltransferase 1	2	2	2,00	1	2|2|0	0,07	0,07	0,07	0,07	0,07	1,50	0,19
RINGwt_z	Q9LPL6	TOM1-like protein 3	2	2	2,00	1	2|2|0	0,07	0,07	0,07	0,07	0,07	1,50	0,19
RINGwt_z	Q9LKA5	Multiple organellar RNA editing factor 8, chloroplastic/mitochondrial	1	1	1,00	1	1|1|0	0,00	0,00	0,00	0,00	0,00	1,50	0,51
RINGwt_z	Q9LSV0	Glyoxylate/succinic semialdehyde reductase 1	1	1	1,00	1	2|0|0	0,00	0,00	0,00	0,00	0,00	1,50	0,51
RINGwt_z	Q9STM4	Zinc finger CCCH domain-containing protein 43	1	1	1,00	1	2|0|0	0,00	0,00	0,00	0,00	0,00	1,50	0,51
RINGwt_z	P52410	3-oxoacyl-[acyl-carrier-protein] synthase I, chloroplastic	1	1	1,00	1	1|1|0	0,00	0,00	0,00	0,00	0,00	1,50	0,51
RINGwt_z	P29976	Phospho-2-dehydro-3-deoxyheptonate aldolase 1, chloroplastic	13	13	13,00	1	13|14|0	0,00	0,00	0,00	0,00	0,00	1,44	0,41
RINGwt_z	O50008	5-methyltetrahydropteroyltriglutamate--homocysteine methyltransferase 1	21	21	21,00	1	23|21|0	0,00	0,00	0,00	0,00	0,00	1,43	0,45
RINGwt_z	P49688	40S ribosomal protein S2-3	19	19	19,00	1	13|14|14	0,00	0,00	0,00	0,00	0,00	1,39	0,45
RINGwt_z	O23515	60S ribosomal protein L15-1	33	33	33,00	1	13|11|48	0,00	0,00	0,00	0,00	0,00	1,38	0,48

Bait: RINGwt_z	Prey	PreyGene	Spec	SpecSum	AvgSpec	NumReplicates	ctrlCounts	AvgP	MaxP	TopoAvgP	TopoMaxP	SaintScore	FoldChange	BFDR
RINGwt_z	Q9LXG1	40S ribosomal protein S9-1	33	33	33,00	1	13|16|43	0,00	0,00	0,00	0,00	0,00	1,38	0,48
RINGwt_z	P46286	60S ribosomal protein L8-1	29	29	29,00	1	13|16|34	0,00	0,00	0,00	0,00	0,00	1,38	0,48
RINGwt_z	Q9FLT0	Ribonuclease TUDOR 2	17	17	17,00	1	19|18|0	0,00	0,00	0,00	0,00	0,00	1,38	0,44
RINGwt_z	Q9FMU6	Mitochondrial phosphate carrier protein 3, mitochondrial	12	12	12,00	1	10|13|3	0,00	0,00	0,00	0,00	0,00	1,38	0,41
RINGwt_z	Q8LF21	Dynamin-related protein 1C	67	67	67,00	1	41|46|60	0,00	0,00	0,00	0,00	0,00	1,37	0,50
RINGwt_z	Q42340	40S ribosomal protein S16-3	25	25	25,00	1	12|11|32	0,00	0,00	0,00	0,00	0,00	1,36	0,47
RINGwt_z	P42697	Dynamin-related protein 1A	95	95	95,00	1	55|61|97	0,00	0,00	0,00	0,00	0,00	1,34	0,50
RINGwt_z	O65719	Heat shock 70 kDa protein 3	130	130	130,00	1	122|127|45	0,00	0,00	0,00	0,00	0,00	1,33	0,51
RINGwt_z	Q9LNB6	Hsp70-Hsp90 organizing protein 1	56	56	56,00	1	44|45|39	0,00	0,00	0,00	0,00	0,00	1,31	0,50
RINGwt_z	F4K1Z0	YTH domain-containing protein ECT3	10	10	10,00	1	8|7|8	0,00	0,00	0,00	0,00	0,00	1,30	0,41
RINGwt_z	Q9LHA8	Heat shock 70 kDa protein 4	118	118	118,00	1	108|122|45	0,00	0,00	0,00	0,00	0,00	1,29	0,51
RINGwt_z	P34788	40S ribosomal protein S18	15	15	15,00	1	6|9|20	0,00	0,00	0,00	0,00	0,00	1,29	0,44
RINGwt_z	Q96266	Glutathione S-transferase F8, chloroplastic	9	9	9,00	1	8|13|0	0,00	0,00	0,00	0,00	0,00	1,29	0,39
RINGwt_z	Q9LQ04	Bifunctional dTDP-4-dehydrorhamnose 3,5-epimerase/dTDP-4-dehydrorhamnose reductase	9	9	9,00	1	11|10|0	0,00	0,00	0,00	0,00	0,00	1,29	0,39
RINGwt_z	Q9FPJ4	Ras-related protein RABD2b	6	6	6,00	1	7|7|0	0,00	0,00	0,00	0,00	0,00	1,29	0,35
RINGwt_z	P22954	Heat shock 70 kDa protein 2	119	119	119,00	1	110|123|51	0,00	0,00	0,00	0,00	0,00	1,26	0,51
RINGwt_z	Q9T029	40S ribosomal protein S25-4	8	8	8,00	1	5|6|8	0,00	0,00	0,00	0,00	0,00	1,26	0,39
RINGwt_z	Q9MAB3	Probable nucleolar protein 5-2	10	10	10,00	1	8|9|7	0,00	0,00	0,00	0,00	0,00	1,25	0,42
RINGwt_z	Q945Q1	Cysteine proteinase inhibitor 1	5	5	5,00	1	4|4|4	0,00	0,00	0,00	0,00	0,00	1,25	0,34
RINGwt_z	Q9CAV0	40S ribosomal protein S3a-1	16	16	16,00	1	13|18|8	0,00	0,00	0,00	0,00	0,00	1,23	0,45
RINGwt_z	Q8W103	Protein CHROMATIN REMODELING 24	11	11	11,00	1	14|13|0	0,00	0,00	0,00	0,00	0,00	1,22	0,43
RINGwt_z	Q9C7X7	Heat shock 70 kDa protein 18	97	97	97,00	1	95|100|45	0,00	0,00	0,00	0,00	0,00	1,21	0,51
RINGwt_z	Q84VW9	Phosphoenolpyruvate carboxylase 3	16	16	16,00	1	24|16|0	0,00	0,00	0,00	0,00	0,00	1,20	0,45

Bait: RINGwt_z	Prey	PreyGene	Spec	SpecSum	AvgSpec	NumReplicates	ctrlCounts	AvgP	MaxP	TopoAvgP	TopoMaxP	SaintScore	FoldChange	BFDR
RINGwt_z	Q9FFT4	Pyruvate decarboxylase 2	2	2	2,00	1	2|3|0	0,03	0,03	0,03	0,03	0,03	1,20	0,23
RINGwt_z	Q93W34	Polyadenylate-binding protein RBP45C	2	2	2,00	1	2|3|0	0,03	0,03	0,03	0,03	0,03	1,20	0,23
RINGwt_z	O04834	GTP-binding protein SAR1A	2	2	2,00	1	2|3|0	0,03	0,03	0,03	0,03	0,03	1,20	0,23
RINGwt_z	Q8LD27	Proteasome subunit beta type-6	2	2	2,00	1	1|4|0	0,04	0,04	0,04	0,04	0,04	1,20	0,21
RINGwt_z	Q9SKU1	Clathrin light chain 1	2	2	2,00	1	2|3|0	0,03	0,03	0,03	0,03	0,03	1,20	0,23
RINGwt_z	Q9SFU0	Protein transport protein Sec24-like At3g07100	2	2	2,00	1	2|3|0	0,03	0,03	0,03	0,03	0,03	1,20	0,23
RINGwt_z	P60039	60S ribosomal protein L7-3	21	21	21,00	1	14|17|22	0,00	0,00	0,00	0,00	0,00	1,19	0,48
RINGwt_z	O81126	Serine/arginine-rich splicing factor RSZ22	9	9	9,00	1	1|0|22	0,00	0,00	0,00	0,00	0,00	1,17	0,41
RINGwt_z	Q9SL67	26S proteasome regulatory subunit 4 homolog B	7	7	7,00	1	9|9|0	0,00	0,00	0,00	0,00	0,00	1,17	0,38
RINGwt_z	Q43291	60S ribosomal protein L21-1	7	7	7,00	1	10|8|0	0,00	0,00	0,00	0,00	0,00	1,17	0,38
RINGwt_z	Q42262	40S ribosomal protein S3a-2	21	21	21,00	1	19|19|17	0,00	0,00	0,00	0,00	0,00	1,15	0,48
RINGwt_z	Q9LT08	26S proteasome non-ATPase regulatory subunit 14 homolog	5	5	5,00	1	3|10|0	0,00	0,00	0,00	0,00	0,00	1,15	0,34
RINGwt_z	Q93VG5	40S ribosomal protein S8-1	28	28	28,00	1	28|32|14	0,00	0,00	0,00	0,00	0,00	1,14	0,49
RINGwt_z	Q42064	60S ribosomal protein L8-3	24	24	24,00	1	14|16|33	0,00	0,00	0,00	0,00	0,00	1,14	0,49
RINGwt_z	P17745	Elongation factor Tu, chloroplastic	14	14	14,00	1	19|16|2	0,00	0,00	0,00	0,00	0,00	1,14	0,45
RINGwt_z	Q9M352	60S ribosomal protein L36-2	8	8	8,00	1	1|1|19	0,00	0,00	0,00	0,00	0,00	1,14	0,40
RINGwt_z	Q42347	60S ribosomal protein L24-1	8	8	8,00	1	0|0|21	0,00	0,00	0,00	0,00	0,00	1,14	0,40
RINGwt_z	Q9LF33	UDP-glucose 6-dehydrogenase 3	8	8	8,00	1	8|13|0	0,00	0,00	0,00	0,00	0,00	1,14	0,40
RINGwt_z	Q9C5U3	26S proteasome regulatory subunit 8 homolog A	8	8	8,00	1	10|11|0	0,00	0,00	0,00	0,00	0,00	1,14	0,41
RINGwt_z	Q94CJ5	Protein RETICULATA-RELATED 4, chloroplastic	6	6	6,00	1	7|9|0	0,00	0,00	0,00	0,00	0,00	1,12	0,37
RINGwt_z	O64843	Polyadenylate-binding protein-interacting protein 7	3	3	3,00	1	4|4|0	0,00	0,00	0,00	0,00	0,00	1,12	0,30
RINGwt_z	P0DH97	Calmodulin-2	3	3	3,00	1	4|4|0	0,00	0,00	0,00	0,00	0,00	1,12	0,30
RINGwt_z	Q9LJE5	YTH domain-containing protein ECT2	21	21	21,00	1	23|27|7	0,00	0,00	0,00	0,00	0,00	1,11	0,48

Bait: RINGwt_z	Prey	PreyGene	Spec	SpecSum	AvgSpec	NumReplicates	ctrlCounts	AvgP	MaxP	TopoAvgP	TopoMaxP	SaintScore	FoldChange	BFDR
RINGwt_z	Q9SIV2	26S proteasome non-ATPase regulatory subunit 2 homolog A	10	10	10,00	1	10|17|0	0,00	0,00	0,00	0,00	0,00	1,11	0,43
RINGwt_z	Q8L5Y6	Cullin-associated NEDD8-dissociated protein 1	49	49	49,00	1	67|62|5	0,00	0,00	0,00	0,00	0,00	1,10	0,50
RINGwt_z	P19456	ATPase 2, plasma membrane-type	16	16	16,00	1	17|27|0	0,00	0,00	0,00	0,00	0,00	1,09	0,47
RINGwt_z	Q9LTT8	Enhancer of mRNA-decapping protein 4	55	55	55,00	1	68|70|15	0,00	0,00	0,00	0,00	0,00	1,08	0,50
RINGwt_z	Q8LPJ7	40S ribosomal protein S26-2	9	9	9,00	1	0|0|25	0,00	0,00	0,00	0,00	0,00	1,08	0,42
RINGwt_z	Q9ZUT9	40S ribosomal protein S5-1	10	10	10,00	1	5|7|16	0,00	0,00	0,00	0,00	0,00	1,07	0,44
RINGwt_z	P51413	60S ribosomal protein L17-2	10	10	10,00	1	5|7|18	0,00	0,00	0,00	0,00	0,00	1,00	0,51
RINGwt_z	Q94BQ2	26S proteasome regulatory subunit 8 homolog B	8	8	8,00	1	10|12|2	0,00	0,00	0,00	0,00	0,00	1,00	0,51
RINGwt_z	Q9SMW7	Basic transcription factor 3	6	6	6,00	1	8|8|2	0,00	0,00	0,00	0,00	0,00	1,00	0,51
RINGwt_z	Q9SIK2	40S ribosomal protein S25-2	4	4	4,00	1	2|4|6	0,00	0,00	0,00	0,00	0,00	1,00	0,51
RINGwt_z	Q9LIK0	Plastidial pyruvate kinase 1, chloroplastic	3	3	3,00	1	4|5|0	0,00	0,00	0,00	0,00	0,00	1,00	0,51
RINGwt_z	Q9ZU46	Receptor protein kinase-like protein ZAR1	2	2	2,00	1	0|0|6	0,00	0,00	0,00	0,00	0,00	1,00	0,51
RINGwt_z	Q949R9	Mitochondrial pyruvate carrier 1	2	2	2,00	1	1|1|4	0,00	0,00	0,00	0,00	0,00	1,00	0,51
RINGwt_z	P47192	Vesicle-associated membrane protein 722	2	2	2,00	1	2|4|0	0,00	0,00	0,00	0,00	0,00	1,00	0,51
RINGwt_z	P0DO44	ATP synthase small subunit 6-A, mitochondrial	1	1	1,00	1	0|0|3	0,00	0,00	0,00	0,00	0,00	1,00	0,51
RINGwt_z	P49692	60S ribosomal protein L7a-1	21	21	21,00	1	13|14|37	0,00	0,00	0,00	0,00	0,00	0,98	0,51
RINGwt_z	Q9LHP1	60S ribosomal protein L7-4	14	14	14,00	1	12|14|17	0,00	0,00	0,00	0,00	0,00	0,98	0,51
RINGwt_z	Q9ZPI1	Lysine--tRNA ligase, cytoplasmic	12	12	12,00	1	15|22|0	0,00	0,00	0,00	0,00	0,00	0,97	0,51
RINGwt_z	Q8L6Y1	Ubiquitin carboxyl-terminal hydrolase 14	7	7	7,00	1	14|8|0	0,00	0,00	0,00	0,00	0,00	0,95	0,51
RINGwt_z	Q9LDD8	Methylcrotonoyl-CoA carboxylase beta chain, mitochondrial	68	68	68,00	1	3|6|209	0,00	0,00	0,00	0,00	0,00	0,94	0,51
RINGwt_z	Q9STX5	Endoplasmin homolog	5	5	5,00	1	7|9|0	0,00	0,00	0,00	0,00	0,00	0,94	0,51
RINGwt_z	Q9LVT8	RGG repeats nuclear RNA binding protein C	5	5	5,00	1	10|6|0	0,00	0,00	0,00	0,00	0,00	0,94	0,51
RINGwt_z	Q9LQ55	Dynamin-2B	72	72	72,00	1	54|60|118	0,00	0,00	0,00	0,00	0,00	0,93	0,51

Bait: RINGwt_z	Prey	PreyGene	Spec	SpecSum	AvgSpec	NumReplicates	ctrlCounts	AvgP	MaxP	TopoAvgP	TopoMaxP	SaintScore	FoldChange	BFDR
RINGwt_z	P49204	40S ribosomal protein S4-2	33	33	33,00	1	27|33|47	0,00	0,00	0,00	0,00	0,00	0,93	0,51
RINGwt_z	P60040	60S ribosomal protein L7-2	20	20	20,00	1	16|23|26	0,00	0,00	0,00	0,00	0,00	0,92	0,51
RINGwt_z	P49205	40S ribosomal protein S17-1	4	4	4,00	1	3|2|8	0,00	0,00	0,00	0,00	0,00	0,92	0,51
RINGwt_z	Q944K2	Dolichyl-diphosphooligosaccharide--protein glycosyltransferase 48 kDa subunit	4	4	4,00	1	6|7|0	0,00	0,00	0,00	0,00	0,00	0,92	0,51
RINGwt_z	Q9SB63	Protein MODIFIER OF SNC1 1	10	10	10,00	1	17|16|0	0,00	0,00	0,00	0,00	0,00	0,91	0,51
RINGwt_z	P16181	40S ribosomal protein S11-1	9	9	9,00	1	7|7|16	0,00	0,00	0,00	0,00	0,00	0,90	0,51
RINGwt_z	Q9STH1	Hsp70-Hsp90 organizing protein 3	3	3	3,00	1	4|6|0	0,00	0,00	0,00	0,00	0,00	0,90	0,51
RINGwt_z	Q9MAH0	Phosphoenolpyruvate carboxylase 1	20	20	20,00	1	34|28|6	0,00	0,00	0,00	0,00	0,00	0,88	0,51
RINGwt_z	P42733	40S ribosomal protein S11-3	5	5	5,00	1	2|2|13	0,00	0,00	0,00	0,00	0,00	0,88	0,51
RINGwt_z	Q9SJQ9	Fructose-bisphosphate aldolase 6, cytosolic	57	57	57,00	1	82|66|48	0,00	0,00	0,00	0,00	0,00	0,87	0,51
RINGwt_z	Q9LZH9	60S ribosomal protein L7a-2	16	16	16,00	1	10|11|34	0,00	0,00	0,00	0,00	0,00	0,87	0,51
RINGwt_z	Q9LFD5	Binding partner of ACD11 1	11	11	11,00	1	14|16|8	0,00	0,00	0,00	0,00	0,00	0,87	0,51
RINGwt_z	Q940B0	60S ribosomal protein L18-3	16	16	16,00	1	13|11|32	0,00	0,00	0,00	0,00	0,00	0,86	0,51
RINGwt_z	O22860	60S ribosomal protein L38	6	6	6,00	1	7|6|8	0,00	0,00	0,00	0,00	0,00	0,86	0,51
RINGwt_z	Q9FPF0	Protein DJ-1 homolog A	2	2	2,00	1	3|3|1	0,00	0,00	0,00	0,00	0,00	0,86	0,51
RINGwt_z	Q9T041	Microtubule-associated protein TORTIFOLIA1	2	2	2,00	1	2|5|0	0,00	0,00	0,00	0,00	0,00	0,86	0,51
RINGwt_z	Q9LF98	Fructose-bisphosphate aldolase 8, cytosolic	86	86	86,00	1	114|102|87	0,00	0,00	0,00	0,00	0,00	0,85	0,51
RINGwt_z	Q9LYK9	40S ribosomal protein S26-3	9	9	9,00	1	3|4|26	0,00	0,00	0,00	0,00	0,00	0,82	0,51
RINGwt_z	Q9SE83	Dynamin-2A	60	60	60,00	1	55|65|102	0,00	0,00	0,00	0,00	0,00	0,81	0,51
RINGwt_z	Q8S3C9	Dynamin-related protein 1D	4	4	4,00	1	4|3|8	0,00	0,00	0,00	0,00	0,00	0,80	0,51
RINGwt_z	P49206	40S ribosomal protein S26-1	9	9	9,00	1	4|4|26	0,00	0,00	0,00	0,00	0,00	0,79	0,51
RINGwt_z	O48847	Transcriptional corepressor LEUNIG_HOMOLOG	5	5	5,00	1	9|10|0	0,00	0,00	0,00	0,00	0,00	0,79	0,51
RINGwt_z	Q9M1R2	Proline--tRNA ligase, cytoplasmic	5	5	5,00	1	10|9|0	0,00	0,00	0,00	0,00	0,00	0,79	0,51

Bait: RINGwt_z	Prey	PreyGene	Spec	SpecSum	AvgSpec	NumReplicates	ctrlCounts	AvgP	MaxP	TopoAvgP	TopoMaxP	SaintScore	FoldChange	BFDR
RINGwt_z	Q9SSD2	Pre-mRNA-processing-splicing factor 8A	7	7	7,00	1	14|13|0	0,00	0,00	0,00	0,00	0,00	0,78	0,51
RINGwt_z	P17094	60S ribosomal protein L3-1	34	34	34,00	1	36|42|58	0,00	0,00	0,00	0,00	0,00	0,75	0,51
RINGwt_z	F4I116	Leucine--tRNA ligase, cytoplasmic	6	6	6,00	1	9|15|0	0,00	0,00	0,00	0,00	0,00	0,75	0,51
RINGwt_z	O04331	Prohibitin-3, mitochondrial	5	5	5,00	1	8|10|2	0,00	0,00	0,00	0,00	0,00	0,75	0,51
RINGwt_z	Q9SID0	Probable fructokinase-1	4	4	4,00	1	8|8|0	0,00	0,00	0,00	0,00	0,00	0,75	0,51
RINGwt_z	P32961	Nitrilase 1	3	3	3,00	1	7|5|0	0,00	0,00	0,00	0,00	0,00	0,75	0,51
RINGwt_z	Q6ICZ8	Nascent polypeptide-associated complex subunit alpha-like protein 3	3	3	3,00	1	6|4|2	0,00	0,00	0,00	0,00	0,00	0,75	0,51
RINGwt_z	Q42586	Orotidine 5'-phosphate decarboxylase	2	2	2,00	1	4|4|0	0,00	0,00	0,00	0,00	0,00	0,75	0,51
RINGwt_z	Q9LTB2	Methionine S-methyltransferase	2	2	2,00	1	4|4|0	0,00	0,00	0,00	0,00	0,00	0,75	0,51
RINGwt_z	Q9LVQ0	Pectinesterase 31	1	1	1,00	1	0|4|0	0,00	0,00	0,00	0,00	0,00	0,75	0,51
RINGwt_z	Q9C5Z1	Eukaryotic translation initiation factor 3 subunit B	13	13	13,00	1	30|25|0	0,00	0,00	0,00	0,00	0,00	0,71	0,51
RINGwt_z	F4K1B1	Putative RNA polymerase II subunit B1 CTD phosphatase RPAP2 homolog	5	5	5,00	1	11|10|0	0,00	0,00	0,00	0,00	0,00	0,71	0,51
RINGwt_z	Q9M8K7	Dual specificity protein phosphatase 1B	4	4	4,00	1	8|9|0	0,00	0,00	0,00	0,00	0,00	0,71	0,51
RINGwt_z	Q8GYU3	Transcriptional elongation regulator MINIYO	4	4	4,00	1	9|8|0	0,00	0,00	0,00	0,00	0,00	0,71	0,51
RINGwt_z	Q96327	ERBB-3 BINDING PROTEIN 1	14	14	14,00	1	31|23|7	0,00	0,00	0,00	0,00	0,00	0,69	0,51
RINGwt_z	Q9FNX5	Dynamin-related protein 1E	9	9	9,00	1	11|12|16	0,00	0,00	0,00	0,00	0,00	0,69	0,51
RINGwt_z	Q8LC83	40S ribosomal protein S24-2	6	6	6,00	1	7|7|12	0,00	0,00	0,00	0,00	0,00	0,69	0,51
RINGwt_z	Q9SS17	40S ribosomal protein S24-1	7	7	7,00	1	8|9|14	0,00	0,00	0,00	0,00	0,00	0,68	0,51
RINGwt_z	O80626	60S ribosomal protein L35-2	5	5	5,00	1	3|4|15	0,00	0,00	0,00	0,00	0,00	0,68	0,51
RINGwt_z	P41127	60S ribosomal protein L13-1	20	20	20,00	1	16|15|58	0,00	0,00	0,00	0,00	0,00	0,67	0,51
RINGwt_z	Q9SRX2	60S ribosomal protein L19-1	14	14	14,00	1	7|8|48	0,00	0,00	0,00	0,00	0,00	0,67	0,51
RINGwt_z	O23254	Serine hydroxymethyltransferase 4	6	6	6,00	1	13|14|0	0,00	0,00	0,00	0,00	0,00	0,67	0,51
RINGwt_z	Q9SJA6	Serine/arginine-rich splicing factor RSZ22A	4	4	4,00	1	0|0|18	0,00	0,00	0,00	0,00	0,00	0,67	0,51

Bait: RINGwt_z	Prey	PreyGene	Spec	SpecSum	AvgSpec	NumReplicates	ctrlCounts	AvgP	MaxP	TopoAvgP	TopoMaxP	SaintScore	FoldChange	BFDR
RINGwt_z	P49201	40S ribosomal protein S23-2	2	2	2,00	1	5|4|0	0,00	0,00	0,00	0,00	0,00	0,67	0,51
RINGwt_z	O80786	DNA replication licensing factor MCM5	2	2	2,00	1	6|3|0	0,00	0,00	0,00	0,00	0,00	0,67	0,51
RINGwt_z	Q8W234	Transcriptional corepressor SEUSS	2	2	2,00	1	4|5|0	0,00	0,00	0,00	0,00	0,00	0,67	0,51
RINGwt_z	O48549	40S ribosomal protein S6-1	15	15	15,00	1	18|22|29	0,00	0,00	0,00	0,00	0,00	0,65	0,51
RINGwt_z	P38666	60S ribosomal protein L24-2	8	8	8,00	1	5|6|27	0,00	0,00	0,00	0,00	0,00	0,63	0,51
RINGwt_z	Q5GM68	Phosphoenolpyruvate carboxylase 2	8	8	8,00	1	20|18|0	0,00	0,00	0,00	0,00	0,00	0,63	0,51
RINGwt_z	P11574	V-type proton ATPase subunit B1	17	17	17,00	1	31|29|24	0,00	0,00	0,00	0,00	0,00	0,61	0,51
RINGwt_z	Q9XI93	Oleosin-B3-like protein	5	5	5,00	1	16|9|0	0,00	0,00	0,00	0,00	0,00	0,60	0,51
RINGwt_z	Q9FUY2	Transcriptional corepressor LEUNIG	2	2	2,00	1	5|5|0	0,00	0,00	0,00	0,00	0,00	0,60	0,51
RINGwt_z	Q9SA73	Obg-like ATPase 1	2	2	2,00	1	6|4|0	0,00	0,00	0,00	0,00	0,00	0,60	0,51
RINGwt_z	Q9SMV6	Protein EXPORTIN 1A	2	2	2,00	1	4|6|0	0,00	0,00	0,00	0,00	0,00	0,60	0,51
RINGwt_z	P51430	40S ribosomal protein S6-2	11	11	11,00	1	17|20|20	0,00	0,00	0,00	0,00	0,00	0,58	0,51
RINGwt_z	P42730	Chaperone protein ClpB1	5	5	5,00	1	10|17|0	0,00	0,00	0,00	0,00	0,00	0,56	0,51
RINGwt_z	Q9FME2	Nuclear transport factor 2	3	3	3,00	1	8|8|0	0,00	0,00	0,00	0,00	0,00	0,56	0,51
RINGwt_z	Q9SU08	Auxilin-related protein 1	3	3	3,00	1	9|7|0	0,00	0,00	0,00	0,00	0,00	0,56	0,51
RINGwt_z	Q38953	Probable pre-mRNA-splicing factor ATP-dependent RNA helicase DEAH5	6	6	6,00	1	18|15|0	0,00	0,00	0,00	0,00	0,00	0,55	0,51
RINGwt_z	Q96250	ATP synthase subunit gamma, mitochondrial	2	2	2,00	1	5|6|0	0,00	0,00	0,00	0,00	0,00	0,55	0,51
RINGwt_z	Q8W4M5	Pyrophosphate--fructose 6-phosphate 1-phosphotransferase subunit beta 1	2	2	2,00	1	3|8|0	0,00	0,00	0,00	0,00	0,00	0,55	0,51
RINGwt_z	Q38882	Phospholipase D alpha 1	73	73	73,00	1	176|159|68	0,00	0,00	0,00	0,00	0,00	0,54	0,51
RINGwt_z	P49690	60S ribosomal protein L23	5	5	5,00	1	3|3|22	0,00	0,00	0,00	0,00	0,00	0,54	0,51
RINGwt_z	P49211	60S ribosomal protein L32-1	5	5	5,00	1	4|3|21	0,00	0,00	0,00	0,00	0,00	0,54	0,51
RINGwt_z	Q0WQ57	Auxilin-related protein 2	3	3	3,00	1	9|8|0	0,00	0,00	0,00	0,00	0,00	0,53	0,51
RINGwt_z	Q8S9J8	Probable clathrin assembly protein At4g32285	3	3	3,00	1	8|9|0	0,00	0,00	0,00	0,00	0,00	0,53	0,51
RINGwt_z	Q9SIU8	Probable protein phosphatase 2C 20	3	3	3,00	1	10|7|0	0,00	0,00	0,00	0,00	0,00	0,53	0,51

Bait: RINGwt_z	Prey	PreyGene	Spec	SpecSum	AvgSpec	NumReplicates	ctrlCounts	AvgP	MaxP	TopoAvgP	TopoMaxP	SaintScore	FoldChange	BFDR
RINGwt_z	F4I1L3	Acetyl-CoA carboxylase 2	27	27	27,00	1	11|11|139	0,00	0,00	0,00	0,00	0,00	0,50	0,51
RINGwt_z	O49160	Eukaryotic translation initiation factor 3 subunit C	5	5	5,00	1	13|17|0	0,00	0,00	0,00	0,00	0,00	0,50	0,51
RINGwt_z	Q0WW26	Coatomer subunit gamma	2	2	2,00	1	4|8|0	0,00	0,00	0,00	0,00	0,00	0,50	0,51
RINGwt_z	O82462	Glutamate--tRNA ligase, cytoplasmic	1	1	1,00	1	0|6|0	0,00	0,00	0,00	0,00	0,00	0,50	0,51
RINGwt_z	P19036	17.4 kDa class I heat shock protein	1	1	1,00	1	0|6|0	0,00	0,00	0,00	0,00	0,00	0,50	0,51
RINGwt_z	P32962	Nitrilase 2	1	1	1,00	1	4|2|0	0,00	0,00	0,00	0,00	0,00	0,50	0,51
RINGwt_z	Q9SVA6	Developmentally-regulated G-protein 3	1	1	1,00	1	3|3|0	0,00	0,00	0,00	0,00	0,00	0,50	0,51
RINGwt_z	Q9ZPY7	Exportin-2	1	1	1,00	1	2|4|0	0,00	0,00	0,00	0,00	0,00	0,50	0,51
RINGwt_z	Q9LTT9	Varicose-related protein	14	14	14,00	1	49|34|5	0,00	0,00	0,00	0,00	0,00	0,48	0,51
RINGwt_z	Q9C5M0	Mitochondrial dicarboxylate/tricarboxylate transporter DTC	10	10	10,00	1	9|9|45	0,00	0,00	0,00	0,00	0,00	0,48	0,51
RINGwt_z	Q9T074	Phosphoenolpyruvate carboxykinase (ATP)	31	31	31,00	1	95|85|17	0,00	0,00	0,00	0,00	0,00	0,47	0,51
RINGwt_z	Q9FMM3	Protein ESSENTIAL FOR POTEXVIRUS ACCUMULATION 1	15	15	15,00	1	55|46|0	0,00	0,00	0,00	0,00	0,00	0,45	0,51
RINGwt_z	Q9LR33	60S ribosomal protein L27a-2	8	8	8,00	1	10|12|31	0,00	0,00	0,00	0,00	0,00	0,45	0,51
RINGwt_z	Q9SF40	60S ribosomal protein L4-1	29	29	29,00	1	23|26|154	0,00	0,00	0,00	0,00	0,00	0,43	0,51
RINGwt_z	P49691	60S ribosomal protein L4-2	28	28	28,00	1	24|27|144	0,00	0,00	0,00	0,00	0,00	0,43	0,51
RINGwt_z	Q38884	Eukaryotic translation initiation factor 3 subunit I	5	5	5,00	1	16|19|0	0,00	0,00	0,00	0,00	0,00	0,43	0,51
RINGwt_z	F4IDQ5	Protein JASON	1	1	1,00	1	4|3|0	0,00	0,00	0,00	0,00	0,00	0,43	0,51
RINGwt_z	Q8LB54	Pre-mRNA-splicing factor 38	1	1	1,00	1	4|3|0	0,00	0,00	0,00	0,00	0,00	0,43	0,51
RINGwt_z	B7ZWR6	Outer envelope protein 61	1	1	1,00	1	3|4|0	0,00	0,00	0,00	0,00	0,00	0,43	0,51
RINGwt_z	P49693	60S ribosomal protein L19-3	5	5	5,00	1	4|6|27	0,00	0,00	0,00	0,00	0,00	0,41	0,51
RINGwt_z	Q9FKA5	Uncharacterized protein At5g39570	12	12	12,00	1	39|36|16	0,00	0,00	0,00	0,00	0,00	0,40	0,51
RINGwt_z	P59224	40S ribosomal protein S13-2	6	6	6,00	1	8|7|30	0,00	0,00	0,00	0,00	0,00	0,40	0,51
RINGwt_z	Q9LFW1	UDP-arabinopyranose mutase 2	2	2	2,00	1	7|8|0	0,00	0,00	0,00	0,00	0,00	0,40	0,51

Bait: RINGwt_z	Prey	PreyGene	Spec	SpecSum	AvgSpec	NumReplicates	ctrlCounts	AvgP	MaxP	TopoAvgP	TopoMaxP	SaintScore	FoldChange	BFDR
RINGwt_z	Q39085	Delta(24)-sterol reductase	2	2	2,00	1	6|9|0	0,00	0,00	0,00	0,00	0,00	0,40	0,51
RINGwt_z	Q8VWF1	SH3 domain-containing protein 2	2	2	2,00	1	8|7|0	0,00	0,00	0,00	0,00	0,00	0,40	0,51
RINGwt_z	Q9LSD0	Ribonucleoside-diphosphate reductase small chain C	2	2	2,00	1	6|9|0	0,00	0,00	0,00	0,00	0,00	0,40	0,51
RINGwt_z	Q96321	Importin subunit alpha-1	1	1	1,00	1	5|3|0	0,00	0,00	0,00	0,00	0,00	0,38	0,51
RINGwt_z	P49637	60S ribosomal protein L27a-3	6	6	6,00	1	10|10|30	0,00	0,00	0,00	0,00	0,00	0,36	0,51
RINGwt_z	O82204	60S ribosomal protein L28-1	3	3	3,00	1	5|4|17	0,00	0,00	0,00	0,00	0,00	0,35	0,51
RINGwt_z	Q94BT0	Sucrose-phosphate synthase 1	2	2	2,00	1	6|4|8	0,00	0,00	0,00	0,00	0,00	0,33	0,51
RINGwt_z	Q9LD90	H/ACA ribonucleoprotein complex subunit 4	2	2	2,00	1	0|0|18	0,00	0,00	0,00	0,00	0,00	0,33	0,51
RINGwt_z	Q05153	FACT complex subunit SSRP1	1	1	1,00	1	4|5|0	0,00	0,00	0,00	0,00	0,00	0,33	0,51
RINGwt_z	Q8VXY4	TIP41-like protein	2	2	2,00	1	8|7|4	0,00	0,00	0,00	0,00	0,00	0,32	0,51
RINGwt_z	O80585	Methylenetetrahydrofolate reductase 2	3	3	3,00	1	17|13|0	0,00	0,00	0,00	0,00	0,00	0,30	0,51
RINGwt_z	Q9LUQ6	60S ribosomal protein L19-2	2	2	2,00	1	0|0|20	0,00	0,00	0,00	0,00	0,00	0,30	0,51
RINGwt_z	Q9C514	40S ribosomal protein S7-1	1	1	1,00	1	3|4|3	0,00	0,00	0,00	0,00	0,00	0,30	0,51
RINGwt_z	F4J5S1	Clustered mitochondria protein	4	4	4,00	1	20|21|0	0,00	0,00	0,00	0,00	0,00	0,29	0,51
RINGwt_z	Q7XZU0	Probable phosphoinositide phosphatase SAC9	3	3	3,00	1	16|16|0	0,00	0,00	0,00	0,00	0,00	0,28	0,51
RINGwt_z	Q9SVR0	60S ribosomal protein L13a-3	3	3	3,00	1	4|10|21	0,00	0,00	0,00	0,00	0,00	0,26	0,51
RINGwt_z	Q9LV09	Protein BOBBER 1	2	2	2,00	1	11|11|1	0,00	0,00	0,00	0,00	0,00	0,26	0,51
RINGwt_z	Q9FIQ0	Probable ADP-ribosylation factor GTPase-activating protein AGD9	3	3	3,00	1	16|15|6	0,00	0,00	0,00	0,00	0,00	0,24	0,51
RINGwt_z	Q9LU44	Splicing factor-like protein 1	2	2	2,00	1	13|12|0	0,00	0,00	0,00	0,00	0,00	0,24	0,51
RINGwt_z	Q9SFU1	60S ribosomal protein L13a-1	4	4	4,00	1	7|12|33	0,00	0,00	0,00	0,00	0,00	0,23	0,51
RINGwt_z	Q38970	Acetyl-CoA carboxylase 1	14	14	14,00	1	22|25|141	0,00	0,00	0,00	0,00	0,00	0,22	0,51
RINGwt_z	O04983	Biotin carboxylase, chloroplastic	12	12	12,00	1	5|9|150	0,00	0,00	0,00	0,00	0,00	0,22	0,51
RINGwt_z	O82647	Pyruvate decarboxylase 1	2	2	2,00	1	14|13|0	0,00	0,00	0,00	0,00	0,00	0,22	0,51
RINGwt_z	P51418	60S ribosomal protein L18a-2	8	8	8,00	1	13|20|81	0,00	0,00	0,00	0,00	0,00	0,21	0,51

Bait: RINGwt_z	Prey	PreyGene	Spec	SpecSum	AvgSpec	NumReplicates	ctrlCounts	AvgP	MaxP	TopoAvgP	TopoMaxP	SaintScore	FoldChange	BFDR
RINGwt_z	Q9LD55	Eukaryotic translation initiation factor 3 subunit A	5	5	5,00	1	41|31|0	0,00	0,00	0,00	0,00	0,00	0,21	0,51
RINGwt_z	Q9FHG2	60S ribosomal protein L32-2	2	2	2,00	1	3|3|23	0,00	0,00	0,00	0,00	0,00	0,21	0,51
RINGwt_z	Q93ZG7	DEAD-box ATP-dependent RNA helicase 38	1	1	1,00	1	8|6|0	0,00	0,00	0,00	0,00	0,00	0,21	0,51
RINGwt_z	Q93ZT6	Eukaryotic translation initiation factor isoform 4G-1	3	3	3,00	1	24|20|0	0,00	0,00	0,00	0,00	0,00	0,20	0,51
RINGwt_z	Q8L716	Splicing factor U2af large subunit B	1	1	1,00	1	0|0|16	0,00	0,00	0,00	0,00	0,00	0,19	0,51
RINGwt_z	O04663	Eukaryotic translation initiation factor isoform 4E	1	1	1,00	1	7|9|0	0,00	0,00	0,00	0,00	0,00	0,19	0,51
RINGwt_z	Q8L793	Polyadenylate-binding protein-interacting protein 3	1	1	1,00	1	8|8|0	0,00	0,00	0,00	0,00	0,00	0,19	0,51
RINGwt_z	Q9SF16	T-complex protein 1 subunit eta	1	1	1,00	1	9|8|0	0,00	0,00	0,00	0,00	0,00	0,18	0,51
RINGwt_z	O81283	Translocase of chloroplast 159, chloroplastic	6	6	6,00	1	52|51|3	0,00	0,00	0,00	0,00	0,00	0,17	0,51
RINGwt_z	Q9LFU5	Probable tRNA (guanine(26)-N(2))-dimethyltransferase 1	4	4	4,00	1	33|28|8	0,00	0,00	0,00	0,00	0,00	0,17	0,51
RINGwt_z	Q08112	40S ribosomal protein S15-1	1	1	1,00	1	3|4|11	0,00	0,00	0,00	0,00	0,00	0,17	0,51
RINGwt_z	O23144	Proton pump-interactor 1	3	3	3,00	1	29|26|0	0,00	0,00	0,00	0,00	0,00	0,16	0,51
RINGwt_z	Q9ZQ47	Glycine-rich domain-containing protein 1	2	2	2,00	1	20|20|0	0,00	0,00	0,00	0,00	0,00	0,15	0,51
RINGwt_z	Q8RXE7	Probable ADP-ribosylation factor GTPase-activating protein AGD14	1	1	1,00	1	11|10|0	0,00	0,00	0,00	0,00	0,00	0,14	0,51
RINGwt_z	Q9M0E2	60S ribosomal protein L28-2	1	1	1,00	1	3|4|16	0,00	0,00	0,00	0,00	0,00	0,13	0,51
RINGwt_z	Q9LUD4	60S ribosomal protein L18a-3	2	2	2,00	1	8|12|39	0,00	0,00	0,00	0,00	0,00	0,10	0,51
RINGwt_z	Q9LFL3	TOM1-like protein 1	1	1	1,00	1	16|13|0	0,00	0,00	0,00	0,00	0,00	0,10	0,51
RINGwt_z	Q9FJX0	Peptidyl-prolyl cis-trans isomerase CYP65	1	1	1,00	1	8|12|12	0,00	0,00	0,00	0,00	0,00	0,09	0,51
RINGwt_z	Q06738	Low-temperature-induced 78 kDa protein	1	1	1,00	1	46|47|4	0,00	0,00	0,00	0,00	0,00	0,03	0,51

Bait: RINGmut	Prey	PreyGene	Spec	SpecSum	AvgSpec	NumReplicates	ctrlCounts	AvgP	MaxP	TopoAvgP	TopoMaxP	SaintScore	FoldChange	BFDR
RINGmut	Q0WV25	Tubulin alpha-4 chain	58	58	58,00	1	0|0|0	1,00	1,00	1,00	1,00	1,00	580,00	0,00
RINGmut	Q8RWZ3	Probable acyl-CoA dehydrogenase IBR3	48	48	48,00	1	0|0|0	1,00	1,00	1,00	1,00	1,00	480,00	0,00
RINGmut	P55737	Heat shock protein 90-2	26	26	26,00	1	0|0|0	1,00	1,00	1,00	1,00	1,00	260,00	0,00
RINGmut	O22254	Putative 60S ribosomal protein L18-1	7	7	7,00	1	0|0|0	1,00	1,00	1,00	1,00	1,00	70,00	0,00
RINGmut	Q9LZ45	Histone H2B.9	7	7	7,00	1	0|0|0	1,00	1,00	1,00	1,00	1,00	70,00	0,00
RINGmut	P57106	Malate dehydrogenase 2, cytoplasmic	7	7	7,00	1	0|0|0	1,00	1,00	1,00	1,00	1,00	70,00	0,00
RINGmut	Q9STY6	40S ribosomal protein S20-2	6	6	6,00	1	0|0|0	1,00	1,00	1,00	1,00	1,00	60,00	0,00
RINGmut	Q9FFR3	6-phosphogluconate dehydrogenase, decarboxylating 3, chloroplastic	6	6	6,00	1	0|0|0	1,00	1,00	1,00	1,00	1,00	60,00	0,00
RINGmut	O04316	Nitrile-specifier protein 4	6	6	6,00	1	0|0|0	1,00	1,00	1,00	1,00	1,00	60,00	0,00
RINGmut	Q8VZ19	60S ribosomal protein L30-2	5	5	5,00	1	0|0|0	1,00	1,00	1,00	1,00	1,00	50,00	0,00
RINGmut	Q9SU58	ATPase 4, plasma membrane-type	5	5	5,00	1	0|0|0	1,00	1,00	1,00	1,00	1,00	50,00	0,00
RINGmut	Q9SRH5	Mitochondrial outer membrane protein porin 1	4	4	4,00	1	0|0|0	1,00	1,00	1,00	1,00	1,00	40,00	0,00
RINGmut	P48006	Elongation factor 1-delta 1	4	4	4,00	1	0|0|0	1,00	1,00	1,00	1,00	1,00	40,00	0,00
RINGmut	Q42556	ATPase 9, plasma membrane-type	4	4	4,00	1	0|0|0	1,00	1,00	1,00	1,00	1,00	40,00	0,00
RINGmut	Q9ZU25	Probable mitochondrial-processing peptidase subunit alpha-1, mitochondrial	4	4	4,00	1	0|0|0	1,00	1,00	1,00	1,00	1,00	40,00	0,00
RINGmut	P10896	Ribulose bisphosphate carboxylase/oxygenase activase, chloroplastic	4	4	4,00	1	0|0|0	1,00	1,00	1,00	1,00	1,00	40,00	0,00
RINGmut	P28769	T-complex protein 1 subunit alpha	4	4	4,00	1	0|0|0	1,00	1,00	1,00	1,00	1,00	40,00	0,00
RINGmut	Q9LS42	Protein CASP	4	4	4,00	1	0|0|0	1,00	1,00	1,00	1,00	1,00	40,00	0,00
RINGmut	Q9FM01	UDP-glucose 6-dehydrogenase 4	3	3	3,00	1	0|0|0	1,00	1,00	1,00	1,00	1,00	30,00	0,00
RINGmut	P59230	60S ribosomal protein L10a-2	3	3	3,00	1	0|0|0	1,00	1,00	1,00	1,00	1,00	30,00	0,00
RINGmut	Q8LCE1	Glutamine synthetase cytosolic isozyme 1-2	3	3	3,00	1	0|0|0	1,00	1,00	1,00	1,00	1,00	30,00	0,00
RINGmut	Q8L3X8	Serine/arginine-rich SC35-like splicing factor SCL30	3	3	3,00	1	0|0|0	1,00	1,00	1,00	1,00	1,00	30,00	0,00

Bait: RINGmut	Prey	PreyGene	Spec	SpecSum	AvgSpec	NumReplicates	ctrlCounts	AvgP	MaxP	TopoAvgP	TopoMaxP	SaintScore	FoldChange	BFDR
RINGmut	P21238	Chaperonin 60 subunit alpha 1, chloroplastic	3	3	3,00	1	0|0|0	1,00	1,00	1,00	1,00	1,00	30,00	0,00
RINGmut	Q07100	Serine/threonine-protein phosphatase PP2A-3 catalytic subunit	3	3	3,00	1	0|0|0	1,00	1,00	1,00	1,00	1,00	30,00	0,00
RINGmut	Q93Y35	26S proteasome non-ATPase regulatory subunit 6 homolog	3	3	3,00	1	0|0|0	1,00	1,00	1,00	1,00	1,00	30,00	0,00
RINGmut	F4I7I0	Alanine aminotransferase 1, mitochondrial	3	3	3,00	1	0|0|0	1,00	1,00	1,00	1,00	1,00	30,00	0,00
RINGmut	Q9FLQ4	2-oxoglutarate dehydrogenase E2 component (dihydrolipoamide succinyltransferase)	34	34	34,00	1	0|0|5	1,00	1,00	1,00	1,00	1,00	20,40	0,00
RINGmut	O80929	60S ribosomal protein L36-1	2	2	2,00	1	0|0|0	0,97	0,97	0,97	0,97	0,97	20,00	0,00
RINGmut	Q8VZB9	60S ribosomal protein L10a-1	2	2	2,00	1	0|0|0	0,97	0,97	0,97	0,97	0,97	20,00	0,00
RINGmut	Q9FXA2	Polyadenylate-binding protein 8	2	2	2,00	1	0|0|0	0,97	0,97	0,97	0,97	0,97	20,00	0,00
RINGmut	Q56XG6	DEAD-box ATP-dependent RNA helicase 15	2	2	2,00	1	0|0|0	0,97	0,97	0,97	0,97	0,97	20,00	0,00
RINGmut	P23321	Oxygen-evolving enhancer protein 1-1, chloroplastic	2	2	2,00	1	0|0|0	0,97	0,97	0,97	0,97	0,97	20,00	0,00
RINGmut	Q9S841	Oxygen-evolving enhancer protein 1-2, chloroplastic	2	2	2,00	1	0|0|0	0,97	0,97	0,97	0,97	0,97	20,00	0,00
RINGmut	P42699	Plastocyanin major isoform, chloroplastic	2	2	2,00	1	0|0|0	0,97	0,97	0,97	0,97	0,97	20,00	0,00
RINGmut	Q9FLV7	B3 domain-containing protein At5g24050	2	2	2,00	1	0|0|0	0,97	0,97	0,97	0,97	0,97	20,00	0,00
RINGmut	P50318	Phosphoglycerate kinase 2, chloroplastic	2	2	2,00	1	0|0|0	0,97	0,97	0,97	0,97	0,97	20,00	0,00
RINGmut	O03042	Ribulose bisphosphate carboxylase large chain	2	2	2,00	1	0|0|0	0,97	0,97	0,97	0,97	0,97	20,00	0,00
RINGmut	Q56WN1	Glutamine synthetase cytosolic isozyme 1-1	2	2	2,00	1	0|0|0	0,97	0,97	0,97	0,97	0,97	20,00	0,00
RINGmut	Q9FMD9	Glutamine synthetase cytosolic isozyme 1-4	2	2	2,00	1	0|0|0	0,97	0,97	0,97	0,97	0,97	20,00	0,00
RINGmut	P93004	Aquaporin PIP2-7	2	2	2,00	1	0|0|0	0,97	0,97	0,97	0,97	0,97	20,00	0,00
RINGmut	Q94AR8	3-isopropylmalate dehydratase large subunit, chloroplastic	2	2	2,00	1	0|0|0	0,97	0,97	0,97	0,97	0,97	20,00	0,00
RINGmut	O49513	Ras-related protein RABA1e	2	2	2,00	1	0|0|0	0,97	0,97	0,97	0,97	0,97	20,00	0,00

Bait: RINGmut	Prey	PreyGene	Spec	SpecSum	AvgSpec	NumReplicates	ctrlCounts	AvgP	MaxP	TopoAvgP	TopoMaxP	SaintScore	FoldChange	BFDR
RINGmut	Q9SB64	Protein NBR1 homolog	2	2	2,00	1	0|0|0	0,97	0,97	0,97	0,97	0,97	20,00	0,00
RINGmut	O22993	Probable inactive ATP-dependent zinc metalloprotease FTSHI 1, chloroplastic	2	2	2,00	1	0|0|0	0,97	0,97	0,97	0,97	0,97	20,00	0,00
RINGmut	Q9SJK3	Protein argonaute 5	2	2	2,00	1	0|0|0	0,97	0,97	0,97	0,97	0,97	20,00	0,00
RINGmut	Q41951	Aquaporin TIP2-1, N-terminally processed	2	2	2,00	1	0|0|0	0,97	0,97	0,97	0,97	0,97	20,00	0,00
RINGmut	P34066	Proteasome subunit alpha type-1-A	2	2	2,00	1	0|0|0	0,97	0,97	0,97	0,97	0,97	20,00	0,00
RINGmut	Q42560	Aconitate hydratase 1	11	11	11,00	1	0|2|0	1,00	1,00	1,00	1,00	1,00	16,50	0,00
RINGmut	Q9SAJ4	Phosphoglycerate kinase 3, cytosolic	11	11	11,00	1	1|1|0	1,00	1,00	1,00	1,00	1,00	16,50	0,00
RINGmut	Q03250	Glycine-rich RNA-binding protein 7	5	5	5,00	1	0|0|1	1,00	1,00	1,00	1,00	1,00	15,00	0,00
RINGmut	Q8H107	2-oxoglutarate dehydrogenase E2 component (dihydrolipoamide succinyltransferase)	29	29	29,00	1	0|0|6	1,00	1,00	1,00	1,00	1,00	14,50	0,00
RINGmut	Q03251	Glycine-rich RNA-binding protein 8	9	9	9,00	1	0|0|2	0,99	0,99	0,99	0,99	0,99	13,50	0,00
RINGmut	Q9SIB9	Aconitate hydratase 3, mitochondrial	16	16	16,00	1	0|4|0	0,99	0,99	0,99	0,99	0,99	12,00	0,00
RINGmut	Q9LVI8	Glutamine synthetase cytosolic isozyme 1-3	4	4	4,00	1	0|1|0	1,00	1,00	1,00	1,00	1,00	12,00	0,00
RINGmut	Q42406	Peptidyl-prolyl cis-trans isomerase CYP18-4	4	4	4,00	1	0|1|0	1,00	1,00	1,00	1,00	1,00	12,00	0,00
RINGmut	P48491	Triosephosphate isomerase, cytosolic	1	1	1,00	1	0|0|0	0,00	0,00	0,00	0,00	0,00	10,00	0,51
RINGmut	Q8W4S4	V-type proton ATPase subunit a3	1	1	1,00	1	0|0|0	0,00	0,00	0,00	0,00	0,00	10,00	0,51
RINGmut	Q9FVE6	Histone deacetylase HDT1	1	1	1,00	1	0|0|0	0,00	0,00	0,00	0,00	0,00	10,00	0,51
RINGmut	Q9ZVF3	MLP-like protein 328	1	1	1,00	1	0|0|0	0,00	0,00	0,00	0,00	0,00	10,00	0,51
RINGmut	Q9M2Y6	Probable pectin methylesterase CGR2	1	1	1,00	1	0|0|0	0,00	0,00	0,00	0,00	0,00	10,00	0,51
RINGmut	Q9SVY0	DNA-directed RNA polymerase I subunit 1	1	1	1,00	1	0|0|0	0,00	0,00	0,00	0,00	0,00	10,00	0,51
RINGmut	Q9SS94	Cell division control protein 48 homolog C	1	1	1,00	1	0|0|0	0,00	0,00	0,00	0,00	0,00	10,00	0,51
RINGmut	Q42601	Carbamoyl-phosphate synthase large chain, chloroplastic	1	1	1,00	1	0|0|0	0,00	0,00	0,00	0,00	0,00	10,00	0,51
RINGmut	Q9LRR2	Terpenoid synthase 17	1	1	1,00	1	0|0|0	0,00	0,00	0,00	0,00	0,00	10,00	0,51

Bait: RINGmut	Prey	PreyGene	Spec	SpecSum	AvgSpec	NumReplicates	ctrlCounts	AvgP	MaxP	TopoAvgP	TopoMaxP	SaintScore	FoldChange	BFDR
RINGmut	O65595	Probable pyruvate kinase, cytosolic isozyme	1	1	1,00	1	0|0|0	0,00	0,00	0,00	0,00	0,00	10,00	0,51
RINGmut	Q9SU63	Aldehyde dehydrogenase family 2 member B4, mitochondrial	1	1	1,00	1	0|0|0	0,00	0,00	0,00	0,00	0,00	10,00	0,51
RINGmut	P45951	DNA-(apurinic or apyrimidinic site) lyase, chloroplastic	1	1	1,00	1	0|0|0	0,00	0,00	0,00	0,00	0,00	10,00	0,51
RINGmut	P93031	GDP-mannose 4,6 dehydratase 2	1	1	1,00	1	0|0|0	0,00	0,00	0,00	0,00	0,00	10,00	0,51
RINGmut	Q8RWF5	Protein DETOXIFICATION 6	1	1	1,00	1	0|0|0	0,00	0,00	0,00	0,00	0,00	10,00	0,51
RINGmut	Q9SN86	Malate dehydrogenase, chloroplastic	1	1	1,00	1	0|0|0	0,00	0,00	0,00	0,00	0,00	10,00	0,51
RINGmut	O65282	20 kDa chaperonin, chloroplastic	1	1	1,00	1	0|0|0	0,00	0,00	0,00	0,00	0,00	10,00	0,51
RINGmut	Q9LXJ2	Cytochrome b-c1 complex subunit 9, mitochondrial	3	3	3,00	1	0|0|1	0,97	0,97	0,97	0,97	0,97	9,00	0,00
RINGmut	Q8LD46	60S ribosomal protein L23a-1	27	27	27,00	1	4|3|3	1,00	1,00	1,00	1,00	1,00	8,10	0,00
RINGmut	Q9FE58	60S ribosomal protein L22-3	5	5	5,00	1	2|0|0	0,93	0,93	0,93	0,93	0,93	7,50	0,01
RINGmut	Q9LX65	V-type proton ATPase subunit H	5	5	5,00	1	0|2|0	0,93	0,93	0,93	0,93	0,93	7,50	0,01
RINGmut	Q9FFC0	Histone H2B.10	7	7	7,00	1	1|2|0	0,99	0,99	0,99	0,99	0,99	7,00	0,00
RINGmut	P39207	Nucleoside diphosphate kinase 1	9	9	9,00	1	2|2|0	1,00	1,00	1,00	1,00	1,00	6,75	0,00
RINGmut	Q9FE65	60S ribosomal protein L34-2	13	13	13,00	1	3|3|0	1,00	1,00	1,00	1,00	1,00	6,50	0,00
RINGmut	Q8LCL3	60S ribosomal protein L27-2	13	13	13,00	1	3|3|0	1,00	1,00	1,00	1,00	1,00	6,50	0,00
RINGmut	Q9FJX3	Mitochondrial outer membrane protein porin 2	10	10	10,00	1	1|4|0	0,95	0,95	0,95	0,95	0,95	6,00	0,01
RINGmut	Q01525	14-3-3-like protein GF14 omega	6	6	6,00	1	1|2|0	0,97	0,97	0,97	0,97	0,97	6,00	0,00
RINGmut	P46077	14-3-3-like protein GF14 phi	6	6	6,00	1	1|2|0	0,97	0,97	0,97	0,97	0,97	6,00	0,00
RINGmut	Q9SAJ6	Glyceraldehyde-3-phosphate dehydrogenase GAPCP1, chloroplastic	4	4	4,00	1	0|0|2	0,86	0,86	0,86	0,86	0,86	6,00	0,02
RINGmut	Q9SHC8	Vesicle-associated protein 1-2, N-terminally processed	2	2	2,00	1	0|1|0	0,79	0,79	0,79	0,79	0,79	6,00	0,02
RINGmut	P42643	14-3-3-like protein GF14 chi	9	9	9,00	1	2|3|0	0,99	0,99	0,99	0,99	0,99	5,40	0,00
RINGmut	P92549	ATP synthase subunit alpha, mitochondrial	32	32	32,00	1	8|10|0	0,99	0,99	0,99	0,99	0,99	5,33	0,00
RINGmut	Q9SIM4	60S ribosomal protein L14-1	7	7	7,00	1	0|0|4	0,87	0,87	0,87	0,87	0,87	5,25	0,02

Bait: RINGmut	Prey	PreyGene	Spec	SpecSum	AvgSpec	NumReplicates	ctrlCounts	AvgP	MaxP	TopoAvgP	TopoMaxP	SaintScore	FoldChange	BFDR
RINGmut	P23686	S-adenosylmethionine synthase 1	24	24	24,00	1	7|7|0	0,98	0,98	0,98	0,98	0,98	5,14	0,00
RINGmut	P42825	Chaperone protein dnaJ 2	15	15	15,00	1	4|5|0	0,98	0,98	0,98	0,98	0,98	5,00	0,00
RINGmut	Q94AW8	Chaperone protein dnaJ 3	10	10	10,00	1	2|4|0	0,95	0,95	0,95	0,95	0,95	5,00	0,01
RINGmut	Q41188	Cold shock protein 2	5	5	5,00	1	1|1|1	0,92	0,92	0,92	0,92	0,92	5,00	0,01
RINGmut	P12411	Tubulin beta-1 chain	63	63	63,00	1	17|21|0	0,98	0,98	0,98	0,98	0,98	4,97	0,00
RINGmut	P59233	Ubiquitin-40S ribosomal protein S27a-3	28	28	28,00	1	8|9|0	0,98	0,98	0,98	0,98	0,98	4,94	0,00
RINGmut	Q9ZT91	Elongation factor Tu, mitochondrial	21	21	21,00	1	6|7|0	0,98	0,98	0,98	0,98	0,98	4,85	0,00
RINGmut	P51419	60S ribosomal protein L27-3	14	14	14,00	1	5|4|0	0,97	0,97	0,97	0,97	0,97	4,67	0,01
RINGmut	P51818	Heat shock protein 90-3	26	26	26,00	1	5|12|0	0,94	0,94	0,94	0,94	0,94	4,59	0,01
RINGmut	P27323	Heat shock protein 90-1	12	12	12,00	1	3|5|0	0,94	0,94	0,94	0,94	0,94	4,50	0,01
RINGmut	P42645	14-3-3-like protein GF14 upsilon	9	9	9,00	1	2|4|0	0,92	0,92	0,92	0,92	0,92	4,50	0,01
RINGmut	Q8RXN4	3-hydroxyisobutyryl-CoA hydrolase-like protein 2, mitochondrial	3	3	3,00	1	0|2|0	0,73	0,73	0,73	0,73	0,73	4,50	0,04
RINGmut	P17562	S-adenosylmethionine synthase 2	25	25	25,00	1	8|9|0	0,96	0,96	0,96	0,96	0,96	4,41	0,01
RINGmut	O23255	Adenosylhomocysteinase 1	38	38	38,00	1	12|14|0	0,96	0,96	0,96	0,96	0,96	4,38	0,01
RINGmut	P59232	Ubiquitin-40S ribosomal protein S27a-2	28	28	28,00	1	8|9|3	1,00	1,00	1,00	1,00	1,00	4,20	0,00
RINGmut	P42644	14-3-3-like protein GF14 psi	11	11	11,00	1	3|5|0	0,90	0,90	0,90	0,90	0,90	4,12	0,01
RINGmut	O24456	Receptor for activated C kinase 1A	20	20	20,00	1	3|12|0	0,85	0,85	0,85	0,85	0,85	4,00	0,02
RINGmut	Q42290	Probable mitochondrial-processing peptidase subunit beta, mitochondrial	8	8	8,00	1	2|4|0	0,86	0,86	0,86	0,86	0,86	4,00	0,02
RINGmut	Q5E924	Glyceraldehyde-3-phosphate dehydrogenase GAPCP2, chloroplastic	4	4	4,00	1	0|0|3	0,74	0,74	0,74	0,74	0,74	4,00	0,03
RINGmut	Q05758	Ketol-acid reductoisomerase, chloroplastic	4	4	4,00	1	1|2|0	0,78	0,78	0,78	0,78	0,78	4,00	0,03
RINGmut	P29515	Tubulin beta-7 chain	95	95	95,00	1	26|36|10	0,97	0,97	0,97	0,97	0,97	3,96	0,00
RINGmut	P93819	Malate dehydrogenase 1, cytoplasmic	14	14	14,00	1	3|3|5	0,99	0,99	0,99	0,99	0,99	3,82	0,00

Bait: RINGmut	Prey	PreyGene	Spec	SpecSum	AvgSpec	NumReplicates	ctrlCounts	AvgP	MaxP	TopoAvgP	TopoMaxP	SaintScore	FoldChange	BFDR
RINGmut	O23016	Probable voltage-gated potassium channel subunit beta	5	5	5,00	1	2|2|0	0,88	0,88	0,88	0,88	0,88	3,75	0,01
RINGmut	Q9LUT2	S-adenosylmethionine synthase 4	30	30	30,00	1	12|13|0	0,76	0,76	0,76	0,76	0,76	3,60	0,03
RINGmut	Q9SEU4	Serine/arginine-rich SC35-like splicing factor SCL33	6	6	6,00	1	0|0|5	0,74	0,74	0,74	0,74	0,74	3,60	0,04
RINGmut	Q9LUW6	DEAD-box ATP-dependent RNA helicase 9, mitochondrial	6	6	6,00	1	3|2|0	0,81	0,81	0,81	0,81	0,81	3,60	0,02
RINGmut	Q8RWV0	Transketolase-1, chloroplastic	6	6	6,00	1	0|5|0	0,74	0,74	0,74	0,74	0,74	3,60	0,04
RINGmut	P29516	Tubulin beta-8 chain	84	84	84,00	1	27|34|10	0,66	0,66	0,66	0,66	0,66	3,55	0,04
RINGmut	P29514	Tubulin beta-6 chain	55	55	55,00	1	16|21|10	1,00	1,00	1,00	1,00	1,00	3,51	0,00
RINGmut	Q96300	14-3-3-like protein GF14 nu	7	7	7,00	1	2|4|0	0,75	0,75	0,75	0,75	0,75	3,50	0,03
RINGmut	Q9C8P0	Pyruvate dehydrogenase E2 component (dihydrolipoamide acetyltransferase)	23	23	23,00	1	0|0|20	0,65	0,65	0,65	0,65	0,65	3,45	0,04
RINGmut	Q9SYG4	Oligouridylate-binding protein 1A	8	8	8,00	1	5|2|0	0,71	0,71	0,71	0,71	0,71	3,43	0,04
RINGmut	Q9FVI6	Homeobox-leucine zipper protein HDG6	9	9	9,00	1	4|4|0	0,76	0,76	0,76	0,76	0,76	3,38	0,03
RINGmut	Q9LQI9	Oligouridylate-binding protein 1B	9	9	9,00	1	5|3|0	0,73	0,73	0,73	0,73	0,73	3,38	0,04
RINGmut	Q56YW9	Tubulin beta-2 chain	104	104	104,00	1	37|41|15	0,14	0,14	0,14	0,14	0,14	3,35	0,16
RINGmut	P29513	Tubulin beta-5 chain	52	52	52,00	1	17|22|8	0,85	0,85	0,85	0,85	0,85	3,32	0,02
RINGmut	Q8RYC2	Putative actin-5	13	13	13,00	1	4|4|4	0,95	0,95	0,95	0,95	0,95	3,25	0,01
RINGmut	Q9SQI8	Pyruvate dehydrogenase E2 component (dihydrolipoamide acetyltransferase)	27	27	27,00	1	0|0|25	0,43	0,43	0,43	0,43	0,43	3,24	0,09
RINGmut	Q9ASR1	Elongation factor 2	28	28	28,00	1	11|15|0	0,42	0,42	0,42	0,42	0,42	3,23	0,09
RINGmut	P53494	Actin-4	29	29	29,00	1	13|15|0	0,26	0,26	0,26	0,26	0,26	3,11	0,12
RINGmut	P53497	Actin-12	29	29	29,00	1	13|15|0	0,26	0,26	0,26	0,26	0,26	3,11	0,12
RINGmut	P29517	Tubulin beta-9 chain	69	69	69,00	1	26|33|8	0,01	0,01	0,01	0,01	0,01	3,09	0,26
RINGmut	P24636	Tubulin beta-4 chain	72	72	72,00	1	29|35|8	0,00	0,00	0,00	0,00	0,00	3,00	0,31
RINGmut	P83483	ATP synthase subunit beta-1, mitochondrial	26	26	26,00	1	9|12|5	0,96	0,96	0,96	0,96	0,96	3,00	0,01
RINGmut	Q9C4Z6	Receptor for activated C kinase 1B	14	14	14,00	1	6|8|0	0,46	0,46	0,46	0,46	0,46	3,00	0,08

Bait: RINGmut	Prey	PreyGene	Spec	SpecSum	AvgSpec	NumReplicates	ctrlCounts	AvgP	MaxP	TopoAvgP	TopoMaxP	SaintScore	FoldChange	BFDR
RINGmut	P54609	Cell division control protein 48 homolog A	7	7	7,00	1	2|5|0	0,55	0,55	0,55	0,55	0,55	3,00	0,06
RINGmut	P92947	Monodehydroascorbate reductase, chloroplastic/mitochondrial	4	4	4,00	1	0|4|0	0,60	0,60	0,60	0,60	0,60	3,00	0,05
RINGmut	Q9LJE4	Chaperonin 60 subunit beta 2, chloroplastic	3	3	3,00	1	1|2|0	0,52	0,52	0,52	0,52	0,52	3,00	0,07
RINGmut	Q9SF85	Adenosine kinase 1	3	3	3,00	1	2|1|0	0,52	0,52	0,52	0,52	0,52	3,00	0,07
RINGmut	Q9SIF2	Heat shock protein 90-5, chloroplastic	3	3	3,00	1	0|3|0	0,58	0,58	0,58	0,58	0,58	3,00	0,05
RINGmut	P92994	Trans-cinnamate 4-monooxygenase	2	2	2,00	1	1|0|1	0,47	0,47	0,47	0,47	0,47	3,00	0,08
RINGmut	F4JFN3	Heat shock protein 90-6, mitochondrial	2	2	2,00	1	0|2|0	0,53	0,53	0,53	0,53	0,53	3,00	0,07
RINGmut	Q8RXN3	Phosphoenolpyruvate/phosphate translocator 1, chloroplastic	2	2	2,00	1	1|1|0	0,47	0,47	0,47	0,47	0,47	3,00	0,08
RINGmut	Q9LKA5	Multiple organellar RNA editing factor 8, chloroplastic/mitochondrial	2	2	2,00	1	1|1|0	0,47	0,47	0,47	0,47	0,47	3,00	0,08
RINGmut	O80446	Pyridoxal 5'-phosphate synthase PDX1-like 4	1	1	1,00	1	0|1|0	0,00	0,00	0,00	0,00	0,00	3,00	0,51
RINGmut	Q2V4F9	SPX domain-containing membrane protein At1g63010	1	1	1,00	1	0|1|0	0,00	0,00	0,00	0,00	0,00	3,00	0,51
RINGmut	Q8RXU5	60S ribosomal protein L37a-2	10	10	10,00	1	0|0|11	0,39	0,39	0,39	0,39	0,39	2,73	0,09
RINGmut	Q9ZU52	Fructose-bisphosphate aldolase 3, chloroplastic	10	10	10,00	1	2|2|7	0,37	0,37	0,37	0,37	0,37	2,73	0,09
RINGmut	P42798	40S ribosomal protein S15a-1	9	9	9,00	1	2|5|3	0,54	0,54	0,54	0,54	0,54	2,70	0,06
RINGmut	Q9FVT2	Probable elongation factor 1-gamma 2	9	9	9,00	1	4|6|0	0,35	0,35	0,35	0,35	0,35	2,70	0,10
RINGmut	Q9SMX3	Mitochondrial outer membrane protein porin 3	29	29	29,00	1	15|16|2	0,01	0,01	0,01	0,01	0,01	2,64	0,27
RINGmut	Q9SJL8	S-adenosylmethionine synthase 3	14	14	14,00	1	8|8|0	0,16	0,16	0,16	0,16	0,16	2,62	0,16
RINGmut	Q42351	60S ribosomal protein L34-1	13	13	13,00	1	3|3|9	0,20	0,20	0,20	0,20	0,20	2,60	0,14
RINGmut	Q9LV28	Receptor for activated C kinase 1C	13	13	13,00	1	5|10|0	0,16	0,16	0,16	0,16	0,16	2,60	0,15
RINGmut	Q9LVA0	BAG family molecular chaperone regulator 7	11	11	11,00	1	6|7|0	0,18	0,18	0,18	0,18	0,18	2,54	0,15
RINGmut	Q8L7B5	Chaperonin CPN60-like 1, mitochondrial	15	15	15,00	1	9|9|0	0,07	0,07	0,07	0,07	0,07	2,50	0,20

Bait: RINGmut	Prey	PreyGene	Spec	SpecSum	AvgSpec	NumReplicates	ctrlCounts	AvgP	MaxP	TopoAvgP	TopoMaxP	SaintScore	FoldChange	BFDR
RINGmut	Q38799	Pyruvate dehydrogenase E1 component subunit beta-1, mitochondrial	5	5	5,00	1	3|3|0	0,34	0,34	0,34	0,34	0,34	2,50	0,10
RINGmut	Q9LUW5	DEAD-box ATP-dependent RNA helicase 53, mitochondrial	18	18	18,00	1	10|9|3	0,06	0,06	0,06	0,06	0,06	2,45	0,20
RINGmut	Q93ZM7	Chaperonin CPN60-like 2, mitochondrial	9	9	9,00	1	3|8|0	0,19	0,19	0,19	0,19	0,19	2,45	0,14
RINGmut	Q9SCM3	40S ribosomal protein S2-4	11	11	11,00	1	7|7|0	0,08	0,08	0,08	0,08	0,08	2,36	0,19
RINGmut	Q9SJT9	Coatomer subunit alpha-2	11	11	11,00	1	7|7|0	0,08	0,08	0,08	0,08	0,08	2,36	0,19
RINGmut	Q94K05	T-complex protein 1 subunit theta	7	7	7,00	1	5|4|0	0,18	0,18	0,18	0,18	0,18	2,33	0,14
RINGmut	P59259	Histone H4	17	17	17,00	1	0|2|20	0,02	0,02	0,02	0,02	0,02	2,32	0,26
RINGmut	P29197	Chaperonin CPN60, mitochondrial	25	25	25,00	1	16|15|2	0,00	0,00	0,00	0,00	0,00	2,27	0,33
RINGmut	Q56WH4	Histone deacetylase HDT2	17	17	17,00	1	11|12|0	0,01	0,01	0,01	0,01	0,01	2,22	0,29
RINGmut	P49200	40S ribosomal protein S20-1	10	10	10,00	1	6|6|3	0,02	0,02	0,02	0,02	0,02	2,00	0,26
RINGmut	Q9LHP2	Serine/arginine-rich SC35-like splicing factor SCL30A	6	6	6,00	1	0|0|9	0,12	0,12	0,12	0,12	0,12	2,00	0,17
RINGmut	O04202	Eukaryotic translation initiation factor 3 subunit F	2	2	2,00	1	0|3|0	0,33	0,33	0,33	0,33	0,33	2,00	0,11
RINGmut	Q9LHA4	V-type proton ATPase subunit d2	2	2	2,00	1	1|2|0	0,23	0,23	0,23	0,23	0,23	2,00	0,13
RINGmut	Q9FGK5	Ras-related protein RABA5a	2	2	2,00	1	2|1|0	0,23	0,23	0,23	0,23	0,23	2,00	0,13
RINGmut	Q93Z16	Dolichyl-diphosphooligosaccharide--protein glycosyltransferase subunit 2	2	2	2,00	1	2|1|0	0,23	0,23	0,23	0,23	0,23	2,00	0,13
RINGmut	O23676	Protein mago nashi homolog	2	2	2,00	1	0|3|0	0,33	0,33	0,33	0,33	0,33	2,00	0,11
RINGmut	Q9SIT1	Receptor-like kinase TMK3	2	2	2,00	1	2|1|0	0,23	0,23	0,23	0,23	0,23	2,00	0,13
RINGmut	P31265	Translationally-controlled tumor protein 1	2	2	2,00	1	0|0|3	0,33	0,33	0,33	0,33	0,33	2,00	0,11
RINGmut	P0CJ46	Actin-1	27	27	27,00	1	14|17|11	0,00	0,00	0,00	0,00	0,00	1,93	0,39
RINGmut	P0CJ47	Actin-3	27	27	27,00	1	14|17|11	0,00	0,00	0,00	0,00	0,00	1,93	0,39
RINGmut	P29511	Tubulin alpha-6 chain	59	59	59,00	1	36|43|13	0,00	0,00	0,00	0,00	0,00	1,92	0,47
RINGmut	F4JWP9	109 kDa U5 small nuclear ribonucleoprotein component GFL	14	14	14,00	1	9|13|0	0,00	0,00	0,00	0,00	0,00	1,91	0,33
RINGmut	Q9LJH8	Oligouridylate-binding protein 1C	14	14	14,00	1	11|7|4	0,00	0,00	0,00	0,00	0,00	1,91	0,32

Bait: RINGmut	Prey	PreyGene	Spec	SpecSum	AvgSpec	NumReplicates	ctrlCounts	AvgP	MaxP	TopoAvgP	TopoMaxP	SaintScore	FoldChange	BFDR
RINGmut	Q9M5K3	Dihydrolipoyl dehydrogenase 1, mitochondrial	7	7	7,00	1	4|7|0	0,03	0,03	0,03	0,03	0,03	1,91	0,23
RINGmut	P0DH99	Elongation factor 1-alpha 1	114	114	114,00	1	69|82|30	0,00	0,00	0,00	0,00	0,00	1,89	0,50
RINGmut	Q9ZW02	Pumilio homolog 3	5	5	5,00	1	4|4|0	0,06	0,06	0,06	0,06	0,06	1,88	0,20
RINGmut	P53496	Actin-11	30	30	30,00	1	17|18|14	0,00	0,00	0,00	0,00	0,00	1,84	0,42
RINGmut	P42794	60S ribosomal protein L11-2	17	17	17,00	1	11|14|3	0,00	0,00	0,00	0,00	0,00	1,82	0,37
RINGmut	Q9LFH5	60S ribosomal protein L12-2	9	9	9,00	1	8|7|0	0,01	0,01	0,01	0,01	0,01	1,80	0,30
RINGmut	Q9LDZ0	Heat shock 70 kDa protein 10, mitochondrial	9	9	9,00	1	9|6|0	0,01	0,01	0,01	0,01	0,01	1,80	0,29
RINGmut	Q8VZG7	Ribonuclease TUDOR 1	9	9	9,00	1	5|10|0	0,01	0,01	0,01	0,01	0,01	1,80	0,29
RINGmut	Q9SRZ6	Cytosolic isocitrate dehydrogenase [NADP]	3	3	3,00	1	2|3|0	0,11	0,11	0,11	0,11	0,11	1,80	0,17
RINGmut	Q42523	Methylcrotonoyl-CoA carboxylase subunit alpha, mitochondrial	146	146	146,00	1	7|13|227	0,00	0,00	0,00	0,00	0,00	1,77	0,50
RINGmut	Q56WH1	Tubulin alpha-3 chain	37	37	37,00	1	24|31|8	0,00	0,00	0,00	0,00	0,00	1,76	0,45
RINGmut	B9DHQ0	Tubulin alpha-5 chain	37	37	37,00	1	24|31|8	0,00	0,00	0,00	0,00	0,00	1,76	0,45
RINGmut	P31414	Pyrophosphate-energized vacuolar membrane proton pump 1	17	17	17,00	1	8|11|10	0,00	0,00	0,00	0,00	0,00	1,76	0,38
RINGmut	P53492	Actin-7	45	45	45,00	1	28|30|19	0,00	0,00	0,00	0,00	0,00	1,75	0,46
RINGmut	Q9SIK2	40S ribosomal protein S25-2	7	7	7,00	1	2|4|6	0,01	0,01	0,01	0,01	0,01	1,75	0,27
RINGmut	Q9SEE9	Serine/arginine-rich splicing factor SR45	7	7	7,00	1	3|3|6	0,01	0,01	0,01	0,01	0,01	1,75	0,27
RINGmut	Q39043	Heat shock 70 kDa protein BIP2	40	40	40,00	1	27|27|16	0,00	0,00	0,00	0,00	0,00	1,71	0,46
RINGmut	Q9FZ76	60S ribosomal protein L6-1	12	12	12,00	1	4|4|13	0,00	0,00	0,00	0,00	0,00	1,71	0,35
RINGmut	O81127	Serine/arginine-rich splicing factor RSZ21	4	4	4,00	1	0|0|7	0,10	0,10	0,10	0,10	0,10	1,71	0,18
RINGmut	Q08682	40S ribosomal protein Sa-1	14	14	14,00	1	9|12|4	0,00	0,00	0,00	0,00	0,00	1,68	0,37
RINGmut	Q9LKR3	Heat shock 70 kDa protein BIP1	39	39	39,00	1	26|28|16	0,00	0,00	0,00	0,00	0,00	1,67	0,47
RINGmut	O23654	V-type proton ATPase catalytic subunit A	10	10	10,00	1	2|5|11	0,00	0,00	0,00	0,00	0,00	1,67	0,34
RINGmut	Q9C9C5	60S ribosomal protein L6-3	11	11	11,00	1	0|0|20	0,00	0,00	0,00	0,00	0,00	1,65	0,34

Bait: RINGmut	Prey	PreyGene	Spec	SpecSum	AvgSpec	NumReplicates	ctrlCounts	AvgP	MaxP	TopoAvgP	TopoMaxP	SaintScore	FoldChange	BFDR
RINGmut	Q9M339	40S ribosomal protein S3-2	18	18	18,00	1	15|18|0	0,00	0,00	0,00	0,00	0,00	1,64	0,41
RINGmut	Q9LZ57	60S ribosomal protein L36-3	6	6	6,00	1	0|0|11	0,02	0,02	0,02	0,02	0,02	1,64	0,25
RINGmut	Q9S9N1	Heat shock 70 kDa protein 5	32	32	32,00	1	15|21|24	0,00	0,00	0,00	0,00	0,00	1,60	0,46
RINGmut	P51427	40S ribosomal protein S5-2	8	8	8,00	1	7|8|0	0,00	0,00	0,00	0,00	0,00	1,60	0,32
RINGmut	P11139	Tubulin alpha-1 chain	17	17	17,00	1	12|16|4	0,00	0,00	0,00	0,00	0,00	1,59	0,41
RINGmut	Q9FX54	Glyceraldehyde-3-phosphate dehydrogenase GAPC2, cytosolic	55	55	55,00	1	41|45|22	0,00	0,00	0,00	0,00	0,00	1,53	0,49
RINGmut	Q9CAX6	40S ribosomal protein S14-2	11	11	11,00	1	11|11|0	0,00	0,00	0,00	0,00	0,00	1,50	0,37
RINGmut	P41916	GTP-binding nuclear protein Ran-1	9	9	9,00	1	7|8|3	0,00	0,00	0,00	0,00	0,00	1,50	0,36
RINGmut	Q9M5K2	Dihydrolipoyl dehydrogenase 2, mitochondrial	6	6	6,00	1	6|6|0	0,00	0,00	0,00	0,00	0,00	1,50	0,31
RINGmut	Q9M9W1	60S ribosomal protein L22-2	4	4	4,00	1	4|3|1	0,01	0,01	0,01	0,01	0,01	1,50	0,26
RINGmut	Q42586	Orotidine 5'-phosphate decarboxylase	4	4	4,00	1	4|4|0	0,02	0,02	0,02	0,02	0,02	1,50	0,25
RINGmut	Q9LHE5	Mitochondrial import receptor subunit TOM40-1, N-terminally processed	4	4	4,00	1	3|5|0	0,02	0,02	0,02	0,02	0,02	1,50	0,25
RINGmut	Q9FMV1	Gamma carbonic anhydrase-like 1, mitochondrial	2	2	2,00	1	2|2|0	0,07	0,07	0,07	0,07	0,07	1,50	0,19
RINGmut	Q95748	NADH dehydrogenase [ubiquinone] iron-sulfur protein 3	2	2	2,00	1	1|3|0	0,10	0,10	0,10	0,10	0,10	1,50	0,18
RINGmut	Q9SA78	Coatomer subunit epsilon-1	1	1	1,00	1	0|2|0	0,00	0,00	0,00	0,00	0,00	1,50	0,51
RINGmut	Q9FLX7	Probable NADH dehydrogenase [ubiquinone] 1 alpha subcomplex subunit 5, mitochondrial	1	1	1,00	1	0|2|0	0,00	0,00	0,00	0,00	0,00	1,50	0,51
RINGmut	Q9LLC1	Biotin carboxyl carrier protein of acetyl-CoA carboxylase 2, chloroplastic	51	51	51,00	1	0|0|103	0,00	0,00	0,00	0,00	0,00	1,49	0,49
RINGmut	Q9FLF0	40S ribosomal protein S9-2	14	14	14,00	1	0|0|29	0,00	0,00	0,00	0,00	0,00	1,45	0,41
RINGmut	P25858	Glyceraldehyde-3-phosphate dehydrogenase GAPC1, cytosolic	50	50	50,00	1	39|41|25	0,00	0,00	0,00	0,00	0,00	1,43	0,49
RINGmut	P51414	60S ribosomal protein L26-1	11	11	11,00	1	2|4|17	0,00	0,00	0,00	0,00	0,00	1,43	0,38
RINGmut	Q9T029	40S ribosomal protein S25-4	9	9	9,00	1	5|6|8	0,00	0,00	0,00	0,00	0,00	1,42	0,37

Bait: RINGmut	Prey	PreyGene	Spec	SpecSum	AvgSpec	NumReplicates	ctrlCounts	AvgP	MaxP	TopoAvgP	TopoMaxP	SaintScore	FoldChange	BFDR
RINGmut	P20649	ATPase 1, plasma membrane-type	15	15	15,00	1	14|18|0	0,00	0,00	0,00	0,00	0,00	1,41	0,43
RINGmut	Q42533	Biotin carboxyl carrier protein of acetyl-CoA carboxylase 1, chloroplastic	133	133	133,00	1	14|14|256	0,00	0,00	0,00	0,00	0,00	1,40	0,51
RINGmut	Q8LBI1	60S ribosomal protein L5-1	21	21	21,00	1	19|21|5	0,00	0,00	0,00	0,00	0,00	1,40	0,45
RINGmut	Q9SIP7	40S ribosomal protein S3-1	19	19	19,00	1	17|18|6	0,00	0,00	0,00	0,00	0,00	1,39	0,45
RINGmut	Q9SIH0	40S ribosomal protein S14-1	13	13	13,00	1	11|11|6	0,00	0,00	0,00	0,00	0,00	1,39	0,42
RINGmut	P31167	ADP,ATP carrier protein 1, mitochondrial	62	62	62,00	1	43|47|45	0,00	0,00	0,00	0,00	0,00	1,38	0,50
RINGmut	P49227	60S ribosomal protein L5-2	17	17	17,00	1	17|20|0	0,00	0,00	0,00	0,00	0,00	1,38	0,44
RINGmut	Q9FMU6	Mitochondrial phosphate carrier protein 3, mitochondrial	12	12	12,00	1	10|13|3	0,00	0,00	0,00	0,00	0,00	1,38	0,41
RINGmut	O64728	Protein STICHEL	5	5	5,00	1	8|3|0	0,00	0,00	0,00	0,00	0,00	1,36	0,31
RINGmut	Q0WNJ6	Clathrin heavy chain 1	25	25	25,00	1	25|31|0	0,00	0,00	0,00	0,00	0,00	1,34	0,47
RINGmut	Q96292	Actin-2	20	20	20,00	1	18|18|9	0,00	0,00	0,00	0,00	0,00	1,33	0,46
RINGmut	Q9LYJ9	DEAD-box ATP-dependent RNA helicase 46	12	12	12,00	1	13|15|0	0,00	0,00	0,00	0,00	0,00	1,29	0,42
RINGmut	P41376	Eukaryotic initiation factor 4A-1	23	23	23,00	1	19|25|10	0,00	0,00	0,00	0,00	0,00	1,28	0,47
RINGmut	O48847	Transcriptional corepressor LEUNIG_HOMOLOG	8	8	8,00	1	9|10|0	0,00	0,00	0,00	0,00	0,00	1,26	0,38
RINGmut	Q8L8Y0	40S ribosomal protein S2-1	12	12	12,00	1	10|11|8	0,00	0,00	0,00	0,00	0,00	1,24	0,43
RINGmut	Q93VB8	40S ribosomal protein S2-2	12	12	12,00	1	10|11|8	0,00	0,00	0,00	0,00	0,00	1,24	0,43
RINGmut	Q9ASS2	Protein FREE1	18	18	18,00	1	17|18|9	0,00	0,00	0,00	0,00	0,00	1,23	0,46
RINGmut	Q9LNC5	110 kDa U5 small nuclear ribonucleoprotein component CLO	13	13	13,00	1	12|20|0	0,00	0,00	0,00	0,00	0,00	1,22	0,44
RINGmut	P40941	ADP,ATP carrier protein 2, mitochondrial	26	26	26,00	1	26|23|16	0,00	0,00	0,00	0,00	0,00	1,20	0,49
RINGmut	Q96293	Actin-8	20	20	20,00	1	20|20|10	0,00	0,00	0,00	0,00	0,00	1,20	0,47
RINGmut	Q9FMG4	Serine/arginine-rich splicing factor SC35	6	6	6,00	1	0|0|15	0,00	0,00	0,00	0,00	0,00	1,20	0,35
RINGmut	Q8LD03	40S ribosomal protein S7-3	6	6	6,00	1	7|8|0	0,00	0,00	0,00	0,00	0,00	1,20	0,36
RINGmut	Q94JQ3	Serine hydroxymethyltransferase 3, chloroplastic	2	2	2,00	1	1|4|0	0,04	0,04	0,04	0,04	0,04	1,20	0,21

Bait: RINGmut	Prey	PreyGene	Spec	SpecSum	AvgSpec	NumReplicates	ctrlCounts	AvgP	MaxP	TopoAvgP	TopoMaxP	SaintScore	FoldChange	BFDR
RINGmut	Q8H136	DEAD-box ATP-dependent RNA helicase 14	31	31	31,00	1	20|21|37	0,00	0,00	0,00	0,00	0,00	1,19	0,49
RINGmut	P41377	Eukaryotic initiation factor 4A-2	23	23	23,00	1	22|27|9	0,00	0,00	0,00	0,00	0,00	1,19	0,48
RINGmut	Q9C522	ATP-citrate synthase beta chain protein 1	24	24	24,00	1	32|27|2	0,00	0,00	0,00	0,00	0,00	1,18	0,48
RINGmut	Q940B0	60S ribosomal protein L18-3	22	22	22,00	1	13|11|32	0,00	0,00	0,00	0,00	0,00	1,18	0,48
RINGmut	Q0WLB5	Clathrin heavy chain 2	23	23	23,00	1	28|31|0	0,00	0,00	0,00	0,00	0,00	1,17	0,48
RINGmut	P49209	60S ribosomal protein L9-1	25	25	25,00	1	26|28|12	0,00	0,00	0,00	0,00	0,00	1,14	0,49
RINGmut	Q42347	60S ribosomal protein L24-1	8	8	8,00	1	0|0|21	0,00	0,00	0,00	0,00	0,00	1,14	0,40
RINGmut	Q9M352	60S ribosomal protein L36-2	8	8	8,00	1	1|1|19	0,00	0,00	0,00	0,00	0,00	1,14	0,40
RINGmut	Q9T043	60S ribosomal protein L14-2	9	9	9,00	1	9|11|4	0,00	0,00	0,00	0,00	0,00	1,12	0,43
RINGmut	P38420	DNA-directed RNA polymerase II subunit 2	3	3	3,00	1	3|5|0	0,00	0,00	0,00	0,00	0,00	1,12	0,30
RINGmut	Q8GUM2	Heat shock 70 kDa protein 9, mitochondrial	26	26	26,00	1	27|28|15	0,00	0,00	0,00	0,00	0,00	1,11	0,49
RINGmut	Q9FJA6	40S ribosomal protein S3-3	14	14	14,00	1	15|17|6	0,00	0,00	0,00	0,00	0,00	1,11	0,46
RINGmut	P0DH91	ADP-ribosylation factor 2-B	10	10	10,00	1	13|14|0	0,00	0,00	0,00	0,00	0,00	1,11	0,43
RINGmut	Q9CAN8	Lysophospholipid acyltransferase 2	7	7	7,00	1	9|10|0	0,00	0,00	0,00	0,00	0,00	1,11	0,40
RINGmut	P49688	40S ribosomal protein S2-3	15	15	15,00	1	13|14|14	0,00	0,00	0,00	0,00	0,00	1,10	0,46
RINGmut	Q42262	40S ribosomal protein S3a-2	20	20	20,00	1	19|19|17	0,00	0,00	0,00	0,00	0,00	1,09	0,48
RINGmut	O04487	Probable elongation factor 1-gamma 1	4	4	4,00	1	5|6|0	0,00	0,00	0,00	0,00	0,00	1,09	0,34
RINGmut	Q9LNU4	26S proteasome non-ATPase regulatory subunit 3 homolog A	5	5	5,00	1	7|7|0	0,00	0,00	0,00	0,00	0,00	1,07	0,37
RINGmut	Q8LF21	Dynamin-related protein 1C	52	52	52,00	1	41|46|60	0,00	0,00	0,00	0,00	0,00	1,06	0,50
RINGmut	Q9FGX1	ATP-citrate synthase beta chain protein 2	23	23	23,00	1	36|30|0	0,00	0,00	0,00	0,00	0,00	1,05	0,49
RINGmut	Q42340	40S ribosomal protein S16-3	19	19	19,00	1	12|11|32	0,00	0,00	0,00	0,00	0,00	1,04	0,48
RINGmut	P22953	Heat shock 70 kDa protein 1	110	110	110,00	1	124|137|58	0,00	0,00	0,00	0,00	0,00	1,03	0,51
RINGmut	P34788	40S ribosomal protein S18	12	12	12,00	1	6|9|20	0,00	0,00	0,00	0,00	0,00	1,03	0,45
RINGmut	P42697	Dynamin-related protein 1A	72	72	72,00	1	55|61|97	0,00	0,00	0,00	0,00	0,00	1,01	0,51

Bait: RINGmut	Prey	PreyGene	Spec	SpecSum	AvgSpec	NumReplicates	ctrlCounts	AvgP	MaxP	TopoAvgP	TopoMaxP	SaintScore	FoldChange	BFDR
RINGmut	Q9LXG1	40S ribosomal protein S9-1	24	24	24,00	1	13|16|43	0,00	0,00	0,00	0,00	0,00	1,00	0,51
RINGmut	Q9MAB3	Probable nucleolar protein 5-2	8	8	8,00	1	8|9|7	0,00	0,00	0,00	0,00	0,00	1,00	0,51
RINGmut	Q94CE5	Gamma-aminobutyrate transaminase POP2, mitochondrial	5	5	5,00	1	7|8|0	0,00	0,00	0,00	0,00	0,00	1,00	0,51
RINGmut	Q8S3C9	Dynamin-related protein 1D	5	5	5,00	1	4|3|8	0,00	0,00	0,00	0,00	0,00	1,00	0,51
RINGmut	O49485	D-3-phosphoglycerate dehydrogenase 1, chloroplastic	3	3	3,00	1	4|5|0	0,00	0,00	0,00	0,00	0,00	1,00	0,51
RINGmut	Q9MAK9	26S proteasome regulatory subunit S10B homolog B	2	2	2,00	1	2|4|0	0,00	0,00	0,00	0,00	0,00	1,00	0,51
RINGmut	Q9SEI3	26S proteasome regulatory subunit 10B homolog A	2	2	2,00	1	2|4|0	0,00	0,00	0,00	0,00	0,00	1,00	0,51
RINGmut	Q940X9	La-related protein 1A	2	2	2,00	1	3|3|0	0,00	0,00	0,00	0,00	0,00	1,00	0,51
RINGmut	P49689	40S ribosomal protein S30	1	1	1,00	1	0|0|3	0,00	0,00	0,00	0,00	0,00	1,00	0,51
RINGmut	Q9LVM1	ABC transporter B family member 25, mitochondrial	1	1	1,00	1	0|0|3	0,00	0,00	0,00	0,00	0,00	1,00	0,51
RINGmut	Q8W4R3	DEAD-box ATP-dependent RNA helicase 30	1	1	1,00	1	1|2|0	0,00	0,00	0,00	0,00	0,00	1,00	0,51
RINGmut	P92966	Serine/arginine-rich splicing factor RS41	1	1	1,00	1	0|0|3	0,00	0,00	0,00	0,00	0,00	1,00	0,51
RINGmut	P49692	60S ribosomal protein L7a-1	21	21	21,00	1	13|14|37	0,00	0,00	0,00	0,00	0,00	0,98	0,51
RINGmut	P25696	Bifunctional enolase 2/transcriptional activator	22	22	22,00	1	27|30|11	0,00	0,00	0,00	0,00	0,00	0,97	0,51
RINGmut	Q9SS17	40S ribosomal protein S24-1	10	10	10,00	1	8|9|14	0,00	0,00	0,00	0,00	0,00	0,97	0,51
RINGmut	Q9ZUT9	40S ribosomal protein S5-1	9	9	9,00	1	5|7|16	0,00	0,00	0,00	0,00	0,00	0,96	0,51
RINGmut	Q9SRX2	60S ribosomal protein L19-1	20	20	20,00	1	7|8|48	0,00	0,00	0,00	0,00	0,00	0,95	0,51
RINGmut	Q9SZ15	Protein HOMOLOG OF MAMMALIAN LYST-INTERACTING PROTEIN 5	19	19	19,00	1	25|22|13	0,00	0,00	0,00	0,00	0,00	0,95	0,51
RINGmut	Q05431	L-ascorbate peroxidase 1, cytosolic	7	7	7,00	1	11|11|0	0,00	0,00	0,00	0,00	0,00	0,95	0,51
RINGmut	Q5XEP2	Hsp70-Hsp90 organizing protein 2	5	5	5,00	1	9|7|0	0,00	0,00	0,00	0,00	0,00	0,94	0,51
RINGmut	Q1EBV4	Protein DNA-DAMAGE INDUCIBLE 1	13	13	13,00	1	19|12|11	0,00	0,00	0,00	0,00	0,00	0,93	0,51
RINGmut	Q9LHA8	Heat shock 70 kDa protein 4	84	84	84,00	1	108|122|45	0,00	0,00	0,00	0,00	0,00	0,92	0,51
RINGmut	Q8LC83	40S ribosomal protein S24-2	8	8	8,00	1	7|7|12	0,00	0,00	0,00	0,00	0,00	0,92	0,51

Bait: RINGmut	Prey	PreyGene	Spec	SpecSum	AvgSpec	NumReplicates	ctrlCounts	AvgP	MaxP	TopoAvgP	TopoMaxP	SaintScore	FoldChange	BFDR
RINGmut	O81126	Serine/arginine-rich splicing factor RSZ22	7	7	7,00	1	1|0|22	0,00	0,00	0,00	0,00	0,00	0,91	0,51
RINGmut	O65719	Heat shock 70 kDa protein 3	88	88	88,00	1	122|127|45	0,00	0,00	0,00	0,00	0,00	0,90	0,51
RINGmut	Q8RWN9	Pyruvate dehydrogenase E2 component (dihydrolipoamide acetyltransferase)	3	3	3,00	1	0|0|10	0,00	0,00	0,00	0,00	0,00	0,90	0,51
RINGmut	P19456	ATPase 2, plasma membrane-type	13	13	13,00	1	17|27|0	0,00	0,00	0,00	0,00	0,00	0,89	0,51
RINGmut	Q9FEF8	rRNA 2'-O-methyltransferase fibrillarin 1	7	7	7,00	1	11|11|2	0,00	0,00	0,00	0,00	0,00	0,88	0,51
RINGmut	Q56WD9	3-ketoacyl-CoA thiolase 2, peroxisomal	5	5	5,00	1	9|8|0	0,00	0,00	0,00	0,00	0,00	0,88	0,51
RINGmut	Q8S9J8	Probable clathrin assembly protein At4g32285	5	5	5,00	1	8|9|0	0,00	0,00	0,00	0,00	0,00	0,88	0,51
RINGmut	Q9LZH9	60S ribosomal protein L7a-2	16	16	16,00	1	10|11|34	0,00	0,00	0,00	0,00	0,00	0,87	0,51
RINGmut	Q9LQ04	Bifunctional dTDP-4-dehydrorhamnose 3,5-epimerase/dTDP-4-dehydrorhamnose reductase	6	6	6,00	1	11|10|0	0,00	0,00	0,00	0,00	0,00	0,86	0,51
RINGmut	Q96266	Glutathione S-transferase F8, chloroplastic	6	6	6,00	1	8|13|0	0,00	0,00	0,00	0,00	0,00	0,86	0,51
RINGmut	Q9C7X7	Heat shock 70 kDa protein 18	68	68	68,00	1	95|100|45	0,00	0,00	0,00	0,00	0,00	0,85	0,51
RINGmut	Q9LJE5	YTH domain-containing protein ECT2	16	16	16,00	1	23|27|7	0,00	0,00	0,00	0,00	0,00	0,84	0,51
RINGmut	Q8LPJ7	40S ribosomal protein S26-2	7	7	7,00	1	0|0|25	0,00	0,00	0,00	0,00	0,00	0,84	0,51
RINGmut	P22954	Heat shock 70 kDa protein 2	79	79	79,00	1	110|123|51	0,00	0,00	0,00	0,00	0,00	0,83	0,51
RINGmut	Q8L5Y6	Cullin-associated NEDD8-dissociated protein 1	37	37	37,00	1	67|62|5	0,00	0,00	0,00	0,00	0,00	0,83	0,51
RINGmut	P46645	Aspartate aminotransferase, cytoplasmic isozyme 1	17	17	17,00	1	27|31|4	0,00	0,00	0,00	0,00	0,00	0,82	0,51
RINGmut	O50008	5-methyltetrahydropteroyltriglutamate--homocysteine methyltransferase 1	12	12	12,00	1	23|21|0	0,00	0,00	0,00	0,00	0,00	0,82	0,51
RINGmut	P46644	Aspartate aminotransferase 3, chloroplastic	6	6	6,00	1	11|11|0	0,00	0,00	0,00	0,00	0,00	0,82	0,51
RINGmut	Q9SEI2	26S proteasome regulatory subunit 6A homolog A	3	3	3,00	1	4|5|2	0,00	0,00	0,00	0,00	0,00	0,82	0,51
RINGmut	P46286	60S ribosomal protein L8-1	17	17	17,00	1	13|16|34	0,00	0,00	0,00	0,00	0,00	0,81	0,51

Bait: RINGmut	Prey	PreyGene	Spec	SpecSum	AvgSpec	NumReplicates	ctrlCounts	AvgP	MaxP	TopoAvgP	TopoMaxP	SaintScore	FoldChange	BFDR
RINGmut	P49693	60S ribosomal protein L19-3	10	10	10,00	1	4|6|27	0,00	0,00	0,00	0,00	0,00	0,81	0,51
RINGmut	Q9FLT0	Ribonuclease TUDOR 2	10	10	10,00	1	19|18|0	0,00	0,00	0,00	0,00	0,00	0,81	0,51
RINGmut	Q9SJF1	GTPase LSG1-2	8	8	8,00	1	12|11|7	0,00	0,00	0,00	0,00	0,00	0,80	0,51
RINGmut	O23515	60S ribosomal protein L15-1	19	19	19,00	1	13|11|48	0,00	0,00	0,00	0,00	0,00	0,79	0,51
RINGmut	Q9LTT8	Enhancer of mRNA-decapping protein 4	40	40	40,00	1	68|70|15	0,00	0,00	0,00	0,00	0,00	0,78	0,51
RINGmut	Q9FVQ1	Nucleolin 1	7	7	7,00	1	14|13|0	0,00	0,00	0,00	0,00	0,00	0,78	0,51
RINGmut	Q9LDD8	Methylcrotonoyl-CoA carboxylase beta chain, mitochondrial	56	56	56,00	1	3|6|209	0,00	0,00	0,00	0,00	0,00	0,77	0,51
RINGmut	Q9CAV0	40S ribosomal protein S3a-1	10	10	10,00	1	13|18|8	0,00	0,00	0,00	0,00	0,00	0,77	0,51
RINGmut	Q9SEI4	26S proteasome regulatory subunit 6B homolog	6	6	6,00	1	9|13|2	0,00	0,00	0,00	0,00	0,00	0,75	0,51
RINGmut	Q9LIA8	UDP-glucose 6-dehydrogenase 2	5	5	5,00	1	10|10|0	0,00	0,00	0,00	0,00	0,00	0,75	0,51
RINGmut	Q9SV20	Coatomer subunit beta-2	4	4	4,00	1	6|10|0	0,00	0,00	0,00	0,00	0,00	0,75	0,51
RINGmut	Q9STX5	Endoplasmin homolog	4	4	4,00	1	7|9|0	0,00	0,00	0,00	0,00	0,00	0,75	0,51
RINGmut	Q945Q1	Cysteine proteinase inhibitor 1	3	3	3,00	1	4|4|4	0,00	0,00	0,00	0,00	0,00	0,75	0,51
RINGmut	Q39189	DEAD-box ATP-dependent RNA helicase 7	3	3	3,00	1	5|7|0	0,00	0,00	0,00	0,00	0,00	0,75	0,51
RINGmut	Q9FQ04	5'-3' exoribonuclease 4	3	3	3,00	1	8|4|0	0,00	0,00	0,00	0,00	0,00	0,75	0,51
RINGmut	O04658	Probable nucleolar protein 5-1	2	2	2,00	1	3|5|0	0,00	0,00	0,00	0,00	0,00	0,75	0,51
RINGmut	Q8W117	Suppressor of mec-8 and unc-52 protein homolog 1	2	2	2,00	1	4|4|0	0,00	0,00	0,00	0,00	0,00	0,75	0,51
RINGmut	O64642	UTP:RNA uridylyltransferase 1	1	1	1,00	1	2|2|0	0,00	0,00	0,00	0,00	0,00	0,75	0,51
RINGmut	Q9LQ55	Dynamin-2B	57	57	57,00	1	54|60|118	0,00	0,00	0,00	0,00	0,00	0,74	0,51
RINGmut	Q9SZY1	Nascent polypeptide-associated complex subunit alpha-like protein 4	6	6	6,00	1	9|9|7	0,00	0,00	0,00	0,00	0,00	0,72	0,51
RINGmut	P41127	60S ribosomal protein L13-1	21	21	21,00	1	16|15|58	0,00	0,00	0,00	0,00	0,00	0,71	0,51
RINGmut	Q42064	60S ribosomal protein L8-3	15	15	15,00	1	14|16|33	0,00	0,00	0,00	0,00	0,00	0,71	0,51
RINGmut	P42733	40S ribosomal protein S11-3	4	4	4,00	1	2|2|13	0,00	0,00	0,00	0,00	0,00	0,71	0,51
RINGmut	Q9SSB5	26S proteasome regulatory subunit 7 homolog A	4	4	4,00	1	7|10|0	0,00	0,00	0,00	0,00	0,00	0,71	0,51

Bait: RINGmut	Prey	PreyGene	Spec	SpecSum	AvgSpec	NumReplicates	ctrlCounts	AvgP	MaxP	TopoAvgP	TopoMaxP	SaintScore	FoldChange	BFDR
RINGmut	P51413	60S ribosomal protein L17-2	7	7	7,00	1	5|7|18	0,00	0,00	0,00	0,00	0,00	0,70	0,51
RINGmut	Q8L7U4	Co-chaperone protein p23-1	9	9	9,00	1	19|18|2	0,00	0,00	0,00	0,00	0,00	0,69	0,51
RINGmut	P49205	40S ribosomal protein S17-1	3	3	3,00	1	3|2|8	0,00	0,00	0,00	0,00	0,00	0,69	0,51
RINGmut	P17094	60S ribosomal protein L3-1	31	31	31,00	1	36|42|58	0,00	0,00	0,00	0,00	0,00	0,68	0,51
RINGmut	Q9LNB6	Hsp70-Hsp90 organizing protein 1	29	29	29,00	1	44|45|39	0,00	0,00	0,00	0,00	0,00	0,68	0,51
RINGmut	Q39172	NADPH-dependent oxidoreductase 2-alkenal reductase	2	2	2,00	1	3|6|0	0,00	0,00	0,00	0,00	0,00	0,67	0,51
RINGmut	Q93VG5	40S ribosomal protein S8-1	16	16	16,00	1	28|32|14	0,00	0,00	0,00	0,00	0,00	0,65	0,51
RINGmut	Q9LYK9	40S ribosomal protein S26-3	7	7	7,00	1	3|4|26	0,00	0,00	0,00	0,00	0,00	0,64	0,51
RINGmut	Q9SB63	Protein MODIFIER OF SNC1 1	7	7	7,00	1	17|16|0	0,00	0,00	0,00	0,00	0,00	0,64	0,51
RINGmut	Q93VP3	Eukaryotic translation initiation factor 5A-2	3	3	3,00	1	8|6|0	0,00	0,00	0,00	0,00	0,00	0,64	0,51
RINGmut	P38666	60S ribosomal protein L24-2	8	8	8,00	1	5|6|27	0,00	0,00	0,00	0,00	0,00	0,63	0,51
RINGmut	Q9SE83	Dynamin-2A	46	46	46,00	1	55|65|102	0,00	0,00	0,00	0,00	0,00	0,62	0,51
RINGmut	P60039	60S ribosomal protein L7-3	11	11	11,00	1	14|17|22	0,00	0,00	0,00	0,00	0,00	0,62	0,51
RINGmut	P49206	40S ribosomal protein S26-1	7	7	7,00	1	4|4|26	0,00	0,00	0,00	0,00	0,00	0,62	0,51
RINGmut	P16181	40S ribosomal protein S11-1	6	6	6,00	1	7|7|16	0,00	0,00	0,00	0,00	0,00	0,60	0,51
RINGmut	O04331	Prohibitin-3, mitochondrial	4	4	4,00	1	8|10|2	0,00	0,00	0,00	0,00	0,00	0,60	0,51
RINGmut	Q39085	Delta(24)-sterol reductase	3	3	3,00	1	6|9|0	0,00	0,00	0,00	0,00	0,00	0,60	0,51
RINGmut	Q9FUY2	Transcriptional corepressor LEUNIG	2	2	2,00	1	5|5|0	0,00	0,00	0,00	0,00	0,00	0,60	0,51
RINGmut	Q9LV27	Target of rapamycin complex subunit LST8-1	2	2	2,00	1	4|4|2	0,00	0,00	0,00	0,00	0,00	0,60	0,51
RINGmut	Q9FFT4	Pyruvate decarboxylase 2	1	1	1,00	1	2|3|0	0,00	0,00	0,00	0,00	0,00	0,60	0,51
RINGmut	Q9SJQ9	Fructose-bisphosphate aldolase 6, cytosolic	36	36	36,00	1	82|66|48	0,00	0,00	0,00	0,00	0,00	0,55	0,51
RINGmut	P60040	60S ribosomal protein L7-2	12	12	12,00	1	16|23|26	0,00	0,00	0,00	0,00	0,00	0,55	0,51
RINGmut	Q96250	ATP synthase subunit gamma, mitochondrial	2	2	2,00	1	5|6|0	0,00	0,00	0,00	0,00	0,00	0,55	0,51
RINGmut	O04019	26S proteasome regulatory subunit 6A homolog B	2	2	2,00	1	4|5|2	0,00	0,00	0,00	0,00	0,00	0,55	0,51

Bait: RINGmut	Prey	PreyGene	Spec	SpecSum	AvgSpec	NumReplicates	ctrlCounts	AvgP	MaxP	TopoAvgP	TopoMaxP	SaintScore	FoldChange	BFDR
RINGmut	P49204	40S ribosomal protein S4-2	19	19	19,00	1	27|33|47	0,00	0,00	0,00	0,00	0,00	0,53	0,51
RINGmut	F4K1Z0	YTH domain-containing protein ECT3	4	4	4,00	1	8|7|8	0,00	0,00	0,00	0,00	0,00	0,52	0,51
RINGmut	Q9LF98	Fructose-bisphosphate aldolase 8, cytosolic	50	50	50,00	1	114|102|87	0,00	0,00	0,00	0,00	0,00	0,50	0,51
RINGmut	Q9SJA6	Serine/arginine-rich splicing factor RSZ22A	3	3	3,00	1	0|0|18	0,00	0,00	0,00	0,00	0,00	0,50	0,51
RINGmut	Q84W89	DEAD-box ATP-dependent RNA helicase 37	1	1	1,00	1	2|4|0	0,00	0,00	0,00	0,00	0,00	0,50	0,51
RINGmut	P47192	Vesicle-associated membrane protein 722	1	1	1,00	1	2|4|0	0,00	0,00	0,00	0,00	0,00	0,50	0,51
RINGmut	O48549	40S ribosomal protein S6-1	11	11	11,00	1	18|22|29	0,00	0,00	0,00	0,00	0,00	0,48	0,51
RINGmut	P51430	40S ribosomal protein S6-2	9	9	9,00	1	17|20|20	0,00	0,00	0,00	0,00	0,00	0,47	0,51
RINGmut	O23212	Splicing factor U2af large subunit A	2	2	2,00	1	2|0|11	0,00	0,00	0,00	0,00	0,00	0,46	0,51
RINGmut	Q9LT08	26S proteasome non-ATPase regulatory subunit 14 homolog	2	2	2,00	1	3|10|0	0,00	0,00	0,00	0,00	0,00	0,46	0,51
RINGmut	Q9LR33	60S ribosomal protein L27a-2	8	8	8,00	1	10|12|31	0,00	0,00	0,00	0,00	0,00	0,45	0,51
RINGmut	Q84VW9	Phosphoenolpyruvate carboxylase 3	6	6	6,00	1	24|16|0	0,00	0,00	0,00	0,00	0,00	0,45	0,51
RINGmut	Q9SF40	60S ribosomal protein L4-1	30	30	30,00	1	23|26|154	0,00	0,00	0,00	0,00	0,00	0,44	0,51
RINGmut	Q9LTT9	Varicose-related protein	13	13	13,00	1	49|34|5	0,00	0,00	0,00	0,00	0,00	0,44	0,51
RINGmut	Q9SIV2	26S proteasome non-ATPase regulatory subunit 2 homolog A	4	4	4,00	1	10|17|0	0,00	0,00	0,00	0,00	0,00	0,44	0,51
RINGmut	P49691	60S ribosomal protein L4-2	28	28	28,00	1	24|27|144	0,00	0,00	0,00	0,00	0,00	0,43	0,51
RINGmut	Q9LF33	UDP-glucose 6-dehydrogenase 3	3	3	3,00	1	8|13|0	0,00	0,00	0,00	0,00	0,00	0,43	0,51
RINGmut	P17745	Elongation factor Tu, chloroplastic	5	5	5,00	1	19|16|2	0,00	0,00	0,00	0,00	0,00	0,41	0,51
RINGmut	Q9ZPI1	Lysine--tRNA ligase, cytoplasmic	5	5	5,00	1	15|22|0	0,00	0,00	0,00	0,00	0,00	0,41	0,51
RINGmut	O80626	60S ribosomal protein L35-2	3	3	3,00	1	3|4|15	0,00	0,00	0,00	0,00	0,00	0,41	0,51
RINGmut	Q9STW6	Heat shock 70 kDa protein 6, chloroplastic	2	2	2,00	1	3|4|8	0,00	0,00	0,00	0,00	0,00	0,40	0,51
RINGmut	Q9FNX5	Dynamin-related protein 1E	5	5	5,00	1	11|12|16	0,00	0,00	0,00	0,00	0,00	0,38	0,51
RINGmut	O64843	Polyadenylate-binding protein-interacting protein 7	1	1	1,00	1	4|4|0	0,00	0,00	0,00	0,00	0,00	0,38	0,51

Bait: RINGmut	Prey	PreyGene	Spec	SpecSum	AvgSpec	NumReplicates	ctrlCounts	AvgP	MaxP	TopoAvgP	TopoMaxP	SaintScore	FoldChange	BFDR
RINGmut	P49637	60S ribosomal protein L27a-3	6	6	6,00	1	10|10|30	0,00	0,00	0,00	0,00	0,00	0,36	0,51
RINGmut	P59224	40S ribosomal protein S13-2	5	5	5,00	1	8|7|30	0,00	0,00	0,00	0,00	0,00	0,33	0,51
RINGmut	P49201	40S ribosomal protein S23-2	1	1	1,00	1	5|4|0	0,00	0,00	0,00	0,00	0,00	0,33	0,51
RINGmut	Q9LTX9	Heat shock 70 kDa protein 7, chloroplastic	2	2	2,00	1	4|5|10	0,00	0,00	0,00	0,00	0,00	0,32	0,51
RINGmut	Q9MAH0	Phosphoenolpyruvate carboxylase 1	7	7	7,00	1	34|28|6	0,00	0,00	0,00	0,00	0,00	0,31	0,51
RINGmut	Q9FKA5	Uncharacterized protein At5g39570	9	9	9,00	1	39|36|16	0,00	0,00	0,00	0,00	0,00	0,30	0,51
RINGmut	Q96327	ERBB-3 BINDING PROTEIN 1	6	6	6,00	1	31|23|7	0,00	0,00	0,00	0,00	0,00	0,30	0,51
RINGmut	Q9SFU1	60S ribosomal protein L13a-1	5	5	5,00	1	7|12|33	0,00	0,00	0,00	0,00	0,00	0,29	0,51
RINGmut	Q9C5U3	26S proteasome regulatory subunit 8 homolog A	2	2	2,00	1	10|11|0	0,00	0,00	0,00	0,00	0,00	0,29	0,51
RINGmut	Q38882	Phospholipase D alpha 1	35	35	35,00	1	176|159|68	0,00	0,00	0,00	0,00	0,00	0,26	0,51
RINGmut	P51418	60S ribosomal protein L18a-2	10	10	10,00	1	13|20|81	0,00	0,00	0,00	0,00	0,00	0,26	0,51
RINGmut	Q38884	Eukaryotic translation initiation factor 3 subunit I	3	3	3,00	1	16|19|0	0,00	0,00	0,00	0,00	0,00	0,26	0,51
RINGmut	Q9M0E2	60S ribosomal protein L28-2	2	2	2,00	1	3|4|16	0,00	0,00	0,00	0,00	0,00	0,26	0,51
RINGmut	Q94BQ2	26S proteasome regulatory subunit 8 homolog B	2	2	2,00	1	10|12|2	0,00	0,00	0,00	0,00	0,00	0,25	0,51
RINGmut	Q9FIQ0	Probable ADP-ribosylation factor GTPase-activating protein AGD9	3	3	3,00	1	16|15|6	0,00	0,00	0,00	0,00	0,00	0,24	0,51
RINGmut	Q93W22	60S ribosomal protein L10-3	3	3	3,00	1	7|7|23	0,00	0,00	0,00	0,00	0,00	0,24	0,51
RINGmut	Q944K2	Dolichyl-diphosphooligosaccharide--protein glycosyltransferase 48 kDa subunit	1	1	1,00	1	6|7|0	0,00	0,00	0,00	0,00	0,00	0,23	0,51
RINGmut	Q9C5Z1	Eukaryotic translation initiation factor 3 subunit B	4	4	4,00	1	30|25|0	0,00	0,00	0,00	0,00	0,00	0,22	0,51
RINGmut	O82647	Pyruvate decarboxylase 1	2	2	2,00	1	14|13|0	0,00	0,00	0,00	0,00	0,00	0,22	0,51
RINGmut	P49211	60S ribosomal protein L32-1	2	2	2,00	1	4|3|21	0,00	0,00	0,00	0,00	0,00	0,21	0,51
RINGmut	Q93ZG7	DEAD-box ATP-dependent RNA helicase 38	1	1	1,00	1	8|6|0	0,00	0,00	0,00	0,00	0,00	0,21	0,51
RINGmut	F4I1L3	Acetyl-CoA carboxylase 2	11	11	11,00	1	11|11|139	0,00	0,00	0,00	0,00	0,00	0,20	0,51
RINGmut	Q8VWF1	SH3 domain-containing protein 2	1	1	1,00	1	8|7|0	0,00	0,00	0,00	0,00	0,00	0,20	0,51

Bait: RINGmut	Prey	PreyGene	Spec	SpecSum	AvgSpec	NumReplicates	ctrlCounts	AvgP	MaxP	TopoAvgP	TopoMaxP	SaintScore	FoldChange	BFDR
RINGmut	Q9C5M0	Mitochondrial dicarboxylate/tricarboxylate transporter DTC	4	4	4,00	1	9|9|45	0,00	0,00	0,00	0,00	0,00	0,19	0,51
RINGmut	P11574	V-type proton ATPase subunit B1	5	5	5,00	1	31|29|24	0,00	0,00	0,00	0,00	0,00	0,18	0,51
RINGmut	Q9SVR0	60S ribosomal protein L13a-3	2	2	2,00	1	4|10|21	0,00	0,00	0,00	0,00	0,00	0,17	0,51
RINGmut	Q08112	40S ribosomal protein S15-1	1	1	1,00	1	3|4|11	0,00	0,00	0,00	0,00	0,00	0,17	0,51
RINGmut	Q9LUD4	60S ribosomal protein L18a-3	3	3	3,00	1	8|12|39	0,00	0,00	0,00	0,00	0,00	0,15	0,51
RINGmut	F4J5S1	Clustered mitochondria protein	2	2	2,00	1	20|21|0	0,00	0,00	0,00	0,00	0,00	0,15	0,51
RINGmut	Q9LUQ6	60S ribosomal protein L19-2	1	1	1,00	1	0|0|20	0,00	0,00	0,00	0,00	0,00	0,15	0,51
RINGmut	Q9T074	Phosphoenolpyruvate carboxykinase (ATP)	9	9	9,00	1	95|85|17	0,00	0,00	0,00	0,00	0,00	0,14	0,51
RINGmut	O81283	Translocase of chloroplast 159, chloroplastic	5	5	5,00	1	52|51|3	0,00	0,00	0,00	0,00	0,00	0,14	0,51
RINGmut	Q9SZI2	Nucleosome assembly protein 1;1	1	1	1,00	1	11|10|0	0,00	0,00	0,00	0,00	0,00	0,14	0,51
RINGmut	Q9LFU5	Probable tRNA (guanine(26)-N(2))-dimethyltransferase 1	3	3	3,00	1	33|28|8	0,00	0,00	0,00	0,00	0,00	0,13	0,51
RINGmut	Q9XI93	Oleosin-B3-like protein	1	1	1,00	1	16|9|0	0,00	0,00	0,00	0,00	0,00	0,12	0,51
RINGmut	F4I116	Leucine--tRNA ligase, cytoplasmic	1	1	1,00	1	9|15|0	0,00	0,00	0,00	0,00	0,00	0,12	0,51
RINGmut	Q9FF90	60S ribosomal protein L13-3	1	1	1,00	1	7|7|14	0,00	0,00	0,00	0,00	0,00	0,11	0,51
RINGmut	O23254	Serine hydroxymethyltransferase 4	1	1	1,00	1	13|14|0	0,00	0,00	0,00	0,00	0,00	0,11	0,51
RINGmut	Q94KE2	Protein TIME FOR COFFEE	2	2	2,00	1	31|34|6	0,00	0,00	0,00	0,00	0,00	0,08	0,51
RINGmut	Q38970	Acetyl-CoA carboxylase 1	4	4	4,00	1	22|25|141	0,00	0,00	0,00	0,00	0,00	0,06	0,51
RINGmut	Q9LD55	Eukaryotic translation initiation factor 3 subunit A	1	1	1,00	1	41|31|0	0,00	0,00	0,00	0,00	0,00	0,04	0,51

Bait: RINGmut_z	Prey	PreyGene	Spec	SpecSum	AvgSpec	NumReplicates	ctrlCounts	AvgP	MaxP	TopoAvgP	TopoMaxP	SaintScore	FoldChange	BFDR
RINGmut_z	P23321	Oxygen-evolving enhancer protein 1-1, chloroplastic	50	50	50,00	1	0|0|0	1,00	1,00	1,00	1,00	1,00	500,00	0,00
RINGmut_z	Q9S841	Oxygen-evolving enhancer protein 1-2, chloroplastic	43	43	43,00	1	0|0|0	1,00	1,00	1,00	1,00	1,00	430,00	0,00
RINGmut_z	Q0WV25	Tubulin alpha-4 chain	36	36	36,00	1	0|0|0	1,00	1,00	1,00	1,00	1,00	360,00	0,00
RINGmut_z	Q9XFT3	Oxygen-evolving enhancer protein 3-1, chloroplastic	30	30	30,00	1	0|0|0	1,00	1,00	1,00	1,00	1,00	300,00	0,00
RINGmut_z	Q8RWZ3	Probable acyl-CoA dehydrogenase IBR3	21	21	21,00	1	0|0|0	1,00	1,00	1,00	1,00	1,00	210,00	0,00
RINGmut_z	O03042	Ribulose bisphosphate carboxylase large chain	20	20	20,00	1	0|0|0	1,00	1,00	1,00	1,00	1,00	200,00	0,00
RINGmut_z	P0DH95	Calmodulin-1	16	16	16,00	1	0|0|0	1,00	1,00	1,00	1,00	1,00	160,00	0,00
RINGmut_z	P0DH96	Calmodulin-4	16	16	16,00	1	0|0|0	1,00	1,00	1,00	1,00	1,00	160,00	0,00
RINGmut_z	P55737	Heat shock protein 90-2	15	15	15,00	1	0|0|0	1,00	1,00	1,00	1,00	1,00	150,00	0,00
RINGmut_z	P10896	Ribulose bisphosphate carboxylase/oxygenase activase, chloroplastic	11	11	11,00	1	0|0|0	1,00	1,00	1,00	1,00	1,00	110,00	0,00
RINGmut_z	P21238	Chaperonin 60 subunit alpha 1, chloroplastic	11	11	11,00	1	0|0|0	1,00	1,00	1,00	1,00	1,00	110,00	0,00
RINGmut_z	Q9ZP06	Malate dehydrogenase 1, mitochondrial	11	11	11,00	1	0|0|0	1,00	1,00	1,00	1,00	1,00	110,00	0,00
RINGmut_z	Q41932	Oxygen-evolving enhancer protein 3-2, chloroplastic	10	10	10,00	1	0|0|0	1,00	1,00	1,00	1,00	1,00	100,00	0,00
RINGmut_z	O65282	20 kDa chaperonin, chloroplastic	9	9	9,00	1	0|0|0	1,00	1,00	1,00	1,00	1,00	90,00	0,00
RINGmut_z	Q9ZVF3	MLP-like protein 328	7	7	7,00	1	0|0|0	1,00	1,00	1,00	1,00	1,00	70,00	0,00
RINGmut_z	Q9LQL0	Glycine cleavage system H protein 3, mitochondrial	7	7	7,00	1	0|0|0	1,00	1,00	1,00	1,00	1,00	70,00	0,00
RINGmut_z	Q9LZ45	Histone H2B.9	6	6	6,00	1	0|0|0	1,00	1,00	1,00	1,00	1,00	60,00	0,00
RINGmut_z	O04316	Nitrile-specifier protein 4	6	6	6,00	1	0|0|0	1,00	1,00	1,00	1,00	1,00	60,00	0,00
RINGmut_z	P50318	Phosphoglycerate kinase 2, chloroplastic	5	5	5,00	1	0|0|0	1,00	1,00	1,00	1,00	1,00	50,00	0,00
RINGmut_z	P57752	Acyl-CoA-binding domain-containing protein 6	5	5	5,00	1	0|0|0	1,00	1,00	1,00	1,00	1,00	50,00	0,00
RINGmut_z	P34790	Peptidyl-prolyl cis-trans isomerase CYP18-3	5	5	5,00	1	0|0|0	1,00	1,00	1,00	1,00	1,00	50,00	0,00
RINGmut_z	O22254	Putative 60S ribosomal protein L18-1	4	4	4,00	1	0|0|0	1,00	1,00	1,00	1,00	1,00	40,00	0,00

Bait: RINGmut_z	Prey	PreyGene	Spec	SpecSum	AvgSpec	NumReplicates	ctrlCounts	AvgP	MaxP	TopoAvgP	TopoMaxP	SaintScore	FoldChange	BFDR
RINGmut_z	P42699	Plastocyanin major isoform, chloroplastic	4	4	4,00	1	0|0|0	1,00	1,00	1,00	1,00	1,00	40,00	0,00
RINGmut_z	Q42589	Non-specific lipid-transfer protein 1	4	4	4,00	1	0|0|0	1,00	1,00	1,00	1,00	1,00	40,00	0,00
RINGmut_z	Q9LD57	Phosphoglycerate kinase 1, chloroplastic	4	4	4,00	1	0|0|0	1,00	1,00	1,00	1,00	1,00	40,00	0,00
RINGmut_z	Q9SW21	Acyl carrier protein 4, chloroplastic	4	4	4,00	1	0|0|0	1,00	1,00	1,00	1,00	1,00	40,00	0,00
RINGmut_z	Q9STY6	40S ribosomal protein S20-2	3	3	3,00	1	0|0|0	1,00	1,00	1,00	1,00	1,00	30,00	0,00
RINGmut_z	Q9SU58	ATPase 4, plasma membrane-type	3	3	3,00	1	0|0|0	1,00	1,00	1,00	1,00	1,00	30,00	0,00
RINGmut_z	Q9SRH5	Mitochondrial outer membrane protein porin 1	3	3	3,00	1	0|0|0	1,00	1,00	1,00	1,00	1,00	30,00	0,00
RINGmut_z	Q8L3X8	Serine/arginine-rich SC35-like splicing factor SCL30	3	3	3,00	1	0|0|0	1,00	1,00	1,00	1,00	1,00	30,00	0,00
RINGmut_z	P48348	14-3-3-like protein GF14 kappa	3	3	3,00	1	0|0|0	1,00	1,00	1,00	1,00	1,00	30,00	0,00
RINGmut_z	Q38900	Peptidyl-prolyl cis-trans isomerase CYP19-1	3	3	3,00	1	0|0|0	1,00	1,00	1,00	1,00	1,00	30,00	0,00
RINGmut_z	P25819	Catalase-2	3	3	3,00	1	0|0|0	1,00	1,00	1,00	1,00	1,00	30,00	0,00
RINGmut_z	P56780	Photosystem II reaction center protein H	3	3	3,00	1	0|0|0	1,00	1,00	1,00	1,00	1,00	30,00	0,00
RINGmut_z	P36210	50S ribosomal protein L12-1, chloroplastic	3	3	3,00	1	0|0|0	1,00	1,00	1,00	1,00	1,00	30,00	0,00
RINGmut_z	Q96262	Plasma membrane-associated cation-binding protein 1	3	3	3,00	1	0|0|0	1,00	1,00	1,00	1,00	1,00	30,00	0,00
RINGmut_z	P10796	Ribulose bisphosphate carboxylase small chain 1B, chloroplastic	3	3	3,00	1	0|0|0	1,00	1,00	1,00	1,00	1,00	30,00	0,00
RINGmut_z	Q9LXC9	Soluble inorganic pyrophosphatase 6, chloroplastic	3	3	3,00	1	0|0|0	1,00	1,00	1,00	1,00	1,00	30,00	0,00
RINGmut_z	Q9LU86	Peroxiredoxin Q, chloroplastic	3	3	3,00	1	0|0|0	1,00	1,00	1,00	1,00	1,00	30,00	0,00
RINGmut_z	P19366	ATP synthase subunit beta, chloroplastic	3	3	3,00	1	0|0|0	1,00	1,00	1,00	1,00	1,00	30,00	0,00
RINGmut_z	Q9ZUU4	RNA-binding protein CP29B, chloroplastic	3	3	3,00	1	0|0|0	1,00	1,00	1,00	1,00	1,00	30,00	0,00
RINGmut_z	P56779	Cytochrome b559 subunit alpha	3	3	3,00	1	0|0|0	1,00	1,00	1,00	1,00	1,00	30,00	0,00
RINGmut_z	Q03250	Glycine-rich RNA-binding protein 7	7	7	7,00	1	0|0|1	1,00	1,00	1,00	1,00	1,00	21,00	0,00
RINGmut_z	Q42556	ATPase 9, plasma membrane-type	2	2	2,00	1	0|0|0	0,97	0,97	0,97	0,97	0,97	20,00	0,00

Bait: RINGmut_z	Prey	PreyGene	Spec	SpecSum	AvgSpec	NumReplicates	ctrlCounts	AvgP	MaxP	TopoAvgP	TopoMaxP	SaintScore	FoldChange	BFDR
RINGmut_z	Q07100	Serine/threonine-protein phosphatase PP2A-3 catalytic subunit	2	2	2,00	1	0|0|0	0,97	0,97	0,97	0,97	0,97	20,00	0,00
RINGmut_z	Q9FXA4	U-box domain-containing protein 26	2	2	2,00	1	0|0|0	0,97	0,97	0,97	0,97	0,97	20,00	0,00
RINGmut_z	Q8GYM1	Glutathione S-transferase U22	2	2	2,00	1	0|0|0	0,97	0,97	0,97	0,97	0,97	20,00	0,00
RINGmut_z	Q39096	Protein EARLY RESPONSIVE TO DEHYDRATION 15	2	2	2,00	1	0|0|0	0,97	0,97	0,97	0,97	0,97	20,00	0,00
RINGmut_z	Q9MA79	Fructose-1,6-bisphosphatase, cytosolic	2	2	2,00	1	0|0|0	0,97	0,97	0,97	0,97	0,97	20,00	0,00
RINGmut_z	Q9LSB4	TSA1-like protein	2	2	2,00	1	0|0|0	0,97	0,97	0,97	0,97	0,97	20,00	0,00
RINGmut_z	Q9ZVA4	EP1-like glycoprotein 3	2	2	2,00	1	0|0|0	0,97	0,97	0,97	0,97	0,97	20,00	0,00
RINGmut_z	Q9ZP05	Malate dehydrogenase 2, peroxisomal	2	2	2,00	1	0|0|0	0,97	0,97	0,97	0,97	0,97	20,00	0,00
RINGmut_z	Q9M1X0	Ribosome-recycling factor, chloroplastic	2	2	2,00	1	0|0|0	0,97	0,97	0,97	0,97	0,97	20,00	0,00
RINGmut_z	P94072	Germin-like protein subfamily 3 member 3	2	2	2,00	1	0|0|0	0,97	0,97	0,97	0,97	0,97	20,00	0,00
RINGmut_z	P60129	Photosystem II reaction center protein L	2	2	2,00	1	0|0|0	0,97	0,97	0,97	0,97	0,97	20,00	0,00
RINGmut_z	Q03251	Glycine-rich RNA-binding protein 8	11	11	11,00	1	0|0|2	1,00	1,00	1,00	1,00	1,00	16,50	0,00
RINGmut_z	Q9FFC0	Histone H2B.10	11	11	11,00	1	1|2|0	1,00	1,00	1,00	1,00	1,00	11,00	0,00
RINGmut_z	Q9SAJ6	Glyceraldehyde-3-phosphate dehydrogenase GAPCP1, chloroplastic	7	7	7,00	1	0|0|2	0,98	0,98	0,98	0,98	0,98	10,50	0,00
RINGmut_z	Q56WN1	Glutamine synthetase cytosolic isozyme 1-1	1	1	1,00	1	0|0|0	0,00	0,00	0,00	0,00	0,00	10,00	0,51
RINGmut_z	Q9FMD9	Glutamine synthetase cytosolic isozyme 1-4	1	1	1,00	1	0|0|0	0,00	0,00	0,00	0,00	0,00	10,00	0,51
RINGmut_z	Q8W4S4	V-type proton ATPase subunit a3	1	1	1,00	1	0|0|0	0,00	0,00	0,00	0,00	0,00	10,00	0,51
RINGmut_z	Q9SN86	Malate dehydrogenase, chloroplastic	1	1	1,00	1	0|0|0	0,00	0,00	0,00	0,00	0,00	10,00	0,51
RINGmut_z	Q7PC79	Exportin-T	1	1	1,00	1	0|0|0	0,00	0,00	0,00	0,00	0,00	10,00	0,51
RINGmut_z	F4KEL0	Subtilisin-like protease SBT5.5	1	1	1,00	1	0|0|0	0,00	0,00	0,00	0,00	0,00	10,00	0,51
RINGmut_z	Q9S757	Bifunctional L-3-cyanoalanine synthase/cysteine synthase C1, mitochondrial	1	1	1,00	1	0|0|0	0,00	0,00	0,00	0,00	0,00	10,00	0,51

Bait: RINGmut_z	Prey	PreyGene	Spec	SpecSum	AvgSpec	NumReplicates	ctrlCounts	AvgP	MaxP	TopoAvgP	TopoMaxP	SaintScore	FoldChange	BFDR
RINGmut_z	Q9C9W5	Glycerate dehydrogenase HPR, peroxisomal	1	1	1,00	1	0|0|0	0,00	0,00	0,00	0,00	0,00	10,00	0,51
RINGmut_z	Q5XF75	Elongation factor Ts, mitochondrial	1	1	1,00	1	0|0|0	0,00	0,00	0,00	0,00	0,00	10,00	0,51
RINGmut_z	P69834	2-C-methyl-D-erythritol 4-phosphate cytidylyltransferase, chloroplastic	1	1	1,00	1	0|0|0	0,00	0,00	0,00	0,00	0,00	10,00	0,51
RINGmut_z	Q96518	Peroxidase 16	1	1	1,00	1	0|0|0	0,00	0,00	0,00	0,00	0,00	10,00	0,51
RINGmut_z	Q9LR64	Photosystem II repair protein PSB27-H1, chloroplastic	1	1	1,00	1	0|0|0	0,00	0,00	0,00	0,00	0,00	10,00	0,51
RINGmut_z	Q9S7I3	Non-specific lipid-transfer protein 2	1	1	1,00	1	0|0|0	0,00	0,00	0,00	0,00	0,00	10,00	0,51
RINGmut_z	Q42406	Peptidyl-prolyl cis-trans isomerase CYP18-4	3	3	3,00	1	0|1|0	0,97	0,97	0,97	0,97	0,97	9,00	0,00
RINGmut_z	Q9SAJ4	Phosphoglycerate kinase 3, cytosolic	5	5	5,00	1	1|1|0	0,98	0,98	0,98	0,98	0,98	7,50	0,00
RINGmut_z	Q41188	Cold shock protein 2	7	7	7,00	1	1|1|1	0,99	0,99	0,99	0,99	0,99	7,00	0,00
RINGmut_z	Q5E924	Glyceraldehyde-3-phosphate dehydrogenase GAPCP2, chloroplastic	7	7	7,00	1	0|0|3	0,92	0,92	0,92	0,92	0,92	7,00	0,01
RINGmut_z	Q8LD46	60S ribosomal protein L23a-1	20	20	20,00	1	4|3|3	1,00	1,00	1,00	1,00	1,00	6,00	0,00
RINGmut_z	P0DH97	Calmodulin-2	16	16	16,00	1	4|4|0	1,00	1,00	1,00	1,00	1,00	6,00	0,00
RINGmut_z	P39207	Nucleoside diphosphate kinase 1	8	8	8,00	1	2|2|0	1,00	1,00	1,00	1,00	1,00	6,00	0,00
RINGmut_z	Q9LJE4	Chaperonin 60 subunit beta 2, chloroplastic	6	6	6,00	1	1|2|0	0,97	0,97	0,97	0,97	0,97	6,00	0,00
RINGmut_z	O23138	Cytochrome c-1	4	4	4,00	1	0|2|0	0,86	0,86	0,86	0,86	0,86	6,00	0,02
RINGmut_z	Q9LXJ2	Cytochrome b-c1 complex subunit 9, mitochondrial	2	2	2,00	1	0|0|1	0,79	0,79	0,79	0,79	0,79	6,00	0,02
RINGmut_z	Q9LPI5	Polyadenylate-binding protein-interacting protein 11	2	2	2,00	1	0|1|0	0,79	0,79	0,79	0,79	0,79	6,00	0,02
RINGmut_z	Q9ZUX4	Uncharacterized protein At2g27730, mitochondrial	2	2	2,00	1	0|0|1	0,79	0,79	0,79	0,79	0,79	6,00	0,02
RINGmut_z	Q9SF85	Adenosine kinase 1	5	5	5,00	1	2|1|0	0,92	0,92	0,92	0,92	0,92	5,00	0,01
RINGmut_z	Q8RWV0	Transketolase-1, chloroplastic	7	7	7,00	1	0|5|0	0,81	0,81	0,81	0,81	0,81	4,20	0,02
RINGmut_z	P46077	14-3-3-like protein GF14 phi	4	4	4,00	1	1|2|0	0,78	0,78	0,78	0,78	0,78	4,00	0,03
RINGmut_z	Q9SIM4	60S ribosomal protein L14-1	5	5	5,00	1	0|0|4	0,74	0,74	0,74	0,74	0,74	3,75	0,03
RINGmut_z	Q9ZT91	Elongation factor Tu, mitochondrial	16	16	16,00	1	6|7|0	0,85	0,85	0,85	0,85	0,85	3,69	0,02

Bait: RINGmut_z	Prey	PreyGene	Spec	SpecSum	AvgSpec	NumReplicates	ctrlCounts	AvgP	MaxP	TopoAvgP	TopoMaxP	SaintScore	FoldChange	BFDR
RINGmut_z	Q9FLQ4	2-oxoglutarate dehydrogenase E2 component (dihydrolipoamide succinyltransferase)	6	6	6,00	1	0|0|5	0,74	0,74	0,74	0,74	0,74	3,60	0,04
RINGmut_z	Q9FJX3	Mitochondrial outer membrane protein porin 2	6	6	6,00	1	1|4|0	0,72	0,72	0,72	0,72	0,72	3,60	0,04
RINGmut_z	Q9SEU4	Serine/arginine-rich SC35-like splicing factor SCL33	6	6	6,00	1	0|0|5	0,74	0,74	0,74	0,74	0,74	3,60	0,04
RINGmut_z	Q9FE65	60S ribosomal protein L34-2	7	7	7,00	1	3|3|0	0,81	0,81	0,81	0,81	0,81	3,50	0,02
RINGmut_z	Q8LCL3	60S ribosomal protein L27-2	7	7	7,00	1	3|3|0	0,81	0,81	0,81	0,81	0,81	3,50	0,02
RINGmut_z	P23686	S-adenosylmethionine synthase 1	16	16	16,00	1	7|7|0	0,75	0,75	0,75	0,75	0,75	3,43	0,03
RINGmut_z	P17562	S-adenosylmethionine synthase 2	18	18	18,00	1	8|9|0	0,55	0,55	0,55	0,55	0,55	3,18	0,06
RINGmut_z	Q8H107	2-oxoglutarate dehydrogenase E2 component (dihydrolipoamide succinyltransferase)	6	6	6,00	1	0|0|6	0,60	0,60	0,60	0,60	0,60	3,00	0,05
RINGmut_z	Q01525	14-3-3-like protein GF14 omega	3	3	3,00	1	1|2|0	0,52	0,52	0,52	0,52	0,52	3,00	0,07
RINGmut_z	P92994	Trans-cinnamate 4-monooxygenase	2	2	2,00	1	1|0|1	0,47	0,47	0,47	0,47	0,47	3,00	0,08
RINGmut_z	P12411	Tubulin beta-1 chain	37	37	37,00	1	17|21|0	0,04	0,04	0,04	0,04	0,04	2,92	0,22
RINGmut_z	P51419	60S ribosomal protein L27-3	8	8	8,00	1	5|4|0	0,36	0,36	0,36	0,36	0,36	2,67	0,10
RINGmut_z	P59233	Ubiquitin-40S ribosomal protein S27a-3	15	15	15,00	1	8|9|0	0,15	0,15	0,15	0,15	0,15	2,65	0,16
RINGmut_z	Q9SQI8	Pyruvate dehydrogenase E2 component (dihydrolipoamide acetyltransferase)	22	22	22,00	1	0|0|25	0,06	0,06	0,06	0,06	0,06	2,64	0,20
RINGmut_z	P27323	Heat shock protein 90-1	7	7	7,00	1	3|5|0	0,35	0,35	0,35	0,35	0,35	2,62	0,10
RINGmut_z	O81127	Serine/arginine-rich splicing factor RSZ21	6	6	6,00	1	0|0|7	0,42	0,42	0,42	0,42	0,42	2,57	0,09
RINGmut_z	O23255	Adenosylhomocysteinase 1	22	22	22,00	1	12|14|0	0,02	0,02	0,02	0,02	0,02	2,54	0,25
RINGmut_z	P42645	14-3-3-like protein GF14 upsilon	5	5	5,00	1	2|4|0	0,33	0,33	0,33	0,33	0,33	2,50	0,11
RINGmut_z	P51818	Heat shock protein 90-3	14	14	14,00	1	5|12|0	0,08	0,08	0,08	0,08	0,08	2,47	0,19
RINGmut_z	P53494	Actin-4	23	23	23,00	1	13|15|0	0,01	0,01	0,01	0,01	0,01	2,46	0,28
RINGmut_z	P53497	Actin-12	23	23	23,00	1	13|15|0	0,01	0,01	0,01	0,01	0,01	2,46	0,28
RINGmut_z	P42643	14-3-3-like protein GF14 chi	4	4	4,00	1	2|3|0	0,31	0,31	0,31	0,31	0,31	2,40	0,12

Bait: RINGmut_z	Prey	PreyGene	Spec	SpecSum	AvgSpec	NumReplicates	ctrlCounts	AvgP	MaxP	TopoAvgP	TopoMaxP	SaintScore	FoldChange	BFDR
RINGmut_z	P29513	Tubulin beta-5 chain	37	37	37,00	1	17|22|8	0,00	0,00	0,00	0,00	0,00	2,36	0,36
RINGmut_z	Q9LHP2	Serine/arginine-rich SC35-like splicing factor SCL30A	7	7	7,00	1	0|0|9	0,25	0,25	0,25	0,25	0,25	2,33	0,13
RINGmut_z	P59232	Ubiquitin-40S ribosomal protein S27a-2	15	15	15,00	1	8|9|3	0,03	0,03	0,03	0,03	0,03	2,25	0,23
RINGmut_z	P42644	14-3-3-like protein GF14 psi	6	6	6,00	1	3|5|0	0,17	0,17	0,17	0,17	0,17	2,25	0,15
RINGmut_z	Q56YW9	Tubulin beta-2 chain	68	68	68,00	1	37|41|15	0,00	0,00	0,00	0,00	0,00	2,19	0,45
RINGmut_z	Q8RXU5	60S ribosomal protein L37a-2	8	8	8,00	1	0|0|11	0,12	0,12	0,12	0,12	0,12	2,18	0,17
RINGmut_z	P29515	Tubulin beta-7 chain	52	52	52,00	1	26|36|10	0,00	0,00	0,00	0,00	0,00	2,17	0,44
RINGmut_z	P83483	ATP synthase subunit beta-1, mitochondrial	18	18	18,00	1	9|12|5	0,00	0,00	0,00	0,00	0,00	2,08	0,31
RINGmut_z	Q9LUT2	S-adenosylmethionine synthase 4	17	17	17,00	1	12|13|0	0,00	0,00	0,00	0,00	0,00	2,04	0,33
RINGmut_z	P29516	Tubulin beta-8 chain	48	48	48,00	1	27|34|10	0,00	0,00	0,00	0,00	0,00	2,03	0,44
RINGmut_z	P29517	Tubulin beta-9 chain	45	45	45,00	1	26|33|8	0,00	0,00	0,00	0,00	0,00	2,01	0,44
RINGmut_z	P92549	ATP synthase subunit alpha, mitochondrial	12	12	12,00	1	8|10|0	0,01	0,01	0,01	0,01	0,01	2,00	0,29
RINGmut_z	Q96300	14-3-3-like protein GF14 nu	4	4	4,00	1	2|4|0	0,14	0,14	0,14	0,14	0,14	2,00	0,16
RINGmut_z	Q9LVM1	ABC transporter B family member 25, mitochondrial	2	2	2,00	1	0|0|3	0,33	0,33	0,33	0,33	0,33	2,00	0,11
RINGmut_z	Q56WH4	Histone deacetylase HDT2	15	15	15,00	1	11|12|0	0,00	0,00	0,00	0,00	0,00	1,96	0,33
RINGmut_z	Q9C8P0	Pyruvate dehydrogenase E2 component (dihydrolipoamide acetyltransferase)	13	13	13,00	1	0|0|20	0,00	0,00	0,00	0,00	0,00	1,95	0,30
RINGmut_z	Q9C4Z6	Receptor for activated C kinase 1B	9	9	9,00	1	6|8|0	0,01	0,01	0,01	0,01	0,01	1,93	0,27
RINGmut_z	P29514	Tubulin beta-6 chain	30	30	30,00	1	16|21|10	0,00	0,00	0,00	0,00	0,00	1,91	0,42
RINGmut_z	P59259	Histone H4	14	14	14,00	1	0|2|20	0,00	0,00	0,00	0,00	0,00	1,91	0,32
RINGmut_z	P24636	Tubulin beta-4 chain	45	45	45,00	1	29|35|8	0,00	0,00	0,00	0,00	0,00	1,88	0,46
RINGmut_z	Q9SJL8	S-adenosylmethionine synthase 3	10	10	10,00	1	8|8|0	0,01	0,01	0,01	0,01	0,01	1,88	0,29
RINGmut_z	Q9SMX3	Mitochondrial outer membrane protein porin 3	20	20	20,00	1	15|16|2	0,00	0,00	0,00	0,00	0,00	1,82	0,39
RINGmut_z	P29197	Chaperonin CPN60, mitochondrial	20	20	20,00	1	16|15|2	0,00	0,00	0,00	0,00	0,00	1,82	0,39

Bait: RINGmut_z	Prey	PreyGene	Spec	SpecSum	AvgSpec	NumReplicates	ctrlCounts	AvgP	MaxP	TopoAvgP	TopoMaxP	SaintScore	FoldChange	BFDR
RINGmut_z	Q9XI93	Oleosin-B3-like protein	15	15	15,00	1	16|9|0	0,00	0,00	0,00	0,00	0,00	1,80	0,36
RINGmut_z	O24456	Receptor for activated C kinase 1A	9	9	9,00	1	3|12|0	0,01	0,01	0,01	0,01	0,01	1,80	0,28
RINGmut_z	Q9LUW6	DEAD-box ATP-dependent RNA helicase 9, mitochondrial	3	3	3,00	1	3|2|0	0,11	0,11	0,11	0,11	0,11	1,80	0,17
RINGmut_z	Q9SRZ6	Cytosolic isocitrate dehydrogenase [NADP]	3	3	3,00	1	2|3|0	0,11	0,11	0,11	0,11	0,11	1,80	0,17
RINGmut_z	Q8LEQ0	60S acidic ribosomal protein P1-3	3	3	3,00	1	2|3|0	0,11	0,11	0,11	0,11	0,11	1,80	0,17
RINGmut_z	Q8RYC2	Putative actin-5	7	7	7,00	1	4|4|4	0,01	0,01	0,01	0,01	0,01	1,75	0,27
RINGmut_z	Q9SEE9	Serine/arginine-rich splicing factor SR45	7	7	7,00	1	3|3|6	0,01	0,01	0,01	0,01	0,01	1,75	0,27
RINGmut_z	Q8L7B5	Chaperonin CPN60-like 1, mitochondrial	10	10	10,00	1	9|9|0	0,00	0,00	0,00	0,00	0,00	1,67	0,33
RINGmut_z	P42825	Chaperone protein dnaJ 2	5	5	5,00	1	4|5|0	0,02	0,02	0,02	0,02	0,02	1,67	0,24
RINGmut_z	P93819	Malate dehydrogenase 1, cytoplasmic	6	6	6,00	1	3|3|5	0,01	0,01	0,01	0,01	0,01	1,64	0,28
RINGmut_z	Q9LV28	Receptor for activated C kinase 1C	8	8	8,00	1	5|10|0	0,00	0,00	0,00	0,00	0,00	1,60	0,32
RINGmut_z	Q9LQI9	Oligouridylate-binding protein 1B	4	4	4,00	1	5|3|0	0,02	0,02	0,02	0,02	0,02	1,50	0,25
RINGmut_z	Q94AW8	Chaperone protein dnaJ 3	3	3	3,00	1	2|4|0	0,05	0,05	0,05	0,05	0,05	1,50	0,21
RINGmut_z	Q949U7	Peroxiredoxin-2E, chloroplastic	3	3	3,00	1	3|3|0	0,04	0,04	0,04	0,04	0,04	1,50	0,21
RINGmut_z	Q42547	Catalase-3	2	2	2,00	1	2|2|0	0,07	0,07	0,07	0,07	0,07	1,50	0,19
RINGmut_z	Q8LCW9	60S acidic ribosomal protein P1-1	2	2	2,00	1	2|2|0	0,07	0,07	0,07	0,07	0,07	1,50	0,19
RINGmut_z	Q9LX65	V-type proton ATPase subunit H	1	1	1,00	1	0|2|0	0,00	0,00	0,00	0,00	0,00	1,50	0,51
RINGmut_z	Q9SI61	Amidophosphoribosyltransferase 1, chloroplastic	1	1	1,00	1	1|1|0	0,00	0,00	0,00	0,00	0,00	1,50	0,51
RINGmut_z	Q42523	Methylcrotonoyl-CoA carboxylase subunit alpha, mitochondrial	123	123	123,00	1	7|13|227	0,00	0,00	0,00	0,00	0,00	1,49	0,50
RINGmut_z	Q9T029	40S ribosomal protein S25-4	9	9	9,00	1	5|6|8	0,00	0,00	0,00	0,00	0,00	1,42	0,37
RINGmut_z	Q42351	60S ribosomal protein L34-1	7	7	7,00	1	3|3|9	0,00	0,00	0,00	0,00	0,00	1,40	0,35
RINGmut_z	Q93ZM7	Chaperonin CPN60-like 2, mitochondrial	5	5	5,00	1	3|8|0	0,00	0,00	0,00	0,00	0,00	1,36	0,31
RINGmut_z	Q9LZ57	60S ribosomal protein L36-3	5	5	5,00	1	0|0|11	0,01	0,01	0,01	0,01	0,01	1,36	0,29

Bait: RINGmut_z	Prey	PreyGene	Spec	SpecSum	AvgSpec	NumReplicates	ctrlCounts	AvgP	MaxP	TopoAvgP	TopoMaxP	SaintScore	FoldChange	BFDR
RINGmut_z	P53496	Actin-11	22	22	22,00	1	17|18|14	0,00	0,00	0,00	0,00	0,00	1,35	0,46
RINGmut_z	P0CJ46	Actin-1	18	18	18,00	1	14|17|11	0,00	0,00	0,00	0,00	0,00	1,29	0,46
RINGmut_z	P0CJ47	Actin-3	18	18	18,00	1	14|17|11	0,00	0,00	0,00	0,00	0,00	1,29	0,46
RINGmut_z	Q9SJT9	Coatomer subunit alpha-2	6	6	6,00	1	7|7|0	0,00	0,00	0,00	0,00	0,00	1,29	0,35
RINGmut_z	Q94F49	Probable histone H2A.5	3	3	3,00	1	0|0|7	0,03	0,03	0,03	0,03	0,03	1,29	0,24
RINGmut_z	Q9S9K7	Probable histone H2AXb	3	3	3,00	1	0|0|7	0,03	0,03	0,03	0,03	0,03	1,29	0,24
RINGmut_z	Q9ASR1	Elongation factor 2	11	11	11,00	1	11|15|0	0,00	0,00	0,00	0,00	0,00	1,27	0,42
RINGmut_z	P0DH99	Elongation factor 1-alpha 1	76	76	76,00	1	69|82|30	0,00	0,00	0,00	0,00	0,00	1,26	0,50
RINGmut_z	Q42533	Biotin carboxyl carrier protein of acetyl-CoA carboxylase 1, chloroplastic	118	118	118,00	1	14|14|256	0,00	0,00	0,00	0,00	0,00	1,25	0,51
RINGmut_z	P53492	Actin-7	32	32	32,00	1	28|30|19	0,00	0,00	0,00	0,00	0,00	1,25	0,49
RINGmut_z	F4JWP9	109 kDa U5 small nuclear ribonucleoprotein component GFL	9	9	9,00	1	9|13|0	0,00	0,00	0,00	0,00	0,00	1,23	0,40
RINGmut_z	Q9FVQ1	Nucleolin 1	11	11	11,00	1	14|13|0	0,00	0,00	0,00	0,00	0,00	1,22	0,43
RINGmut_z	Q9FMG4	Serine/arginine-rich splicing factor SC35	6	6	6,00	1	0|0|15	0,00	0,00	0,00	0,00	0,00	1,20	0,35
RINGmut_z	Q56WH1	Tubulin alpha-3 chain	25	25	25,00	1	24|31|8	0,00	0,00	0,00	0,00	0,00	1,19	0,48
RINGmut_z	B9DHQ0	Tubulin alpha-5 chain	25	25	25,00	1	24|31|8	0,00	0,00	0,00	0,00	0,00	1,19	0,48
RINGmut_z	P29511	Tubulin alpha-6 chain	36	36	36,00	1	36|43|13	0,00	0,00	0,00	0,00	0,00	1,17	0,49
RINGmut_z	O81126	Serine/arginine-rich splicing factor RSZ22	9	9	9,00	1	1|0|22	0,00	0,00	0,00	0,00	0,00	1,17	0,41
RINGmut_z	Q9LLC1	Biotin carboxyl carrier protein of acetyl-CoA carboxylase 2, chloroplastic	39	39	39,00	1	0|0|103	0,00	0,00	0,00	0,00	0,00	1,14	0,50
RINGmut_z	Q9M352	60S ribosomal protein L36-2	8	8	8,00	1	1|1|19	0,00	0,00	0,00	0,00	0,00	1,14	0,40
RINGmut_z	P11139	Tubulin alpha-1 chain	12	12	12,00	1	12|16|4	0,00	0,00	0,00	0,00	0,00	1,12	0,44
RINGmut_z	Q9FVI6	Homeobox-leucine zipper protein HDG6	3	3	3,00	1	4|4|0	0,00	0,00	0,00	0,00	0,00	1,12	0,30
RINGmut_z	Q9M9W1	60S ribosomal protein L22-2	3	3	3,00	1	4|3|1	0,00	0,00	0,00	0,00	0,00	1,12	0,31
RINGmut_z	Q9LUW5	DEAD-box ATP-dependent RNA helicase 53, mitochondrial	8	8	8,00	1	10|9|3	0,00	0,00	0,00	0,00	0,00	1,09	0,42

Bait: RINGmut_z	Prey	PreyGene	Spec	SpecSum	AvgSpec	NumReplicates	ctrlCounts	AvgP	MaxP	TopoAvgP	TopoMaxP	SaintScore	FoldChange	BFDR
RINGmut_z	Q9CAX6	40S ribosomal protein S14-2	8	8	8,00	1	11|11|0	0,00	0,00	0,00	0,00	0,00	1,09	0,42
RINGmut_z	Q9ZU52	Fructose-bisphosphate aldolase 3, chloroplastic	4	4	4,00	1	2|2|7	0,00	0,00	0,00	0,00	0,00	1,09	0,34
RINGmut_z	Q39043	Heat shock 70 kDa protein BIP2	25	25	25,00	1	27|27|16	0,00	0,00	0,00	0,00	0,00	1,07	0,49
RINGmut_z	Q9LKR3	Heat shock 70 kDa protein BIP1	25	25	25,00	1	26|28|16	0,00	0,00	0,00	0,00	0,00	1,07	0,49
RINGmut_z	Q9C9C5	60S ribosomal protein L6-3	7	7	7,00	1	0|0|20	0,00	0,00	0,00	0,00	0,00	1,05	0,40
RINGmut_z	Q9FX54	Glyceraldehyde-3-phosphate dehydrogenase GAPC2, cytosolic	36	36	36,00	1	41|45|22	0,00	0,00	0,00	0,00	0,00	1,00	0,51
RINGmut_z	P25858	Glyceraldehyde-3-phosphate dehydrogenase GAPC1, cytosolic	35	35	35,00	1	39|41|25	0,00	0,00	0,00	0,00	0,00	1,00	0,51
RINGmut_z	Q9S9N1	Heat shock 70 kDa protein 5	20	20	20,00	1	15|21|24	0,00	0,00	0,00	0,00	0,00	1,00	0,51
RINGmut_z	P41916	GTP-binding nuclear protein Ran-1	6	6	6,00	1	7|8|3	0,00	0,00	0,00	0,00	0,00	1,00	0,51
RINGmut_z	Q9LFH5	60S ribosomal protein L12-2	5	5	5,00	1	8|7|0	0,00	0,00	0,00	0,00	0,00	1,00	0,51
RINGmut_z	Q8LD03	40S ribosomal protein S7-3	5	5	5,00	1	7|8|0	0,00	0,00	0,00	0,00	0,00	1,00	0,51
RINGmut_z	Q42290	Probable mitochondrial-processing peptidase subunit beta, mitochondrial	2	2	2,00	1	2|4|0	0,00	0,00	0,00	0,00	0,00	1,00	0,51
RINGmut_z	Q9ZU46	Receptor protein kinase-like protein ZAR1	2	2	2,00	1	0|0|6	0,00	0,00	0,00	0,00	0,00	1,00	0,51
RINGmut_z	Q9LVT8	RGG repeats nuclear RNA binding protein C	5	5	5,00	1	10|6|0	0,00	0,00	0,00	0,00	0,00	0,94	0,51
RINGmut_z	Q9M339	40S ribosomal protein S3-2	10	10	10,00	1	15|18|0	0,00	0,00	0,00	0,00	0,00	0,91	0,51
RINGmut_z	P42798	40S ribosomal protein S15a-1	3	3	3,00	1	2|5|3	0,00	0,00	0,00	0,00	0,00	0,90	0,51
RINGmut_z	Q9SIP7	40S ribosomal protein S3-1	12	12	12,00	1	17|18|6	0,00	0,00	0,00	0,00	0,00	0,88	0,51
RINGmut_z	Q9T043	60S ribosomal protein L14-2	7	7	7,00	1	9|11|4	0,00	0,00	0,00	0,00	0,00	0,88	0,51
RINGmut_z	P42697	Dynamin-related protein 1A	62	62	62,00	1	55|61|97	0,00	0,00	0,00	0,00	0,00	0,87	0,51
RINGmut_z	Q96292	Actin-2	13	13	13,00	1	18|18|9	0,00	0,00	0,00	0,00	0,00	0,87	0,51
RINGmut_z	Q9SRX2	60S ribosomal protein L19-1	18	18	18,00	1	7|8|48	0,00	0,00	0,00	0,00	0,00	0,86	0,51
RINGmut_z	P34788	40S ribosomal protein S18	10	10	10,00	1	6|9|20	0,00	0,00	0,00	0,00	0,00	0,86	0,51
RINGmut_z	Q9SIH0	40S ribosomal protein S14-1	8	8	8,00	1	11|11|6	0,00	0,00	0,00	0,00	0,00	0,86	0,51

Bait: RINGmut_z	Prey	PreyGene	Spec	SpecSum	AvgSpec	NumReplicates	ctrlCounts	AvgP	MaxP	TopoAvgP	TopoMaxP	SaintScore	FoldChange	BFDR
RINGmut_z	Q42347	60S ribosomal protein L24-1	6	6	6,00	1	0|0|21	0,00	0,00	0,00	0,00	0,00	0,86	0,51
RINGmut_z	O04848	Probable histone H2AXa	2	2	2,00	1	0|0|7	0,00	0,00	0,00	0,00	0,00	0,86	0,51
RINGmut_z	Q96293	Actin-8	14	14	14,00	1	20|20|10	0,00	0,00	0,00	0,00	0,00	0,84	0,51
RINGmut_z	Q9LNC5	110 kDa U5 small nuclear ribonucleoprotein component CLO	9	9	9,00	1	12|20|0	0,00	0,00	0,00	0,00	0,00	0,84	0,51
RINGmut_z	P41376	Eukaryotic initiation factor 4A-1	15	15	15,00	1	19|25|10	0,00	0,00	0,00	0,00	0,00	0,83	0,51
RINGmut_z	P31414	Pyrophosphate-energized vacuolar membrane proton pump 1	8	8	8,00	1	8|11|10	0,00	0,00	0,00	0,00	0,00	0,83	0,51
RINGmut_z	Q9LZH9	60S ribosomal protein L7a-2	15	15	15,00	1	10|11|34	0,00	0,00	0,00	0,00	0,00	0,82	0,51
RINGmut_z	Q9M5K3	Dihydrolipoyl dehydrogenase 1, mitochondrial	3	3	3,00	1	4|7|0	0,00	0,00	0,00	0,00	0,00	0,82	0,51
RINGmut_z	P49692	60S ribosomal protein L7a-1	17	17	17,00	1	13|14|37	0,00	0,00	0,00	0,00	0,00	0,80	0,51
RINGmut_z	P49200	40S ribosomal protein S20-1	4	4	4,00	1	6|6|3	0,00	0,00	0,00	0,00	0,00	0,80	0,51
RINGmut_z	Q8VZG7	Ribonuclease TUDOR 1	4	4	4,00	1	5|10|0	0,00	0,00	0,00	0,00	0,00	0,80	0,51
RINGmut_z	Q8L7U4	Co-chaperone protein p23-1	10	10	10,00	1	19|18|2	0,00	0,00	0,00	0,00	0,00	0,77	0,51
RINGmut_z	Q9ASS2	Protein FREE1	11	11	11,00	1	17|18|9	0,00	0,00	0,00	0,00	0,00	0,75	0,51
RINGmut_z	P42794	60S ribosomal protein L11-2	7	7	7,00	1	11|14|3	0,00	0,00	0,00	0,00	0,00	0,75	0,51
RINGmut_z	Q5XEP2	Hsp70-Hsp90 organizing protein 2	4	4	4,00	1	9|7|0	0,00	0,00	0,00	0,00	0,00	0,75	0,51
RINGmut_z	Q9SV20	Coatomer subunit beta-2	4	4	4,00	1	6|10|0	0,00	0,00	0,00	0,00	0,00	0,75	0,51
RINGmut_z	Q9SIK2	40S ribosomal protein S25-2	3	3	3,00	1	2|4|6	0,00	0,00	0,00	0,00	0,00	0,75	0,51
RINGmut_z	Q945Q1	Cysteine proteinase inhibitor 1	3	3	3,00	1	4|4|4	0,00	0,00	0,00	0,00	0,00	0,75	0,51
RINGmut_z	P32961	Nitrilase 1	3	3	3,00	1	7|5|0	0,00	0,00	0,00	0,00	0,00	0,75	0,51
RINGmut_z	P38420	DNA-directed RNA polymerase II subunit 2	2	2	2,00	1	3|5|0	0,00	0,00	0,00	0,00	0,00	0,75	0,51
RINGmut_z	P31167	ADP,ATP carrier protein 1, mitochondrial	33	33	33,00	1	43|47|45	0,00	0,00	0,00	0,00	0,00	0,73	0,51
RINGmut_z	Q08682	40S ribosomal protein Sa-1	6	6	6,00	1	9|12|4	0,00	0,00	0,00	0,00	0,00	0,72	0,51
RINGmut_z	Q9FJA6	40S ribosomal protein S3-3	9	9	9,00	1	15|17|6	0,00	0,00	0,00	0,00	0,00	0,71	0,51
RINGmut_z	Q56WD9	3-ketoacyl-CoA thiolase 2, peroxisomal	4	4	4,00	1	9|8|0	0,00	0,00	0,00	0,00	0,00	0,71	0,51

Bait: RINGmut_z	Prey	PreyGene	Spec	SpecSum	AvgSpec	NumReplicates	ctrlCounts	AvgP	MaxP	TopoAvgP	TopoMaxP	SaintScore	FoldChange	BFDR
RINGmut_z	Q9SSB5	26S proteasome regulatory subunit 7 homolog A	4	4	4,00	1	7|10|0	0,00	0,00	0,00	0,00	0,00	0,71	0,51
RINGmut_z	Q9LJH8	Oligouridylate-binding protein 1C	5	5	5,00	1	11|7|4	0,00	0,00	0,00	0,00	0,00	0,68	0,51
RINGmut_z	Q8LF21	Dynamin-related protein 1C	33	33	33,00	1	41|46|60	0,00	0,00	0,00	0,00	0,00	0,67	0,51
RINGmut_z	O23654	V-type proton ATPase catalytic subunit A	4	4	4,00	1	2|5|11	0,00	0,00	0,00	0,00	0,00	0,67	0,51
RINGmut_z	Q9SJA6	Serine/arginine-rich splicing factor RSZ22A	4	4	4,00	1	0|0|18	0,00	0,00	0,00	0,00	0,00	0,67	0,51
RINGmut_z	P25696	Bifunctional enolase 2/transcriptional activator	15	15	15,00	1	27|30|11	0,00	0,00	0,00	0,00	0,00	0,66	0,51
RINGmut_z	P49693	60S ribosomal protein L19-3	8	8	8,00	1	4|6|27	0,00	0,00	0,00	0,00	0,00	0,65	0,51
RINGmut_z	Q9C522	ATP-citrate synthase beta chain protein 1	13	13	13,00	1	32|27|2	0,00	0,00	0,00	0,00	0,00	0,64	0,51
RINGmut_z	Q9SB63	Protein MODIFIER OF SNC1 1	7	7	7,00	1	17|16|0	0,00	0,00	0,00	0,00	0,00	0,64	0,51
RINGmut_z	Q9LYJ9	DEAD-box ATP-dependent RNA helicase 46	6	6	6,00	1	13|15|0	0,00	0,00	0,00	0,00	0,00	0,64	0,51
RINGmut_z	Q9SCM3	40S ribosomal protein S2-4	3	3	3,00	1	7|7|0	0,00	0,00	0,00	0,00	0,00	0,64	0,51
RINGmut_z	Q93VP3	Eukaryotic translation initiation factor 5A-2	3	3	3,00	1	8|6|0	0,00	0,00	0,00	0,00	0,00	0,64	0,51
RINGmut_z	Q8H136	DEAD-box ATP-dependent RNA helicase 14	16	16	16,00	1	20|21|37	0,00	0,00	0,00	0,00	0,00	0,62	0,51
RINGmut_z	P46286	60S ribosomal protein L8-1	13	13	13,00	1	13|16|34	0,00	0,00	0,00	0,00	0,00	0,62	0,51
RINGmut_z	P41377	Eukaryotic initiation factor 4A-2	12	12	12,00	1	22|27|9	0,00	0,00	0,00	0,00	0,00	0,62	0,51
RINGmut_z	Q8LBI1	60S ribosomal protein L5-1	9	9	9,00	1	19|21|5	0,00	0,00	0,00	0,00	0,00	0,60	0,51
RINGmut_z	Q9LDZ0	Heat shock 70 kDa protein 10, mitochondrial	3	3	3,00	1	9|6|0	0,00	0,00	0,00	0,00	0,00	0,60	0,51
RINGmut_z	Q9FVT2	Probable elongation factor 1-gamma 2	2	2	2,00	1	4|6|0	0,00	0,00	0,00	0,00	0,00	0,60	0,51
RINGmut_z	Q9FFT4	Pyruvate decarboxylase 2	1	1	1,00	1	2|3|0	0,00	0,00	0,00	0,00	0,00	0,60	0,51
RINGmut_z	Q9LDD8	Methylcrotonoyl-CoA carboxylase beta chain, mitochondrial	43	43	43,00	1	3|6|209	0,00	0,00	0,00	0,00	0,00	0,59	0,51
RINGmut_z	P17745	Elongation factor Tu, chloroplastic	7	7	7,00	1	19|16|2	0,00	0,00	0,00	0,00	0,00	0,57	0,51
RINGmut_z	Q9FZ76	60S ribosomal protein L6-1	4	4	4,00	1	4|4|13	0,00	0,00	0,00	0,00	0,00	0,57	0,51
RINGmut_z	Q9LQ55	Dynamin-2B	43	43	43,00	1	54|60|118	0,00	0,00	0,00	0,00	0,00	0,56	0,51

Bait: RINGmut_z	Prey	PreyGene	Spec	SpecSum	AvgSpec	NumReplicates	ctrlCounts	AvgP	MaxP	TopoAvgP	TopoMaxP	SaintScore	FoldChange	BFDR
RINGmut_z	P20649	ATPase 1, plasma membrane-type	6	6	6,00	1	14|18|0	0,00	0,00	0,00	0,00	0,00	0,56	0,51
RINGmut_z	P0DH91	ADP-ribosylation factor 2-B	5	5	5,00	1	13|14|0	0,00	0,00	0,00	0,00	0,00	0,56	0,51
RINGmut_z	P57691	60S acidic ribosomal protein P0-3	3	3	3,00	1	5|11|0	0,00	0,00	0,00	0,00	0,00	0,56	0,51
RINGmut_z	P22953	Heat shock 70 kDa protein 1	59	59	59,00	1	124|137|58	0,00	0,00	0,00	0,00	0,00	0,55	0,51
RINGmut_z	P40941	ADP,ATP carrier protein 2, mitochondrial	12	12	12,00	1	26|23|16	0,00	0,00	0,00	0,00	0,00	0,55	0,51
RINGmut_z	P49209	60S ribosomal protein L9-1	12	12	12,00	1	26|28|12	0,00	0,00	0,00	0,00	0,00	0,55	0,51
RINGmut_z	Q9FGX1	ATP-citrate synthase beta chain protein 2	12	12	12,00	1	36|30|0	0,00	0,00	0,00	0,00	0,00	0,55	0,51
RINGmut_z	Q42262	40S ribosomal protein S3a-2	10	10	10,00	1	19|19|17	0,00	0,00	0,00	0,00	0,00	0,55	0,51
RINGmut_z	Q05431	L-ascorbate peroxidase 1, cytosolic	4	4	4,00	1	11|11|0	0,00	0,00	0,00	0,00	0,00	0,55	0,51
RINGmut_z	Q940B0	60S ribosomal protein L18-3	10	10	10,00	1	13|11|32	0,00	0,00	0,00	0,00	0,00	0,54	0,51
RINGmut_z	Q9LJE5	YTH domain-containing protein ECT2	10	10	10,00	1	23|27|7	0,00	0,00	0,00	0,00	0,00	0,53	0,51
RINGmut_z	O65719	Heat shock 70 kDa protein 3	51	51	51,00	1	122|127|45	0,00	0,00	0,00	0,00	0,00	0,52	0,51
RINGmut_z	P51414	60S ribosomal protein L26-1	4	4	4,00	1	2|4|17	0,00	0,00	0,00	0,00	0,00	0,52	0,51
RINGmut_z	F4K1Z0	YTH domain-containing protein ECT3	4	4	4,00	1	8|7|8	0,00	0,00	0,00	0,00	0,00	0,52	0,51
RINGmut_z	P41127	60S ribosomal protein L13-1	15	15	15,00	1	16|15|58	0,00	0,00	0,00	0,00	0,00	0,51	0,51
RINGmut_z	P49688	40S ribosomal protein S2-3	7	7	7,00	1	13|14|14	0,00	0,00	0,00	0,00	0,00	0,51	0,51
RINGmut_z	Q9LHA8	Heat shock 70 kDa protein 4	46	46	46,00	1	108|122|45	0,00	0,00	0,00	0,00	0,00	0,50	0,51
RINGmut_z	Q9SZ15	Protein HOMOLOG OF MAMMALIAN LYST-INTERACTING PROTEIN 5	10	10	10,00	1	25|22|13	0,00	0,00	0,00	0,00	0,00	0,50	0,51
RINGmut_z	Q1EBV4	Protein DNA-DAMAGE INDUCIBLE 1	7	7	7,00	1	19|12|11	0,00	0,00	0,00	0,00	0,00	0,50	0,51
RINGmut_z	P51413	60S ribosomal protein L17-2	5	5	5,00	1	5|7|18	0,00	0,00	0,00	0,00	0,00	0,50	0,51
RINGmut_z	Q9M5K2	Dihydrolipoyl dehydrogenase 2, mitochondrial	2	2	2,00	1	6|6|0	0,00	0,00	0,00	0,00	0,00	0,50	0,51
RINGmut_z	Q9LF46	2-hydroxyacyl-CoA lyase	2	2	2,00	1	6|6|0	0,00	0,00	0,00	0,00	0,00	0,50	0,51
RINGmut_z	Q6ICZ8	Nascent polypeptide-associated complex subunit alpha-like protein 3	2	2	2,00	1	6|4|2	0,00	0,00	0,00	0,00	0,00	0,50	0,51
RINGmut_z	P47192	Vesicle-associated membrane protein 722	1	1	1,00	1	2|4|0	0,00	0,00	0,00	0,00	0,00	0,50	0,51

Bait: RINGmut_z	Prey	PreyGene	Spec	SpecSum	AvgSpec	NumReplicates	ctrlCounts	AvgP	MaxP	TopoAvgP	TopoMaxP	SaintScore	FoldChange	BFDR
RINGmut_z	Q949R9	Mitochondrial pyruvate carrier 1	1	1	1,00	1	1|1|4	0,00	0,00	0,00	0,00	0,00	0,50	0,51
RINGmut_z	O82462	Glutamate--tRNA ligase, cytoplasmic	1	1	1,00	1	0|6|0	0,00	0,00	0,00	0,00	0,00	0,50	0,51
RINGmut_z	P49227	60S ribosomal protein L5-2	6	6	6,00	1	17|20|0	0,00	0,00	0,00	0,00	0,00	0,49	0,51
RINGmut_z	P38666	60S ribosomal protein L24-2	6	6	6,00	1	5|6|27	0,00	0,00	0,00	0,00	0,00	0,47	0,51
RINGmut_z	Q9C7X7	Heat shock 70 kDa protein 18	37	37	37,00	1	95|100|45	0,00	0,00	0,00	0,00	0,00	0,46	0,51
RINGmut_z	P49205	40S ribosomal protein S17-1	2	2	2,00	1	3|2|8	0,00	0,00	0,00	0,00	0,00	0,46	0,51
RINGmut_z	P22954	Heat shock 70 kDa protein 2	43	43	43,00	1	110|123|51	0,00	0,00	0,00	0,00	0,00	0,45	0,51
RINGmut_z	Q9LUQ6	60S ribosomal protein L19-2	3	3	3,00	1	0|0|20	0,00	0,00	0,00	0,00	0,00	0,45	0,51
RINGmut_z	Q42064	60S ribosomal protein L8-3	9	9	9,00	1	14|16|33	0,00	0,00	0,00	0,00	0,00	0,43	0,51
RINGmut_z	Q96266	Glutathione S-transferase F8, chloroplastic	3	3	3,00	1	8|13|0	0,00	0,00	0,00	0,00	0,00	0,43	0,51
RINGmut_z	Q9LHG8	Protein ELC	1	1	1,00	1	3|2|2	0,00	0,00	0,00	0,00	0,00	0,43	0,51
RINGmut_z	Q9LNB6	Hsp70-Hsp90 organizing protein 1	18	18	18,00	1	44|45|39	0,00	0,00	0,00	0,00	0,00	0,42	0,51
RINGmut_z	P51430	40S ribosomal protein S6-2	8	8	8,00	1	17|20|20	0,00	0,00	0,00	0,00	0,00	0,42	0,51
RINGmut_z	P19456	ATPase 2, plasma membrane-type	6	6	6,00	1	17|27|0	0,00	0,00	0,00	0,00	0,00	0,41	0,51
RINGmut_z	O50008	5-methyltetrahydropteroyltriglutamate--homocysteine methyltransferase 1	6	6	6,00	1	23|21|0	0,00	0,00	0,00	0,00	0,00	0,41	0,51
RINGmut_z	Q8L8Y0	40S ribosomal protein S2-1	4	4	4,00	1	10|11|8	0,00	0,00	0,00	0,00	0,00	0,41	0,51
RINGmut_z	Q93VB8	40S ribosomal protein S2-2	4	4	4,00	1	10|11|8	0,00	0,00	0,00	0,00	0,00	0,41	0,51
RINGmut_z	Q94CE5	Gamma-aminobutyrate transaminase POP2, mitochondrial	2	2	2,00	1	7|8|0	0,00	0,00	0,00	0,00	0,00	0,40	0,51
RINGmut_z	Q8S3C9	Dynamin-related protein 1D	2	2	2,00	1	4|3|8	0,00	0,00	0,00	0,00	0,00	0,40	0,51
RINGmut_z	Q9SE83	Dynamin-2A	29	29	29,00	1	55|65|102	0,00	0,00	0,00	0,00	0,00	0,39	0,51
RINGmut_z	Q9SS17	40S ribosomal protein S24-1	4	4	4,00	1	8|9|14	0,00	0,00	0,00	0,00	0,00	0,39	0,51
RINGmut_z	Q9MAB3	Probable nucleolar protein 5-2	3	3	3,00	1	8|9|7	0,00	0,00	0,00	0,00	0,00	0,38	0,51
RINGmut_z	Q9FEF8	rRNA 2'-O-methyltransferase fibrillarin 1	3	3	3,00	1	11|11|2	0,00	0,00	0,00	0,00	0,00	0,38	0,51
RINGmut_z	Q8L716	Splicing factor U2af large subunit B	2	2	2,00	1	0|0|16	0,00	0,00	0,00	0,00	0,00	0,38	0,51

Bait: RINGmut_z	Prey	PreyGene	Spec	SpecSum	AvgSpec	NumReplicates	ctrlCounts	AvgP	MaxP	TopoAvgP	TopoMaxP	SaintScore	FoldChange	BFDR
RINGmut_z	Q8L5Y6	Cullin-associated NEDD8-dissociated protein 1	16	16	16,00	1	67|62|5	0,00	0,00	0,00	0,00	0,00	0,36	0,51
RINGmut_z	Q8LC83	40S ribosomal protein S24-2	3	3	3,00	1	7|7|12	0,00	0,00	0,00	0,00	0,00	0,35	0,51
RINGmut_z	Q8GUM2	Heat shock 70 kDa protein 9, mitochondrial	8	8	8,00	1	27|28|15	0,00	0,00	0,00	0,00	0,00	0,34	0,51
RINGmut_z	Q96327	ERBB-3 BINDING PROTEIN 1	7	7	7,00	1	31|23|7	0,00	0,00	0,00	0,00	0,00	0,34	0,51
RINGmut_z	P17094	60S ribosomal protein L3-1	15	15	15,00	1	36|42|58	0,00	0,00	0,00	0,00	0,00	0,33	0,51
RINGmut_z	Q9FKA5	Uncharacterized protein At5g39570	10	10	10,00	1	39|36|16	0,00	0,00	0,00	0,00	0,00	0,33	0,51
RINGmut_z	O23515	60S ribosomal protein L15-1	8	8	8,00	1	13|11|48	0,00	0,00	0,00	0,00	0,00	0,33	0,51
RINGmut_z	Q08112	40S ribosomal protein S15-1	2	2	2,00	1	3|4|11	0,00	0,00	0,00	0,00	0,00	0,33	0,51
RINGmut_z	Q39172	NADPH-dependent oxidoreductase 2-alkenal reductase	1	1	1,00	1	3|6|0	0,00	0,00	0,00	0,00	0,00	0,33	0,51
RINGmut_z	Q9SJQ9	Fructose-bisphosphate aldolase 6, cytosolic	21	21	21,00	1	82|66|48	0,00	0,00	0,00	0,00	0,00	0,32	0,51
RINGmut_z	Q9FLT0	Ribonuclease TUDOR 2	4	4	4,00	1	19|18|0	0,00	0,00	0,00	0,00	0,00	0,32	0,51
RINGmut_z	Q9ZPI1	Lysine--tRNA ligase, cytoplasmic	4	4	4,00	1	15|22|0	0,00	0,00	0,00	0,00	0,00	0,32	0,51
RINGmut_z	P49211	60S ribosomal protein L32-1	3	3	3,00	1	4|3|21	0,00	0,00	0,00	0,00	0,00	0,32	0,51
RINGmut_z	Q9LF98	Fructose-bisphosphate aldolase 8, cytosolic	30	30	30,00	1	114|102|87	0,00	0,00	0,00	0,00	0,00	0,30	0,51
RINGmut_z	O48549	40S ribosomal protein S6-1	7	7	7,00	1	18|22|29	0,00	0,00	0,00	0,00	0,00	0,30	0,51
RINGmut_z	P60040	60S ribosomal protein L7-2	6	6	6,00	1	16|23|26	0,00	0,00	0,00	0,00	0,00	0,28	0,51
RINGmut_z	Q9SF40	60S ribosomal protein L4-1	18	18	18,00	1	23|26|154	0,00	0,00	0,00	0,00	0,00	0,27	0,51
RINGmut_z	Q0WNJ6	Clathrin heavy chain 1	5	5	5,00	1	25|31|0	0,00	0,00	0,00	0,00	0,00	0,27	0,51
RINGmut_z	Q42340	40S ribosomal protein S16-3	5	5	5,00	1	12|11|32	0,00	0,00	0,00	0,00	0,00	0,27	0,51
RINGmut_z	P59224	40S ribosomal protein S13-2	4	4	4,00	1	8|7|30	0,00	0,00	0,00	0,00	0,00	0,27	0,51
RINGmut_z	Q9LTT8	Enhancer of mRNA-decapping protein 4	13	13	13,00	1	68|70|15	0,00	0,00	0,00	0,00	0,00	0,25	0,51
RINGmut_z	Q9LXG1	40S ribosomal protein S9-1	6	6	6,00	1	13|16|43	0,00	0,00	0,00	0,00	0,00	0,25	0,51
RINGmut_z	Q93VG5	40S ribosomal protein S8-1	6	6	6,00	1	28|32|14	0,00	0,00	0,00	0,00	0,00	0,24	0,51
RINGmut_z	P46645	Aspartate aminotransferase, cytoplasmic isozyme 1	5	5	5,00	1	27|31|4	0,00	0,00	0,00	0,00	0,00	0,24	0,51

Bait: RINGmut_z	Prey	PreyGene	Spec	SpecSum	AvgSpec	NumReplicates	ctrlCounts	AvgP	MaxP	TopoAvgP	TopoMaxP	SaintScore	FoldChange	BFDR
RINGmut_z	Q9SZY1	Nascent polypeptide-associated complex subunit alpha-like protein 4	2	2	2,00	1	9|9|7	0,00	0,00	0,00	0,00	0,00	0,24	0,51
RINGmut_z	P60039	60S ribosomal protein L7-3	4	4	4,00	1	14|17|22	0,00	0,00	0,00	0,00	0,00	0,23	0,51
RINGmut_z	Q9LR33	60S ribosomal protein L27a-2	4	4	4,00	1	10|12|31	0,00	0,00	0,00	0,00	0,00	0,23	0,51
RINGmut_z	Q9FNX5	Dynamin-related protein 1E	3	3	3,00	1	11|12|16	0,00	0,00	0,00	0,00	0,00	0,23	0,51
RINGmut_z	O82204	60S ribosomal protein L28-1	2	2	2,00	1	5|4|17	0,00	0,00	0,00	0,00	0,00	0,23	0,51
RINGmut_z	P49691	60S ribosomal protein L4-2	14	14	14,00	1	24|27|144	0,00	0,00	0,00	0,00	0,00	0,22	0,51
RINGmut_z	Q9ZUT9	40S ribosomal protein S5-1	2	2	2,00	1	5|7|16	0,00	0,00	0,00	0,00	0,00	0,21	0,51
RINGmut_z	Q9FHG2	60S ribosomal protein L32-2	2	2	2,00	1	3|3|23	0,00	0,00	0,00	0,00	0,00	0,21	0,51
RINGmut_z	P49204	40S ribosomal protein S4-2	7	7	7,00	1	27|33|47	0,00	0,00	0,00	0,00	0,00	0,20	0,51
RINGmut_z	Q9STW6	Heat shock 70 kDa protein 6, chloroplastic	1	1	1,00	1	3|4|8	0,00	0,00	0,00	0,00	0,00	0,20	0,51
RINGmut_z	Q38882	Phospholipase D alpha 1	25	25	25,00	1	176|159|68	0,00	0,00	0,00	0,00	0,00	0,19	0,51
RINGmut_z	Q9FME2	Nuclear transport factor 2	1	1	1,00	1	8|8|0	0,00	0,00	0,00	0,00	0,00	0,19	0,51
RINGmut_z	Q9SL67	26S proteasome regulatory subunit 4 homolog B	1	1	1,00	1	9|9|0	0,00	0,00	0,00	0,00	0,00	0,17	0,51
RINGmut_z	Q9LTX9	Heat shock 70 kDa protein 7, chloroplastic	1	1	1,00	1	4|5|10	0,00	0,00	0,00	0,00	0,00	0,16	0,51
RINGmut_z	Q0WLB5	Clathrin heavy chain 2	3	3	3,00	1	28|31|0	0,00	0,00	0,00	0,00	0,00	0,15	0,51
RINGmut_z	O80626	60S ribosomal protein L35-2	1	1	1,00	1	3|4|15	0,00	0,00	0,00	0,00	0,00	0,14	0,51
RINGmut_z	Q8LPJ7	40S ribosomal protein S26-2	1	1	1,00	1	0|0|25	0,00	0,00	0,00	0,00	0,00	0,12	0,51
RINGmut_z	O82647	Pyruvate decarboxylase 1	1	1	1,00	1	14|13|0	0,00	0,00	0,00	0,00	0,00	0,11	0,51
RINGmut_z	O23254	Serine hydroxymethyltransferase 4	1	1	1,00	1	13|14|0	0,00	0,00	0,00	0,00	0,00	0,11	0,51
RINGmut_z	Q9FLF0	40S ribosomal protein S9-2	1	1	1,00	1	0|0|29	0,00	0,00	0,00	0,00	0,00	0,10	0,51
RINGmut_z	Q9SJF1	GTPase LSG1-2	1	1	1,00	1	12|11|7	0,00	0,00	0,00	0,00	0,00	0,10	0,51
RINGmut_z	Q9T074	Phosphoenolpyruvate carboxykinase (ATP)	6	6	6,00	1	95|85|17	0,00	0,00	0,00	0,00	0,00	0,09	0,51
RINGmut_z	O04983	Biotin carboxylase, chloroplastic	5	5	5,00	1	5|9|150	0,00	0,00	0,00	0,00	0,00	0,09	0,51
RINGmut_z	P49206	40S ribosomal protein S26-1	1	1	1,00	1	4|4|26	0,00	0,00	0,00	0,00	0,00	0,09	0,51

Bait: RINGmut_z	Prey	PreyGene	Spec	SpecSum	AvgSpec	NumReplicates	ctrlCounts	AvgP	MaxP	TopoAvgP	TopoMaxP	SaintScore	FoldChange	BFDR
RINGmut_z	Q9LYK9	40S ribosomal protein S26-3	1	1	1,00	1	3|4|26	0,00	0,00	0,00	0,00	0,00	0,09	0,51
RINGmut_z	Q9SVR0	60S ribosomal protein L13a-3	1	1	1,00	1	4|10|21	0,00	0,00	0,00	0,00	0,00	0,09	0,51
RINGmut_z	Q9LTT9	Varicose-related protein	2	2	2,00	1	49|34|5	0,00	0,00	0,00	0,00	0,00	0,07	0,51
RINGmut_z	Q9SFU1	60S ribosomal protein L13a-1	1	1	1,00	1	7|12|33	0,00	0,00	0,00	0,00	0,00	0,06	0,51
RINGmut_z	Q9C5Z1	Eukaryotic translation initiation factor 3 subunit B	1	1	1,00	1	30|25|0	0,00	0,00	0,00	0,00	0,00	0,05	0,51
RINGmut_z	F4I1L3	Acetyl-CoA carboxylase 2	2	2	2,00	1	11|11|139	0,00	0,00	0,00	0,00	0,00	0,04	0,51